PREDICTION OF STABILITY LIMITS FOR BINARY AND TERNARY SYSTEMS USING THE NRTL LIQUID PHASE MODEL

by

Fahad M. Al-Sadoon

A Thesis Presented to the Faculty of the
American University of Sharjah
College of Engineering
in Partial Fulfillment
of the Requirements
for the Degree of

Master of Science in
Chemical Engineering

Sharjah, United Arab Emirates

January 2013

Approval Signatures

We, the undersigned, approve the Master's Thesis of Fahad M. Al-Sadoon.

Prediction of Stability Limits For Binary & Ternary Systems Using The NRTL Liquid Phase Model:

Signature **Date of Signature** (dd/mm/yyyy)

_____ _____

Dr. Naif Darwish
Professor, Department of Chemical Engineering
Thesis Advisor

_____ _____

Dr. Taleb Ibrahim
Professor, Department of Chemical Engineering
Thesis Committee Member

_____ _____

Dr. Zarook Shareefdeen
Associate Professor, Department of Chemical Engineering

Thesis Committee Member

_____ _____

Dr. Mohamed Al-Sayyah
Associate Professor, Dept. of Biology, Chemistry & Environment
Thesis Committee Member

_____ _____

Dr. Naif Darwish
Head, Department of Chemical Engineering

_____ _____

Dr. Hany El Kadi
Associate Dean, College of Engineering

_____ _____

Dr. Yousef Al Assaf
Dean, College of Engineering

_____ _____

Dr. Khaled Assaleh
Director of Graduate Studies

Acknowledgments

All praises to Allah for giving me the strength and ability to finish this thesis.

I would like to express my profound gratitude to my Professor Dr. Naif Darwish, for his guidance, effort, and support in every aspect during the course of this thesis. I thank him for giving me the opportunity to pursue research of my interest.

Special thanks goes to the thesis committee: Dr. Taleb Ibrahim, Dr. Zarook Shareefdeen, and Dr. Mohammad Al-Sayyah for their time and effort put in reviewing this thesis.

I take this opportunity to thank and show my gratitude to my parents for their endless love and support in all aspects of my life. I would like to also thank my brother and sister, Ihab and Safia, for their encouragement to always pursue my dreams and for being my role models.

I thank my colleague, Ibrahim Masoud, for making this trip pleasurable. I am indebted to my colleagues and friends Saeid Rahimi and Sami Hassouneh for their continuous support & encouragement to grow professionally.

Abstract

Stability limits (spinodal loci) were determined for 53 binary systems and 26 ternary systems. Rigorous thermodynamic criteria for spinodal limits and criticality conditions in terms of mixture Gibbs free energy were derived from the NRTL model. The highly nonlinear coupled algebraic equations were solved using a Matlab® code employing a double precision strategy to minimize round-off errors. The generated critical temperatures and compositions were compared with literature, when available, and found in good agreement.

The binary systems studied contain six groups: acetonitrile + hydrocarbons, N-formylmorpholine (NFM)+ alkanes, perfluoroalkanes + n-alkanes, sulfolane + hydrocarbons, 1,3- propanediol + ionic liquids, and N-methyl-α -pyrrolidone + n-alkanes. Additionally, the ternary systems analyzed belong to six groups; 2-propanol + water + alkanes, 2-propanone + water + alcohols, ethyl acetate + water + carboxylic acids, dibutyl ether + alcohols + water, water + ethanol + toluenes, and water + ethanol + benzene. Additionally, a ternary system consisting of limonene + linalool + 2-Aminoethanol was studied for temperatures of 298.15 K, 308.15 K, and 318.15 K.

For binary systems, literature reported data for critical temperatures and compositions exists for 44 out of the 53 binary systems studied. The average difference between literature and values obtained in the study is ± 0.58 K, while 75% of the critical temperatures obtained deviated less than 1 K. The average difference in critical compositions from literature reported values is 1.8 mol%. However, critical conditions are not reported in literature for any ternary systems except limonene + linalool + 2-aminoethanol, where the maximum difference in critical composition is 0.7 mol%. The results obtained indicate the model developed in this thesis can accurately predict the stability limits.

The results of the binary system were found to obey the universal exponent and follow simple power law with β of 0.3126 & 0.3623 for binodal and spinodal points, respectively. In addition, the critical exponent of susceptibility (γ) has been deduced to follow the expanded power law and the regressed value of γ is -0.8468.

Search Terms: Stability, critical temperature, critical point, spinodal loci, NRTL, critical exponent, binary liquid systems, ternary liquid systems, liquid-liquid equilibrium

Table of Contents

List of Figures

List of Tables

Chapter 1
Introduction

1.1 Background

The stability limits of a certain liquid mixture define the conditions (i.e., temperature, pressure, and composition) beyond which the system cannot maintain its homogenous phase and must split into two or more phases to attain a stable thermodynamic state. Stability is a concept of immense importance in Liquid-Liquid Equilibria (LLE) studies. All phase transitions are affiliated with the concept of stability. Any system, at given conditions, will retain its current state only if it is thermodynamically stable. Similarly, if the system at these conditions is deemed thermodynamically unstable, it will undergo phase transition to achieve a stable thermodynamic state. [1]

However, there is a third state referred to as metastable state, when the system is somewhat stable and can only withstand small disturbances [1]. As soon as the system is exposed to large disturbances, it will spontaneously become unstable and initiate phase transition to achieve a stable state. For example, it is normally expected that water boils at 100°C under atmospheric pressure, but it would be possible to heat water well above 100°C and still maintain it in a liquid state [2]. Under such conditions, water would be a superheated liquid and is categorized as being in a metastable state. Superheating can be achieved using pure water and by taking precautions to eliminate any impurities in the system, as well as eliminating external disturbances such as vibrations or quick heating. In fact, the more superheating is desired, the more precautions need to be taken. Likewise, water can be supercooled below 0 °C if the same precautions are taken. Liquid water has been experimentally reported in the range from -41 °C to 280 °C [2-4]. Liquid water between 0 °C to -41 °C and between 100 °C to 280 °C is referred to as thermodynamically metastable (i.e., stable only with respect to small disturbances). In

case of large disturbances, it will promote spontaneous immediate phase transformation. The relative size of disturbances is dependent on the degree of superheating. For a high degree of superheating, a large disturbance would be as small as a nuclear particle. This phenomenon is not limited to water but applicable to all liquid systems [2]. Under all circumstances, liquids cannot be superheated indefinitely; there is a practical limit that defines the limits of stability even in the complete absence of any sort of disturbances. Spinodal curves define the limit of stability for any phase transition and are frequently illustrated on the phase diagram.

Beside the fundamental significance of phase stability, it has currently many industrial applications in different areas of modern technology. For example, in separation processes, which constitute of 40%-80% of capital and operating investment [5], phase stability limits determine the conditions for phase splitting and consequently the required hardware facilities for further separation and purification [6].

Phase stability is extensively used to predict accurately the number of phases and the conditions at which these phases exist. This is needed prior to calculation of equilibrium compositions of each phase. Most reliable algorithms used in LLE calculations are the ones based on stability analysis [7].

The concept of phase stability plays an important role in polymer science and engineering as it helps to produce microstructures of high dispersion to improve the physical properties [8]. In fact, different polymer structures are obtained by the route of polymer phase separation. Phase separation of polymers can either take place by nucleation and growth or by spinodal decomposition [1, 2]. These phase separation paths will result in totally different polymer structures. Nucleation and growth phase separation happens when the liquid mixture is brought from the stable homogenous region into metastable region. At this point, the system will either proceed into phase splitting or form two phases to assume a stable low energy state, or it will exist as a single homogenous metastable state. On the other hand, spinodal decomposition occurs when the system is quenched into an unstable phase.

In the late 1960s, the U.S. Bureau of Mines carried out studies to address the safety concerns regarding LNG transport and operation. It was observed, by mere coincidence, that the LNG spill over water caused vapor explosions. In literature this is commonly referred to as Rapid Phase Transition (RPT) [2]. The contact between water, hot and non-volatile liquid, and LNG, cold and volatile liquid, will promote superheating of LNG, where superheating can proceed up to the homogenous nucleation temperature where a sudden and explosive rapid evaporation of LNG takes place. Vapor explosions or RPT are rapid and spontaneous and as such produce a shockwave that may damage equipment and cause personnel injuries [9, 10]. This kind of explosion is not related to fire or chemical reaction, rather it is a rapid vapor expansion. Nevertheless, the severity of RPT explosion is no different than a traditional explosion. Experimental work simulating RPT explosion achieved an explosion which is equivalent to 1817 kg of TNT in magnitude [9]. In fact, for a very large spill, an overpressure rate reaching up to 1000 m^3/min has been observed [11].

Rapid Phase Transitions were notably addressed through the Superheated Liquid Theory (SLT) by Reid and coauthors [2, 12-15]. According to the SLT, the homogenous nucleation lies on the spinodal curve and represents the absolute limit for superheating of liquid LNG. However, boiling can take place before reaching to homogenous nucleation in the presence of impurities and suspended particles. Moreover, superheated liquid theory stipulates that in order for vapor explosion to occur, the following criteria must also be satisfied [2, 15]

$$T_h > 0.9 \cdot T_c \qquad (1.1)$$

Where T_h refers to hot liquid temperature and T_C refers to critical temperature of the superheated (cold) liquid. This is due to the fact that most liquids can be superheated up to 90% of their critical temperature. Additionally, experimental work reveals that vapor explosion cannot happen if the temperature of hot [2] liquid is higher than 99% of the cold liquid's critical temperature. Therefore, the range of temperatures for vapor explosion is expressed [2, 15] as:

$$0.99 > \frac{T_h}{T_c} > 0.9 \qquad (1.2)$$

RPT is also a safety concern in some industries, such as in nuclear power plants, refrigeration units, and paper industry [2, 12-17]. In nuclear power plants, there is a concern that overheating of a reactor's core will melt the fuel cell and will trigger vapor explosion with the water used as coolant. Though there has been no incident in the nuclear power generation industry, vapor explosions have been witnessed in laboratory scale experiments and researchers deduced that these conditions are favorable for RPT.

Similar to vapor explosions, Boiling Liquid Expanding Vapor Explosion (BLEVE) produces explosions of a comparable scale to those witnessed in RPT. BLEVE is defined as "a sudden release of a large mass of pressurized superheated liquid to the atmosphere" as per The Centre for Chemical Process Safety [18, 19]. BELEVE is cited as being responsible for 1000 fatalities and over 10,000 personal injuries, as well as for billions of dollars of damaged assets [19]. BELEVE is frequently encountered in tank farms, tank trucks and railroad car accidents, where liquefied vapor such as LNG and LPG is stored [2, 20]. It has been observed that, during such accidents, there are two consecutive explosions occurring sequentially. The second explosion is comparably much more severe than the initial explosion. The first explosion will trigger superheating of the liquid content through sudden adiabatic depressuring, which will eventually lead to homogenous nucleation. Reid [20, 21] explains in terms of his Super Heat Limit (SLT) theory that quick depressuring or rapid heating will force the liquid to penetrate into the metastable region without actually boiling. However, as soon as the system reaches the limits of stability, it will induce homogenous nucleation and result in a disastrous explosion.

Phase stability problems also occur in oil production fields, where it is necessary to avoid the precipitation of asphaltenes that may result in clogging of the flow lines and oil wells. Asphaltenes are high molecular substances found in crude oil at the bottom of distillation [22, 23]. They are highly viscous substances, and thus their precipitation is undesirable as it can affect the production of oil by reducing its throughput. Moreover, they can increase

the corrosion rates, as well as produce excessive pressure drops. One of the methods used to predict asphaltene precipitation is to treat it as liquid-liquid and use stability analysis to predict the phase splitting of asphaltene from crude oil [22].

Furthermore, hydrate formation is another problem that is frequently encountered in wellheads and flow lines. Gas hydrates are complex crystalline structures that have an "ice-like" appearance, formed in the presence of free water and light hydrocarbon gases such as methane [24]. Gas hydrate formation is a serious problem as it can lead to pipeline and equipment clogging, and can reduce pipeline capacity by exacerbating pressure drop. The conventional method for hydrate inhibition is by methanol or glycol injection [24, 25]. Methanol/Glycol will thermodynamically stabilize the system by lowering the hydrate formation temperature at a certain pressure. However, this method results in substantial operating cost as it requires huge amounts of methanol or glycol to be injected. In addition, there is an extra capital cost to be considered for separation units installed for methanol/glycol recovery.

A promising hypothesis is recently being explored to use kinetic inhibitors to prevent gas hydrates [2, 26-27]. These inhibitors will work on suppressing hydrate formation kinetically rather than thermodynamically, as is the case with methanol injection. Thus, the system is effectively metastable. Kinetic- based recovery techniques overcomes the shortcomings of conventional injection as only a small amount of kinetic inhibitor is required to achieve hydrate inhibition. This concept is still in the research phase, where the pursuit of suitable kinetic inhibitors is currently under investigation . Promising results were obtained by using polyvinylpirolidone and hydroxyethylcellouse [2], and hyperbranched poly(ester amide)s [28].

Metastable states are not limited to industrial applications, and there are many occurrences in nature. For example, water, and specifically liquid water, is undeniably essential for all life aspects. Organisms living in subzero temperatures are in threat of potential water freezing that will subsequently terminate all molecular activity. Organisms living under these conditions develop means to suppress water freezing by

producing anti-freeze proteins that inhibit water freezing and maintain water in liquid state below 0 °C, effectively keeping water in metastable state [2, 29]. Anti-freeze protein are found in Polar and Antarctic fish [2, 30] and land animals beetles, spiders, and mites [31] The most prominent explanation on how these proteins inhibit water freezing is by adsorbing onto ice embryos thus preventing ice embryo from acting as nucleating site and preventing further formation of ice [32, 33].

In fact, the vast majority of supercooled liquids in nature are found in clouds [2]. Supercooled water will often be formed in the middle and high clouds that are in the range from 5 to 13 km from the earth's surface. The temperature of water at those heights is well below zero and temperatures as low as -40 °C were recorded in high clouds [34, 35]. Supercooling of water is possible at those heights due to the absence of airborne particles that act as nucleating sites. In low clouds up to 3 km, supercooling is quite rare as there is no shortage of airborne particles such as dust or salt, resulting from the evaporation of sea water. Airborne particles facilitate phase transition by acting as nucleating sites for crystal formation. This knowledge serves as the basis of cloud seeding, whereby dispersal of dry ice into the clouds facilitates the phase transition of supercooled water to ice. Silver iodide has hexagonal symmetry acts as an ideal shape for nucleating sites [2, 36].

The main goal of this thesis is to determine the stability limits of binary and ternary liquid mixtures based on the well-established stability criteria [1]. These criteria require the availability of a reliable liquid phase model describing the thermodynamic behavior of the liquid system under study. In this work, the well-known Non-Random-Two-Liquid (NRTL) model will be employed.

This thesis is organized in the following manner: Chapter 1 is dedicated to the applications of phase stability, the theoretical background relevant to this work, and the methodology towards determining phase stability limits. First, the phase behavior and stability concept is thoroughly discussed along with describing the common types of phase behavior for binary and ternary liquid mixtures. The NRTL model will be also

discussed and presented. Next, experimental and theoretical methods of finding stability limits will be described. Chapter 1 will be concluded by the methodology section, which will feature the needed derivations to develop a model together with the solution approach adopted to find stability limits. Chapter 2 will present the results of predicting stability limits for certain binary and ternary mixtures of industrial importance. Comparisons with experimental data, whenever such data are available, will be attempted. Chapter 3 will furnish the concluding remarks and observation of this work, together with the suggested recommendations for further work.

1.2 Literature Survey

As advanced before, the stability limits of a certain liquid mixture define the conditions (i.e. temperature, pressure, and composition) beyond which the system cannot maintain its homogenous phase and must split into two or more phases to attain a stable thermodynamic state. Stability analysis serves as a tool to determine these conditions. In simple terms, a system is said to be stable if it maintains its phase with respect to large disturbances [1] in its thermodynamic properties (T, P, composition, etc). A stable isolated system will always be at the maximum of its entropy or equivalently, the overall Gibbs free energy must be at minimum [1]. Unstable isolated systems are unable to maintain its homogenous phase and will split into two or more phases to achieve a stable condition of minimum overall Gibbs free energy. Metastable state can be considered as an intermediate state, where the system can still maintain its homogeneity and is relatively stable to small disturbances but will spontaneously split into two or more phases when exposed to large pressure, temperature, and composition fluctuations.

1.2.1 Phase Behaviour and The Concept of Stability

For liquid components to be mixed and form a stable homogenous or miscible liquid at constant temperature and pressure, the overall Gibbs free energy of mixing (ΔG^M) must be at its minimum. Therefore, for a single phase stable liquid system the ΔG^M must be always negative over the entire composition range. This is illustrated in figure 1.2-1 where the ΔG^M for the binary system at T1 is always negative; thus a single phase is

maintained throughout the composition range. As for T2 & T3, maintaining a single phase will not achieve a global m of ΔG^M and the actual minima is guaranteed by phase splitting. In particular, at T2 global minima of ΔG^M is achieved by having two distinct phases (L1 & L2) with composition of x_1^{L1} and x_1^{L2}, as illustrated in figure 1.2-1.

x_1^{L1} and x_1^{L2} are part of the binodal curve, depicted by the solid line on figure 1.2-1, which defines the solubility diagram i.e. defines the compositions of coexisting phases for a temperature range.

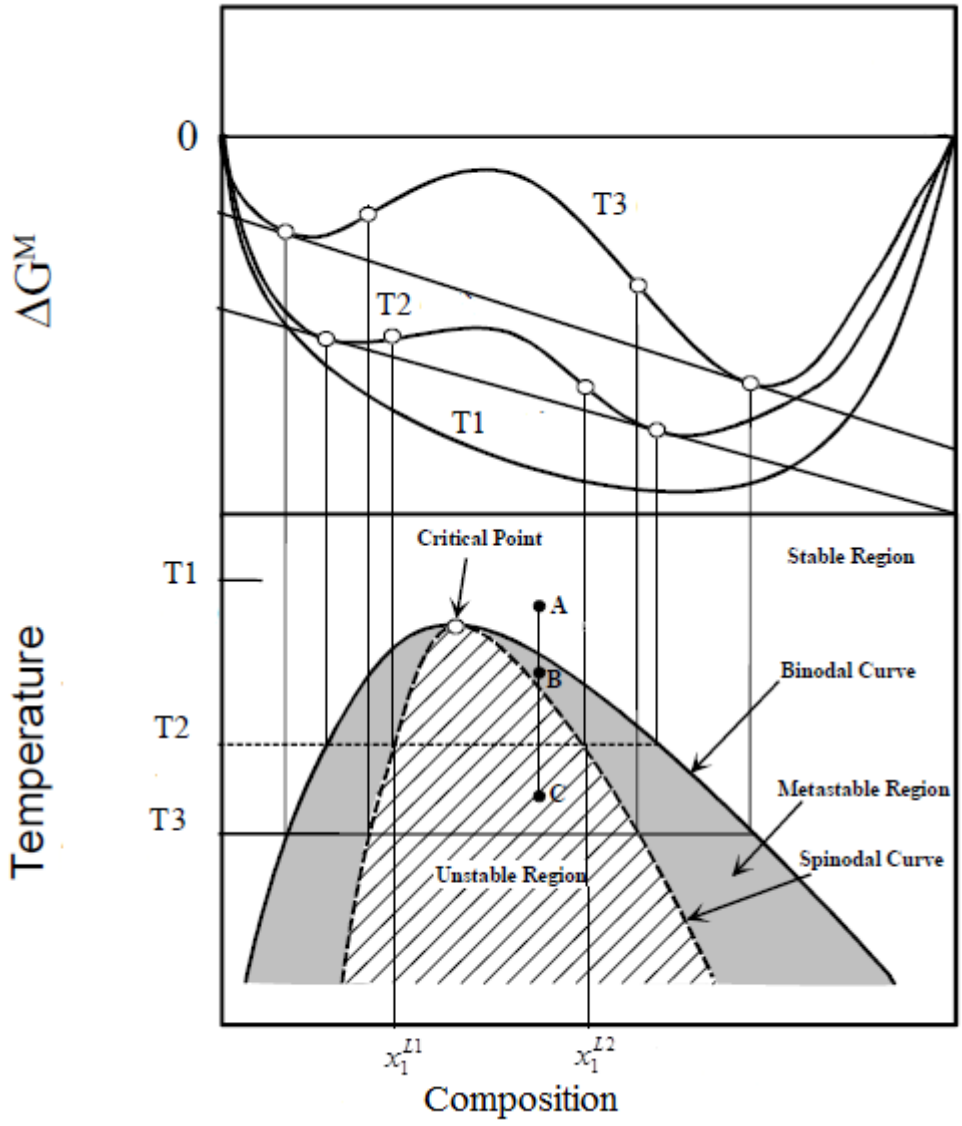

Figure 1.2-1 Binary system with phase splitting [46]

Graphically, the binodal curve sets the boundary for the two phase equilibrium. Outside of the binodal curve, the mixture will be of a single stable homogenous phase. Inside the binodal curve, the system can no longer be completely stable and will normally split into two phases to achieve a global minimum in ΔG^M and therefore a stable state (at constant T and P and overall mass). Under special circumstances, the liquid mixture can still retain a single homogenous phase in some portions, beyond the binodal curve where it is regarded as thermodynamically metastable. The metastable region is shown as the shaded region in figure 1.2-1. Metastability can be achieved experimentally by ensuring that any variation in the system such as cooling, heating, and mixing take place slowly and smoothly, in absence of any nucleation sites. Any perturbations large enough will force the liquid mixture to split to achieve a stable state where ΔG^M is at its minimum. However, anywhere beyond the spinodal curve, the binary mixture cannot retain its homogeneity and must split into two phases, irrespective of how carefully the experiment is carried out. The Spinodal curve defines the limit for the possible existence of metastable systems. Inside the spinodal curve, the system is unstable and cannot physically exist and will lead to phase separation. Overall, figure 1.2-1 shows three distinct regions. The first region where the system is of stable single phase region located anywhere outside the binodal curve. Second, metastable region defined by the area between the binodal and spinodal curve, where the system is only stable with respect to small disturbances. Third, the unstable region positioned inside the spinodal curve, where the system must split into two phases to achieve more stable state with a minimum in its energy. Theoretically, spinodal and binodal curves must converge at a single unique point, as shown in figure 1.2-1, referred to as the critical point.

In light of the above, three distinctive routes for phase transition can be observed; heterogeneous nucleation, homogenous nucleation, and spinodal decomposition. Heterogeneous nucleation is simply the phase splitting that occurs at the binodal curve, as shown in figure 1.2-1 for T2 where the system consist of two phases (L1 & L2) with compositions of x_1^{L1} and x_1^{L2}. This is the most frequent form of phase transition as there are always impurities, irregularities in shape, and suspended particles acting as nucleating sites and promoting heterogeneous phase transition. However, if these nucleating sites are

eliminated, phase transition occurs by penetrating deep beyond the binodal curve into the metastable region, at point B, for phase transition as depicted in figure 1.2-1. This process is known as homogenous nucleation or nucleation and growth. This kind of phase transition, as opposed to heterogeneous nucleation, will suddenly grow from the state of apparent stability to a sudden and spontaneous phase transition [1, 2].
Spinodal decomposition is a phase transition that arises from within the unstable region at point C as shown in figure 1.2-1. This type of transition is possible by introducing large and rapid change to the system, for example by quenching, and it has to be done in the vicinity of the critical point.

The critical temperature is a unique point and important property of any system. For example, for pure components, the liquid and vapor densities approach each other, and the two phases cannot be distinguished from each other. It is also important for multi-component mixtures, as it sets the limit for the two phase region envelope, and provides the best scaling parameter for temperature. Substantial amount of literature has been developed for finding or predicting the critical temperature. Various experimental methods such as light scattering [2] and more advanced experimental methods such as pulse induced critical scattering [37] proved to be successful and highly reliable. Yet, experimental data on critical temperature measurements are scarce and limited. This is mainly because experimental work is demanding or it cannot be carried out at high temperatures, where some systems will suffer from thermal decomposition [38]. Therefore, analytical predictive methods, such as those based on the NRTL model, used in this thesis, become of high importance.

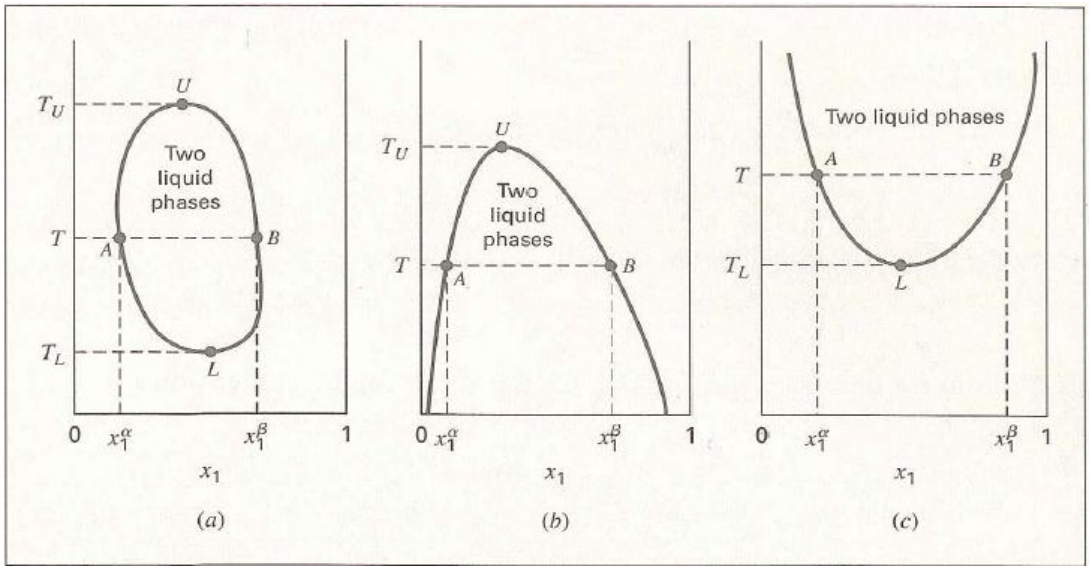

Figure 1.2-2 Three types of constant-pressure liquid/liquid solubility diagram. [39]

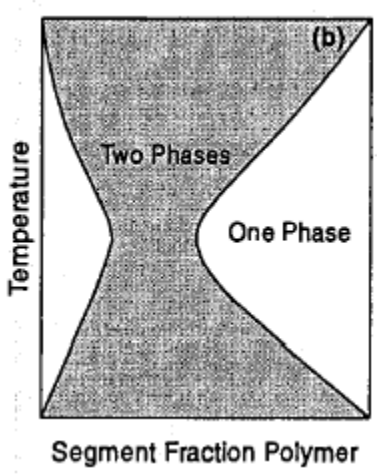

Figure 1.2-3 Hour-glass trend for polymers [41]

As shown in figure 1.2-2 a), the critical point represents conditions at which two or more phases converge to a single homogeneous phase. It sets the maximum limit for the existence of LLE. The critical temperature shown in figure 1.2-2 b) is referred to as upper critical solution temperature (UCST) where the system has only upper limit for LLE. While figure 1.2-2 c) depicts another type of critical temperature that represents a lower limit and is called a lower critical solution (LCST). UCST will form if the binodal curve intersects the freezing curve, and LCST will form if the binodal curve intersects the VLE bubble point curve [39]. Another type, which is less frequently observed [40], is the presence of both LCST and UCST, where LLE is only possible between LCST and

UCST, as shown in figure 1.2-2 a). Seldom, a system can has no critical temperature as shown in figure 1.2-3. This type of behavior is only observed in high molecular weight polymers [41]. This phenomenon is referred to as hour-glass. The system will never have high complete miscibility (homogenous phase) over all the composition and temperature range [41]. Table 1.2-1 presents examples of binary LLE systems with different critical solution temperature behavior.

Table 1.2-1 Example of binary systems with different critical temperature behaviour

System	Classification	Reference
Carbon Disulphide (1)+ Acetic Acid anhydride (2)	UCST	[42]
Ethanenitrile (1)+ Cyclopentane (2)	UCST	[43]
B-U3000 (polymer) (1)+ 1-Butanol (2)	UCST	[44]
3-Buten-2-one (1)+ Water (2)	UCST and LCST	[45]
Glycerol (1)+ Amine Benzyl Ethyl (2)	UCST and LCST	[47]
Furan Tetrahydron (1)+ Water (2)	UCST and LCST	[48]
polystyrene (1)+ Tert-butyl acetate (2)	LCST	[49]
Polystyrene (1)+ poly(vinyl methyl ether) (2)	LCST	[50]
Water (1) + *n*-heptyl polyglycol ethers	LCST	[51]
t-butyl acetate (1)+ poly(ethylene glycol) (2)	No CST	[52]

The phase behavior of a ternary systems are defined based on their binary counterpart and their temperature. The most common type of phase behavior is shown in figure 1.2-4. Figure 1.2-4 (a), represents a ternary system where the two binary systems [1+2] and [2+3] exhibit UCST, and system [2+3] has higher UCST. It can be observed that if the ternary system is at a temperature higher than the critical temperature of both binary systems, then the ternary system will be homogenous in single phase as shown in the first ternary plot of figure 1.2-4 (b). Similarly, when mixed below the critical temperatures of the binary systems, the ternary will be heterogeneous and it will have no critical temperature. By increasing the temperature the heterogeneous region will shrink and indicate a unique critical temperature, as shown in figure 1.2-4 (b). The critical temperature for this system varies between the critical temperatures, in increasing

fashion, of subsystems [1+2] and [2+3] as shown in figure 1.2-4 (c). Other types of phase behaviors for ternary systems are well explained in literature and interested reader can refer to the following references [38, 40].

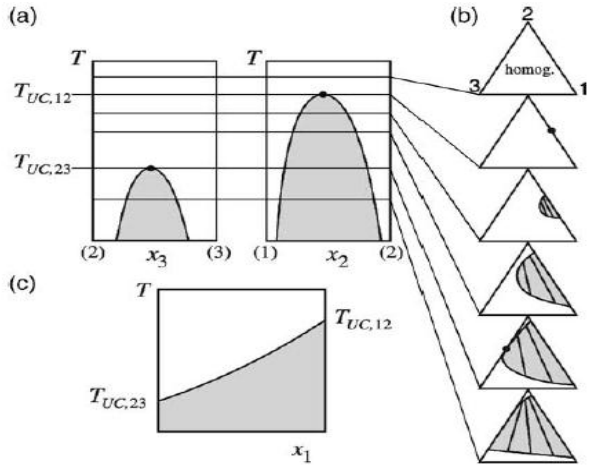

Figure 1.2-4 Liquid-Liquid ternary system: a) Two binary systems [1+2] & [2+3]showing both UCST. b) Mixing of two binary systems at different temperature. C) The critical temperature behaviour with composition [38]

1.2.2 Excess Gibbs Energy & NRTL Model

In thermodynamics, excess properties characterize non-ideality of real mixtures. It is defined as the difference of real thermodynamic properties from ideal solution properties [1]. It may be written as

$$M^E = M - M^{id} \tag{1.3}$$

where "*id*" refers to ideal solution and "*M*" is the real property of a mixture. The prevailing assumption in an ideal solution is that the interactions between all species in the mixture are identical. This implies that interactions between molecules of species "A" and "B" are identical to the interactions of species "A" molecules amongst themselves. This generally holds true for species of almost identical nature such as isomers. This, of course, is not true for real mixtures where the interaction between different species will always differ. The deviation from an ideal solution is further increased as the species become more dissimilar. Excess properties are a convenient way to study the deviation of

liquid mixtures from ideal solution [39]. Excess Gibbs energy is an important excess property. It is defined as [1]

$$\overline{G}^{E} = \sum RT \cdot \ln \gamma_i \qquad (1.4)$$

Where R is the universal gas constant, T is the temperature, and γ_i is the activity coefficient, which is specific to each species in the liquid mixture. The activity coefficient accounts for nonideal behavior that arises due to the difference of chemical species in a liquid mixture. The Gibbs free energy of a real mixture may be written as:

$$G_m = \underbrace{\sum x_i G_i^{pure} + RT \sum x_i \ln x_i}_{\text{Gibbs energy of Ideal Solution}} + \overbrace{\overline{G}^{E}}^{\text{Excess Gibbs}} \qquad (1.5)$$

Inclusion of the activity coefficient enables the full representation of a real mixture. Gm,i is the Gibbs energy of pure component. Looking at equation 1, it can be realized that the actual property is the summation of ideal solution and excess property. In equation 3, the first two terms correspond to ideal solution and GE is the excess property.

Non Random Two Liquid (NRTL) model is a Gibbs Excess (G^E) model, derived by Renon & Prausnitz in 1968 [41], and it is used to find the activity coefficient of liquids. Activity coefficient is a function of composition, temperature and pressure. Pressure, however has a weak effect and is not considered in the NRTL model. Therefore, it is only applicable for low to moderate pressure models. It belongs to local composition models where it is assumed that the local composition near to the molecules is different from the overall liquid mixtures [39], which results from differences in molecular size and interaction energies between them. NRTL equations of G^E and activity coefficient for multi-component are presented as follows:

$$\frac{G^E}{RT} = \sum_{i=1}^{N} x_i \frac{\sum_{j=1}^{N} x_j G_{ji} \tau_{ji}}{\sum_{j=1}^{N} x_j G_{ji}} \tag{1.6}$$

$$\tau_{ji} = \frac{g_{ji} - g_{jj}}{RT} \tag{1.7}$$

$$G_{ji} = e^{-\alpha_{ji}\tau_{ji}} \tag{1.8}$$

$$\ln \gamma_i = \frac{\sum_{j=1}^{N} x_j G_{ji} \tau_{ji}}{\sum_{j=1}^{N} x_j G_{ji}} + \sum_{j=1}^{N} \frac{x_j G_{ji}}{\sum_{k=1}^{N} x_k G_{kj}} \left(\tau_{ij} - \frac{\sum_{k=1}^{N} x_k G_{kj} \tau_{kj}}{\sum_{k=1}^{N} x_k G_{kj}} \right) \tag{1.9}$$

Where g_{ji} and g_{jj} are the energy interaction parameters and τ_{ji} and G_{ji} are simply dimensionless parameters related to g_{ji}. α_{ji} is a non-randomness parameter, and γ_j is the activity coefficient. The first Local composition model was established by Wilson in 1964 and it was called Wilson model [39]. However, Wilson model suffered from the inability to predict partial miscibility of liquid mixtures and it could not be applied to Liquid- Liquid Equilibrium (LLE) calculations [41]. New models came along such as NRTL & UNIQUAC that are capable of predicting partial miscibility and perform very well for LLE calculations [41]. The UNIQUAC model is more complex mathematically and it has the advantages of having two adjustable parameters instead of three, and smaller dependence on temperature [41]. The α_{ji} parameter in NRTL can be fixed without sacrificing the accuracy of the results, and this reduces the adjustable parameters to two. Typical values of α_{ji} range between 0.2 to 0.47 and the usual choice of alpha is either 0.2 or 0.3 [41]. NRTL is powerful in predicting the LLE in highly non-ideal liquid mixtures and performs as well as UNIQUAC models [40]. In addition, better results can be obtained by making the $g_{ji} - g_{jj}$ function of temperature.

1.2.3 Determining Phase Stability Limits

Experimental works are the most reliable means to find the stability limits. Various experimental procedures are developed to obtain the liquid-liquid equilibrium compositions, including the cloud point [63] and volumetric [64, 65] methods. The same methods can also measure critical point—with relative accuracy—depending on the method employed. The cloud point method is a common and simple method that can be used to find the critical point of liquid-liquid systems. The experimental composition is measured by utilizing a homogenous mixture and heating / cooling until visual inspection determines the mixture to be cloudy—indicating phase splitting. The experiment is usually repeated and the average is taken to minimize error [66]. Further improvement can be achieved by using a laser beam to detect the cloud point to eliminate errors caused by visual inspection. As for volumetric method, the compositions are measured indirectly by measuring the volume of the liquid equilibrium phases. Volumetric method is not suitable near the critical region if LLE data have a relatively flat slope near the critical point [65].

One of the well suited methods to experimentally determine stability limits is by the light scattering technique [2, 67- 68]. This technique was originally developed to experimentally measure the cloud points (binodal curve) with high accuracy. Nevertheless, it has proved to be a powerful tool to predict spinodal curve and critical temperature.

Debye [69, 70] derived the following equation to find the critical temperature:

$$I = \frac{T \cdot P(\varphi)}{\left[a(T - Tc) + b \cdot \sin^2\left(\frac{\varphi}{2}\right) \right]} \tag{1.10}$$

Where a and b are constants and $P(\varphi)$ is the particle scattering factor. The light intensity will diverge at the direction of (θ=0) when T=Tc.

Early works were restricted to study systems that are under atmospheric pressure and were only exposed to temperature pulses. Recent improvements allowed the study of systems at elevated pressures by enabling pressure and temperature pulses, this method is

referred to as Pulsed Induced Scattering (PICS) [70]. There are further more advanced light scattering techniques such as Pressure Pulsed Induced Scatter (PPICS) [71] and Small Angle Light Scattering (SALS) [72] that are currently used in researched literature.

Unfortunately, there are limited experimental data for measured critical points for LLE as they require experiments to be carried over a wide temperature range, which is often quite challenging. In effect, nearly 80% of reported experimental data have a temperature range of 0-35 °C [38] and as a result, most reported critical points are predicted theoretically.

There are many different routes towards theoretically calculating stability limits and critical loci for mixtures. In essence, all of these methods are different facets of the same rigorous thermodynamic criteria as depicted by Gibbs [1]. Nevertheless, the phase stability problem is usually approached either by minimization or solving highly coupled nonlinear equations (will be detailed later) based on Gibbs criteria.

The basis of minimization technique is that a stable system must have a minimum in Gibbs energy and thus:

$$d(\Delta G)_{P,T} = 0 \tag{1.11}$$

This criterion is considered as necessary but insufficient for stability. Most minimization techniques use only this criterion to attempt to find global minima. The most notable minimization technique based on this criterion is tangent plane analysis, which was first set up by Baker [6, 73-74]. This test will simply check if the system is capable of achieving a lower energy state if it were allowed to split. Tangent plane analysis finds the tangent plane distance D, expressed as

$$D(x) = g_m(x) - g_m(z) - \sum_{i=1}^{n}\left(\frac{\partial g_m}{\partial x_i}\right)(x_i - z_i) \tag{1.12}$$

Where g_m is the Gibbs function of mixture, x_i is the mole fraction, and z_i are the mole fractions of the feed. If D is found to be negative, at certain conditions, phase splitting will occur. The points at which D becomes negative can be found by solving the following equations

$$\left[\left(\frac{\partial g_m}{\partial x_i}\right)-\left(\frac{\partial g_m}{\partial x_n}\right)\right]-\left[\left(\frac{\partial g_m}{\partial x_i}\right)-\left(\frac{\partial g_m}{\partial x_n}\right)\right]_Z = 0 \tag{1.13}$$

$$\sum_{i=1}^{n} x_i = 1 \tag{1.14}$$

Michelsen [6, 75] was the first to develop computer algorithm to find stability limits based on tangent plane analysis (eqns 1.13 & 1.14). The strength of tangent plane analysis lies in its simplicity. It can be used with nonlinear LLE models such as NRTL and UNIQUAC to produce reasonable results and greatly reduce computing time. However, tangent plane analysis is strongly dependent on the accuracy of the initially specified guess. If the initially specified guess is inappropriate, it may diverge or lead to a trivial solution or find local minima. Several algorithms were developed to improve stability limits prediction namely differential geometry method [73, 76], homotopy-continuation method [73, 77], branch and bound optimization [78], and interval analysis method [79], but all these algorithms do not provide a theoretical guarantee for finding a global minima [79]. Thus, the reliability of the obtained results will always be questionable. On the other hand, reliable results are obtained by applying all the necessary and sufficient conditions of stability. This will guarantee reliable results and will drastically reduce the convergence problems. However, application of all stability criteria on LLE models such as NRTL and UNIQUAC, which are already nonlinear in nature, will result in highly nonlinear equations and may prove to be unfeasible for multi-component system.

1.3 Methodology

The method adopted here is entirely based on the rigorous approach presented by Tester and Modell [1]. The relevant equations from NRTL will be developed in this section. As the NRTL model does not account for pressure, this model will only be applicable at low to moderate pressures, where pressure has little effect on liquids at this range.
The criteria of stability of thermodynamic systems is best explored using the energy representation, i.e., $U^t = f\left(S^t, V^t, N_1, N_2, .., N_n\right)$ because then other Legendre transforms

such as H^t, G^t, and A^t can easily be employed to develop more convenient criteria of stability. In terms of U^t, the starting point for stability criteria development is the requirement that the second order variations in U^t, which is a second order quadratic, be greater than zero, i.e.,:

$$\delta^2 U^t = K\sum_{i=1}^{n+2}\sum_{j=1}^{n+2}\frac{\delta^2 U^t}{\delta x_i x_j}\delta x_i \delta x_j \succ 0 \tag{1.15}$$

In this expression x stands for the independent variables S^t, V^t, N_1,..,N_n. It can be shown that the expression above is equivalent to [2]:

$$y^{(m-2)}_{(m-1)(m-1)} = 0 \tag{1.16}$$

Here, $m = n+2$ and $y^{(m-2)}$ represents the order of the Legendre transform (Refer to Appendix I for discussion of Legendre Transforms), and subscript (m-1) represents independent variable derivative. For Example, A_{SV} is the second derivative of Helmholtz with respect to entropy and volume. Actually, equation (1.16) is a general criteria for stability that provides necessary and sufficient conditions for stability, where

If, $y^{(m-2)}_{(m-1)(m-1)} > 0$ system is stable

Or if, $y^{(m-2)}_{(m-1)(m-1)} = 0$ system is on the limit of stability

Or if, $y^{(m-2)}_{(m-1)(m-1)} < 0$ system is unstable

A critical point lies on the limit of stability and it is stable. This can be clearly observed graphically where the spinodal and binodal curves converge to a common point of tangency. Consequently, any system at its critical point shall obey both the limit of stability and the critical point criterion. The necessary and sufficient conditions for critical conditions are therefore[1]:

$$y^{(m-2)}_{(m-1)(m-1)} = 0 \tag{1.17}$$

$$y^{(m-2)}_{(m-1)(m-1)(m-1)} = 0 \tag{1.18}$$

Since the critical point is a stable state, then it will also satisfy the following

$$y^{(m-2)}_{(m-1)(m-1)(m-1)(m-1)} > 0 \tag{1.19}$$

If equation (1.19) equals zero, then the lowest even-order, non-vanishing derivative of $y^{(m-2)}$ must be positive. For example, for a binary system, where m= 4, the following should be applicable

$$y^2_{33} = 0 \qquad \text{(Spinodal curve)} \tag{1.20}$$

$$y^2_{333} = 0 \qquad \text{(Critical point)} \tag{1.21}$$

$$y^2_{3333} \geq 0\,, \qquad \text{or if =0, then} \tag{1.23}$$

$$y^2_{33333} \geq 0 \tag{1.24}$$

If equation (1.24) equals zero, then the next derivative should be checked until the equation gets satisfied.

1.3.1 Binary Systems

First, expanding equations (1.6 & 1.9) to obtain NRTL model for binary component:

$$\frac{G^E}{RT} = x_1 x_2 \left(\frac{G_{21}\tau_{21}}{x_1 + x_2 G_{21}} \right) + x_1 x_2 \left(\frac{G_{12}\tau_{12}}{x_2 + x_1 G_{12}} \right) \tag{1.25}$$

$$\ln \gamma_1 = x_2^{\,2} \left[\tau_{21} \left(\frac{G_{21}}{x_1 + x_2 G_{21}} \right)^2 + \frac{G_{12}\tau_{12}}{\left(x_2 + x_1 G_{12}\right)^2} \right] \tag{1.26}$$

$$\ln \gamma_2 = x_1^{\,2} \left[\tau_{12} \left(\frac{G_{12}}{x_2 + x_1 G_{12}} \right)^2 + \frac{G_{21}\tau_{21}}{\left(x_1 + x_2 G_{21}\right)^2} \right] \tag{1.27}$$

Staring with U as the basis function applied for binary system that contains species A and B,

$$\overline{U} = f(S, V, N_1, N_2) \tag{1.28}$$

Over bar refers to extensive properties. Therefore, $\overline{U}$ refers to Total internal energy of the system and U refers to internal energy per unit mass or mole. Applying Equation (1.16) and using Legendre transforms (Refer to Appendix I for discussion of Legendre Transforms) to obtain an expression to find the spinodal curve:

$$y_{33}^2 = \left(\frac{\partial^2 \overline{G}}{\partial N_1^2}\right)_{T,P,N_2} = 0 \tag{1.29}$$

Note that $y^{(2)}$ is the second Legendre transform of $U^t = f\left(S^t, V^t, N_1, N_2, .., N_n\right)$ i.e., $y^{(2)} = G^t = G^t(T, P, N_1, N_2, , \ldots, N_n)$. For binary mixtures (n = 2).

Using the chemical potential definition $\mu_1 = \left(\frac{\partial \overline{G}}{\partial N_1}\right)_{T,P,N_2}$ which can be written as

$$\mu_1 = G_{pure} + RT\ln(x_1\gamma_1) \tag{1.30}$$

The expression can be further simplified into,

$$\left(\frac{\partial^2 \overline{G}}{\partial N_1^2}\right)_{T,P,N_2} = \left(\frac{\partial \mu_1}{\partial N_1}\right)_{T,P,N_2} = 0 \qquad \Rightarrow \left(\frac{\partial \mu_1}{\partial x_1}\right)_{T,P} = 0 \tag{1.31}$$

Next, substituting the expression of activity coefficient obtained from NRTL model in equation (1.30) and applying equation (1.31), the final expression becomes

$$\left(\frac{\partial \mu_1}{\partial x_1}\right)_{T,P} = -2x_2\left[\tau_{21}\left(\frac{G_{21}}{x_1 + x_2 G_{21}}\right)^2 + \frac{G_{12}\tau_{12}}{\left(x_1 G_{12} + x_2\right)^2}\right] - 2x_2{}^2\left[\frac{\tau_{21}G_{21}{}^2\left(1 - G_{21}\right)}{\left(x_1 + x_2 G_{21}\right)^3} + \frac{G_{12}\tau_{12}\left(G_{12} - 1\right)}{\left(x_1 G_{12} + x_2\right)^3}\right] + \frac{1}{x_1} \tag{1.32}$$

In view of the phase rule, a non-reactive binary system in a single phase at the stability limit has two degrees of freedom as shown below [39]:

$$F = 2 + N - \pi - r - s = 2 + 2 - 1 - 0 - 1 = 2 \tag{1.33}$$

Where F stands for the number of degrees of freedom, n is the number of species, π is the number of phases, r is the number of independent chemical reactions, and s stands for any external special constraint that is not accounted for in phase and chemical reaction equilibria. In this case there is one special constraint, i.e., s = 1, which is the above stability criterion. Therefore, for a binary system at a fixed pressure and x_1, the spinodal

limit criterion (equation 1.33 above) can be solved for the temperature at the stability limit.

Equation (1.33) is a function of temperature and mole fraction of species 1. Even though, temperature is not explicitly expressed above but G_{ij} and τ_{ij} are functions of temperature. The mole fraction of species 1 is varied and the corresponding temperatures are found that satisfy equation (1.32). These temperatures and mole fraction of species 1 define the spinodal curve. Matlab® is used to solve this equation and the code can be found in appendix III.

Now, the critical point can be found by applying the criteria for stable equilibrium presented in equation (1.18). Applying it for a binary system we obtain:

$$y_{333}^{2} = \left(\frac{\partial^3 \overline{G}}{\partial N_1^3} \right)_{T,P,N_2} = 0 \tag{1.34}$$

Using the definition for chemical potential and using mole fractions instead of moles, equation (1.34) can be simplified to

$$\left(\frac{\partial^3 \mu_1}{\partial N_1^3} \right)_{T,P,N_2} \equiv \left(\frac{\partial^2 \mu_1}{\partial N_1^2} \right)_{T,P,N_2} \equiv 0 \qquad \Rightarrow \left(\frac{\partial^2 \mu_1}{\partial x_1^2} \right)_{T,P} = 0 \tag{1.35}$$

Similarly, using the definition of chemical potential with the NRTL model to obtain an equation for the critical point determination, as shown below:

$$\left(\frac{\partial^2 \mu_1}{\partial x_1^{\,2}} \right)_{T,P} = 2\left[\tau_{21}\left(\frac{G_{21}}{x_1 + x_2 G_{21}} \right)^2 + \frac{G_{12}\tau_{12}}{\left(x_1 G_{12} + x_2\right)^2} \right] + 8x_2 \left[\frac{\tau_{21} G_{21}^{\,2}\left(1 - G_{21}\right)}{\left(x_1 + x_2 G_{21}\right)^3} + \frac{G_{12}\tau_{12}\left(G_{12} - 1\right)}{\left(x_1 G_{12} + x_2\right)^3} \right]$$
$$+ 6x_2^{\,2} \left[\frac{\tau_{21} G_{21}^{\,2}\left(1 - G_{21}\right)^2}{\left(x_1 + x_2 G_{21}\right)^4} + \frac{G_{12}\tau_{12}\left(G_{12} - 1\right)^2}{\left(x_1 G_{12} + x_2\right)^4} \right] - \frac{1}{x_1^{\,2}} \tag{1.36}$$

There are two special constraints corresponding to the critical point of a mixture. The phase rule in this case gives for a non-reactive, binary mixture a single degree of freedom. For a binary mixture at a given pressure, stability limit criterion (equation 1.32) and the criticality criterion (equation 1.36) must be solved simultaneously for the temperature (T) and the mole fraction (x_1). The Matlab® code can be found in appendix III.

1.3.2 Ternary Systems

The G^E function and activity coefficients for ternary components obtained by expanding equations (1.6 & 1.9) and the following expressions are obtained:

$$\frac{G^E}{RT} = x_1\left(\frac{x_2G_{21}\tau_{21} + x_3G_{31}\tau_{31}}{x_1 + x_2G_{21} + x_3G_{31}}\right) + x_2\left(\frac{x_1G_{12}\tau_{12} + x_3G_{32}\tau_{32}}{x_1G_{12} + x_2 + x_3G_{32}}\right) + x_3\left(\frac{x_1G_{13}\tau_{13} + x_2G_{23}\tau_{23}}{x_1G_{13} + x_2G_{23} + x_3}\right)$$

(1.37)

$$\ln\gamma_1 = \frac{x_2G_{21}\tau_{21} + x_3G_{31}\tau_{31}}{x_1 + x_2G_{21} + x_3G_{31}} - \frac{x_1}{x_1 + x_2G_{21} + x_3G_{31}}\cdot\left(\frac{x_2G_{21}\tau_{21} + x_3G_{31}\tau_{31}}{x_1 + x_2G_{21} + x_3G_{31}}\right)$$
$$+ \frac{x_2G_{12}}{x_1G_{12} + x_2 + +x_3G_{32}}\cdot\left(\tau_{12} - \frac{x_1G_{12}\tau_{12} + x_3G_{32}\tau_{32}}{x_1G_{12} + x_2 + +x_3G_{32}}\right) + \frac{x_3G_{13}}{x_1G_{13} + x_2G_{23} + x_3}\cdot\left(\tau_{13} - \frac{x_1G_{13}\tau_{13} + x_2G_{23}\tau_{23}}{x_1G_{13} + x_2G_{23} + x_3}\right)$$

(1.38)

$$\ln\gamma_2 = \frac{x_1G_{12}\tau_{12} + x_3G_{32}\tau_{32}}{x_1G_{12} + x_2 + x_3G_{32}} + \frac{x_1G_{21}}{x_1 + x_2G_{21} + x_3G_{31}}\cdot\left(\tau_{21} - \frac{x_2G_{21}\tau_{21} + x_3G_{31}\tau_{31}}{x_1 + x_2G_{21} + x_3G_{31}}\right)$$
$$- \frac{x_2}{x_1G_{12} + x_2 + +x_3G_{32}}\cdot\left(\frac{x_1G_{12}\tau_{12} + x_3G_{32}\tau_{32}}{x_1G_{12} + x_2 + +x_3G_{32}}\right) + \frac{x_3G_{13}}{x_1G_{13} + x_2G_{23} + x_3}\cdot\left(\tau_{23} - \frac{x_1G_{13}\tau_{13} + x_2G_{23}\tau_{23}}{x_1G_{13} + x_2G_{23} + x_3}\right)$$

(1.39)

$$\ln\gamma_3 = \frac{x_1G_{13}\tau_{13} + x_2G_{23}\tau_{23}}{x_1G_{13} + x_2G_{23} + x_3} + \frac{x_1G_{31}}{x_1 + x_2G_{21} + x_3G_{31}}\cdot\left(\tau_{31} - \frac{x_2G_{21}\tau_{21} + x_3G_{31}\tau_{31}}{x_1 + x_2G_{21} + x_3G_{31}}\right)$$
$$+ \frac{x_2G_{32}}{x_1G_{12} + x_2 + +x_3G_{32}}\cdot\left(\tau_{32} - \frac{x_1G_{12}\tau_{12} + x_3G_{32}\tau_{32}}{x_1G_{12} + x_2 + +x_3G_{32}}\right) - \frac{x_3}{x_1G_{13} + x_2G_{23} + x_3}\cdot\left(\frac{x_1G_{13}\tau_{13} + x_2G_{23}\tau_{23}}{x_1G_{13} + x_2G_{23} + x_3}\right)$$

(1.40)

U is chosen again to be the basis function for ternary system analysis. Where U for ternary system is a function of the following:

$$\overline{U} = f(S, V, N_1, N_2, N_3) \tag{1.41}$$

With the use of equation (1.16), it follows that for a ternary system to be at the limits of stability, it shall obey the following criteria:

$$y_{44}^{(3)} \equiv \left(\frac{\partial^2 G'}{\partial N_2^2} \right)_{T,P,\mu_1,N_3} = 0 \qquad (1.42)$$

Equation (1.39) is difficult to deal with, since the derivation has to be carried out at constant μ_1 which is difficult to do analytically. This can be overcome by transforming in terms of lower order Legendre transform as shown by Tester [1] and the following expression is obtained:

$$\Im_2 = \begin{bmatrix} \left(\frac{\partial^2 \overline{G}^M}{\partial x_1^2} \right)_{T,P,x_2} & \left(\frac{\partial^2 \overline{G}^M}{\partial x_2^2} \right) \\ \left(\frac{\partial^2 \overline{G}^M}{\partial x_2^2} \right) & \left(\frac{\partial^2 \overline{G}^M}{\partial x_2^2} \right)_{T,P,x_1} \end{bmatrix} = 0 \qquad (1.43)$$

$$\left| \Im_2 \right| = \left(\frac{\partial^2 \overline{G}^M}{\partial x_1^2} \right)_{T,P,x_2} \left(\frac{\partial^2 \overline{G}^M}{\partial x_2^2} \right)_{T,P,x_1} - \left[\left(\frac{\partial^2 \overline{G}^M}{\partial x_2^2} \right)_{T,P,x_1} \right]^2 = 0 \qquad (1.44)$$

Where

$$\overline{G}^M = \sum x_i G_{m,i} + RT \sum x_i \ln x_i + G^E \qquad (1.45)$$

$G_{m,i}$ is the molar Gibbs energy of the pure component at the pressure and temperature of the system. The differentials terms in equations (1.43 & 1.44) are attached in Appendix II. Next, these differentials can be substituted into equation (1.44) to reach a useful form, which can be used to solve for the spinodal curve. Equation (1.44) is a function of four variables; temperature, pressure and composition (two variables). Applying the phase rule, for a non-reactive ternary system in a single phase at the stability limit has three degrees of freedom as shown below [39]:

$$F = 2 + N - \pi - r - s = 2 + 3 - 1 - 0 - 1 = 3 \qquad (1.46)$$

Usually, liquid-liquid equilibrium data are reported at constant temperature and pressure; this sets two variables. Therefore, equation (1.44) can be solved by varying the value of x_1 and finding the corresponding values of x_2. The Matlab® used to solve this equation is attached in appendix III.

Next, equation (1.18) is applied to find the critical point of a ternary system:

$$y_{444}^{(3)} \equiv \left(\frac{\partial^3 G'}{\partial N_2^3} \right)_{T,P,\mu_1,N_3} = 0 \tag{1.47}$$

As noted earlier, any system at the critical point shall satisfy two criteria: the limit of stability criteria (1.16), and the critical point criteria shown in equation (1.18). Therefore, equations (1.44) & (1.47) are solved simultaneously to find the critical points. As performed earlier for limit of stability, equation (1.47) is transformed in terms of lower order Legendre transforms to get a more useful expression. This results to:

$$\mathrm{M}_2 \equiv \begin{bmatrix} \left(\frac{\partial^2 \overline{G}^M}{\partial x_1^2} \right)_{T,P,x_2} & \left(\frac{\partial^3 \overline{G}^M}{\partial x_1 \partial x_2} \right)_{T,P,x_1} \\ \frac{\partial \zeta_2}{\partial N_1} & \frac{\partial \zeta_2}{\partial N_2} \end{bmatrix} = 0 \tag{1.48}$$

Where

$$\frac{\partial \zeta_2}{\partial N_1} = \left(\frac{\partial^2 \overline{G}^M}{\partial x_1^2} \right)_{T,P,x_2} \left(\frac{\partial^3 \overline{G}^M}{\partial x_2^2 \cdot \partial x_1} \right)_{T,P,x_2} + \left(\frac{\partial^3 \overline{G}^M}{\partial x_1^3} \right)_{T,P,x_2} \left(\frac{\partial^2 \overline{G}^M}{\partial x_2^2} \right)_{T,P,x_1} - 2 \cdot \left(\frac{\partial^2 \overline{G}^M}{\partial x_2 \cdot \partial x_1} \right)_{T,P,x_1} \left(\frac{\partial^3 \overline{G}^M}{\partial x_1^2 \cdot \partial x_2} \right)_{T,P,x_1} \tag{1.49}$$

And

$$\frac{\partial \zeta_2}{\partial N_2} = \left(\frac{\partial^2 \overline{G}^M}{\partial x_1^2} \right)_{T,P,x_2} \left(\frac{\partial^3 \overline{G}^M}{\partial x_2^3} \right)_{T,P,x_1} + \left(\frac{\partial^3 \overline{G}^M}{\partial x_1^2 \partial x_2} \right)_{T,P,x_1} \left(\frac{\partial^2 \overline{G}^M}{\partial x_2^2} \right)_{T,P,x_1} - 2 \cdot \left(\frac{\partial^2 \overline{G}^M}{\partial x_2 \cdot \partial x_1} \right)_{T,P,x_1} \left(\frac{\partial^3 \overline{G}^M}{\partial x_2^2 \cdot \partial x_1} \right)_{T,P,x_2} \tag{1.50}$$

The differential terms are derived and presented in Appendix II. Now, the partial differentials are substituted in equations (1.49) and (1.50), to find the determinant of this matrix and finally arrive to,

$$\begin{aligned} |M_2| = & \left[\left(\frac{\partial^2 \overline{G}^M}{\partial x_2^2} \right)_{T,P,x_1}^2 \right] \left(\frac{\partial^3 \overline{G}^M}{\partial x_1^3} \right)_{T,P,x_2} + 3 \left[\left(\frac{\partial^2 \overline{G}^M}{\partial x_1 \partial x_2} \right)_{T,P}^2 \right] \left(\frac{\partial^3 \overline{G}^M}{\partial x_2^2 \partial x_1} \right)_{T,P} \\ & - 3 \left(\frac{\partial^3 \overline{G}^M}{\partial x_1^2 \partial x_2} \right)_{T,P} \left(\frac{\partial^2 \overline{G}^M}{\partial x_2^2} \right)_{T,P,x_1} \left(\frac{\partial^2 \overline{G}^M}{\partial x_1 \partial x_2} \right)_{T,P} - \left(\frac{\partial^3 \overline{G}^M}{\partial x_2^3} \right)_{T,P,x_1} \left(\frac{\partial^2 \overline{G}^M}{\partial x_1^2} \right)_{T,P,x_2}^2 \left(\frac{\partial^2 \overline{G}^M}{\partial x_1 \partial x_2} \right)_{T,P}^2 = 0 \end{aligned} \tag{1.51}$$

As shown by the phase rule, a non-reactive ternary system has two degree of freedom. Therefore, solving equations (1.51) & (1.44) simultaneously is sufficient to find the critical compositions for ternary system at constant temperature and pressure. The Matlab® program used to solve for ternary critical conditions is given in appendix III.

1.3.3 Critical Universality

It is well-known that the liquid–gas critical point is associated with a number of important properties; certain thermodynamic properties diverge as the critical temperature T_c or density ρ_c is approached with the divergence obeying a power-law form in $|T - T_c|$ or $|\rho - \rho_c|$, whereas other thermodynamic properties show a non-divergent power-law. The exponents that go with these power laws are called critical exponents. A striking observation associated with these critical exponents is the fact that for large classes of systems, known as universality classes, the same critical exponents were found. For example, the difference in densities of the coexisting liquid and vapour phases ($\rho_L - \rho_G$) for a vapour-liquid system and the magnetization (M) of a magnetic system, were found to follow the same power law in $\varepsilon = (T-T_c)/T_c$, i.e., :

$$\rho_L - \rho_G = |\varepsilon|^{\beta} \tag{1.52}$$

$$M = |\varepsilon|^{\beta} \tag{1.53}$$

With a common value of $\beta = 0.326 \pm 0.002$ [80-83]. In general, critical universality principle implies that the behaviour of "order parameters", such as ($\rho_L - \rho_G$), follow a simple power law as a certain "field variable", such as ($T-T_c$), approaches the critical value. table 1.3-1, borrowed from [80], summarizes the corresponding order parameters for three kinds of phase transformation, together with some recent best estimates of the most popular "primary" critical exponents (α, β, γ, ν).

Table 1.3-1 Current Values of Some Common Critical Exponents [80]

Exponent	Value	Vapor–Liquid	Liquid–Liquid	Magnetic
α	-0.110 ± 0.003	$C_V \sim \epsilon^{\alpha}$	$C_{p,x} \sim \epsilon^{\alpha}$	$C_H \sim \epsilon^{\alpha}$
β	0.326 ± 0.002	$\rho_L - \rho_G \sim (-\epsilon)^{\beta}$	$x_1' - x_1'' \sim (-\epsilon)^{\beta}$	$M \sim (-\epsilon)^{\beta}$
γ	-1.239 ± 0.002	$\chi \sim \epsilon^{\gamma}$	$\chi \sim \epsilon^{\gamma}$	$\chi \sim \epsilon^{\gamma}$
ν	-0.630 ± 0.001	$\xi \sim \epsilon^{\nu}$	$\xi \sim \epsilon^{\nu}$	$\xi \sim \epsilon^{\nu}$

This phenomenon of universality indicates that near a critical point, short-range interactions between specific pairs or clusters of particles become of lower significance than long-range interactions, which are typically robust towards the details of an interaction potential. Thus, it is possible to obtain information about all of the systems in a universality class by studying its physically simplest members, a thing reminiscent of the corresponding state principle (CSP). However, universality is more far reaching a concept than the CSP [80].

As indicated in table 1.3-1, two order parameters of relevance to the liquid-liquid systems are ($x_1' - x_1''$), the difference in mole fraction of species 1 in the two coexisting phases, and susceptibility (χ), which is related to the chemical potential of species (1) according to:

$$\chi = \frac{x_2}{\left(\partial \mu_1 \big/ \partial x_1\right)_{T,P}} \tag{1.54}$$

Therefore, critical universality implies that:

$$x_1^{'} - x_1^{''} = \varepsilon^{\gamma} \tag{1.55}$$

and

$$\chi = \varepsilon^{\gamma} \tag{1.56}$$

Experimental values of χ are easily calculated from the reported experimental data and the optimized NRTL model, taking $\left(\partial \mu_1 \big/ \partial x_1\right)_{T,P}$ from equation (1.32), the final form of χ is as follow:

$$\chi = \frac{-x_2}{2x_2\left[\tau_{21}\left(\frac{G_{21}}{x_1 + x_2 G_{21}}\right)^2 + \frac{G_{12}\tau_{12}}{\left(x_1 G_{12} + x_2\right)^2}\right] + 2{x_2}^2\left[\frac{\tau_{21}{G_{21}}^2\left(1 - G_{21}\right)}{\left(x_1 + x_2 G_{21}\right)^3} + \frac{G_{12}\tau_{12}\left(G_{12} - 1\right)}{\left(x_1 G_{12} + x_2\right)^3}\right] - \frac{1}{x_1}} \cdot \frac{1}{RT} \tag{1.57}$$

The approach of universal criticality shown above can only applied for the binary systems of this thesis. As for ternary system, all data points are taken at constant temperature, thus, the same approached cannot be followed for ternary systems.

1.3.4 NRTL Regression & Experimental Data

The first step in initiating the needed calculations is optimizing the NRTL model to have a good fit of experimental data, so that the experimental data are replaced by the model. To accomplish this objective, liquid-liquid equilibrium (LLE) experimental data, which must be of good quality are needed . Normally, NRTL binary interaction parameters (refer to eqn 1.7) are given along with the reported LLE experimental data. If NRTL binary parameters are not available, LLE data is regressed to fit NRTL model using Aspen Plus® by applying maximum likelihood objective function [87], defined as

$$OF = \sum_{k=1}^{N} \left\{ \left(\frac{T_k^{calc} - T_k^{\exp}}{\sigma_{Tk}} \right)^2 + \sum_{i=1}^{N-1} \sum_{j=1}^{N-1} \left(\frac{x_{ij}^{calc} - x_{ij}^{\exp}}{\sigma_{xijk}} \right)^2 \right\} \tag{1.58}$$

N refers to the number of experimental data points; the superscript "*calc"* and "*exp"* correspond to the calculated and experimental values, respectively. σ is the standard deviation in k group.

The objective functions above find the optimized temperature dependent binary interaction parameters of NRTL model in the form

$$\tau_{ij} = a_{ij} + \frac{b_{ij}}{T} + c_{ij} \ln T + d_{ij} \cdot T \tag{1.59}$$

The results of the regression are a_{ij}, b_{ij}, and d_{ij}. The regressed constants must minimize the percent of absolute average deviation (AAD%), defined

$$AAD\% = \frac{1}{N} \sum_{i=1}^{N} \left| \frac{x_1^{calc} - x_1^{\exp}}{x_1^{\exp}} \right| \times 100 \tag{1.60}$$

In any case, to ensure meaningful and accurate results the following consideration were taken in selecting experimental data:

- In order to try draw meaningful conclusions on the behavior of stability limits and critical temperatures, systems studied must belong to the same homologues group (e.g., alkanols, ethers, aqueous, etc)
- Experimental data must be taken from reliable sources. In this thesis, all experimental data are acquired from reliable resources such as DECHEMA and widely accepted journals such as phase equilibria and chemical engineering journals
- Though there is no established consistency test for LLE experimental work, it is acceptable, to a reasonable extent, to rely on intuition to evaluate the quality of experimental data.
- Enough experimental data points must be available to produce good regression of NRTL and subsequently accurate calculation of stability limits. Therefore, any system must have at least 10 experimental data and preferentially those points are close to the critical temperature.
- The regressed NRTL parameters must produce maximum AAD% of 10 compared to experimental data.

1.3.5 Solution Approach

The objective of this thesis is to derive a model to predict the spinodal curves and critical temperatures for binary and ternary liquid systems. Once the stability criteria are applied and the necessary mathematical derivations are obtained, the next step becomes implementing a robust numerical approach to solve for the unknowns using the derived (highly nonlinear) mathematical model. The procedure taken towards the final solution (the algorithm) consist of the following solution steps

1. Data regression for experimental data using the NRTL model to determine the model parameters (in case they are not available). The regression results should preferentially have ADD% less than 5%.
2. Solving for the binodal curve:
    a. Binary system: experimental data are usually reported as mole fractions for the two phases at certain temperature and constant pressure. The system has two degrees of freedom. However, since LLE are measured at constant pressure, only one degree of freedom remains. Therefore, experimental temperatures were used in the calculation of the binodal curve to satisfy the phase rule. The binodal curve for binary system were calculated by solving the following equations (equilibrium criteria) simultaneously to find mole fractions of species 1 and 2 in both phases:

$$x_1^{\alpha}\gamma_1^{\alpha} = x_1^{\beta}\gamma_1^{\beta} \quad (1.61)$$

$$x_2^{\alpha}\gamma_2^{\alpha} = x_2^{\beta}\gamma_2^{\beta} \quad (1.62)$$

    b. Ternary system: experimental data points for ternary system are reported as the mole fractions of all species in both phases. The experiment is taken at constant temperature and pressure, which reduces the degrees of freedom to one. Using one of the species mole fraction is enough to construct the binodal curve. For ternary system, the following equations must be solved simultaneously to find the binodal curve:

$$x_1^{\alpha}\gamma_1^{\alpha} = x_1^{\beta}\gamma_1^{\beta} \quad (1.63)$$

$$x_2^{\alpha}\gamma_2^{\alpha} = x_2^{\beta}\gamma_2^{\beta} \quad (1.64)$$

$$x_3^{\alpha}\gamma_3^{\alpha} = x_3^{\beta}\gamma_3^{\beta} \quad (1.65)$$

$$x_1^{\alpha} + x_2^{\alpha} + x_3^{\alpha} = 1 \quad (1.66)$$

$$x_1^{\beta} + x_2^{\beta} + x_3^{\beta} = 1 \quad (1.67)$$

3. Finding the critical temperature: solving equations (1.32 & 1.36) for binary system and equations (1.44 & 1.51) for ternary system. The critical point must graphically lie on the highest point of the binodal curve.
4. Spinodal curve can be constructed using equation (1.32) and equation (1.44) for binary and ternary systems, respectively. The spinodal curve should join the binodal curve only at the critical temperature.

Chapter 2
Results & Discussion

2.1 Binary systems

The stability limits were determined for 53 binary systems based on the methodology outlined in the previous chapter. All binary systems are segregated into 6 groups, each binary system within a group shares same solvent with all other group members. There are at least 3 binary systems in a group and the largest group has 17 binary systems. The group solvents vary from being organic solvents, inorganic solvents, and ionic solvents.

2.1.1 Acetonitrile + Hydrocarbons

Table 2.1-1 shows the different binary systems studied for Acetonitrile + Hydrocarbons, together with the references citing their available experimental range data in the literature. The binary systems are taken from two references. For acetonitrile + alkanes (C8-C16), the interaction parameters required by the NRTL model for the optimum fit of the binodal equilibrium data of each binary system were reported in the literature [88]. While acetonitrile + branched hydrocarbons were regressed in this thesis. Binary interaction parameters and the percent Absolute Average Deviations (AAD %) of the regression are reported in tables 2.1-2 and 2.1-3, respectively.

Table 2.1-1 Range of temperature and composition for Acetonitrile (1) + Hydrocarbons (2)

System (Acetonitrile+ alkanes)	Temperature range (K)	Composition range
Octane [88]	347.54-364.83	0.287-0.908
Nonane [88]	339.71-373	0.354-0.948
Decane [88]	351.77-380.53	0.251-0.951
Undecane [88]	372.7-377.69	0.551-0.859
Dodecane [88]	368.13-394.27	0.559-0.895
Tridecane [88]	374.09-400.96	0.534-0.917
Tetradecane [88]	400.89-405.41	0.726-0.814

System (Acetonitrile+ alkanes)	Temperature range (K)	Composition range
Pentadecane [88]	400.72-411.12	0.6108-0.9481
Cyclopentane [89]	319.08-331.76	0.286-0.797
Cyclohexane [89]	333.03-348.68	0.228-0.827
Cyclooctane [89]	355.2-371.79	0.281-0.866
Methylcyclopentane [89]	330.97-341.43	0.219-0.814
Methylcyclohexane [89]	342.8-352.45	0.267-0.817
2,2 Dimethylbutane [89]	337.18-341.98	0.325-0.771
2,3 Dimethylbutane [89]	335.29-343.22	0.301-0.799
2-Methylpentane [89]	337.26-346.35	0.259-0.709
3-Methylpentane [89]	333.7-345.9	0.217-0.715

The regression of acetonitrile + branched hydrocarbons experimental data was performed to find NRTL binary interaction parameters. Aspen Plus ® V 7.3 was used for this purpose by employing the maximum likelihood objective function to find the optimum binary interaction parameter capable of fitting the experimental data. The temperature dependent binary interaction model used for these binary systems is shown below:

$$\tau_{ij} = a_{ij} + \frac{b_{ij}}{T} + c_{ij}\ln T + d_{ij}\cdot T \qquad (2.2)$$

Where aij, bij, and dij are constants tabulated for each binary system in table 2.1-2.

Table 2.1-2 Binary interaction parameters for Acetonitrile (1) + Branched hydrocarbons (2)

	ij=12	ij=21
Acetonitrile(1) + Cyclopentane(2)		
Aij (J/ mol)	7.45179601	16.1042842
Bij (J/ mol)	-8332.81	-10000
Cij (J/ mol)	11	11
Dij (J/ mol)	-10000	-0.146
αij	0.3	
Acetonitrile(1) + Cyclohexane(2)		
Aij (J/ mol)	-2.971	-8.717

	ij=12	ij=21
Bij (J/ mol)	1510.299	3464.093
αij	0.3	
Acetonitrile(1) + Cyclooctane(2)		
Aij (J/ mol)	64.212	63.145
Bij (J/ mol)	-24568.595	-30000
Cij (J/ mol)	16.054	21.695
Dij (J/ mol)	-0.246	-0.297
αij	0.2	
Acetonitrile(1) + Methylcyclopentane(2)		
Aij (J/ mol)	-5.962	-4.012
Bij (J/ mol)	2454.262	1733.362
αij	0.2	
Acetonitrile(1) + Methylcyclohexane(2)		
Aij (J/ mol)	56.671	-38.905
Bij (J/ mol)	-5377.019	4155.335
Cij (J/ mol)	11	5.511
Dij (J/ mol)	-0.261	-0.009
αij	0.3	
Acetonitrile(1) + 2,2 Dimethylbutane(2)		
Aij (J/ mol)	-1.196	-13.888
Bij (J/ mol)	950.942	5087.616
αij	0.3	
Acetonitrile(1) + 2,3Dimethylbutane(2)		
Aij (J/ mol)	47.206	21.963
Bij (J/ mol)	-2963.185	3686.489
Cij (J/ mol)	-6.341	-5.472
αij	0.2	
Acetonitrile(1) + 2-Methylpentane (2)		
Aij (J/ mol)	-11.730	7.951
Bij (J/ mol)	-10000	-10000
Cij (J/ mol)	14.064	13.393
Dij (J/ mol)	-0.116	-0.163

	ij=12	ij=21
αij	0.2	
Acetonitrile(1) + 3-Methylpentane (2)		
Aij (J/ mol)	-5.188	-7.629
Bij (J/ mol)	2324.297	3004.302
αij	0.3	

Figures 2.1-1 to 2.1-17 show graphical results of the regression for acetonitrile + branched hydrocarbons and the percent absolute average deviation is tabulated in table 2.1-3. It can be concluded from the figures and AAD% that the regression was performed successfully and the experimental data are well reproduced over the experimental temperature range.

Table 2.1-3:The percent absolute average deviations (AAD%) of NRTL model for acetonitrile (1) + branched hydrocarbons (2) binary systems

System (Acetonitrile+ alkanes)	**Acetonitrile phase**	**Branched hydrocarbons phase**
Cyclopentane	3.98	1.46
Cyclohexane	5.50	2.10
Cyclooctane	1.95	0.78
Methylcyclopentane	3.50	1.72
Methylcyclohexane	6.99	2.21
2,2 Dimethylbutane	3.22	1.53
2,3 Dimethylbutane	1.83	1.70
2-Methylpentane	2.71	2.06
3-Methylpentane	4.61	1.31

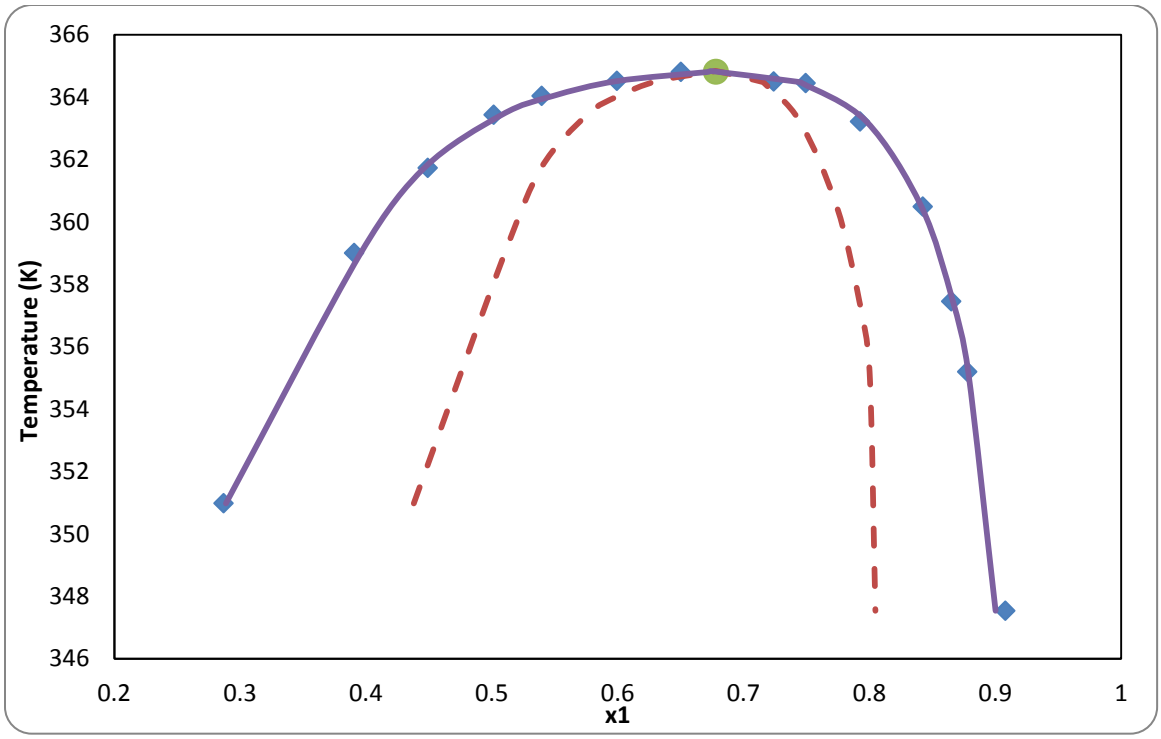

Figure 2.1-1: Binodal & Spinodal curves for Acetonitrile (1) + Octane(2)Experimental points (■), Binodal curve from NRTL (—), Spinodal curve (- -), and critical point (•).

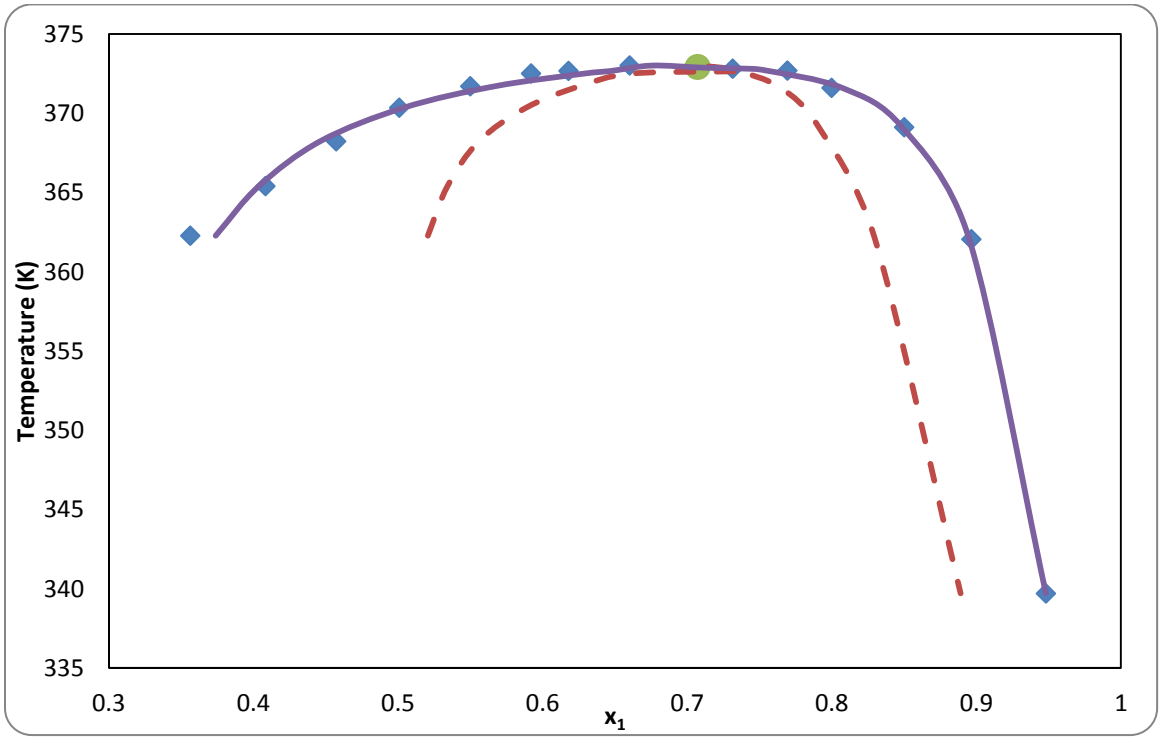

Figure 2.1-2: Binodal & Spinodal curves for Acetonitrile (1) + Nonane (2) Experimental points (■), Binodal curve from NRTL (—), Spinodal curve (- -), and critical point (•).

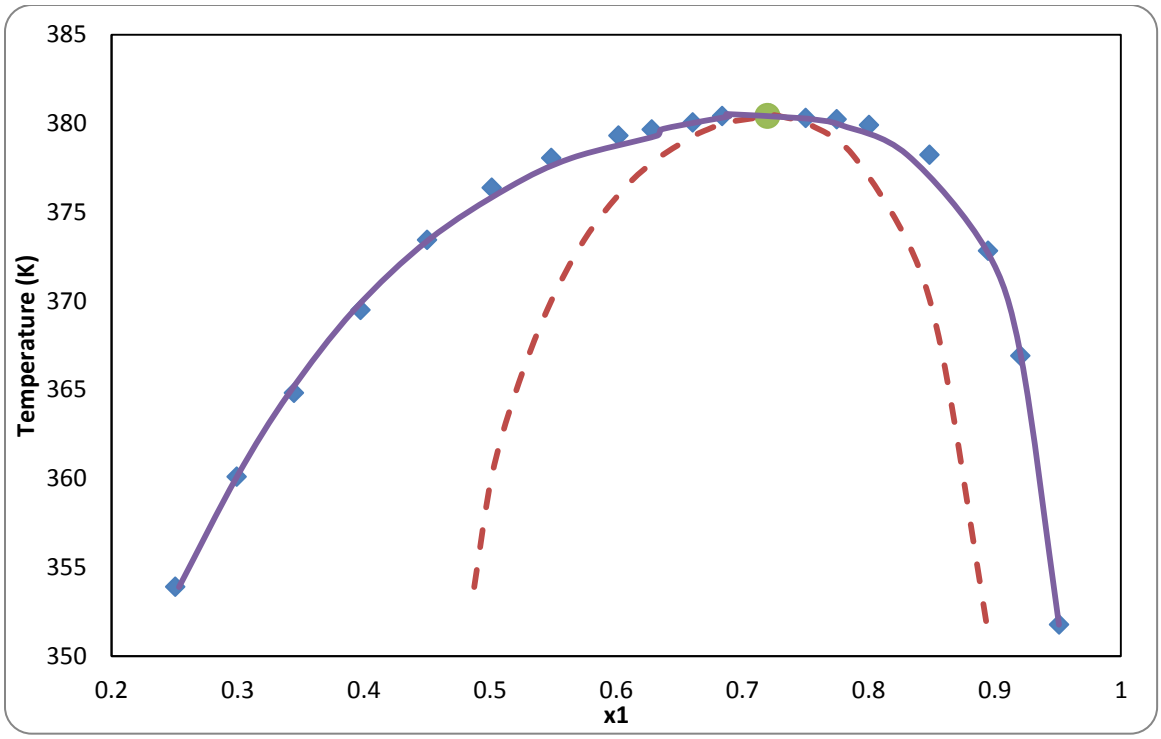

Figure 2.1-3: Binodal & Spinodal curves for Acetonitrile (1) + Decane (2) Experimental points (■), Binodal curve from NRTL (—), Spinodal curve (- -), and critical point (•).

Figures 2.1-1 to 2.1-17, illustrate the graphical results for binodal curve (from experimental data and from NRTL), spinodal curve, and critical temperature for each binary system. In general, all binodal curves constructed using NRTL show good agreement with the experimental data over the experimental temperature range with the exception of acetonitrile + tetradecane, where the binodal curve from NRTL could not be solved using the tabulated NRTL binary interaction parameters. The calculations for these systems have either converged to trivial solution or failed to converge due to mathematical singularity. The most plausible explanation could be that the experimental data for acetonitrile + tetradecane have only 5 K range and taken in the vicinity of critical region, where the system shows non-analytical behaviour with flat slope in the close proximity of critical region. Thus, it would not be practical to expect NRTL to be capable of constructing the binodal curve within this range.

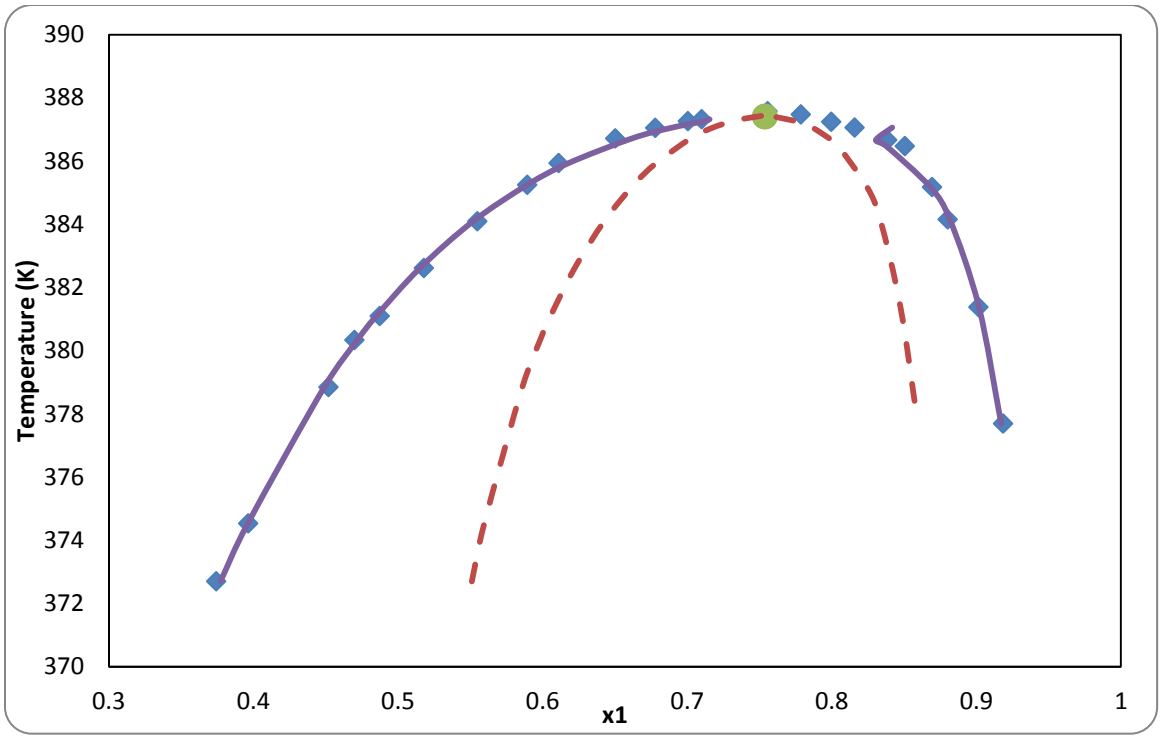

Figure 2.1-4: Binodal & Spinodal curves for Acetonitrile (1) + Undecane (2) Experimental points (■), Binodal curve from NRTL (—), Spinodal curve (- -), and critical point (•).

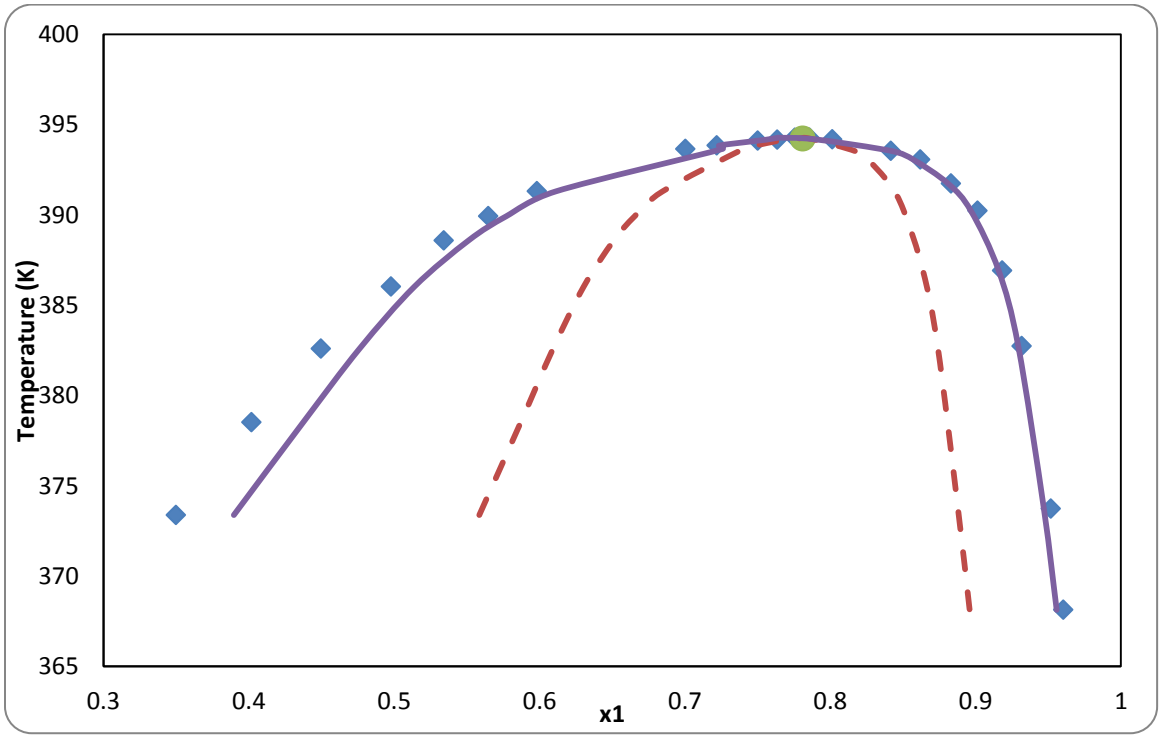

Figure 2.1-5: Binodal & Spinodal curves for Acetonitrile (1) + Dodecane (2) Experimental points (■), Binodal curve from NRTL (—), Spinodal curve (- -), and critical point (•).

For the binary systems of acetonitrile + undecane (figure 2.1-4), acetonitrile + pentadecane (figure 2.1-8), NRTL had failed to find the equilibrium conditions near the critical region. Likewise binary systems of acetonitrile + methylcyclohexane (figure 2.1-13), and acetonitrile +2,2 dimethylbutane (figure 2.1-14), and acetonitrile +2-Methylpentane (figure 2.1-16), the binodal curves were poorly reproduced from NRTL model when compared to experimental data. Yet, this is still within the acceptable margin of error, as the objective function attempts to find the optimized binary interactions parameters that minimize the difference between the calculated and experimental data over all the experimental data. Therefore, the calculated equilibrium composition might show poor results in specific regions in the binodal curve.

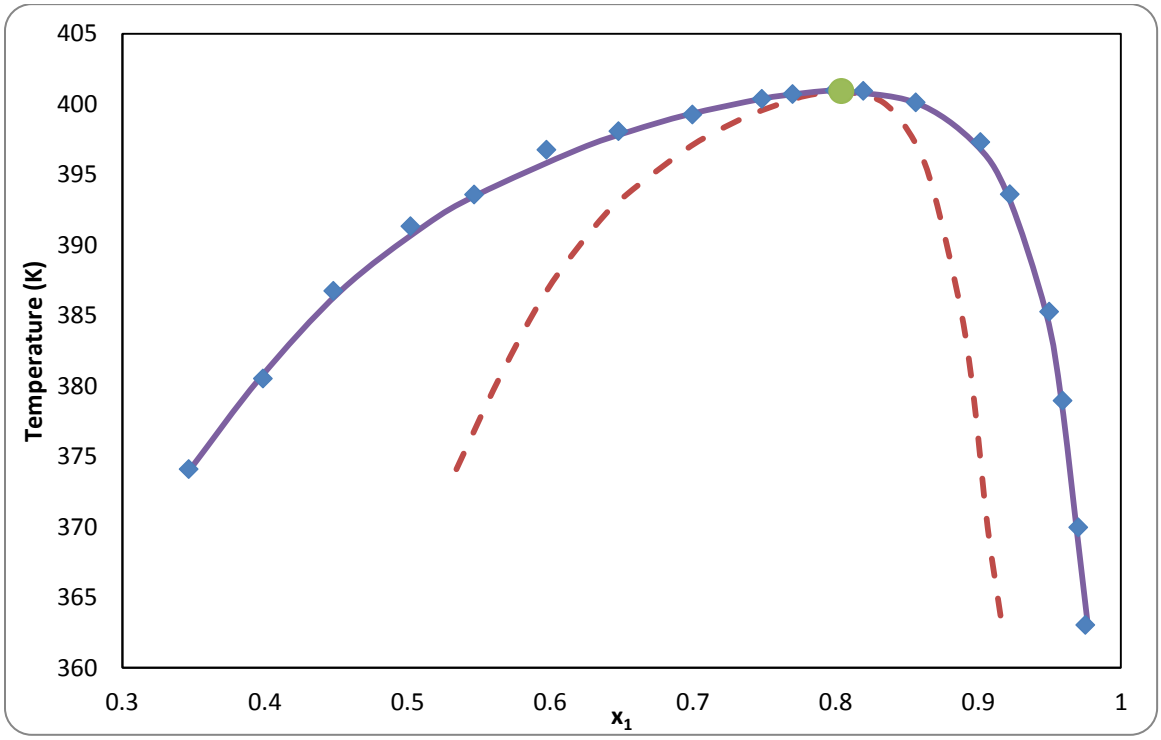

Figure 2.1-6 Binodal & Spinodal curves for Acetonitrile (1) + Tridecane (2) Experimental points (■), Binodal curve from NRTL (—), Spinodal curve (- -), and critical point (•).

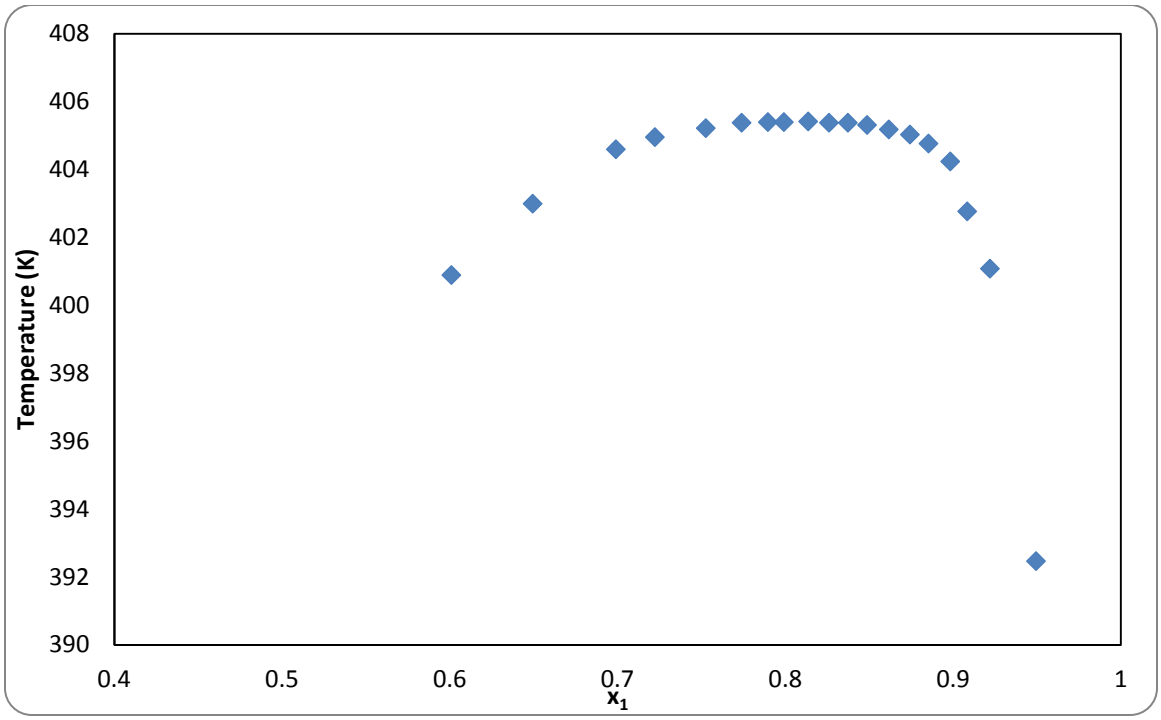

Figure 2.1-7 Binodal & Spinodal curves for Acetonitrile (1) + Tetradecane (2) Experimental points (■).

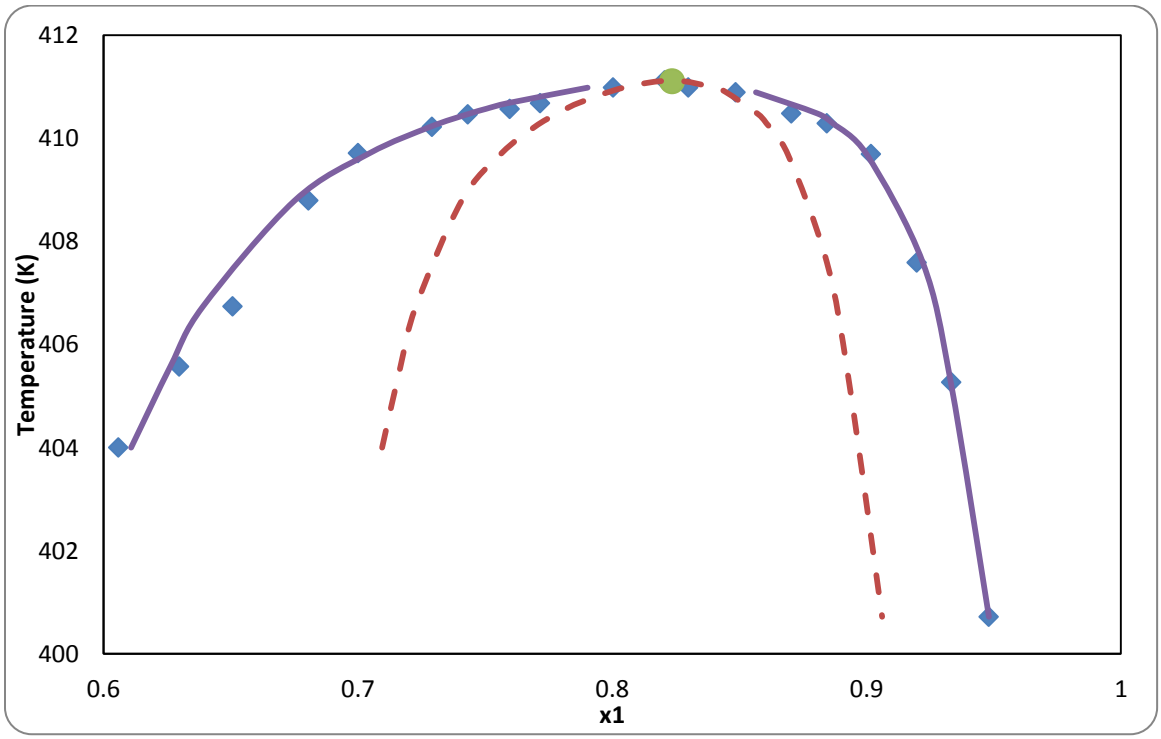

Figure 2.1-8: Binodal & Spinodal curves for Acetonitrile (1) + Pentadecane (2) Experimental points (■), Binodal curve from NRTL (—), Spinodal curve (- -), and critical point (•).

All binary systems studied here show Upper Critical Solution Temperature (UCST) as shown in all figures. Critical temperatures for all binary systems are given in table 2.1-4 and they are also depicted as a solid circle in figures 2.1-1 to 2.1-17. For most binary systems studied, the results show precise convergence of the spinodal to the binodal curve at the critical point of the mixture. This, in addition to the good fit of the NRTL model to the binodal experimental data, gives confidence in the predicted spinodal curves for the different systems. Unfortunately, experimentally determined stability limits are lacking for most liquid mixtures. Nevertheless, critical temperatures calculated show good agreement with other literature work as shown in table 2.1-4.

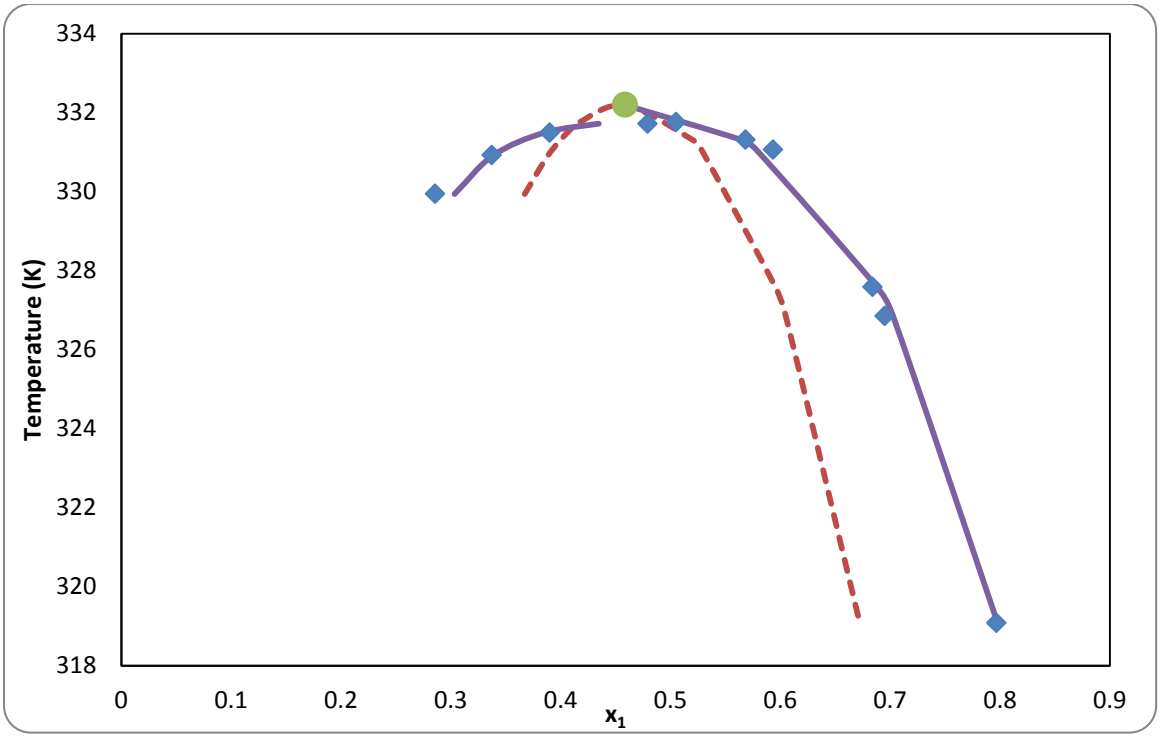

Figure 2.1-9: Binodal & Spinodal curves for Acetonitrile (1) + Cyclopentane (2) Experimental points (■), Binodal curve from NRTL (—), Spinodal curve (- -), and critical point (•).

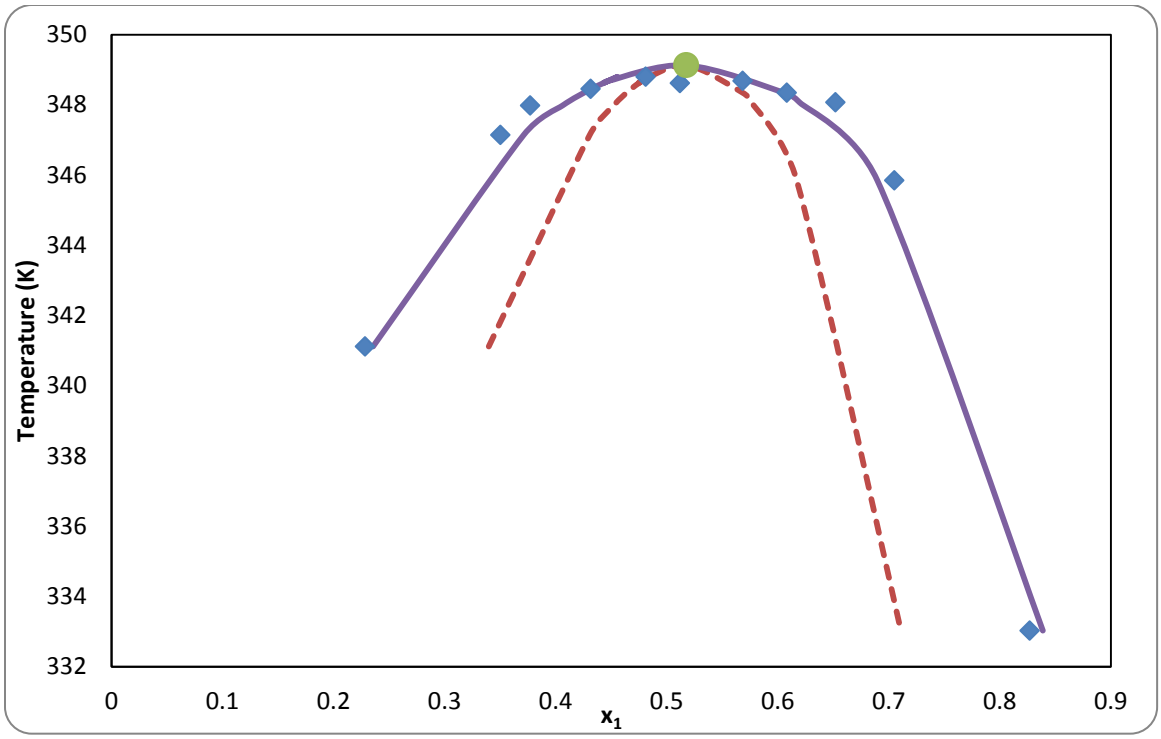

Figure 2.1-10: Binodal & Spinodal curves for Acetonitrile (1) + Cyclohexane (2) Experimental points (■), Binodal curve from NRTL (—), Spinodal curve (- -), and critical point (•).

It is interesting to note that for all binary systems studied, the metastable regions, where a single phase of the two species can be maintained homogenous without splitting (i.e., the region bounded by the spinodal (dashed curve) and the bimodal(slid curve), penetrate deep into the two-phase region under the binodal curve. For example, for Acetonitrile (1) + Pentadecane(2) (Figure 2-8) at a temperature of 404 K, a homogeneous mixture that is supposed to split into two phases of x_1= 0.63 (acetonitrile-rich phase) and x_1 = 0.95 (pentadecane–rich phase) can be maintained as a single homogeneous phase without splitting up to x_1 = 0. 72 starting from pure acetonitrile on the left and up to x_1 = 0.9 starting from pure pentadecane the right.

Table 2.1-4 Critical temperature & composition determined for Acetonitrile + Hydrocarbons with reported literature values.

	Critical Temperature (K)		Critical Composition	
System (Acetonitrile + hydrocarbons)	**This work**	**Literature**	**This work**	**Literature**
Octane	364.8	364.84 [88]	0.678	0.6781 [88]
Nonane	372.89	372.96 [88]	0.707	0.6928 [88]
Decane(2)	380.41	380.45 [88]	0.72	0.7203 [88]
Undecane	387.40	385.7 [90]	0.754	0.77 [90]
Dodecane	394.20	393.1 [89]	0.781	0.781 [89]
Tridecane	400.90	399.83 [88]	0.804	0.7907 [88]
Tetradecane	405.40	405.4 [88]	0.814	0.8142 [88]
Pentadecane	411.10	411.12 [88]	0.824	0.8236 [88]
Cyclopentane	332.19	331.68 [89]	0.459	0.4551 [89]
Cyclohexane	349.12	348.78 [89]	0.518	0.5036 [89]
Cyclooctane	371.73	371.48 [89]	0.595	0.6067 [89]
Methylcyclopentane	341.55	341.17 [89]	0.512	0.5076 [89]
Methylcyclohexane	352.42	352.39 [89]	0.547	0.5519 [89]
2,2 Dimethylbutane	342.16	341.86 [89]	0.571	0.562 [89]
2,3 Dimethylbutane	343.38	343.26 [89]	0.559	0.5464 [89]
2-Methylpentane	347.05	346.66 [89]	0.543	0.5631 [89]
3-Methylpentane	346.46	346.05 [89]	0.556	0.5542 [89]

The spinodal curves for the different binary systems studied here are consistent with the reported experimental binodal equilibrium data. That is, they are lying nicely within the binodal and soundly converge to the binodal data at the critical point. It must be noted that acetonitrile + methylcyclohexane demonstrates a contradiction in the expected analytical behavior by intersecting the binodal curve near the critical region. Inspecting the results graphically in figure 2.1-13, it is quick to conclude that the experimental data

were regressed ineffectively. This leads to erroneous binary interactions parameters and subsequently, poor results for spinodal and binodal curve.

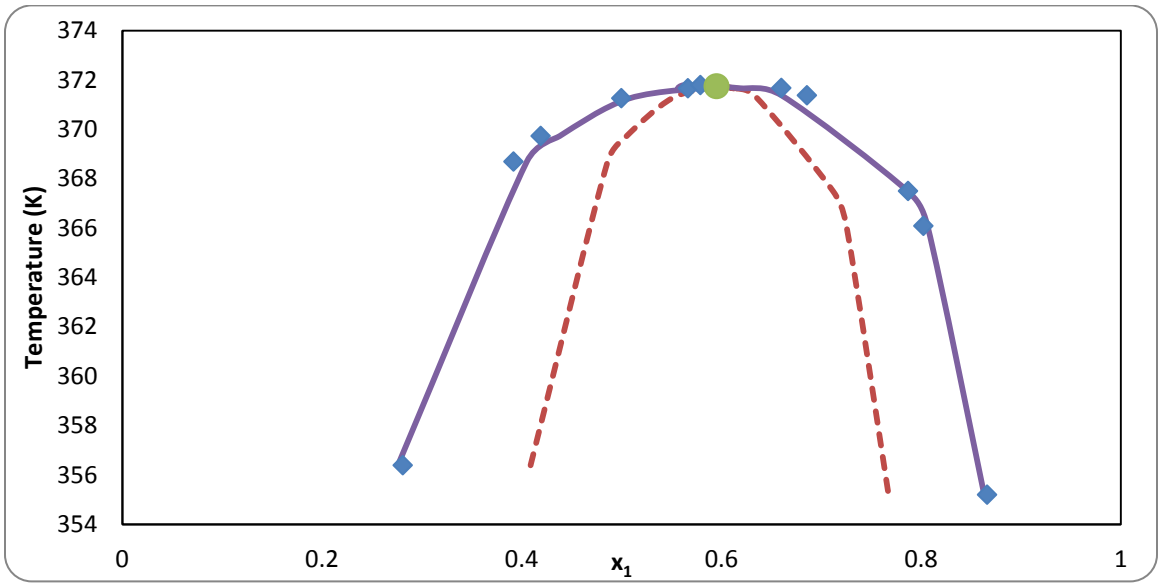

Figure 2.1-11: Binodal & Spinodal curves for Acetonitrile (1) + Cyclooctane (2) Experimental points (■), Binodal curve from NRTL (—), Spinodal curve (- -), and critical point (•).

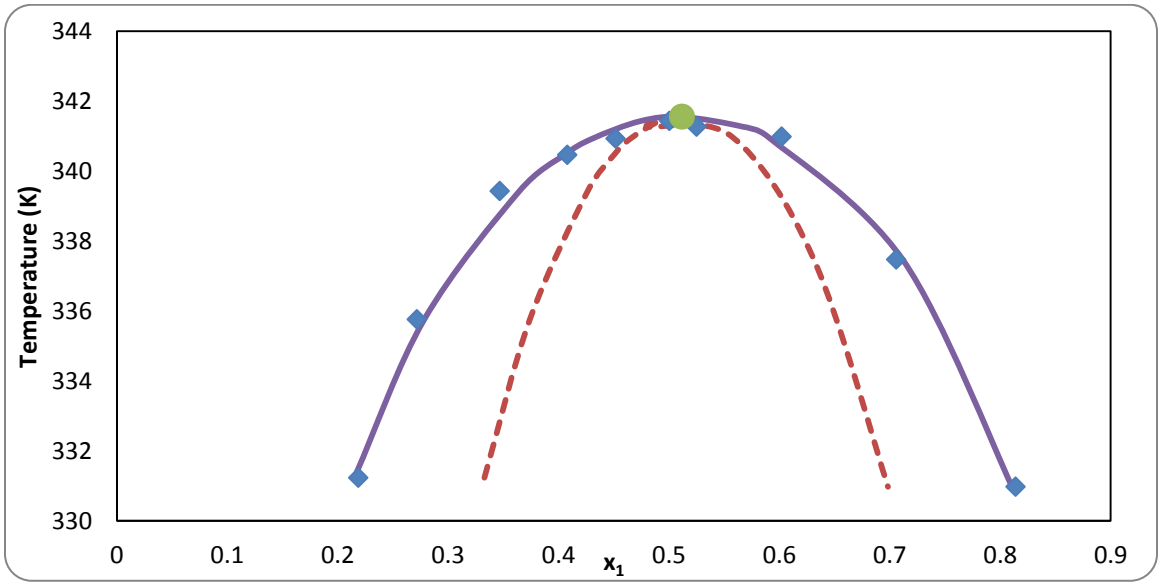

Figure 2.1-12: Binodal & Spinodal curves for Acetonitrile (1) + Methylcyclopentane (2) Experimental points (■), Binodal curve from NRTL (—), Spinodal curve (- -), and critical point (•).

The calculated critical temperatures, together with the calculated composition for the different binary systems studied here are summarized in table 2.1-4. Shown also in the same table, are experimental values reported in the literature. The critical temperatures

found for acetonitrile + hydrocarbons show good agreement with values reported in literature [89].

The mutual solubility increases as the size of the n-alkane increases, as expected. The increase in critical temperature follows linear fashion, as shown in figure 2.4-18, and there is an average increase of 6.6 K for critical temperatures in n-alkanes series.

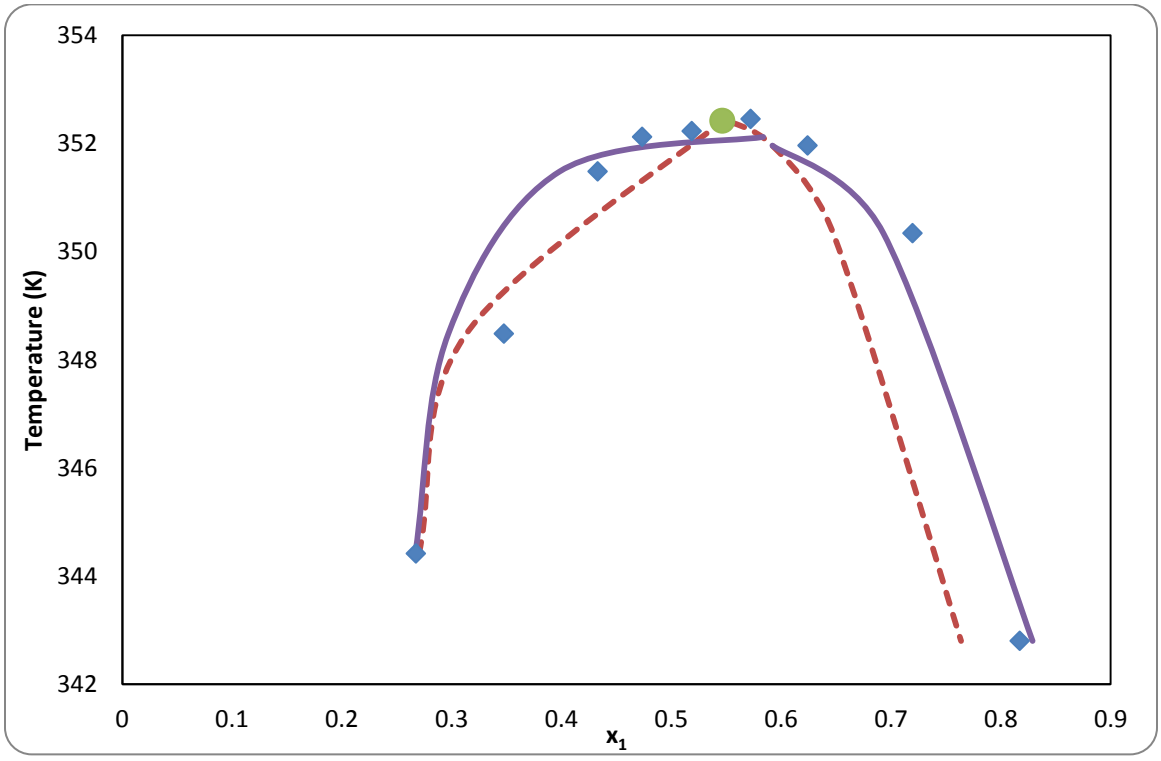

Figure 2.1-13: Binodal & Spinodal curves for Acetonitrile (1) + Methylcyclohexane (2) Experimental points (■), Binodal curve from NRTL (—), Spinodal curve (- -), and critical point (•).

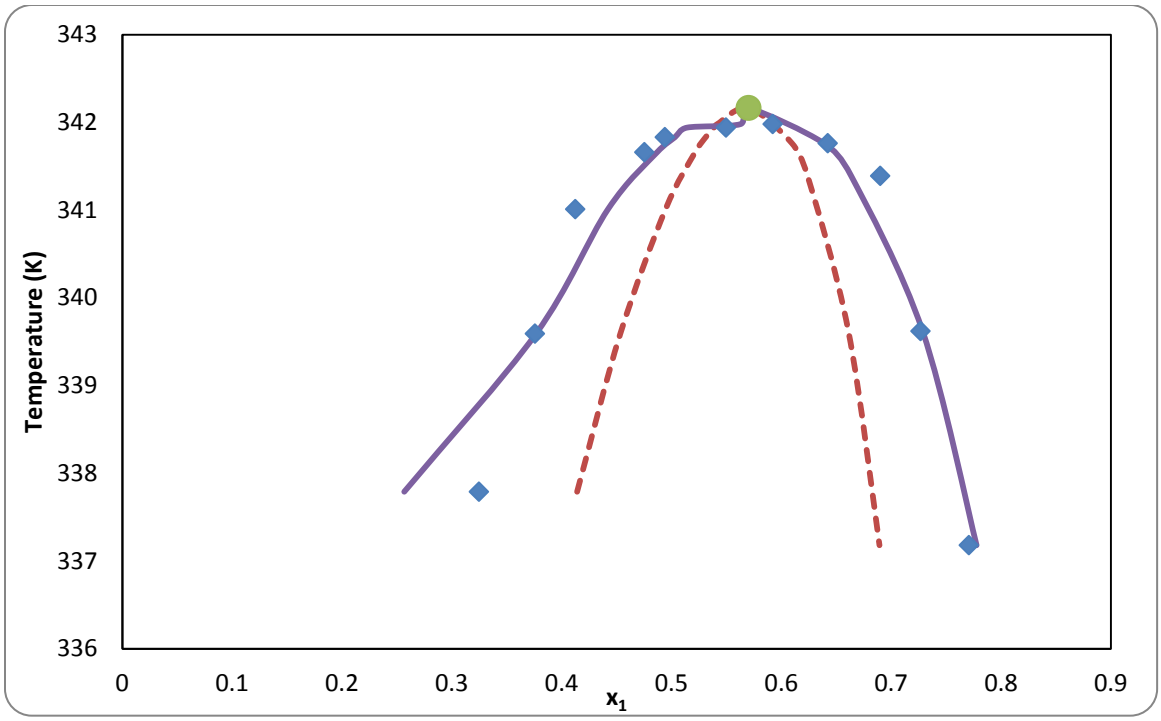

Figure 2.1-14: Binodal & Spinodal curves for Acetonitrile (1) + 2,2 Dimethylbutane (2) Experimental points (■), Binodal curve from NRTL (—), Spinodal curve (- -), and critical point (•).

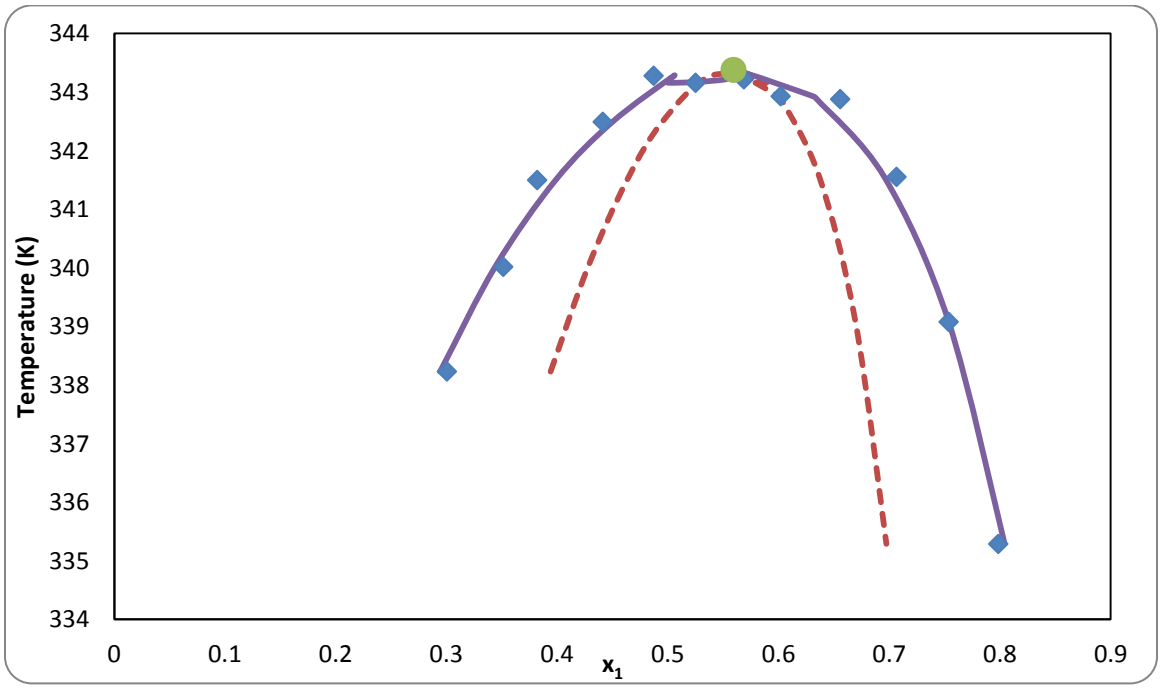

Figure 2.1-15: Binodal & Spinodal curves for Acetonitrile (1) + 2,3 Dimethylbutane (2) Experimental points (■), Binodal curve from NRTL (—), Spinodal curve (- -), and critical point (•).

The critical temperature found for binary systems of different isomers are nearly identical. Namely, for acetonitrile + 2-methylpentane and acetonitrile + 2-methylpentane there is only a 0.5 K difference in critical temperature. Likewise, there is a 1 K difference for acetonitrile + 2,2 dimethylbutane and acetonitrile + 2,3 dimethylbutane. Moreover, acetonitrile + cycloalkanes (cyclopentane, cyclohexane, and cyclooctane) showed, similar to n-alkanes, an increase in critical temperature with the increase of molecular size.

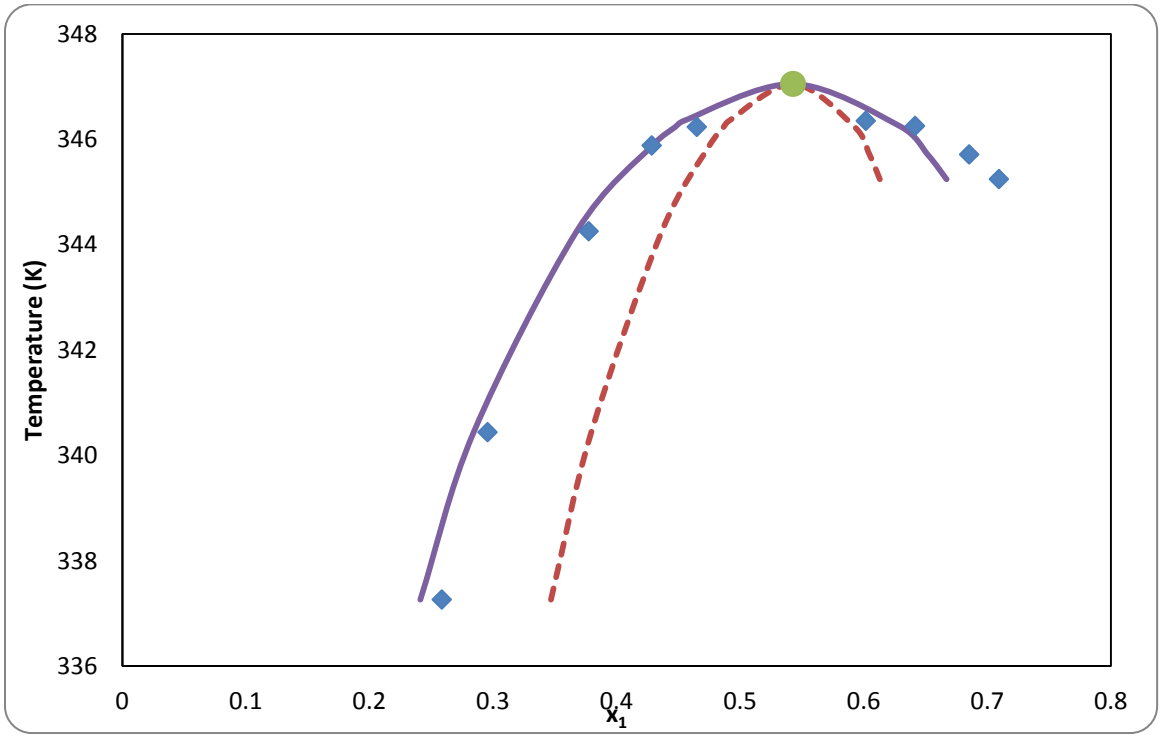

Figure 2.1-16: Binodal & Spinodal curves for Acetonitrile (1) + 2-Methylpentane (2) Experimental points (■), Binodal curve from NRTL (—), Spinodal curve (- -), and critical point (•).

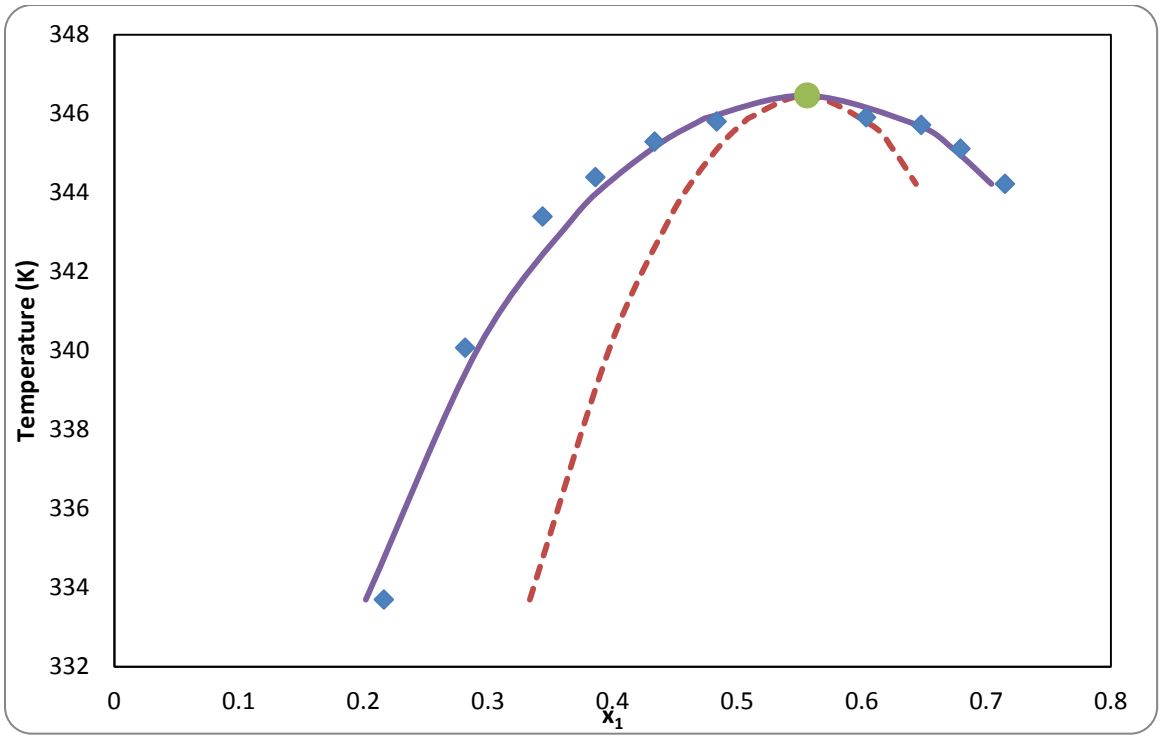

Figure 2.1-17: Binodal & Spinodal curves for Acetonitrile (1) + 3-Methylpentane (2) Experimental points (■), Binodal curve from NRTL (—), Spinodal curve (- -), and critical point (•).

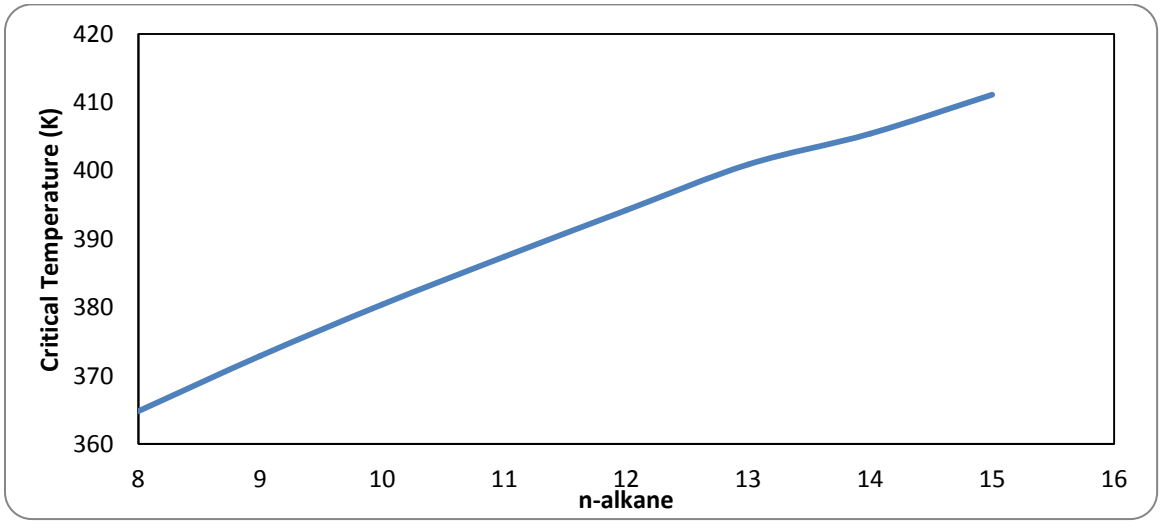

Figure 2.1-18: Critical Temperatures of n-alkanes series

2.1.2 Perfluoroalkane + n-Alkane

The experimental data range including their reference for perfluoroalkanes + alkanes are shown in table 2.1-5. Perfluoroalkanes are used as oxygen carriers in blood substitutes, and in the synthesis of fluorous phase organic using fluorous catalysis [91].

Perfluoroalkanes have the same chemical structures as those of alkanes, yet they differ in physical properties; they possess higher densities and vapor pressures, lower surface tensions, and higher gas solubilities in comparison to their corresponding alkanes [91].

The interaction parameters required by the NRTL model for the optimum fit of the binodal equilibrium data of each binary system were reported in the literature [91].

Table 2.1-5 Range of temperature and composition for Perfluoroalkane (1) + n-alkane (2) systems [91].

System (Perfuloroalkanes+ alkanes)	Temperature range (K)	Composition range
n-hexane [91]	347.54-364.83	0.287-0.908
n-octane [91]	281.67-334.83	0.051-0.906
n-octane [91]	304.97-349.5	0.050-0.873

Figures 2.1-19, 2.1-20, & 2.1-20 illustrate the binodal and spinodal curves along with critical temperature for Perfluorohexane (1)+ Hexane (2), Perfluorohexane (1)+ Octane (2), and Perfluorooctane (1)+Octane (2). For each binary system, the spinodal curve was generated by solving the stability limit criterion. The critical temperature of each binary at the reported pressure of the experimental data was determined by solving the two highly coupled stability and criticality criteria.

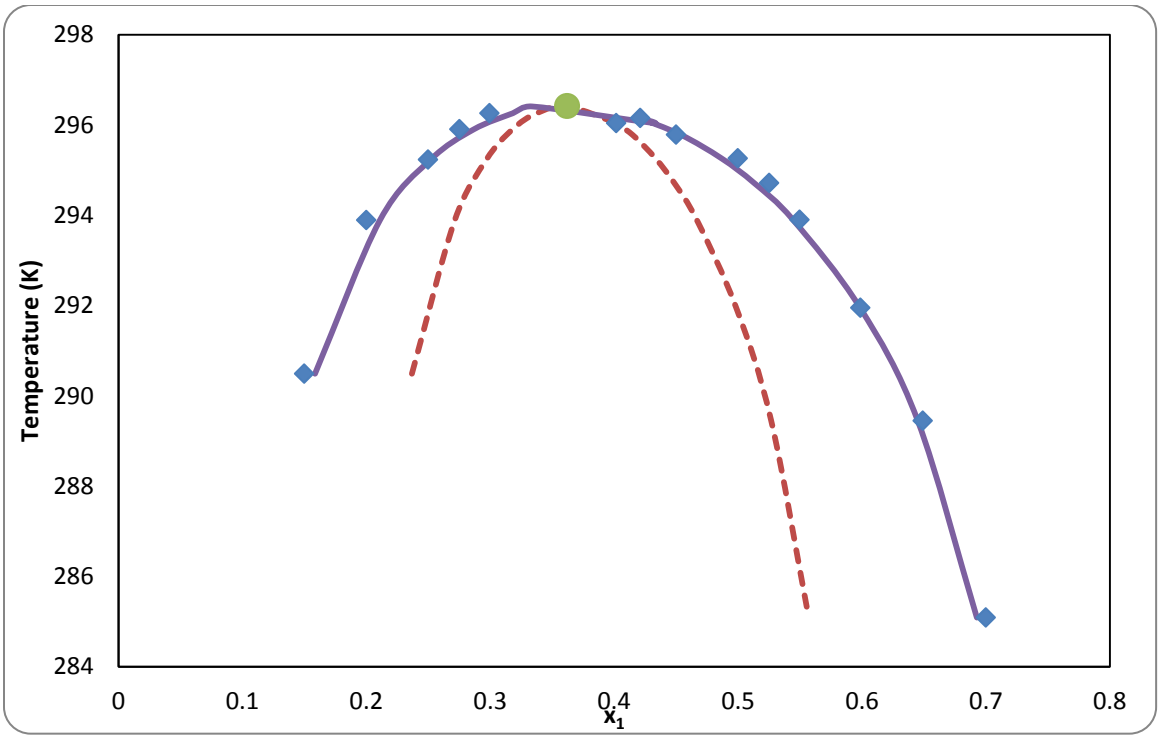

Figure 2.1-19: Binodal & Spinodal curves for Perfluorohexane (1) + Hexane (2). Experimental points (■), Binodal curve from NRTL (—), Spinodal curve (- -), and critical point (•).

The results of the spinodal curve for each system are consistent with the expected analytical behaviour. The spinodal converge to the binodal curve precisely at the critical temperature. Moreover, NRTL model was able to perfectly reproduce fit the experimental data assuring the accuracy of the results.

It is interesting to note that perfuloroalkanes binary systems have wider metastable range in the alkane rich phase (from the right). Graphically, the extent of penetration of metastable region is higher from the right (above x_1=0.4) .

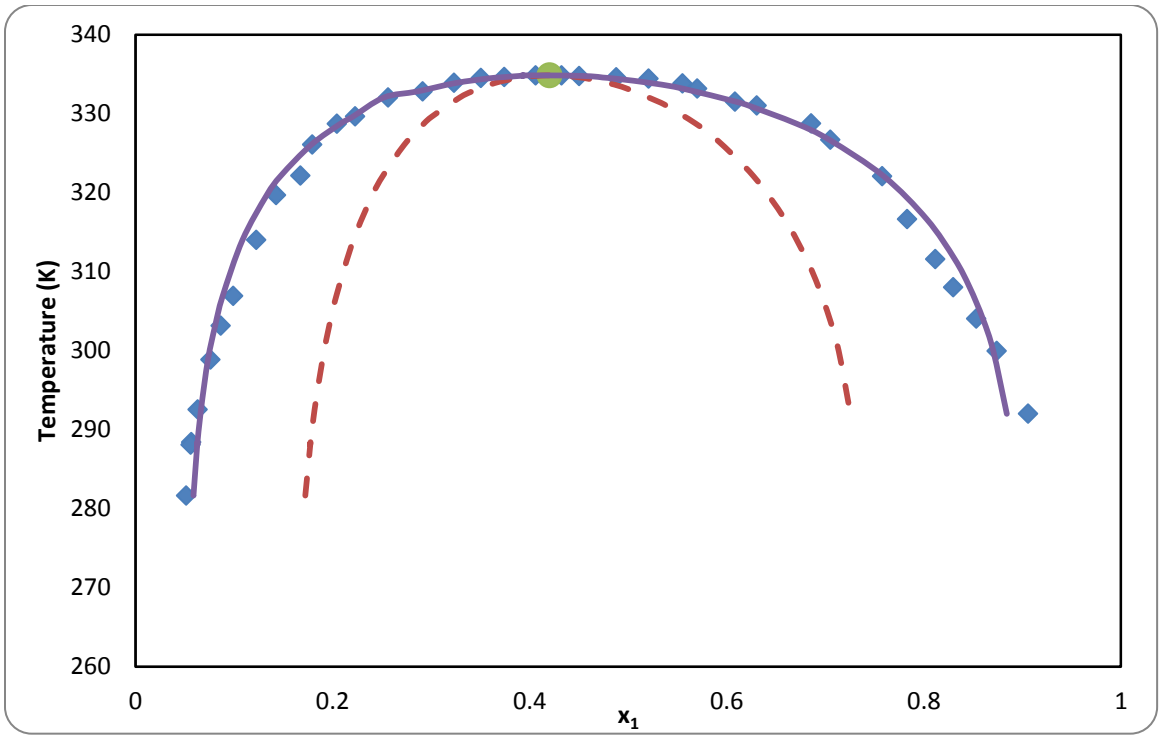

Figure 2.1-20: Binodal & Spinodal curves for Perfluorohexane (1) + Octane (2). Experimental points (■), Binodal curve from NRTL (—), Spinodal curve (- -), and critical point (•).

All perfuloroalkanes binary systems exhibit upper critical solution temperature. The results of critical temperatures, and critical composition are tabulated in table 2.1-6 along with reported literature values. The predicted critical temperatures showed good agreement with the ones reported in literature.

The good quality results can be attributed to the good quality of the experimental data. The wide temperature range taken presents the experimental binodal curve properly including the critical region. This has assisted the accurate regression of NRTL parameters, which were subsequently used for the calculation of the spinodal curve and critical temperature.

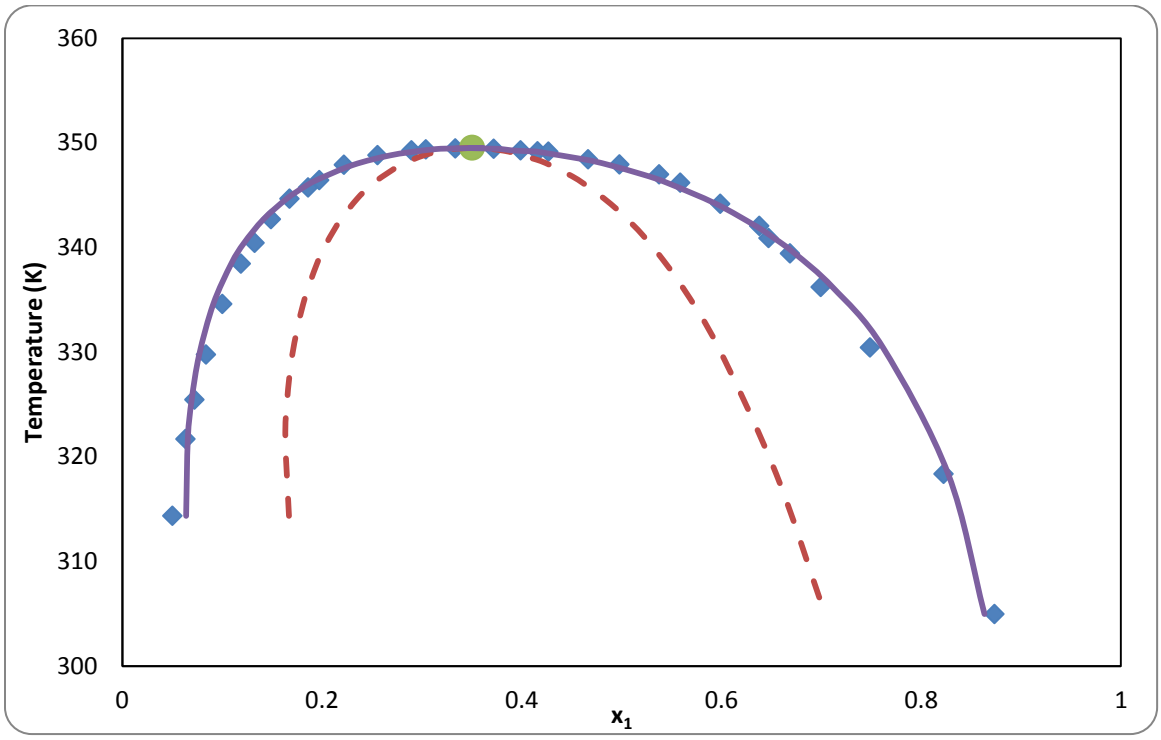

Figure 2.1-21: Binodal & Spinodal curves for Perfluorooctane (1) + Octane (2). Experimental points (■), Binodal curve from NRTL (—), Spinodal curve (- -), and critical point (•).

Table 2.1-6 Critical temperature & composition determined for Acetonitrile + Hydrocarbons with literature reported data.

	Critical Temperature (K)		Critical composition	
System	**This work**	**Literature**	**This work**	**Literature**
Perfulorohexane(1)+ Hexane(2)	296.41	295.8 [91]	0.362	0.37 [91]
Perfulorohexane(1)+ Octane(2)	334.84	331.5 [91]	0.42	0.45 [91]
Perfulorooctane(1)+ Octane(2)	349.52	349.4 [91]	0.351	0.36 [91]

2.1.3 Alkanes + N-formylmorpholine

N-Formylmorpholine (NFM) is an important solvent used to extract undesired constituents from hydrocarbon mixtures [92]. Aromatics content in gasoline and reformate that are produced by catalytic reforming of naphtha, for example, are restricted by environmental regulations, and can be, minimized by extractive distillation using NFM to selectively remove aromatics from these products, which can then be used as feedstock for petrochemical processes. The experimental data range of NFM binary systems are presented in table 2.1-7 along with their references. Seven binary systems for NFM are studied here covering NFM + alkanes and branched alkanes.

Table 2.1-7 Range of temperature and composition for n-Alkanes (1) + N-formylmorpholine (2) systems

System (+N-Formylmorpholine)	Temperature range (K)	Composition range
Pentane [93]	304.49-388.1	0.039-0.994
Hexane [93]	299.46-413.33	0.031-0.986
Heptane [93]	301.12-412.16	0.024-0.988
Octane [93]	297-416.18	0.012-0.973
Methylcyclopentane [92]	300.27-398.73	0.067-0.984
Methylcyclohexane [92]	301.24-402.28	0.063-0.979
Ethylcyclohexane [92]	297.85-409.63	0.027-0.979

The binary interaction parameters of branched alkanes + NMF for NRTL model were reported in literature [92]. As for NMF + alkanes, the optimum binary parameters were regressed, in this thesis, and shown in table 2.1-8.

the energy interaction parameters (g_{ij}-g_{jj}) were correlated considering temperature dependencies using the model shown below:

$$\tau_{ij} = a_{ij} + \frac{b_{ij}}{T} + c_{ij} \ln T \qquad (2.4)$$

The coefficients a_{ij}, b_{ij}, and c_{ij} are presented in tables 2.1-8.

Table 2.1-8 Binary interaction parameters for n-Alkanes (1) + NFM (2) systems.

binary interaction parameters							
	a_{12}	a_{21}	b_{12}/K	b_{21}/K	c_{12}	c_{21}	α_{ij}
Pentane	-3.174	-1.499	2116.58	982.848	-	-	0.2
Hexane	27.304	80	-48.240	-3350.755	-4.233	11.713	0.2
Heptane	-5.059	1.678	2512.54	166.132	-	-	0.2
Octane	-1.993	-0.871	1351.61	1120.431	-	-	0.2

Table 2.1-9:The percent absolute average deviations (AAD%) of NRTL model for alkanes (1) + NFM (2) binary systems

System (NFM+ alkanes)	n-Alkane rich phase	NFM rich phase
Pentane	0.30	11.3
Hexane	0.16	3.84
Heptane	0.38	2.73
Octane	0.5	9.34

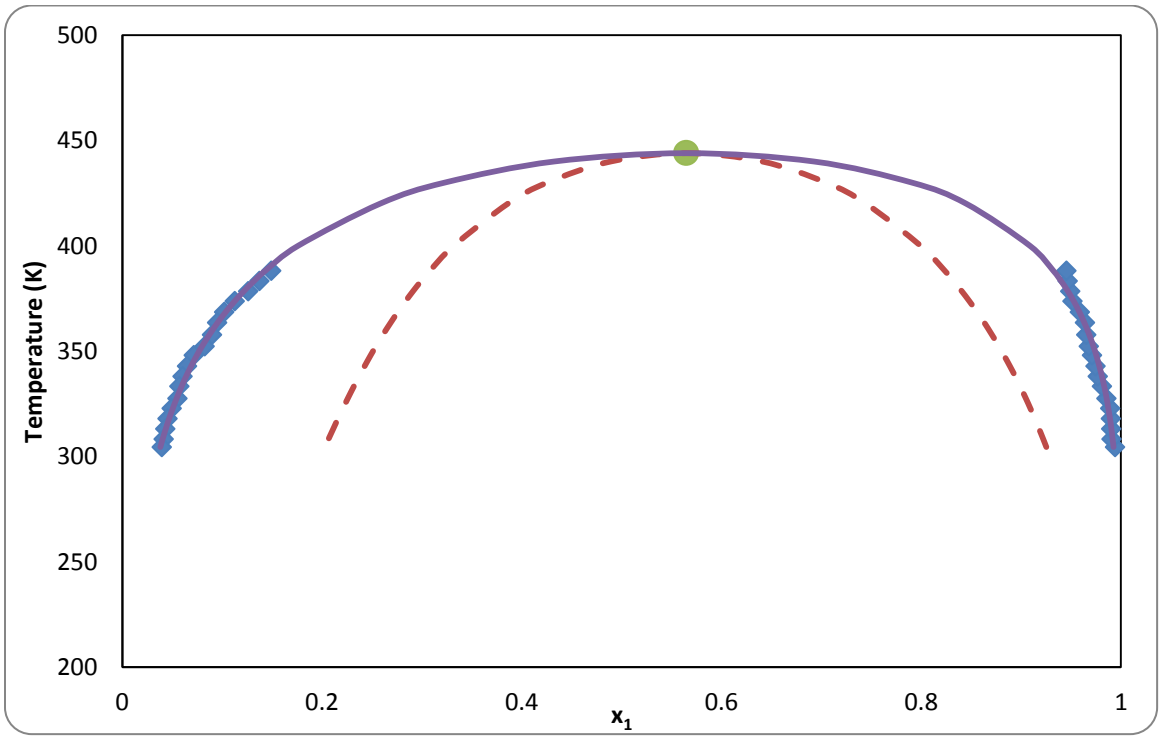

Figure 2.1-22: Binodal & Spinodal curves for Pentane (1) + NFM (2). Experimental points (■), Binodal curve from NRTL (—), Spinodal curve (- -), and critical point (•).

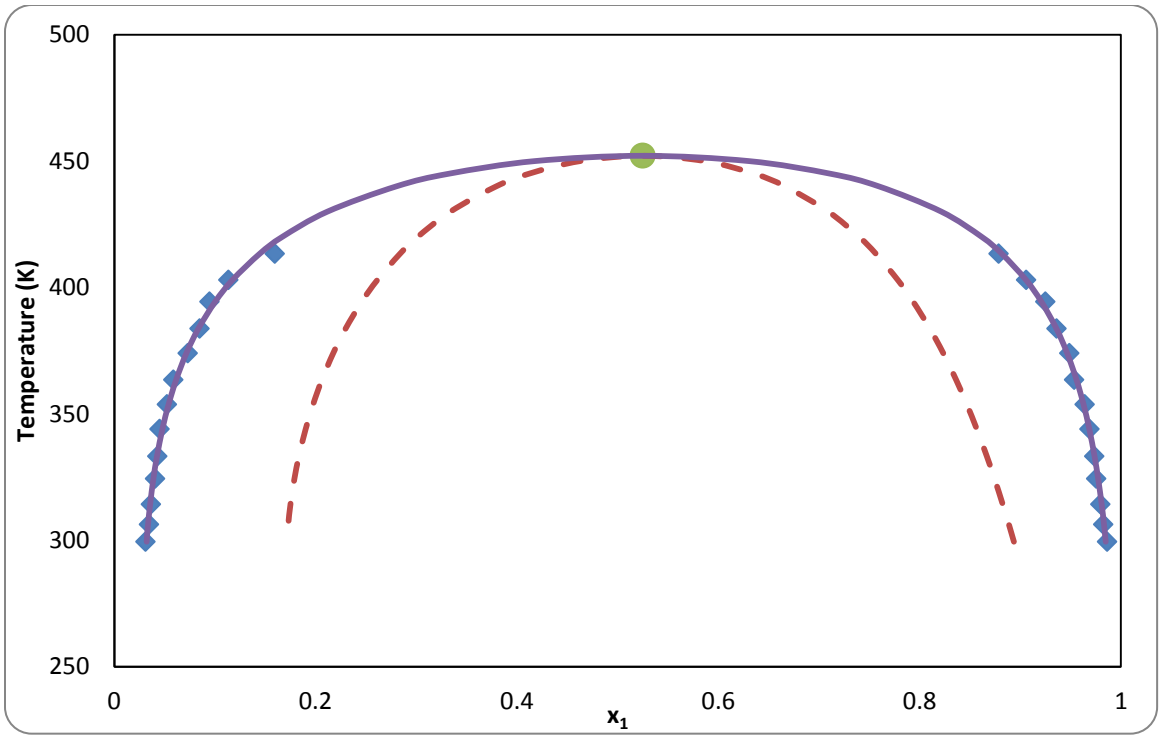

Figure 2.1-23: Binodal & Spinodal curves for Hexane (1) + NFM (2). Experimental points (■), Binodal curve from NRTL (—), Spinodal curve (- -), and critical point (•).

The percent absolute average deviations for each regression are reported in table 2.1-9. The binary parameters optimized for alkanes + NFM were able to reproduce the experimental binodal curve generally with a satisfactory accuracy. However, the AAD% for NFM + pentane is 11.3%, which is considered too high and this can be confirmed graphically from figure 2.1-22. The calculated binodal curve seems to have conflict with the experimental data for NFM rich phase ($x_1 \approx 0.94$). At 400 K, the calculated binodal curve shows a slope towards the left contradicting the somehow vertical line defined by the experimental curve. This will certainly affect the successive calculations of the spinodal and critical temperature, as the precision of these calculations will depend entirely on the accuracy of the binary parameters of NRTL. The extent at which this affects the results is difficult to assess in the absence of literature values to be compared with.

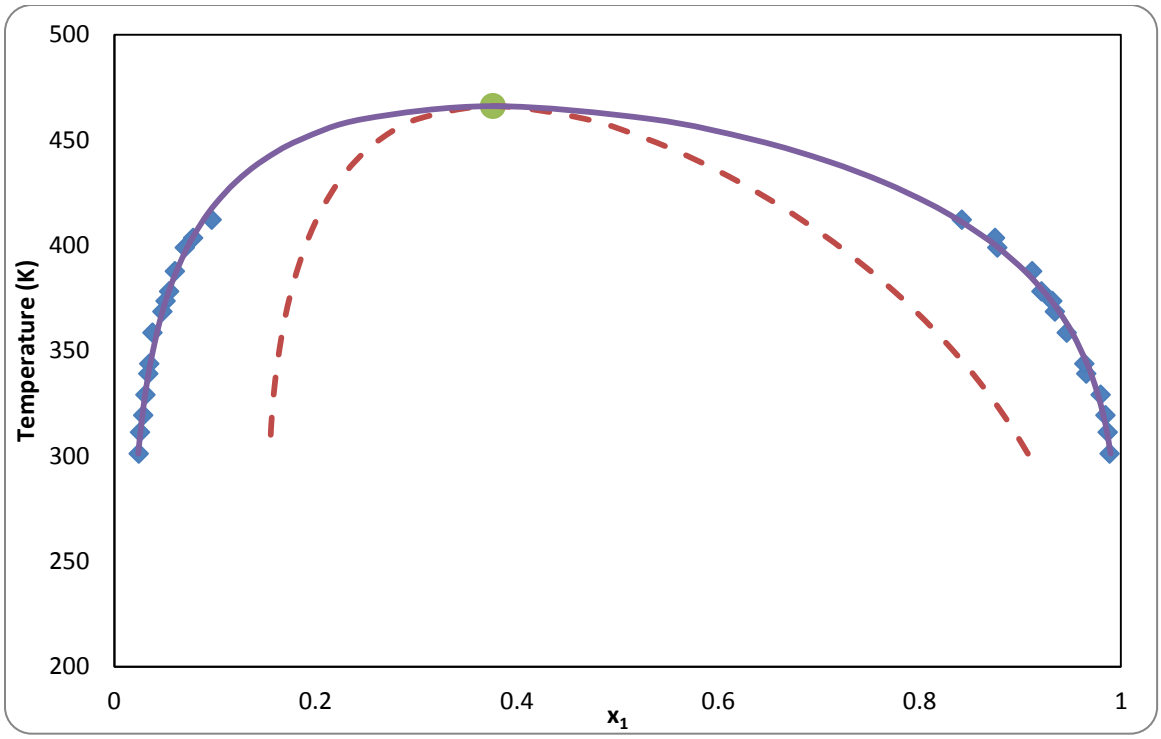

Figure 2.1-24: Binodal & Spinodal curves for Heptane (1) + NFM (2). Experimental points (■), Binodal curve from NRTL (—), Spinodal curve (- -), and critical point (•).

The results of the binodal curve, spinodal curve, and critical temperature are illustrated in figures 2.1-22 to 2.1-28 for NFM binary systems. Each of the binary system treated in this series conforms to the anticipated theoretical behaviour, having spinodal and binodal curve converging at exactly the critical temperature. Yet, branched alkanes + NFM exhibit non-analytical behaviour of flat slope in the close proximity of the critical region. Luckily, experimental data points are available near the critical region to tune the binary interaction parameters so it can reproduce the experimental binodal curve effectively.

All NFM binary systems exhibit Upper Critical Solution Temperature (UCST). For alkanes + NFM systems, the mutual solubility increases with size i.e. the critical temperature increases, as expected. The increase in critical temperature follows a linear trend and there is an average increase of 11.9 K for critical temperatures in n-alkanes series.

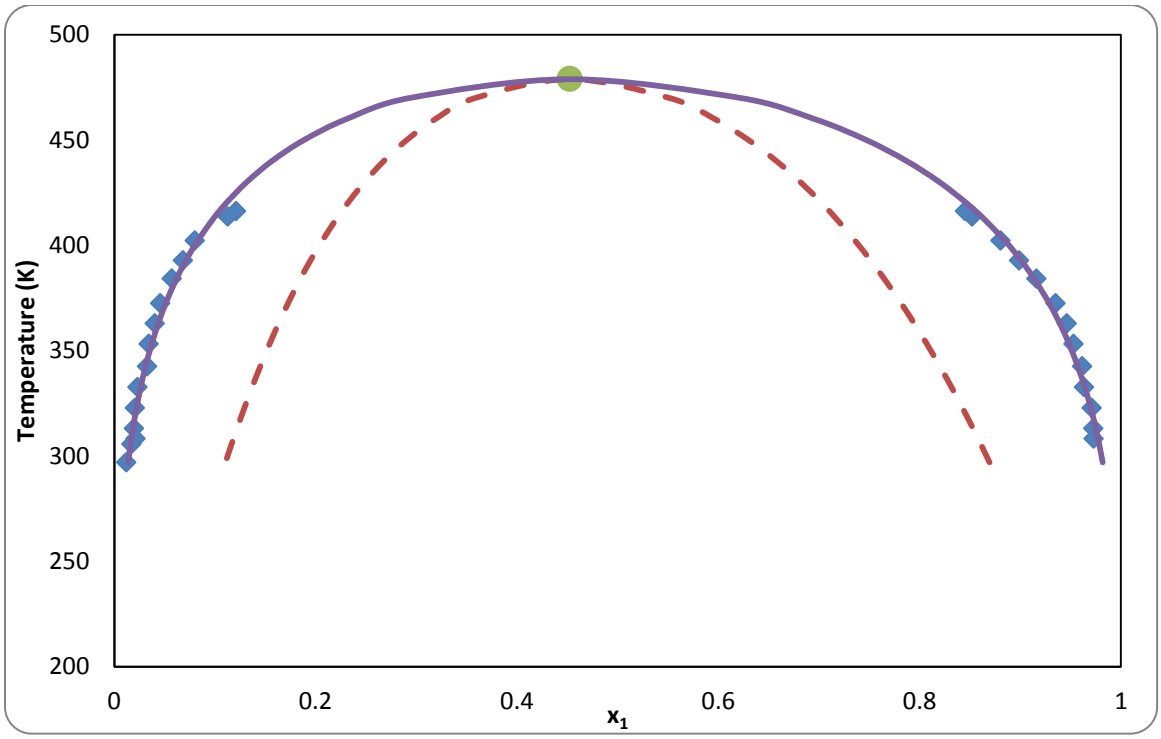

Figure 2.1-25: Binodal & Spinodal curves for Octane (1) + NFM (2). Experimental points (■), Binodal curve from NRTL (—), Spinodal curve (- -), and critical point (•).

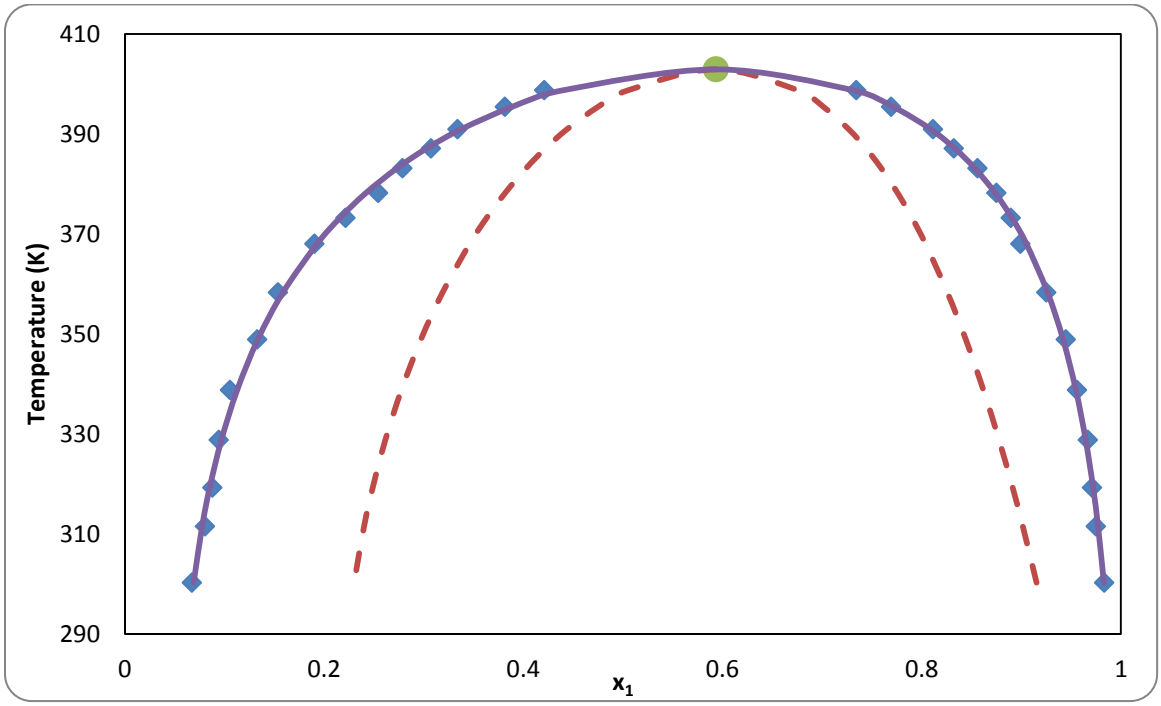

Figure 2.1-26: Binodal & Spinodal curves for Methylcyclopentane (1) + NFM (2). Experimental points (■), Binodal curve from NRTL (—), Spinodal curve (- -), and critical point (•).

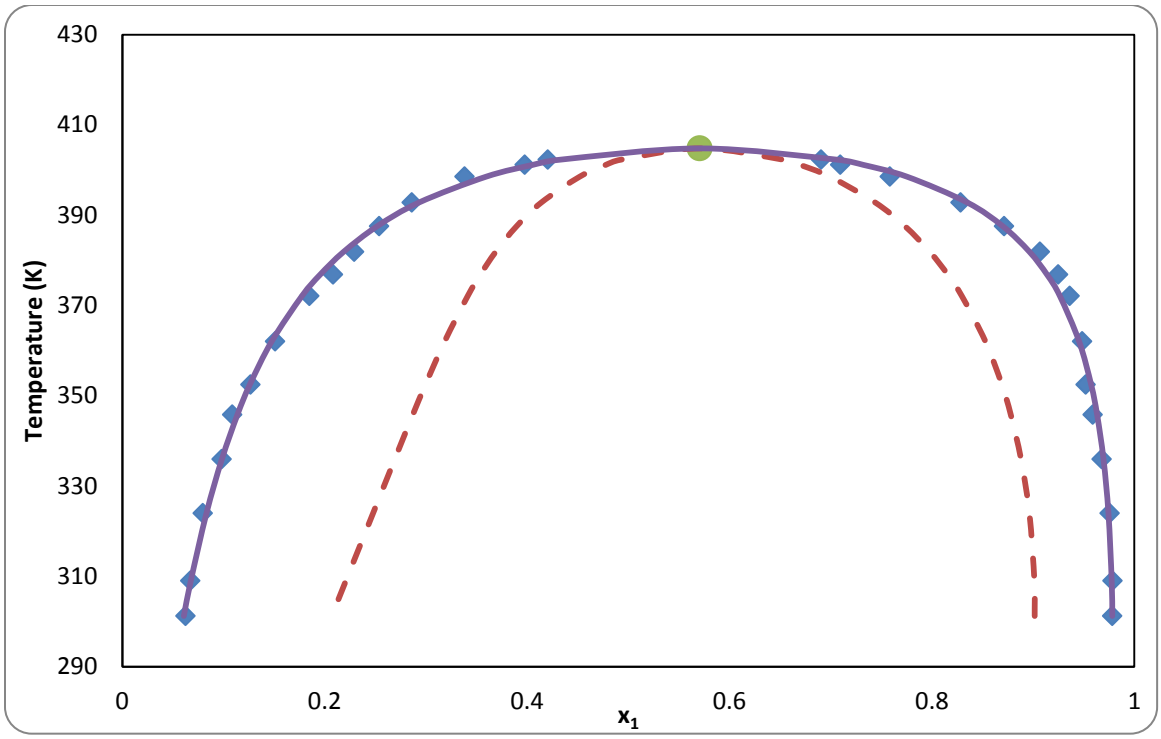

Figure 2.1-27: Binodal & Spinodal curves for Methylcyclohexane(1) + NFM (2). Experimental points (■), Binodal curve from NRTL (—), Spinodal curve (- -), and critical point (•).

The critical temperatures calculated for this series are tabulated in table 2.1-10 together with their corresponding critical compositions. Reported literatures values of critical temperature are also shown in table 2.1-10. The critical temperatures found for Formylmorpholine (NFM) + branched Cyclohexanes agree reasonably well with the literature. Despite a lack of literature data for the critical temperatures of n-alkanes+NMF, graphical results indicate accurate prediction of critical temperatures.

The mutual solubility increases as the size of the cycloalkane increases, as expected. Nevertheless, it is interesting to note that the contribution of the cycloalkane size has less effect on the critical temperature than the branch size. Going from methylcyclopentane to methycyclohexane has an effect of increasing the critical temperature by only 2 K, while the difference between methylcyclohexane and ethylcyclohexane produces a difference of almost 10 K. In addition, it can be observed that increasing the size of the components decreases the critical composition.

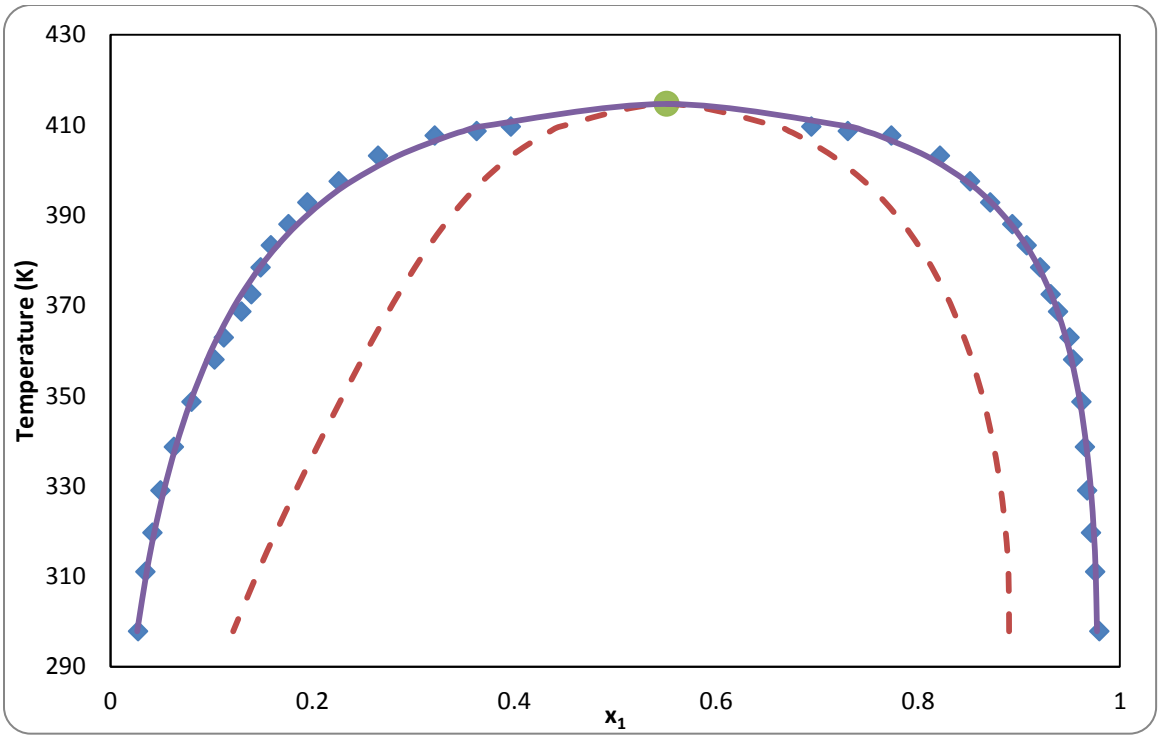

Figure 2.1-28: Binodal & Spinodal curves for Ethylcyclohexane (1) + NFM (2). Experimental points (■), Binodal curve from NRTL (—), Spinodal curve (- -), and critical point (•).

It is worth mentioning that NFM binary systems exhibit symmetry in spinodal curve. As a result of this symmetry, predicting the critical temperature is difficult using tangent plane analysis as it may lead to trivial solution.

Table 2.1-10 Critical temperature & composition determined for n-Alkanes (1)+ NFM (2) with reported literature data.

	Critical Temperature (K)		Critical composition	
System (+NFM)	**This work**	**Literature**	**This work**	**Literature**
Methycyclopentane	402.91	403.29 [92]	0.594	0.5933 [92]
Methylcyclohexane	404.8	404.78 [92]	0.571	0.5707 [92]
Ethylcyclohexane	414.65	414.73 [92]	0.551	0.5509 [92]
Pentane	443.92	-	0.565	-
Hexane	452.08	-	0.525	-
Heptane	466.07	-	0.377	-
Octane	478.85	-	0.453	-

2.1.4 Hydrocarbons + Sulfolane

In this section, stability limits were determined for Sulfolane + n-alkanes and Sulfolane + cycloalkanes, as shown in table 2.1-11 along with their cited references. Experimental data were correlated using NRTL model and regressions for all systems were performed using Aspen Plus®. Maximum Likelihood objective function was employed to find the optimum binary parameters of NRTL to fit the experimental data. The percent absolute average deviations (AAD %) of the regression are shown in table 2.1-12.

Table 2.1-11 Range of temperature and composition for Hydrocarbons (1) + Sulfolane (2) systems.

System (+ Sulfolane)	Temperature range (K)	Composition range
Pentane [87]	304.31-380.35	0.058-0.998
Hexane [87]	300.3-429.93	0.009-0.999
Heptane [87]	309.09-429.24	0.006-0.999
Octane [87]	298.15-373.15	0.009-0.999
Methylcyclopentane [94]	304.32-444.67	0.027-0.986
Methylcyclohexane [94]	303.96-464.91	0.019-0.999
Ethylcyclohexane [94]	314.29-451.15	0.013-0.993

Temperature dependent binary interaction model (equation) to correlate NRTL model was used to have enhanced prediction of LEE equilibrium composition near the critical region:

$$\tau_{ij} = A_{ij} + \frac{B_{ij}}{T} + C_{ij}\ln T + D_{ij}\cdot T \qquad (2.5)$$

The coefficients A_{ij}, B_{ij}, and C_{ij} are shown in table 2.1-12.The non-randomness parameter (α) was chosen to be 0.2 for all systems.

Table 2.1-12 Binary interaction parameters for Hydrocarbons (1) + Sulfolane (2) binary systems, α =0.2 for all systems.

	ij=12	ij=21
Pentane(1) + Sulfolane(2)		
Aij (J/ mol)	-44.299	-3.497
Bij (J/ mol)	9190.924	7572.914
Cij (J/ mol)	3.288	-7.661
Dij (J/ mol)	0.0073	0.078
Hexane(1) + Sulfolane(2)		
Aij (J/ mol)	-100	13.539
Bij (J/ mol)	7619.619	794.673
Cij (J/ mol)	14.008	-2.359
Heptane(1) + Sulfolane(2)		
Aij (J/ mol)	2.296	-100
Bij (J/ mol)	2680.388	6286.565
Cij (J/ mol)	-1.023	14.355
Octane(1) + Sulfolane(2)		
Aij (J/ mol)	-100	-20.278
Bij (J/ mol)	7928.152	2243.733
Cij (J/ mol)	13.757	2.761
Methylcyclopentane(1) + Sulfolane(2)		
Aij (J/ mol)	0.166	-1.957
Bij (J/ mol)	840.012	1233.143
Methylcyclohexane(1) + Sulfolane(2)		
Aij (J/ mol)	-1.938	-1.497
Bij (J/ mol)	1821.563	1029.268
Ethylcyclohexane(1) + Sulfolane(2)		
Aij (J/ mol)	-1.657	-2.769
Bij (J/ mol)	1601.083	1770.724

Figures 2.1-29 to 2.1-35, illustrate the binodal curve calculated using the regressed NRTL binary interaction parameters, along with the experimental data point. The percent absolute average deviations of the regression are given in table 2.1-13. Overall, the

regressed binary parameters of NMP binary systems were capable to reconstruct the binodal curve with reasonable accuracy.

Table 2.1-13 The percent absolute average deviations (AAD%) of NRTL model for Hydrocarbons (1) + Sulfolane (2) systems.

System (+ Sulfolane)	Hydrocarbon rich phase	Sulfolane rich phase
Pentane	0.189	0.50
Hexane	0.14	6.35
Heptane	15.90	0.17
Octane	0.11	3.61
Methylcyclopentane	0.26	4.86
Methylcyclohexane	0.27	8.90
Ethylcyclohexane	0.30	4.40

Though most AAD% are less than 5% for n-alkanes + Sulfolane indicating accurate regression of experimental data, it must be noted that the results of Heptane + Sulfolane, Octane + Sulfolane and to some extent Hexane + Sulfolane must be used with caution. The experimental data available are distant from the critical point and graphically do not depict any trend of binodal curve, whereas the experimental binodal curve is given as almost two horizontal lines. Consequently, it is not practical to expect regressed binary parameters to predict the binodal curve at higher temperatures. Therefore, binodal curve obtained from NRTL can only accurately predict the phase equilibrium in the region where experimental data were regressed.

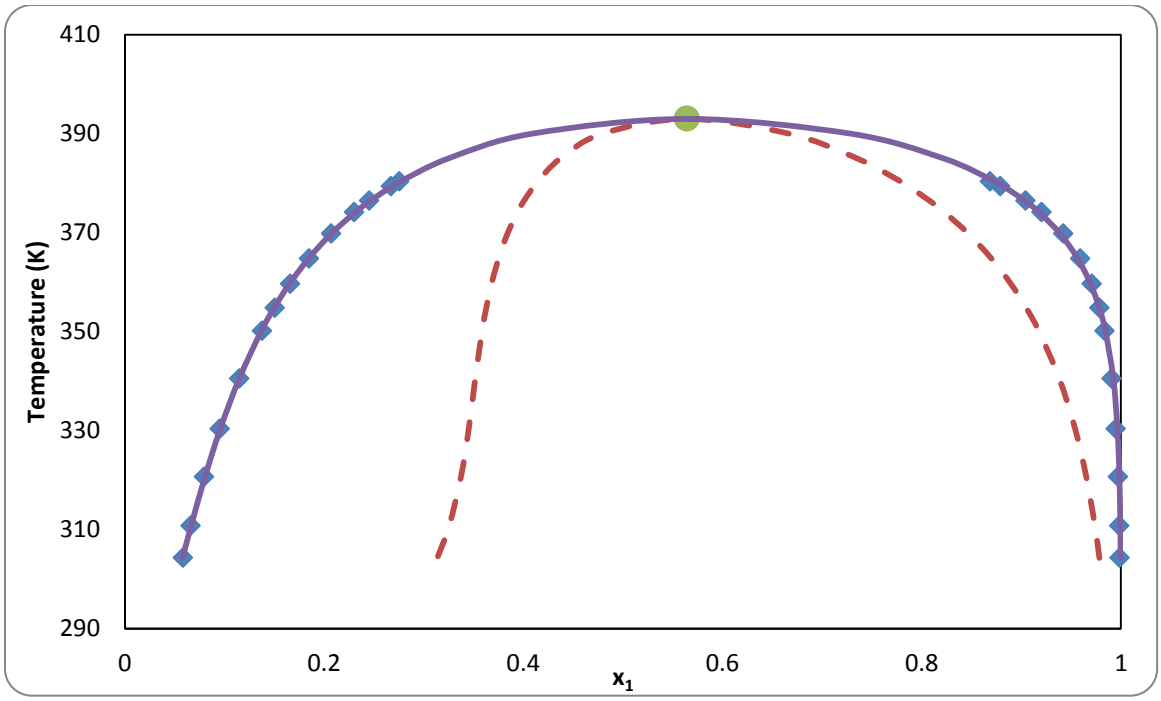

Figure 2.1-29:Binodal & Spinodal curves for Pentane (1) + Sulfolane (2) Experimental points (■), Binodal curve from NRTL (—), Spinodal curve (- -), and critical point (•).

For all branched cycloalkanes + Sulfolane there seems to be less prediction of equilibrium compositions in Sulfolane rich phase (x_1>0.9). This can be attributed to the fact that the composition of sulfolane over a wide range of temperature is relatively constant as depicted by the vertical line of sulfolane rich phase. This behaviour would be very difficult to be accurately predicted by NRTL, as evident in this case. Moreover, attaining AAD% less than 10% is considered a very good result and as apparent from figures 2.1-33 to 2.1-35, there seems to be good representation of predicted binodal curve from NRTL.

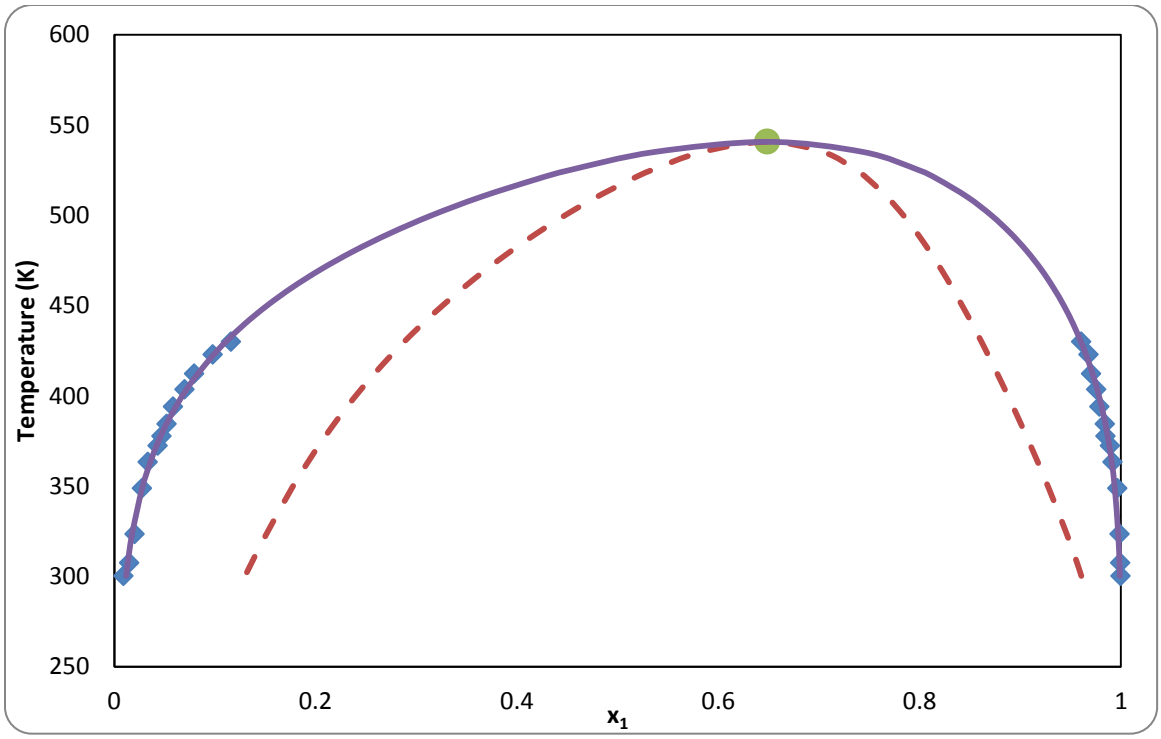

Figure 2.1-30: Binodal & Spinodal curves for Hexane (1) + Sulfolane (2) Experimental points (■), Binodal curve from NRTL (—), Spinodal curve (- -), and critical point (•).

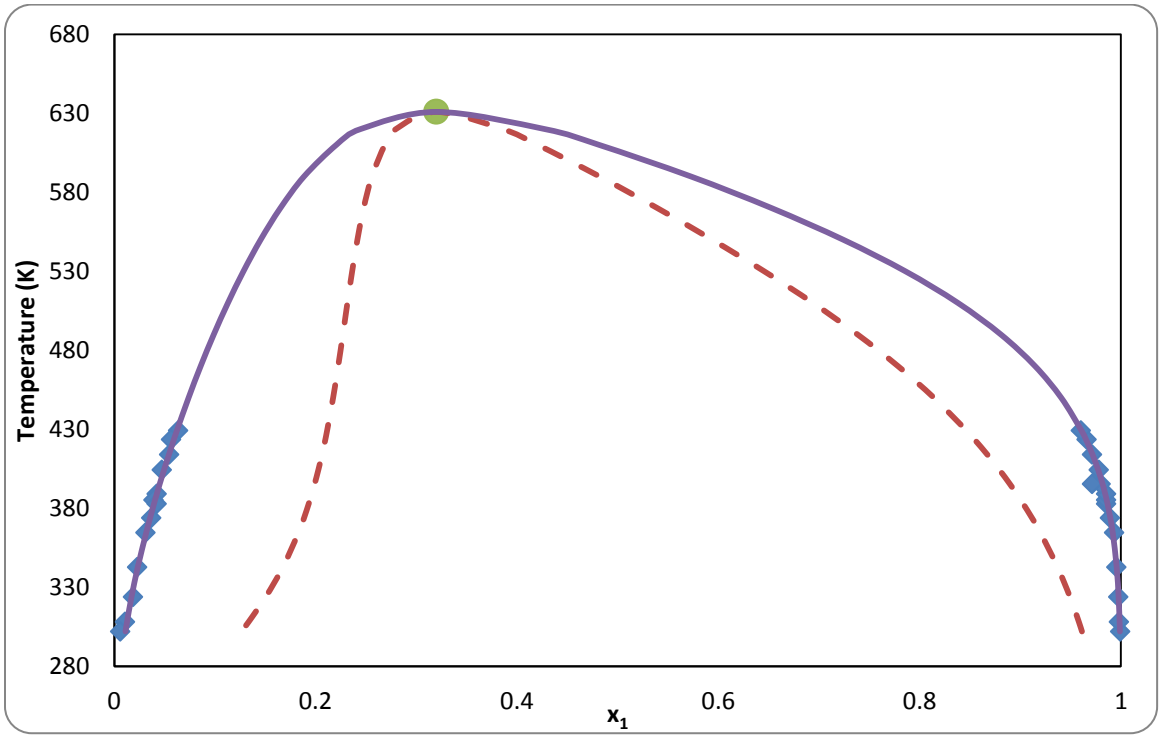

Figure 2.1-31: Binodal & Spinodal curves for Heptane (1) + Sulfolane (2) Experimental points (■), Binodal curve from NRTL (—), Spinodal curve (- -), and critical point (•).

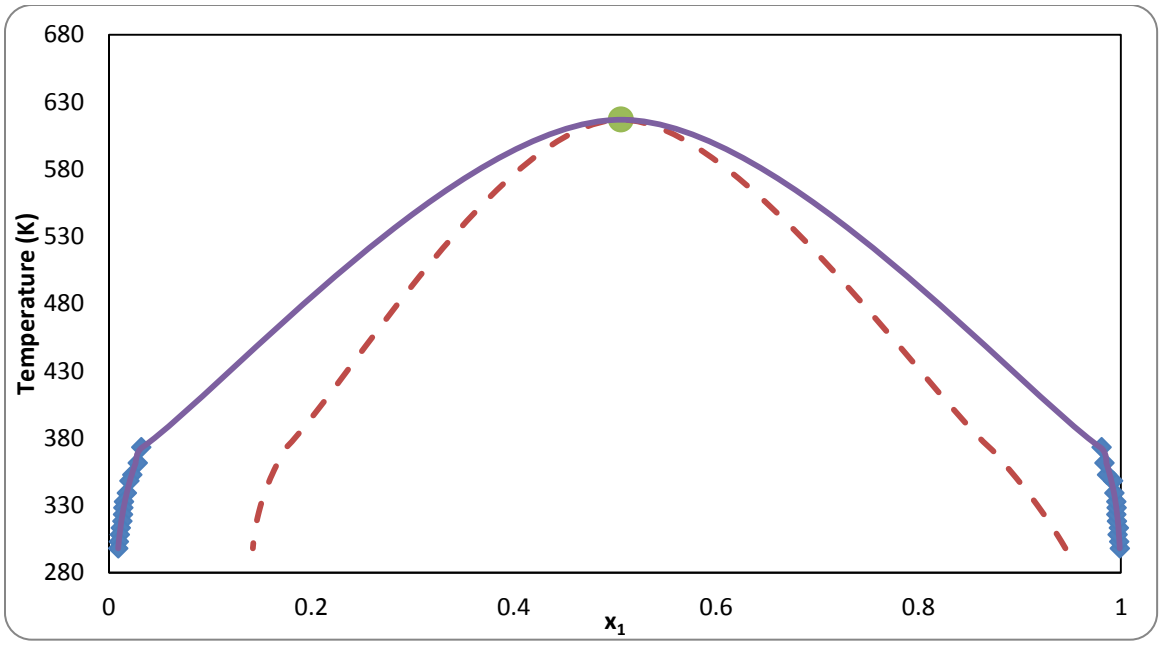

Figure 2.1-32: Binodal & Spinodal curves for Octane (1) + Sulfolane (2) Experimental points (■), Binodal curve from NRTL (—), Spinodal curve (- -), and critical point (•).

The predicted spinodal curves and critical points are depicted in figures 2.1-29 to 2.1-35, for all Sulfolane binary systems. All binary systems studied follow the expected theoretical behaviour, having the binodal and spinodal curve converge at precisely the critical temperature. However, Heptane + Sulfolane exhibit an odd trend of being highly skewed to the left. It starts symmetrical at low temperatures and shows a sudden shift in spinodal curve. Similar trend is shown by Hexane + Sulfolane to a lesser extent and being shifted to the left. As mentioned earlier, due to lack of enough well-presented experimental data that led to poor correlation of NRTL model, it is expected to reach inaccurate results in spinodal curve.

High degree of symmetry for spinodal curves is maintained throughout branched cycloalkane + Sulfolane, where the critical composition falls between 0.55-0.6.

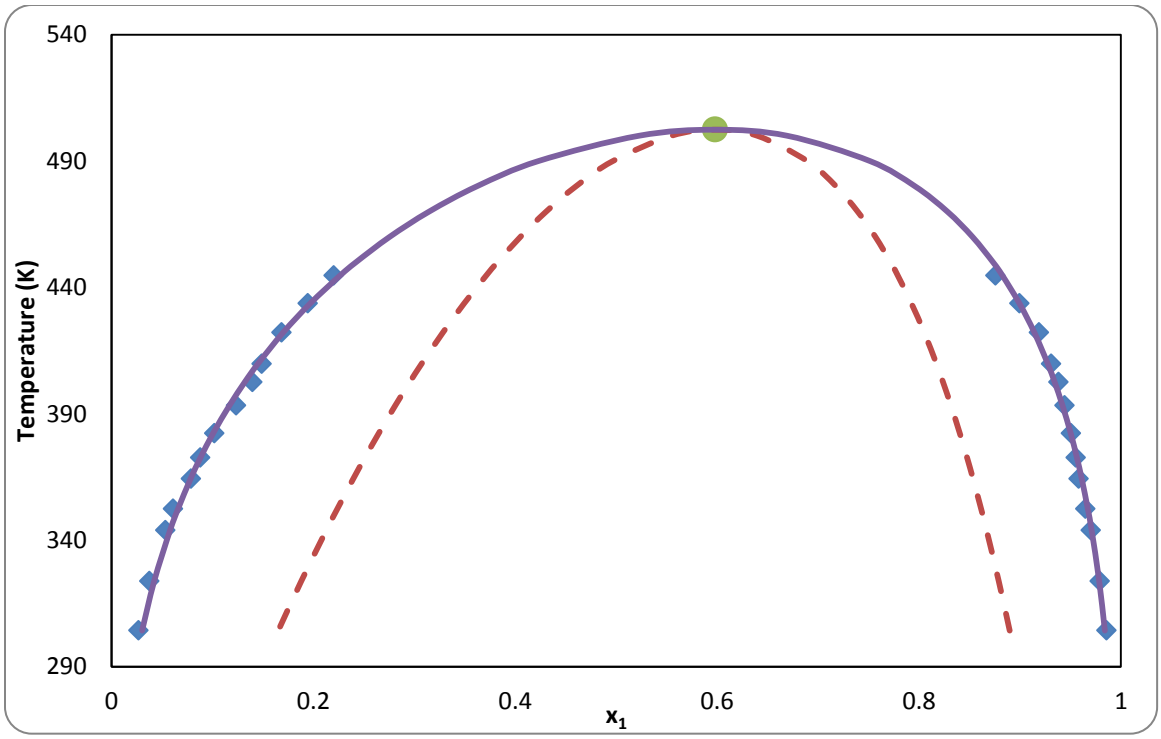

Figure 2.1-33: Binodal & Spinodal curves for Methylcyclopentane(1) + Sulfolane(2)Experimental points (■), Binodal curve from NRTL (—), Spinodal curve (- -), and critical point (•).

The critical temperatures calculated for this series are tabulated in table 2.1-14 together with their corresponding critical compositions. Unfortunately, there were no experimental data nor calculated critical temperatures and compositions reported in literature to compare the results obtained here. It must be mentioned the calculated critical temperatures and compositions for Hexane, Heptane, and Octane + Sulfolane must be used with caution due to the poor correlation of binary parameters of NRTL.

All binary systems of Sulfolane have Upper Critical Solution Temperature (UCST), which is quite common for most binary systems. There is confirmed trend of having critical temperature increasing with n-alkane size, if results obtained from Heptane + Sulfolane are ignored. Additionally, there was no pronounced trend shown for branched cycloalkanes + Sulfolane for critical temperature with increasing neither the cycloalkane size nor branch size. There is only 1 K difference in critical temperature between Methylcyclopentane and Ethylcyclohexane.

Moreover, there was a decrease in critical temperature observed moving from Methylcyclopentane to Methylcyclohexane indicating there is a possible decrease in temperature, as the cycloalkane size grew larger. In any case, no definite trend can be established as there are only three binary systems for cycloalkanes + Sulfolane.

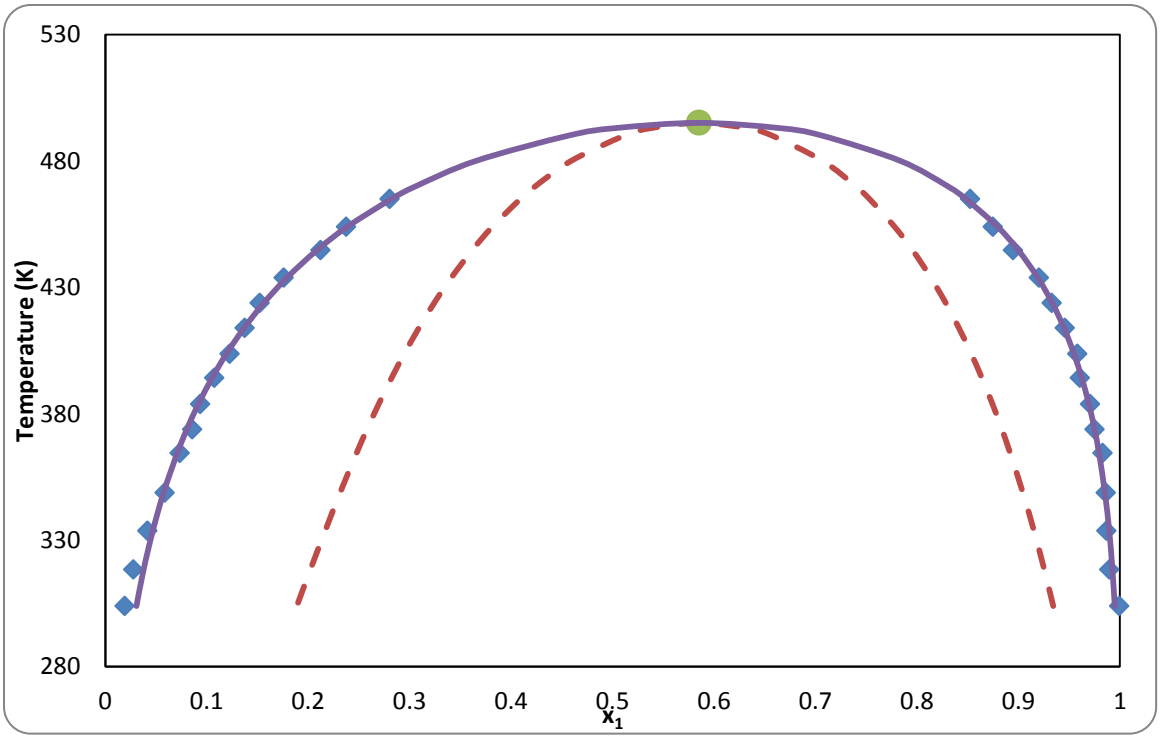

Figure 2.1-34: Binodal & Spinodal curves for Methylcyclohexane(1) + Sulfolane (2) Experimental points (■), Binodal curve from NRTL (—), Spinodal curve (- -), and critical point (•).

As evident from the results obtained for Hexane, Heptane, and Octane + Sulfolane the prediction of stability limits is highly dependent on the experimental data range. That's because the binary parameters of NRTL are obtained by regressing the experimental data and the binary parameters are used in NRTL along with stability criteria to find the stability limits. This proves that even though we employ highly rigorous method to find the stability limits, its weakness lies in the available experimental data range and certainly in the quality of the regression.

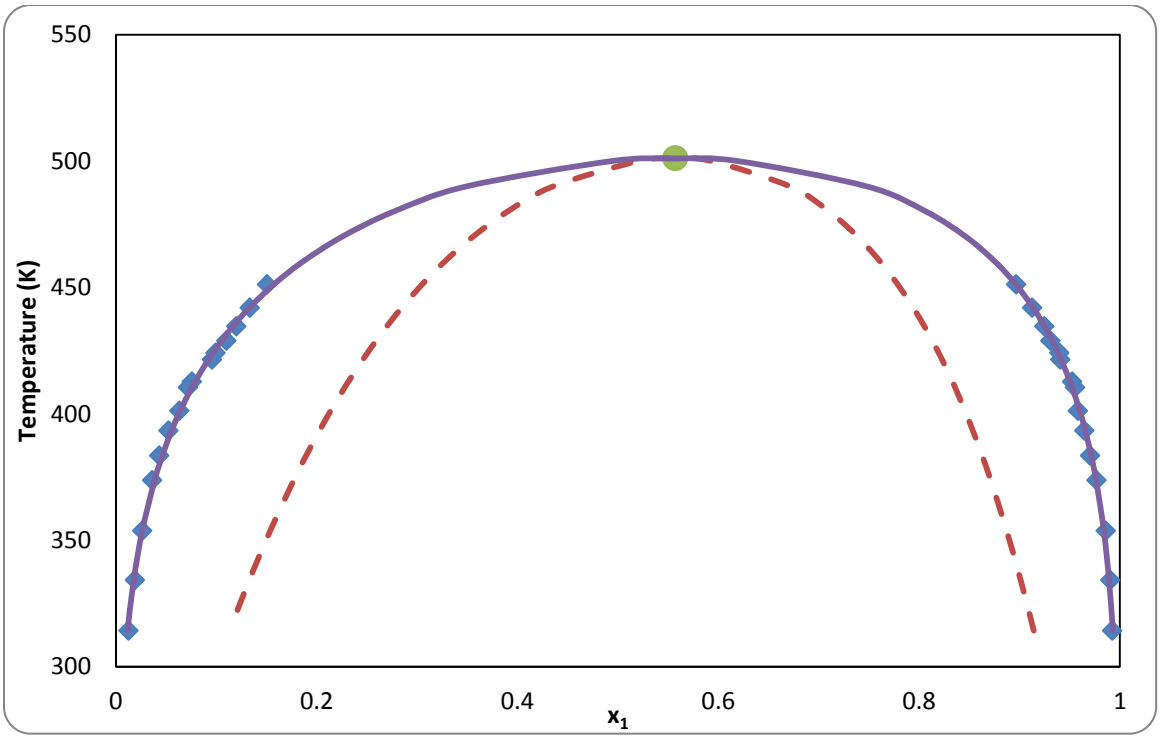

Figure 2.1-35: Binodal & Spinodal curves for Ethylcyclohexane(1) + Sulfolane (2) Experimental points (■), Binodal curve from NRTL (—), Spinodal curve (- -), and critical point (•).

Table 2.1-14 Critical temperature & composition determined for Hydrocarbons (1) + Sulfolane (2) binary systems.

	Critical Temperature (K)		Critical composition	
System (+ Sulfolane)	**This work**	**Literature**	**This work**	**Literature**
Pentane	392.98	-	0.5643	-
Hexane	540.64	-	0.6489	-
Heptane	630.86	-	0.3201	-
Octane	616.75	-	0.506	-
Methylcyclopentane	502.4	-	0.5982	-
Methylcyclohexane	495.04	-	0.5852	-
Ethylcyclohexane	501.0	-	0.5573	-

2.1.5 1,3-Propanediol + Ionic Liquids

We intend to examine if stability limits can be predicted for ionic liquids binary systems using the same methodology used in this thesis. The experimental data range of 1,3 propanediol (PDO) + ionic liquids: 1-butyl- 3 methylimidazolium hexafluorophosphate [bmim][PF6], 1-butyl-3-methylimidazolium tetrafluoroborate [bmim][BF4], and1-ethyl-3-methylimidazolium tetrafluoroborate [emim][BF4] are given in table 2.1-15. The binary interaction parameters of NRTL were found in literature and used here for further analysis [95].

Table 2.1-15 Range of temperature and composition for 1,3-Propanediol (1) + Ionic Liquids (2) systems [95].

System (1,3 Proanediol (PDO)+ alkanes)	Temperature range (K)	Composition range
1-butyl- 3 methylimidazoliumhexafluorophosphate [bmim][PF6] [95]	287.8-323.4	0.114-0.994
1-butyl- 3-methylimidazolium tetrafluoroborate [bmim][BF4] [95]	286.7-291.9	0.540-0.894
1-ethyl-3-methylimidazolium tetrafluoroborate [emim][BF4] [95]	286.6-303.3	0.238-0.970

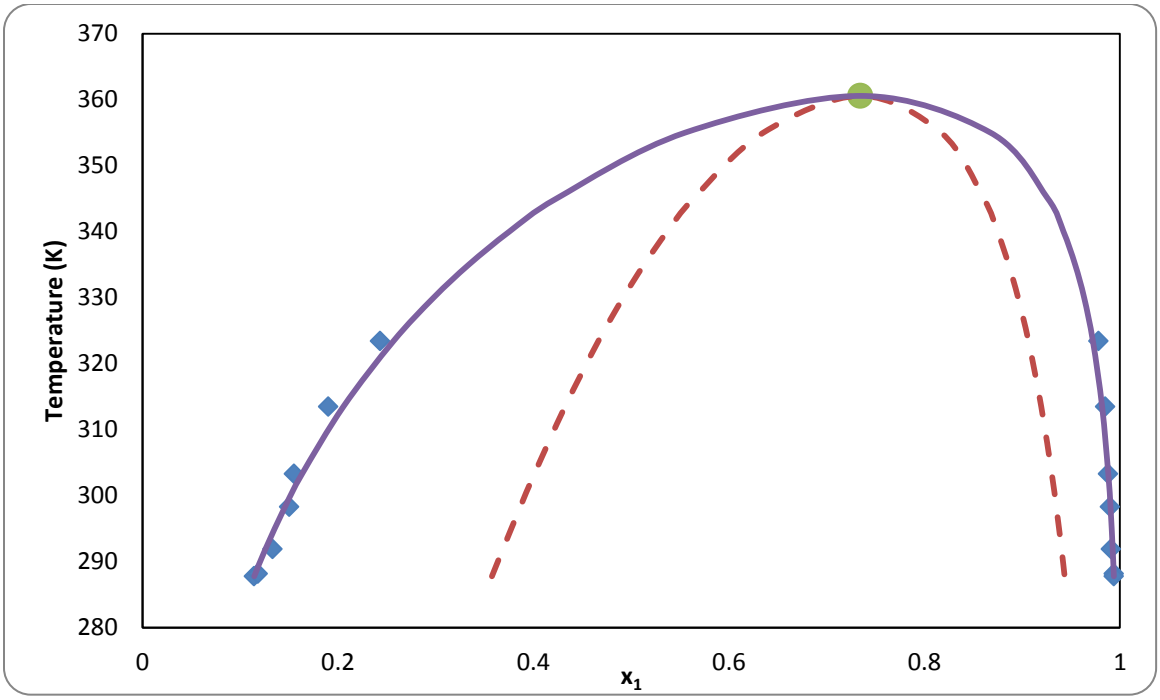

Figure 2.1-36:Binodal & Spinodal curves for 1,3-Propanediol (1) +1-butyl-3- Methylimidazolium hexafluorophosphate(2) Experimental points (■), Binodal curve from NRTL (—), Spinodal curve (- -), and critical point (•).

Figures 2.1-36, 2-37, & 2.1-38 illustrate the binodal and spinodal curves along with critical temperature for PDO (1)+[bmim][PF6] (2), PDO (1)+ [bmim][BF4] (2), and PDO (1)+[bmim][BF4] (2). For each binary system, solving the stability limit criterion generated the spinodal curve while calculating the two highly coupled stability and criticality criteria determined the critical temperature of each binary at the reported pressure of the experimental data.

The results of spinodal curve conform to the expected theoretical behavior, where the spinodal and binodal curve intersect exactly at the critical temperature. All spinodal curves of PDO binary systems appear to be skewed to the right resulting in a wider metastable region in ionic rich phase (x_1<0.4).

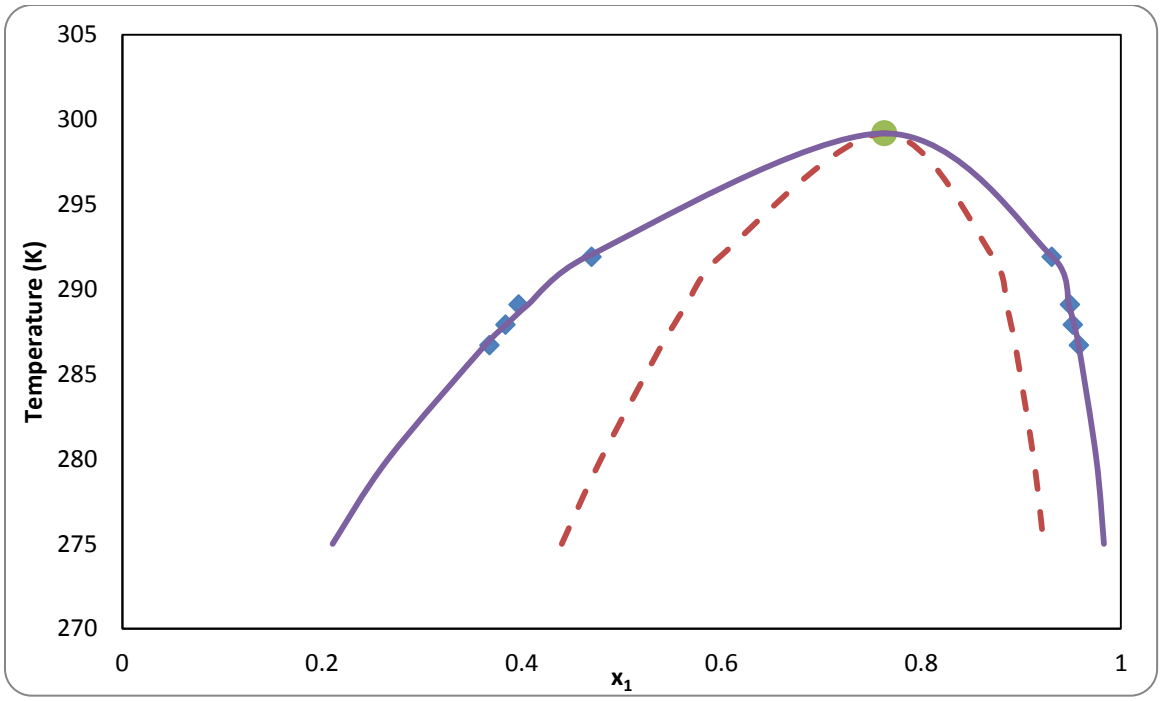

Figure 2.1-37:Binodal & Spinodal curves for 1,3-Propanediol (1) + 1-butyl-3-Methylimidazolium tetrafluoroborate(2) Experimental points (■), Binodal curve from NRTL (—), Spinodal curve (- -), and critical point (•).

All ionic-liquids binary systems showed Upper Critical Solution Temperature (UCST) as expected since all monoalcohol + ionic liquid mixtures reported in literature have shown UCST [95]. It is interesting to note here that increasing the alkyl group on the cation will decrease the UCST. As shown for [bmim][BF4] and [emim][BF4], where the alkyl group was changed from butyl to ethyl, the UCST decreased from 360.57 K to 310.43 K as shown in table 2.1-16. On the contrary, increasing anion size will increase the UCST.

The critical temperatures and compositions determined for ionic liquids binary systems are given in table 2.1-16 along with the reported literature values. Critical temperatures and compositions calculated here concur well with the reported literature.

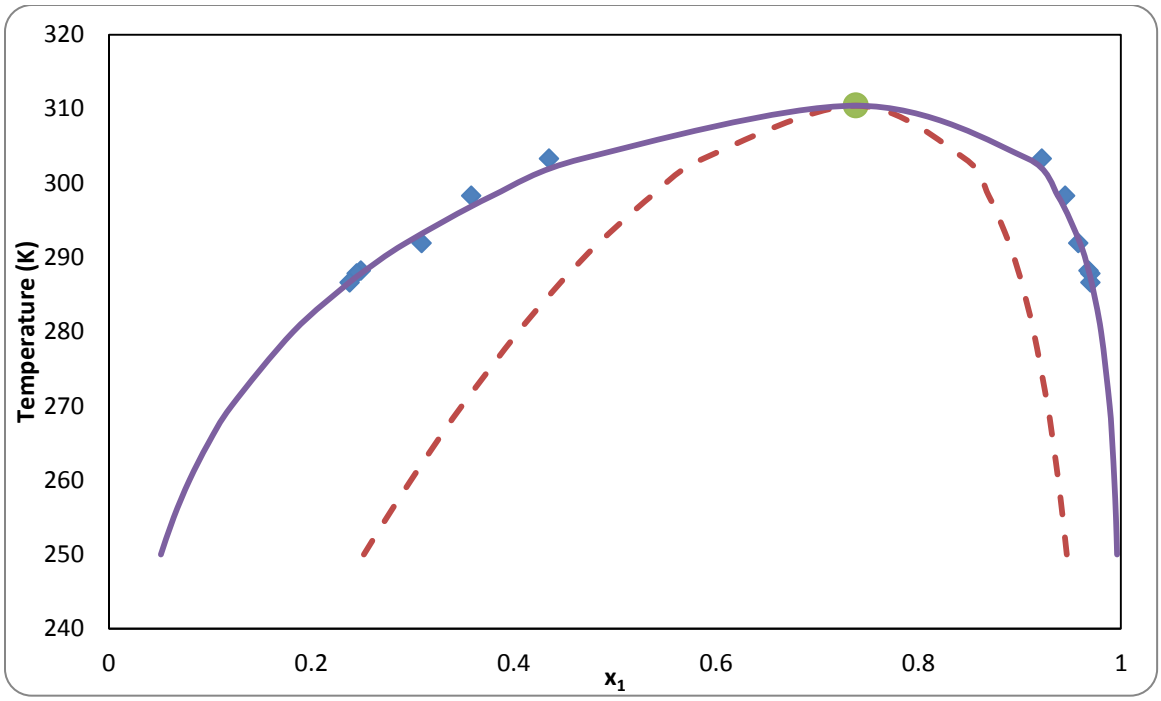

Figure 2.1-38: Binodal & Spinodal curves for 1,3-Propanediol (1) +1-ethyl-3-methylimidazolium tetrafluoroborate(2) Experimental points (■), Binodal curve from NRTL (—), Spinodal curve (- -), and critical point (•).

Table 2.1-16 Critical temperature & composition determined for 1,3-Propanediol (1) + Ionic Liquids (2) systems with values found in literature.

	Critical Temperature (K)		Critical composition	
System (1,3 Proanediol (PDO)+ alkanes)	**This work**	**Literature**	**This work**	**Literature**
1-butyl- 3 methylimidazoliumhexafluorophosphate [bmim][PF6]	360.57	360 [95]	0.734	0.74 [95]
1-butyl- 3-methylimidazolium tetrafluoroborate [bmim][BF4]	299.18	299 [95]	0.763	0.74 [95]
1-ethyl-3-methylimidazolium tetrafluoroborate [emim][BF4]	310.43	310 [95]	0.738	0.77 [95]

2.1.6 N-methyl-α -pyrrolidone+ n-alkanes

Table 2.1-17 shows the different binary systems studied for N-methyl-α -pyrrolidone (NMP)+ Hydrocarbons, together with the references citing their available experimental range data in the literature. For NMP + alkanes (C10-C14), the interaction parameters required by the NRTL model for the optimum fit of the binodal equilibrium data of binary systems were reported in the literature [96]. As for all other binary systems, the energy binary interactions parameters of NRTL were regressed; the percent absolute average deviations (AAD %) of the regression are shown in table 2.1-18. It must be noted that there are there are two experimental data points of NMP+decane binary system, as highlighted in table 2.1-17.

Table 2.1-17 Range of temperature and composition for N-methyl-α –pyrrolidone (1) + n-Alkanes (2) systems.

System (N-methyl-α -pyrrolidone+)	Temperature range (K)	Composition range
Hexane [96]	284.92-323.53	0.056-0.854
Octane [96]	279.4-329.54	0.133-0.930
Decane [96]	293.88-309.35	0.161-0.942
Decane [97]	322.14-336.78	0.292-0.733
Undecane [96]	308.35-340.78	0.103-0.858
Dodecane [96]	317.95-344.75	0.229-0.779
Tridecane [96]	329.65-348.15	0.224-0.919
Tetradecane [96]	332.66-354.61	0.415-0.849
Cyclohexane [97]	278.02-289.13	0.105-0.692
Cyclooctane [97]	286.35-291.49	0.173-0.681
2-Methylpentane [97]	281.03-325.89	0.076-0.871
3-Methylpentane [97]	282.36-319.42	0.099-0.847
Isooctane [97]	286.52-327.15	0.068-0.895
2,2-Dimethylbutane [97]	279.88-322.87	0.069-0.855
2,3-Dimethylbutane [97]	283.2-316.03	0.074-0.820

The regression of NMP systems experimental data was performed to find NRTL binary interaction parameters. Aspen Plus ® V 7.3 was used for this purpose by employing the maximum likelihood objective function to find the optimum binary interaction parameter capable of fitting the experimental data. The temperature dependent binary interaction model used for these binary systems is shown below:

$$\tau_{ij} = A_{ij} + \frac{B_{ij}}{T} + C_{ij} \ln T \tag{2.8}$$

The coefficients A_{ij},B_{ij}, and C_{ij} are presented in table 2.1-18.

Table 2.1-18 Binary interaction parameters for N-methyl-α –pyrrolidone (1) + n-Alkanes (2) systems.

	ij=12	ij=21
NMP (1)+ Hexane (2)		
Aij (J/ mol)	80	80
Bij (J/ mol)	-3179.548	-1692.818
Cij (J/ mol)	-12.008	-12.670
αij	0.2	
NMP (1)+ Octane (2)		
Aij (J/ mol)	80.000	80.000
Bij (J/ mol)	-2546.762	-1977.108
Cij (J/ mol)	-12.227	-12.556
αij	0.3	
NMP (1)+ Decane (2)		
Aij (J/ mol)	-80	-64.955
Bij (J/ mol)	4257.145	6716.399
Cij (J/ mol)	11.879	7.888
αij	0.3	
NMP (1)+ Cyclohexane (2)		
Aij (J/ mol)	195.399	215.567
Bij (J/ mol)	-7908.375	-5808.449
Cij (J/ mol)	-29.514	-34.178
αij	0.3	

	ij=12	ij=21
NMP (1)+ Cyclooctane (2)		
Aij (J/ mol)	183.139	207.739
Bij (J/ mol)	-11146.129	-1422.765
Cij (J/ mol)	-25.377	-35.494
αij	0.2	
NMP (1)+ 2-Methylpentane (2)		
Aij (J/ mol)	80	80
Bij (J/ mol)	-2776.229	-2441.183
Cij (J/ mol)	-12.243	-12.236
αij	0.2	
NMP (1)+ 3-Methylpentane (2)		
Aij (J/ mol)	100	100
Bij (J/ mol)	-3561.097	-3454.273
Cij (J/ mol)	-15.300	-15.167
αij	0.2	
NMP (1)+ Isooctane (2)		
Aij (J/ mol)	80	80
Bij (J/ mol)	-2776.229	-2441.183
Cij (J/ mol)	-12.243	-12.236
αij	0.2	
NMP (1)+ 2,2-Dimethylbutane (2)		
Aij (J/ mol)	100	100
Bij (J/ mol)	-3709.745	-3382.301
Cij (J/ mol)	-15.222	-15.187
αij	0.2	
NMP (1)+ 2,3-Dimethylbutane (2)		
Aij (J/ mol)	100	100
Bij (J/ mol)	-4074.621	-2648.436
Cij (J/ mol)	-15.006	-15.643
αij	0.2	

Figures 2.1-39 to 2.1-53, illustrate the binodal curve calculated using the regressed NRTL binary interaction parameters, along with the experimental data point. The percent absolute average deviations of the regression are given in table 2.1-19. Overall, the regressed binary parameters of NMP binary systems were capable to reconstruct the binodal curve to satisfactory precision. NMP + decane show high AAD% of 14.78 in hydrocarbon rich phase, this is evident from figure 2.1-42, where the binodal curve from NRTL fails to follow the trend of experimental data points at low (less than 0.6) mole fraction.

Table 2.1-19 The percent absolute average deviations (AAD%) of NRTL model for NMP (1) + hydrocarbons (2) binary systems.

System (Acetonitrile+ alkanes)	Hydrocarbon phase	NMP phase
Hexane	0.72	1.74
Octane	0.81	1.87
Decane	2.22	14.78
Cyclohexane	1.37	4.00
Cyclooctane	0.30	2.55
2-Methylpentane	3.28	2.22
3-Methylpentane	4.76	3.76
Isooctane	2.03	2.11
2,2-Dimethylbutane	4.48	3.17
2,3-Dimethylbutane	3.10	1.68

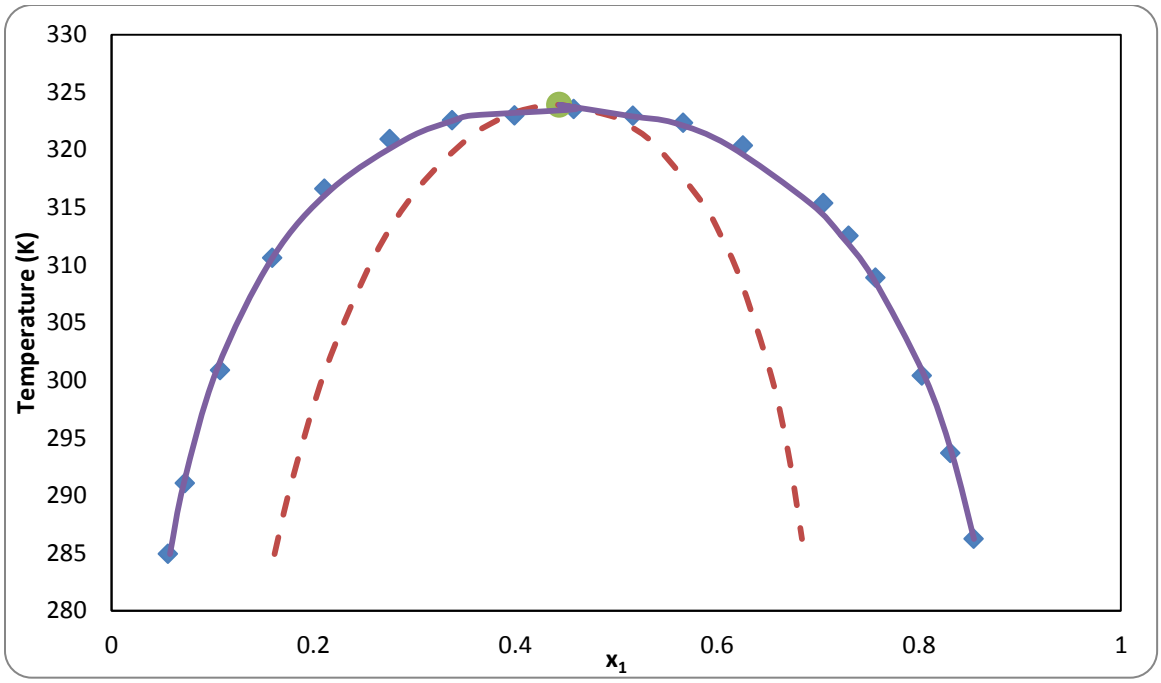

Figure 2.1-39: Binodal & Spinodal curves for N-methyl-α-pyrrolidone (1) + Hexane (2) Experimental points (■), Binodal curve from NRTL (—), Spinodal curve (- -), and criticalpoint (•).

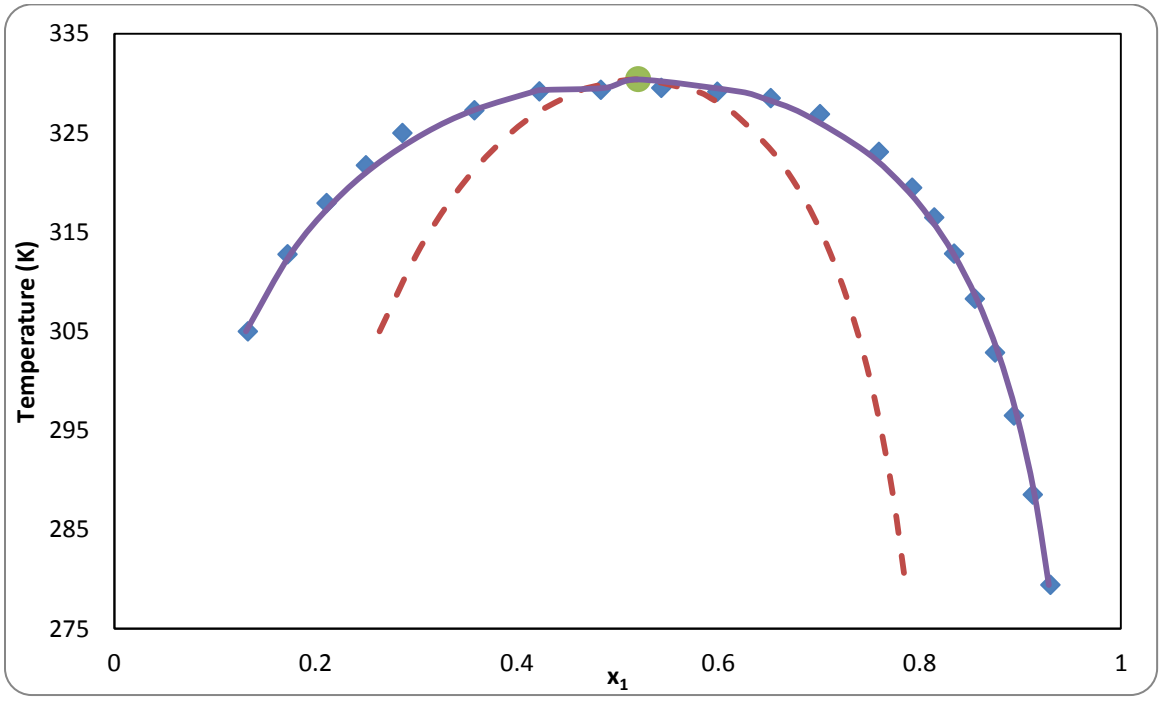

Figure 2.1-40: Binodal & Spinodal curves for N-methyl-α-pyrrolidone (1) + Octane (2) Experimental points (■), Binodal curve from NRTL (—), Spinodal curve (- -), and critical point (•).

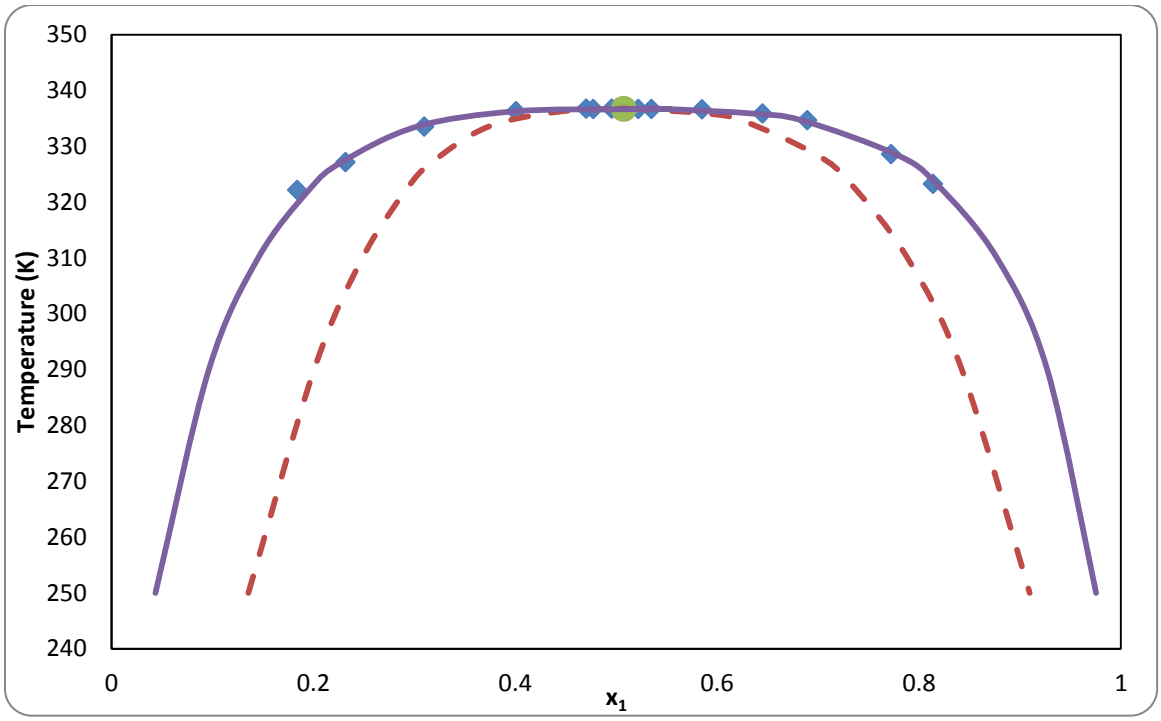

Figure 2.1-41: Binodal & Spinodal curves for N-methyl-α-pyrrolidone(1) + Decane(2) Experimental points (■), Binodal curve from NRTL (—), Spinodal curve (- -), and critical point (•).

The results of the binodal curve, spinodal curve, and critical temperature are illustrated in figures 2.1-39 to 2.1-53 for NMP binary systems. All the binary systems treated in this series conform to the anticipated theoretical behaviour, with both spinodal and binodal curves converging at exactly the critical temperature. Moreover, most of NMP binary systems exhibit non-analytical behaviour of flat slope in close proximity of the critical region. Coincidentally, experimental data points are available near the critical region to tune the binary interaction parameters so it can reproduce the experimental binodal curve effectively. For NMP+ (decane, undecane, dodecane, tridecane, and tetradecane), the non-randomness parameter taken was -1.This is rarely found in literature as the author [96] explains that it is due to the highly non-ideal nature of NMP.

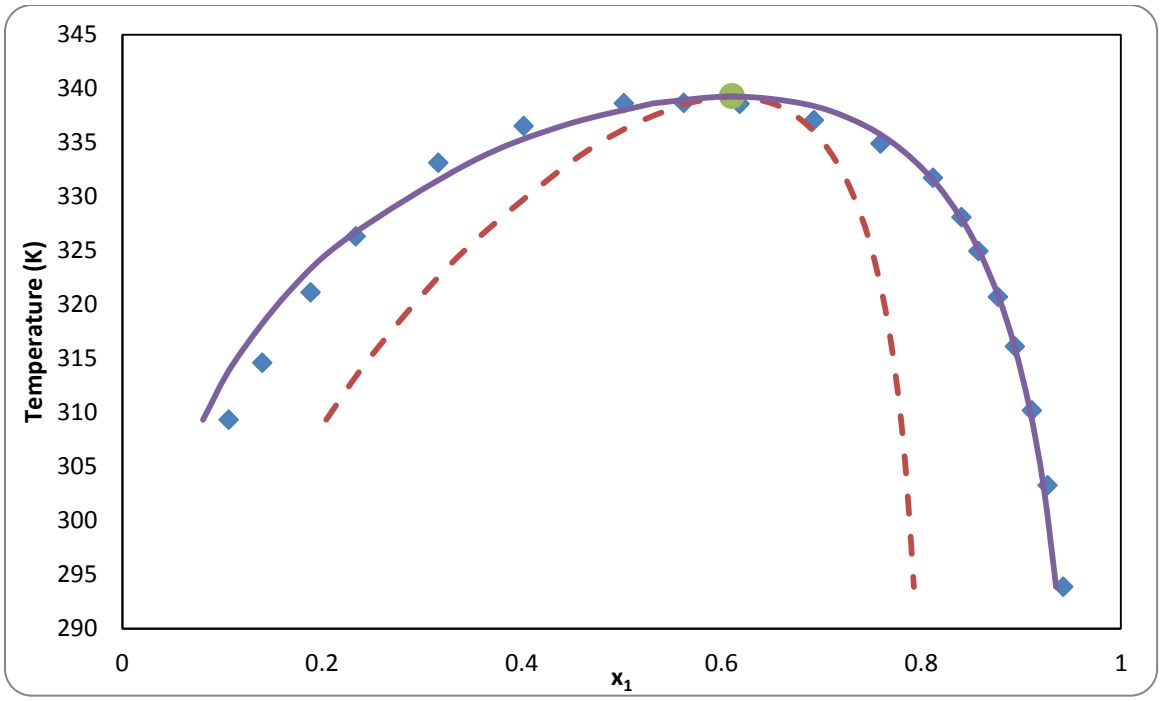

Figure 2.1-42: Binodal & Spinodal curves for N-methyl-α-pyrrolidone (1) + Decane (2) Experimental points (■), Binodal curve from NRTL (—), Spinodal curve (- -), and critical point (•).

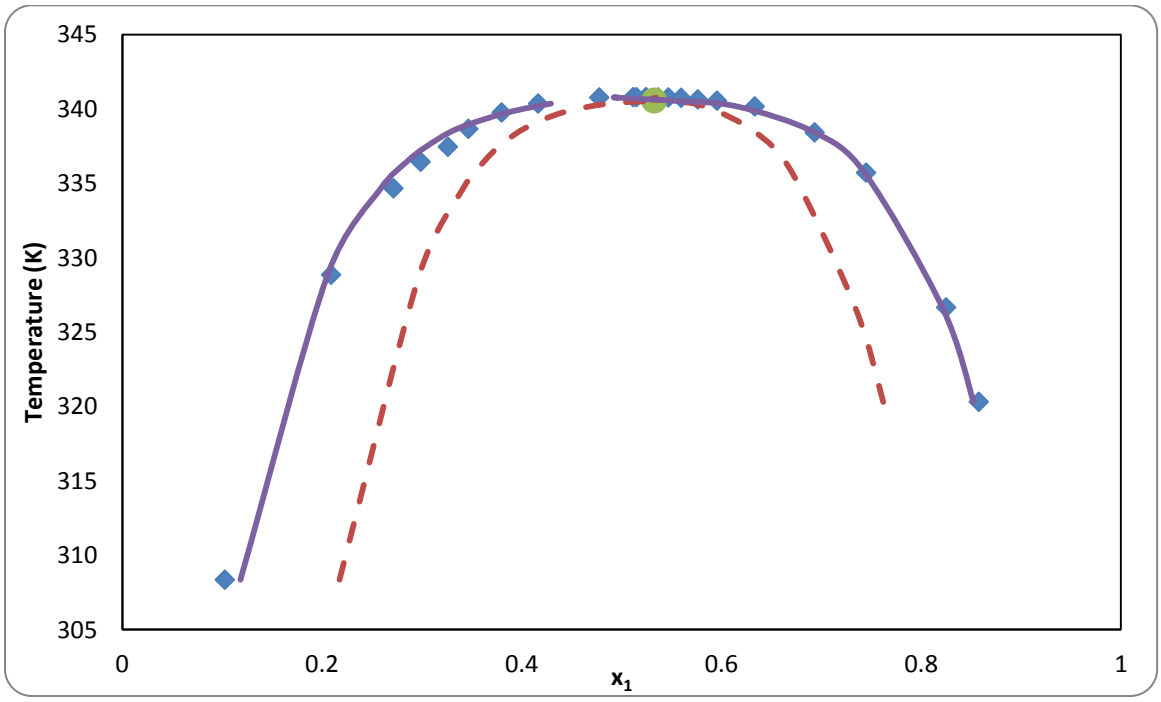

Figure 2.1-43: Binodal & Spinodal curves for N-methyl-α-pyrrolidone (1) + Undecane (2) Experimental points (■), Binodal curve from NRTL (—), Spinodal curve (- -), and critical point (•).

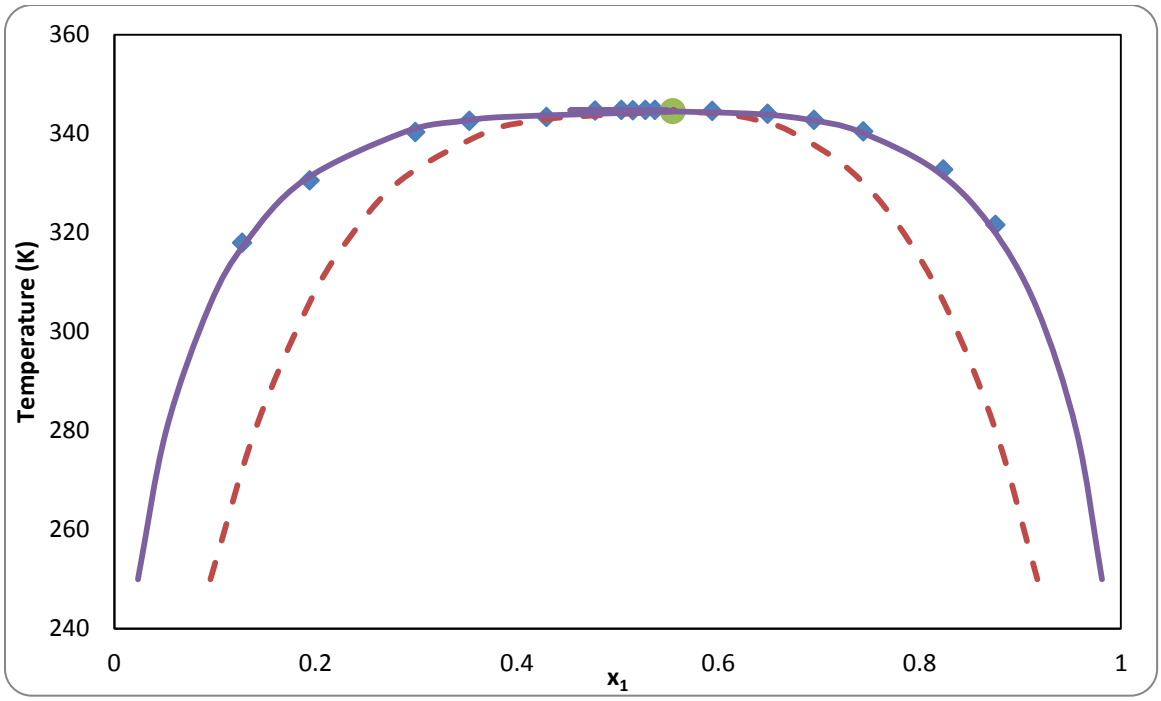

Figure 2.1-44: Binodal & Spinodal curves for N-methyl-α-pyrrolidone (1) + Dodecane (2) Experimental points (■), Binodal curve from NRTL (—), Spinodal curve (- -), and critical point (•).

There is a high degree of symmetry maintained for all spinodal curves of NMP + alkanes, as shown in figures 2.1-39 to 2.1-46. However, there is inconsistency regarding the size of the metastable region. In alkane binary systems, except for +decane +undecane and dodecane, the metastable region in alkane rich phase is wider than NMP rich phase (x_1<0.5). i.e. the metastable region can be penetrated to higher extent from the left. In NMP binary systems with decane, undecane, and dodecane the spinodal curve is symmetrical and maintains almost identical metastable areas on both sides.

It is also observed that spinodal curves do not show specific trend, even for isomers. For example, NMP + 2-Methylpentane exhibit identical trend of spinodal curve to NMP + 3-Methylpentane. Then again, dissimilar spinodal curves predicted for NMP + 2,2-Dimethylbutane and NMP + 2,3-Dimethylbutane. This proves that there is no specific trend for spinodal curves of NMP binary systems.

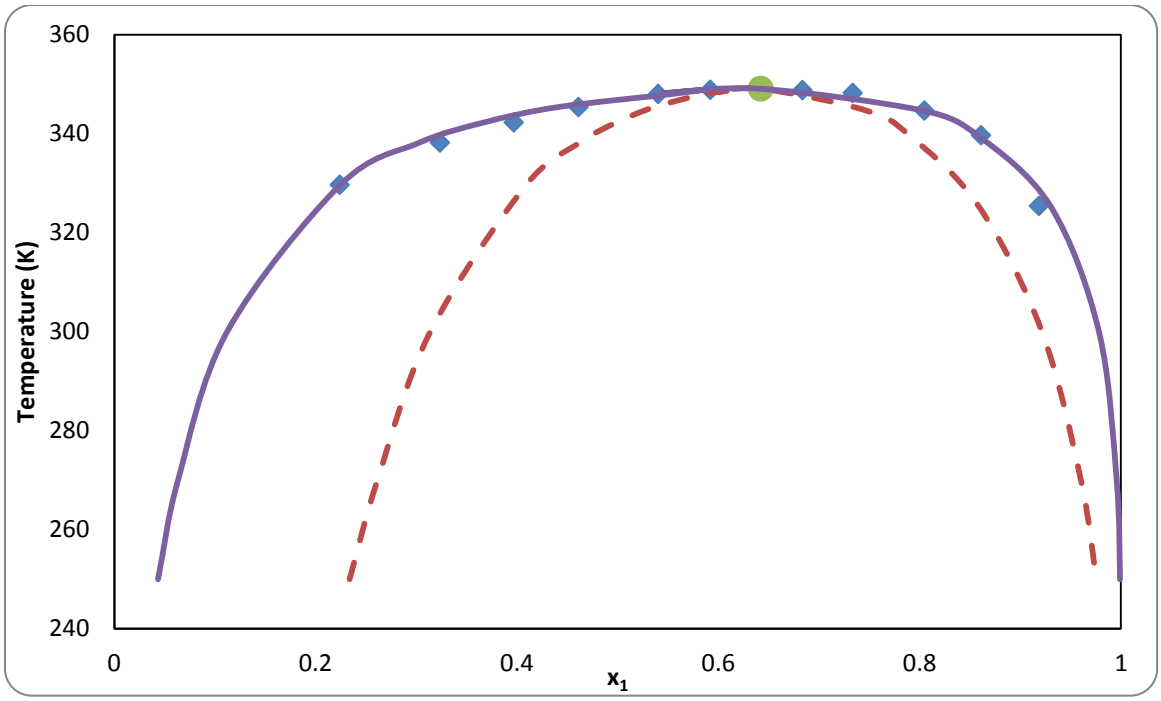

Figure 2.1-45: Binodal & Spinodal curves for N-methyl-α-pyrrolidone (1) + Tridecane (2) Experimental points (■), Binodal curve from NRTL (—), Spinodal curve (- -), and critical point (•).

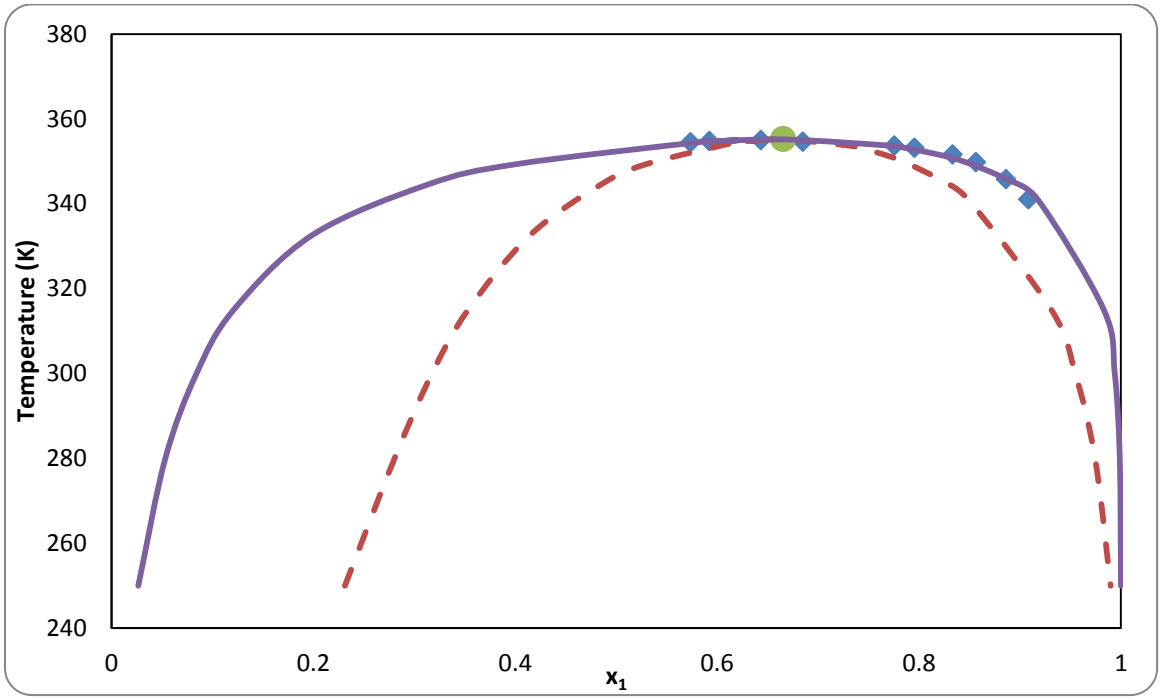

Figure 2.1-46: Binodal & Spinodal curves for N-methyl-α-pyrrolidone (1) + Tetradecane (2) Experimental points (■), Binodal curve from NRTL (—), Spinodal curve (- -), and critical point (•).

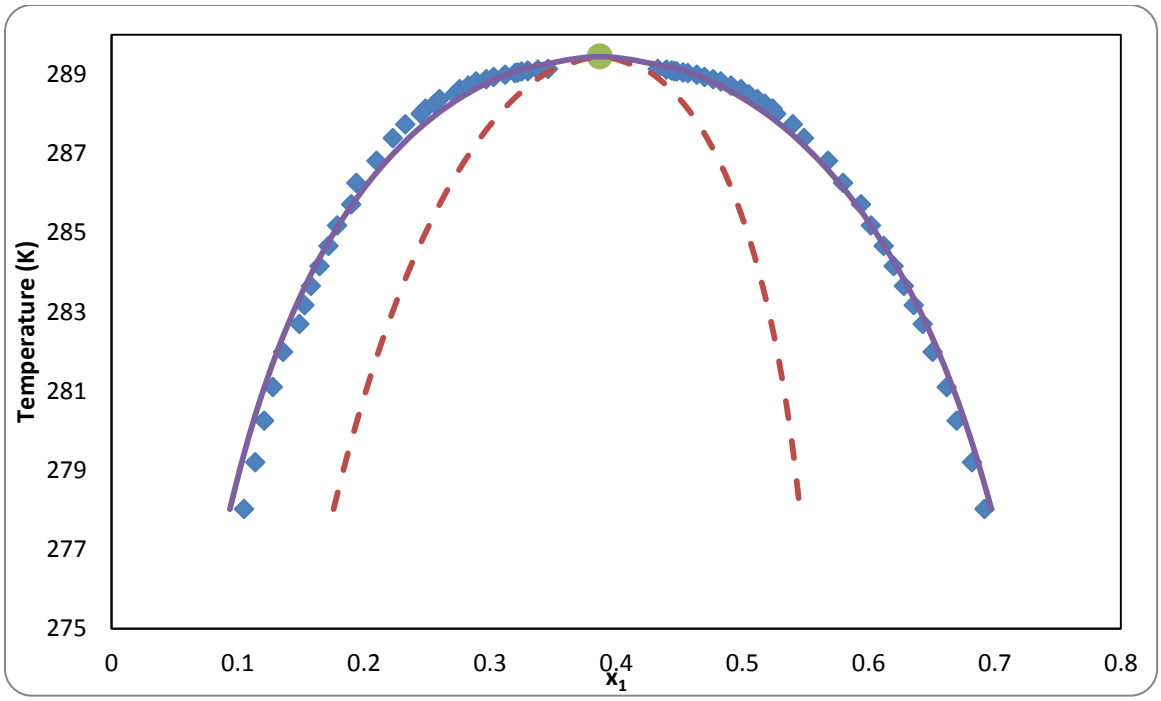

Figure 2.1-47 Binodal & Spinodal curves for N-methyl-α-pyrrolidone (1) + Cyclohexane (2) Experimental points (■), Binodal curve from NRTL (—), Spinodal curve (- -), and critical point (•).

All NMP binary systems exhibit Upper Critical Solution Temperature (UCST). For NMP + alkanes systems, the mutual solubility increases with size i.e. the critical temperature increases, as expected. The increase in critical temperature follows a linear pattern and there is an average increase of 4.5 K for critical temperatures in n-alkanes series. The critical composition varies from 0.4 to 0.66, making the spinodal and binodal curve skew to the right with increasing alkane chain size.

The critical temperatures calculated for this series are tabulated in table 2.1-20 together with their corresponding critical compositions. Available reported literatures values of critical temperature are also shown in table 2.1-20. In general, critical temperatures found NMP binary systems agree reasonably well with literature reported values.

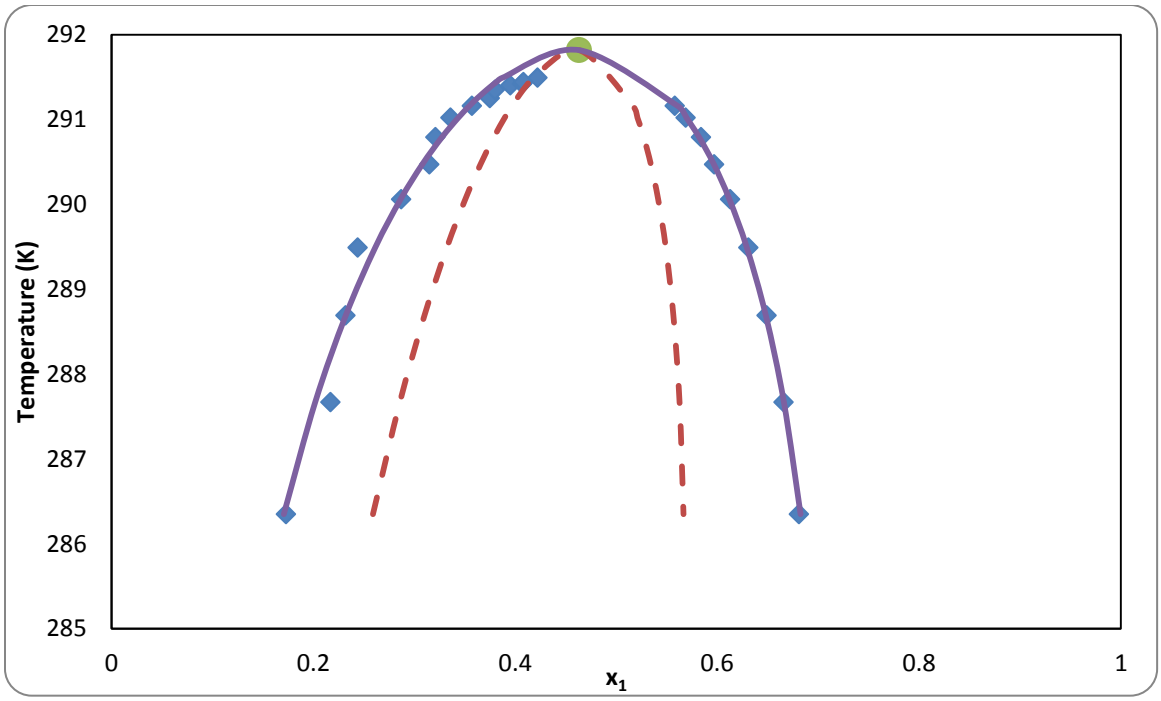

Figure 2.1-48 Binodal & Spinodal curves for N-methyl-α-pyrrolidone (1) + Cyclooctane (2) Experimental points (■), Binodal curve from NRTL (—), Spinodal curve (- -), and critical point (•).

As mentioned earlier, two experimental data sets were used for NMP + Decane, both shown in figures 2.1-41 & 2.1-42 and table 2.1-18. The calculation of critical temperature and composition vary widely using the two experimental sets. The critical temperatures found were 339.28 K and 336.64 K, where their critical compositions were calculated at, 0.611 and 0.508, respectively. This, in addition to having literature values confirmed both results. The discrepancy essentially lies in the experimental data. As shown in figures 2.1-41 & 42, both experimental binodal curves show flat slope at different temperatures in the vicinity of critical region. No plausible explanation can be provided for the inconsistency in experimental measurement. Nevertheless, this proves that the prediction of critical temperature and compositions is highly dependent on the accuracy of experimental data.

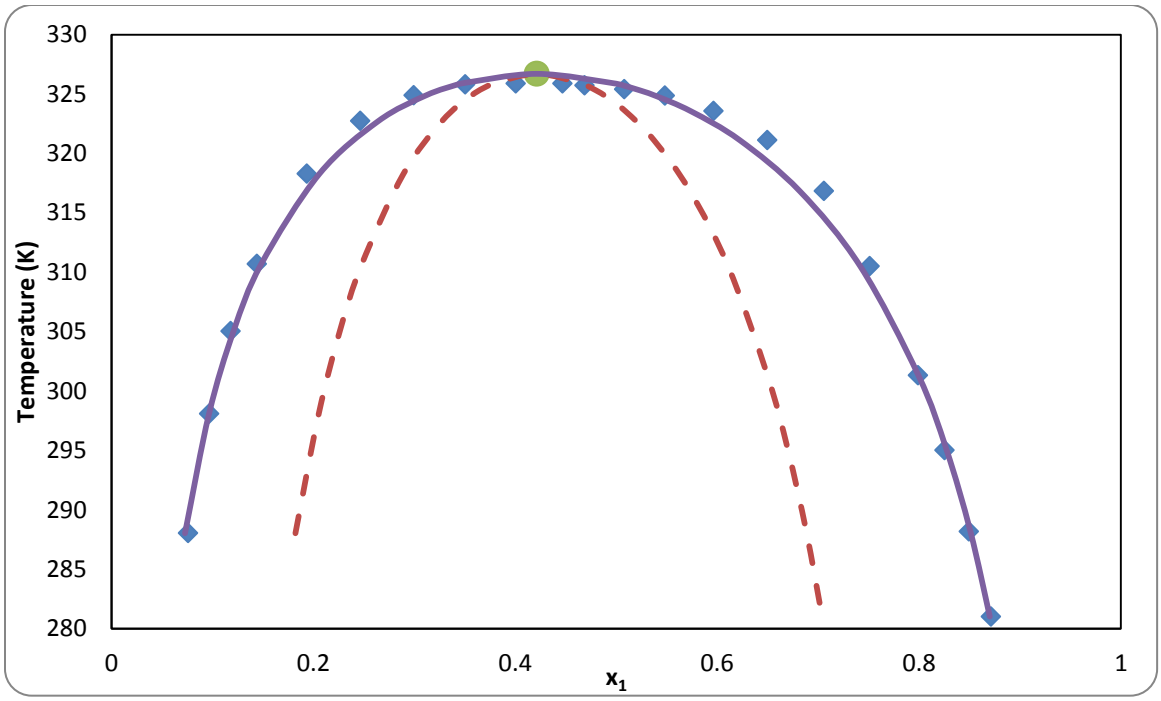

Figure 2.1-49 Binodal & Spinodal curves for N-methyl-α-pyrrolidone (1) + 2-Methylpentane (2) Experimental points (■), Binodal curve from NRTL (—), Spinodal curve (- -), and critical point (•).

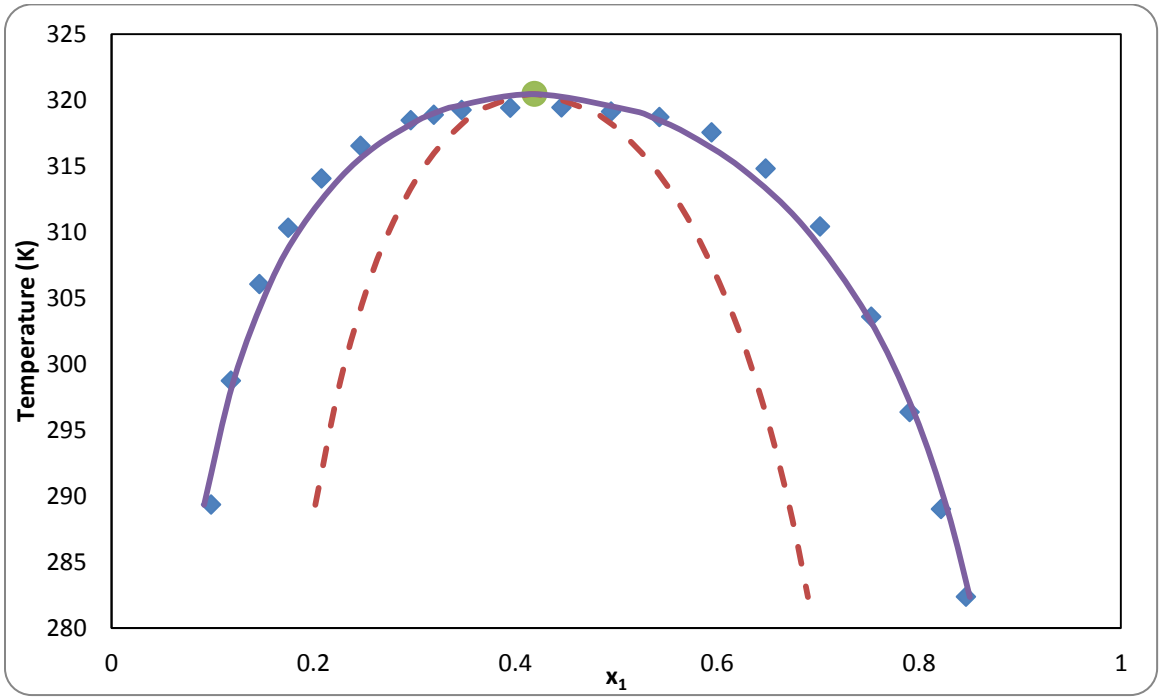

Figure 2.1-50 Binodal & Spinodal curves for N-methyl-α-pyrrolidone (1) + 3-Methylpentane (2) Experimental points (■), Binodal curve from NRTL (—), Spinodal curve (- -), and critical point (•).

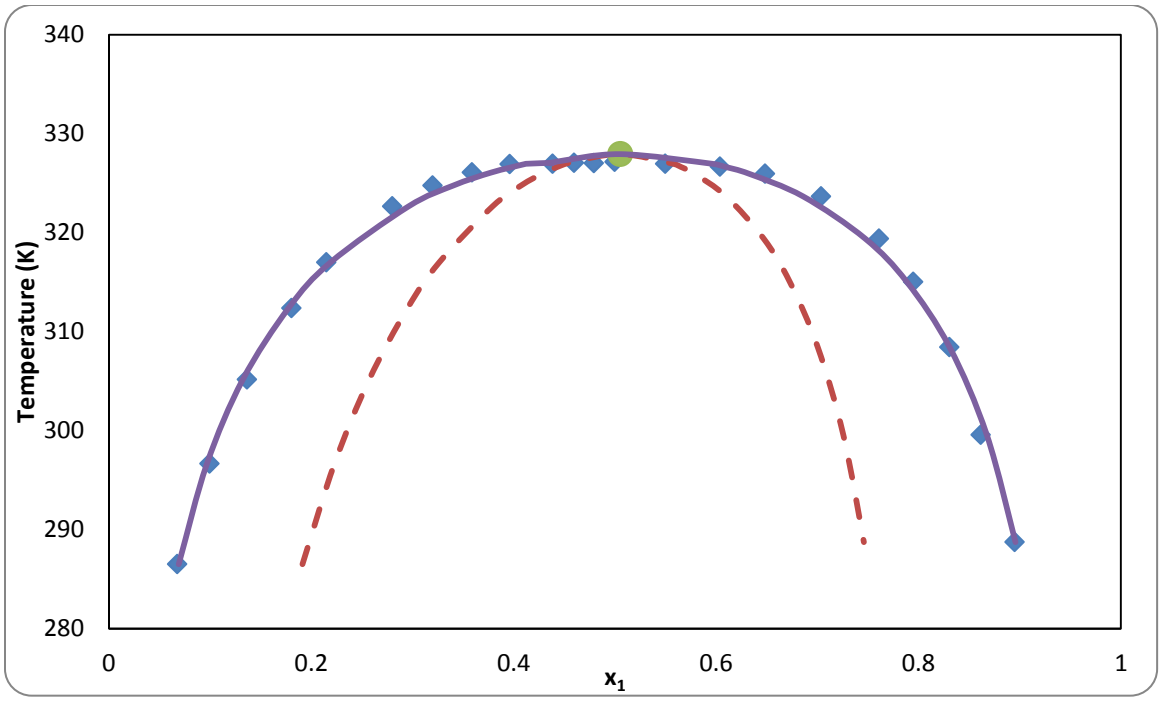

Figure 2.1-51: Binodal & Spinodal curves for N-methyl-α-pyrrolidone (1) + Isooctane (2) Experimental points (■), Binodal curve from NRTL (—), Spinodal curve (- -), and critical point (•).

NMP + 2,2 Dimethylbutane and 2,3 Dimethylbutane have critical temperatures of 323.98 K and 316.43 K, respectively. This contradicts the intuitive assumption that isomers should have the same critical compositions. Similar tendency was observed for NMP binary systems with 2-Methylpentane and 3-Methylpentane. It must be noted that this observation was not seen in Acetonitrile + 2,2 Dimethylbutane 2,3 Dimethylbutane, 2-methylpentane, and 3-methylpentane. Another unusual trend witnessed for NMP binary systems of cyclohexane and cyclooctane where the difference in critical temperature is only 1 K. It would normally be expected to hold a much higher difference in critical temperatures.

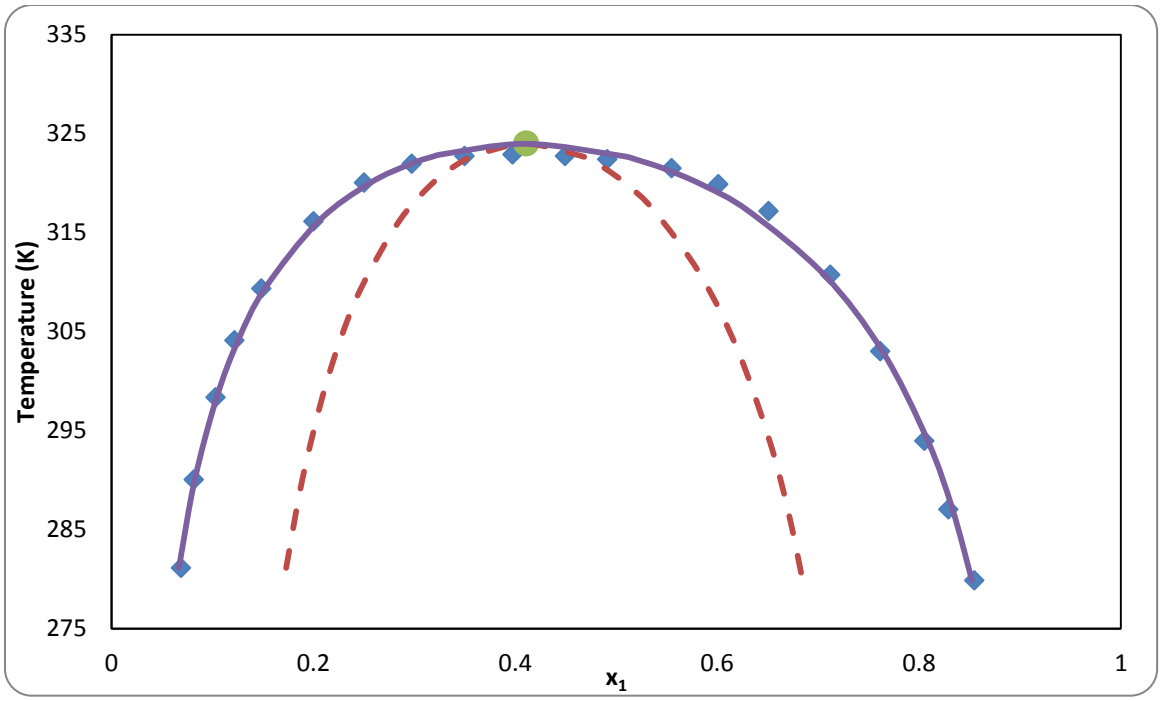

Figure 2.1-52 Binodal & Spinodal curves for N-methyl-α-pyrrolidone (1) + 2,2-Dimethylbutane (2) Experimental points (■), Binodal curve from NRTL (—), Spinodal curve (- -), and critical point (•).

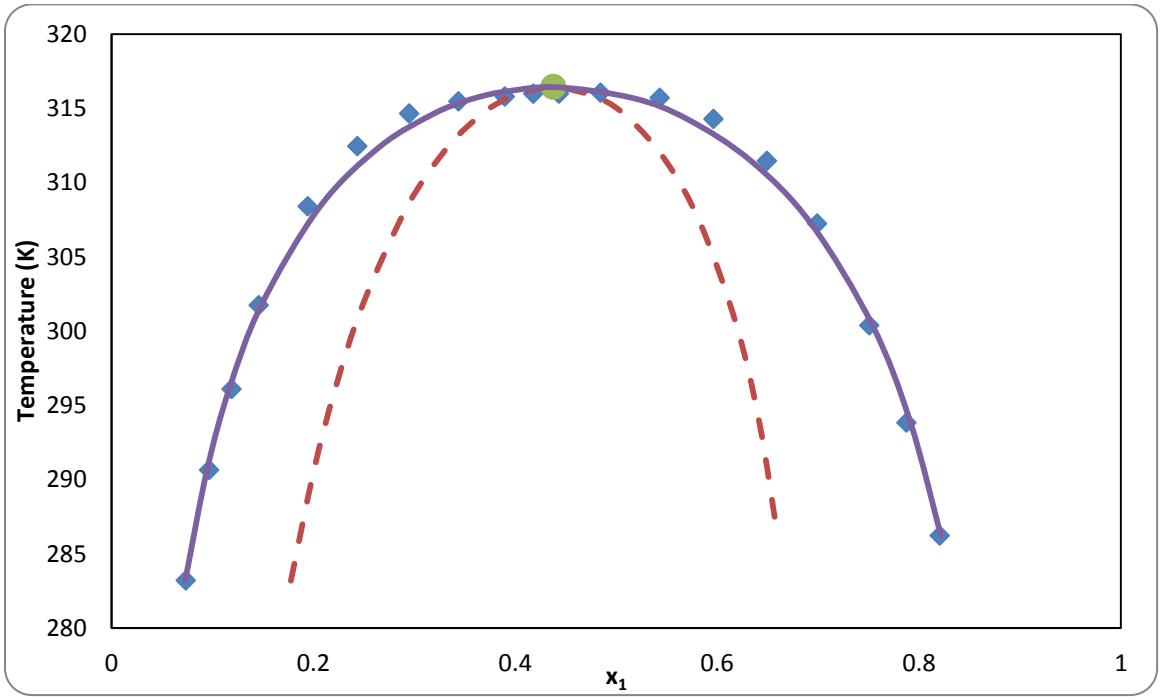

Figure 2.1-53 Binodal & Spinodal curves for N-methyl-α-pyrrolidone (1) + 2,3-Dimethylbutane (2) Experimental points (■), Binodal curve from NRTL (—), Spinodal curve (- -), and critical point (•).

Table 2.1-20 Critical temperature & composition determined for N-methyl-α-pyrrolidone (1) + Hydrocarbons (2) with values found in literature.

	Critical Temperature (K)		Critical composition	
System (NMP + hydrocarbons)	**This work**	**Literature**	**This work**	**Literature**
Hexane	323.90	322.92 [96]	0.444	0.4460 [96]
Octane	330.38	328.99 [96]	0.521	0.5289 [96]
Decane	339.28	338.03 [96]	0.611	0.5919 [96]
Decane	336.64	336.72 [97]	0.508	0.511 [97]
Undecane	340.56	340.8 [96]	0.533	0.523 [96]
Dodecane	344.50	344.7 [96]	0.555	0.530 [96]
Tridecane	349.05	348.9 [96]	0.643	0.630 [96]
Tetradecane	355.17	354.9 [96]	0.666	0.645 [96]
Cyclohexane	289.44	289.39 [97] 289.2 [98]	0.387	0.3185 [97] 0.616 [98]
Cyclooctane	291.82	290.17 [97] 291.5 [98]	0.463	0.4272 [97] 0.547 [98]
2-Methylpentane	326.7	325.49 [97]	0.421	0.4219 [97]
3-Methylpentane	320.44	319.04 [97]	0.419	0.4124 [97]
Isooctane	327.93	326.93 [97]	0.505	0.5081 [97]
2,2-Dimethylbutane	323.98	322.32 [97]	0.411	0.4055 [97]
2,3-Dimethylbutane	316.43	315.88 [97]	0.438	0.4320 [97]

2.2 Critical Universality

Figures 2.2-1 to 2.2-3 illustrate the behavior of ($x_1' - x_1''$), and χ against ε over the whole range of experimental data processed in this thesis. In addition table 2.2-1, show the model equations used and the regressed constants. The binodal and spinodal curve is presented as a simple power law as shown below

$$x_1^{'} - x_1^{''} = A(-\varepsilon)^{\beta}$$

And for χ, it was found that the form of extended series of power law shows better representation and it is taken as

$$\chi = \varepsilon^{\gamma}(1 + B\varepsilon^{x})$$

where γ and β are the critical constants. A,B, and x are regression constants. The predicted constants are reported in table 2.2-1, along with R^2.

Table 2.2-1 Results for regression of critical exponents

	β or γ	**A or B**	**x**	**R^2**
Binodal curve	0.3126	1.478	-	0.945
Spinodal curve	0.3623	1.114	-	0.968
susceptibility	-0.8468	-1.00	-4.867×10^{-6}	0.615

The asymptotic behavior of these order parameters are very clear in the near-critical region (that around ε = 0). For the binodal curve, the predicted value of β from figure 2.2-1 is 0.3126 as compared to 0.326 reported in table 1.3-1 which is approximately 4% deviation. The regression seems to have exact prediction of the calculated points in the vicinity of critical region for $x_1' - x_1''$ range of 0-0.2. large divergence is observed for temperatures far from critical region, specifically for $x_1' - x_1''$ above 0.9.

The critical exponent (β) for the spinodal curve is found to be 0.3623. The curve appears to agree reasonably well with the calculated data near the critical region. There is noticeable data scattered for data fruther from the critical region, the scatter becomes more pronounced for $x_1' - x_1''$ above 0.4. There are no reported literature value of β for the spinodal curve.

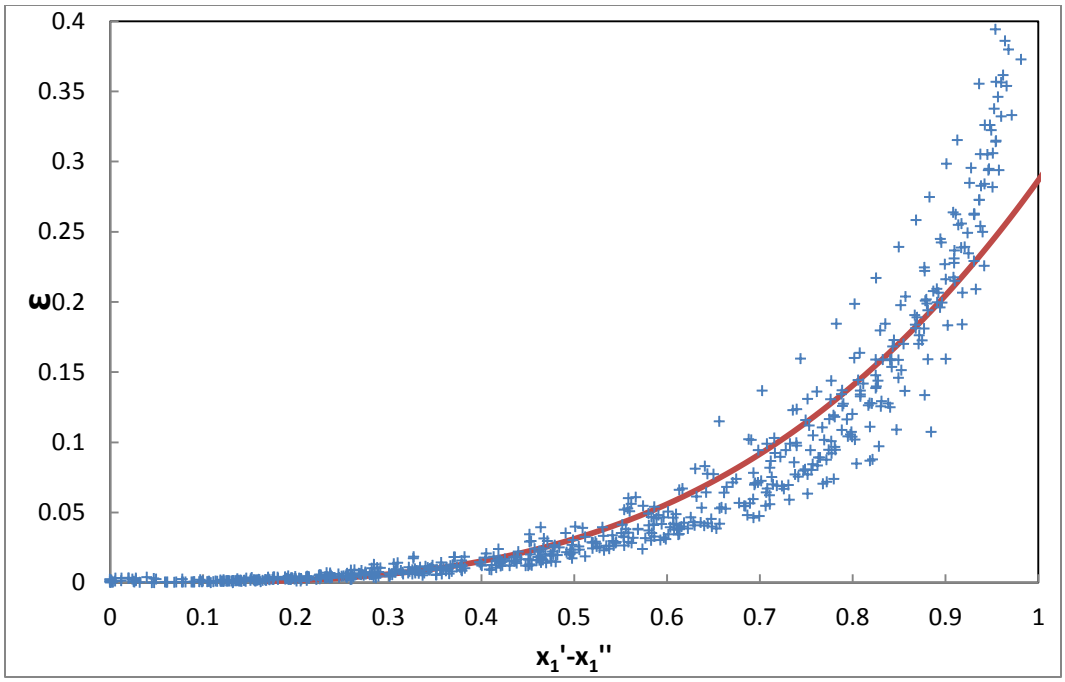

Figure 2.2-1 ε vs x_1'-x_1'' for binodal curve (+) and the regressed power model (--).

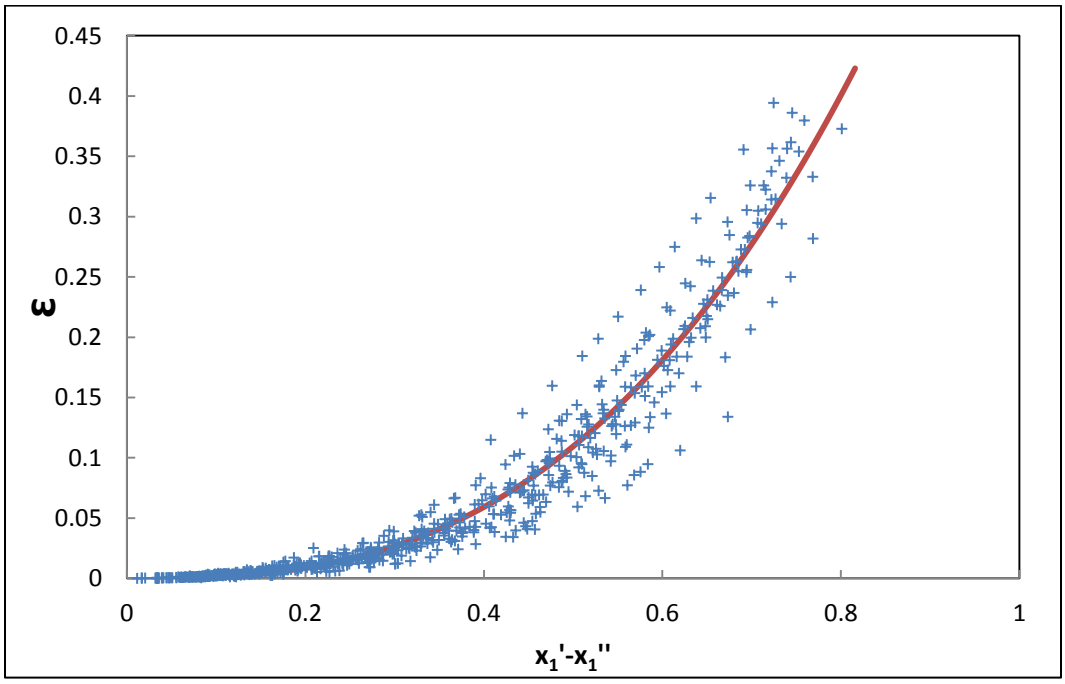

Figure 2.2-2 ε vs x1'-x1'' for spinodal curve (+) and the regressed power model (--).

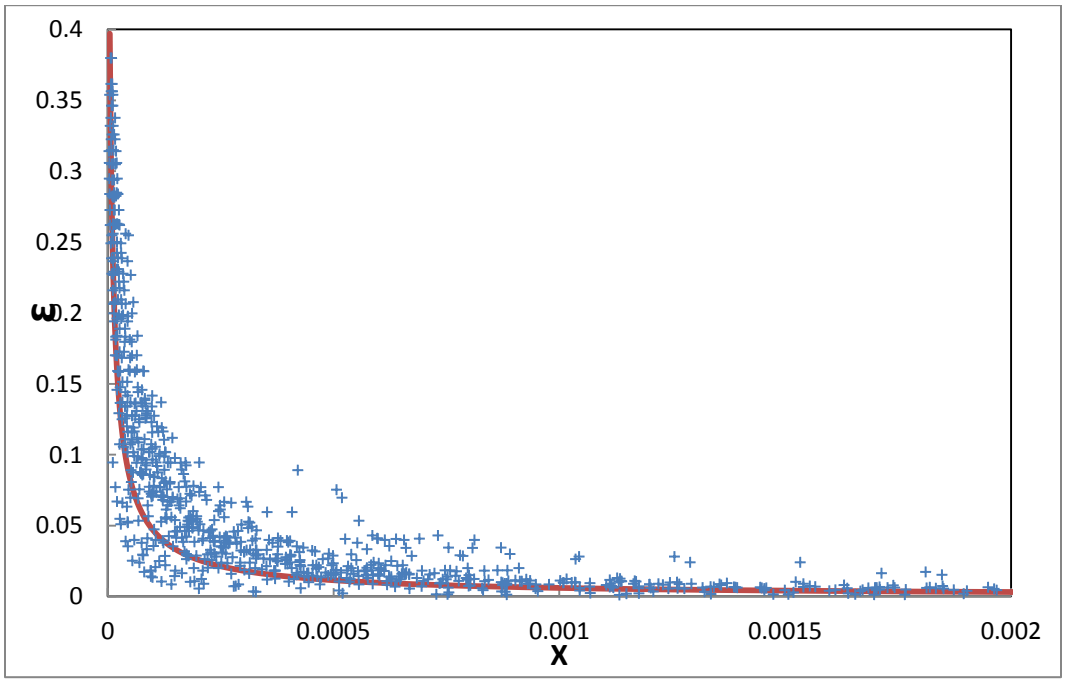

Figure 2.2-3 ε vs χ for spinodal curve (+) and the regressed power model (--).

The calculated isothermal susceptibility (χ) for the binary systems is -0.8468 which contradicts the reported universal exponent (γ) of -1.239 as shown in table 1.3-1. The regressed model has R^2 value of 0.6146, signaling that approximately 40% of the results fallout from the regressed equation. There is high degree of scatter of calculated data near the critical region (around $\varepsilon = 0$), as shown in figure 2.2-3 suggesting there is no definitive trend for χ in this region. This can be either attributed to erroneous experimental data points near the critical region or deficiency of NRTL model to predict χ which is calculated by differentiating the experimental data points, and if errors do exist, it will be amplified and this can suggest the high scatter near the critical region. Conversely, it must be pointed that that χ is calculated from NRTL, which is considered as classical liquid phase model, and it is well known in literature that classical models lacks the ability to account for long-range concentration fluctuations on the thermodynamic properties that becomes dominant near the critical region [84-86]. The NRTL model, therefore, may fail to predict thermodynamic properties of the system near the critical region.

2.3 Ternary systems

The stability limits were determined for 26 ternary systems based on the methodology outlined in the previous chapter. Segregated into 7 groups, each ternary system shares the same other two species with all other group members. There are at least 3 binary systems in each group considered with the exception of Limonene (1) + Linalool (2) + 2-Aminoethanol (3), where there contains only a single ternary system studied at different temperatures. All ternary systems are listed below, together with their parent group and reference:

- 2-Propanol + Water + Alkanes
    - 2-Propanol (1) + Water (2) + Hexane (3) [99].
    - 2-Propanol (1) + Water (2) + Heptane (3) [99].
    - 2-Propanol (1) + Water (2) + Octane (3) [99].
    - 2-Propanol (1) + Water (2) + Nonane (3) [99].
- 2-Propanone + Water + Alcohols
    - 2-Propanone (1) + Water (2) + Butanol (3) [99, 100].
    - 2-Propanone (1) + Water (2) + Hexanol (3) [99, 100].
    - 2-Propanone (1) + Water (2) + Heptanol (3) [99, 101].
    - 2-Propanone (1) + Water (2) + Octanol (3) [99].
- Ethyl Acetate + Water + Carboxylic Acids
    - Ethyl Acetate (1) + Water (2) + Formic Acid (3) [99, 102].
    - Ethyl Acetate (1) + Water (2) + Acetic Acid (3) [99, 103].
    - Ethyl Acetate (1) + Water (2) + Propanoic Acid (3) [99].
- Dibutyl Ether + Alcohols + Water
    - Dibutyl Ether (1) + Methanol (2) + Water (3) [104].
    - Dibutyl Ether (1) + Ethanol (2) + Water (3) [104].
    - Dibutyl Ether (1) + 1-Propanol (2) + Water (3) [104].
    - Dibutyl Ether (1) + 2-Propanol (2) + Water (3) [104].
    - Dibutyl Ether (1) + Butanol (2) + Water (3) [104].
- Water + Ethanol + Toluenes
    - Water (1) + Ethanol (2) + Toluene (3) [99, 105].

    - Water (1) + Ethanol (2) + 2-Chloro Toluene (3) [99, 106].
    - Water (1) + Ethanol (2) + 3-Chloro Toluene (3) [99, 106].
    - Water (1) + Ethanol (2) + 4-Chloro Toluene (3) [99, 106]
- Water + Ethanol + Benzene
    - Water (1) + Ethanol (2) + Benzene (3) [99, 107].
    - Water (1) + Ethanol (2) + Toluene (3) [99, 105].
    - Water (1) + Ethanol (2) + 1,2 Dimethyl Benzene (3) [99, 106].
    - Water (1) + Ethanol (2) + 1,3 Dimethyl Benzene (3) [99, 106].
- Limonene + Linalool + 2-Aminoethanol [108]
    - Limonene (1) + Linalool (2) + 2-Aminoethanol (3) @ 298.15 K.
    - Limonene (1) + Linalool (2) + 2-Aminoethanol (3) @ 298.15 K.
    - Limonene (1) + Linalool (2) + 2-Aminoethanol (3) @ 298.15 K.

2.3.1 2-Propanol + Water + Alkanes

The stability limits were determined for 2-Propanol (1) + Water (2) + Hexane (3), 2-Propanol (1) + Water (2) + Heptane (3), 2-Propanol (1) + Water (2) + Octane (3), and 2-Propanol (1) + Water (2) + Nonane (3). The LLE data for the ternary systems were taken from DECHEMA Vol 3 [99], where the optimized binary interaction parameters required by the NRTL mode are reported in the same reference as well. The experimental data points were collected at 298.15 K.

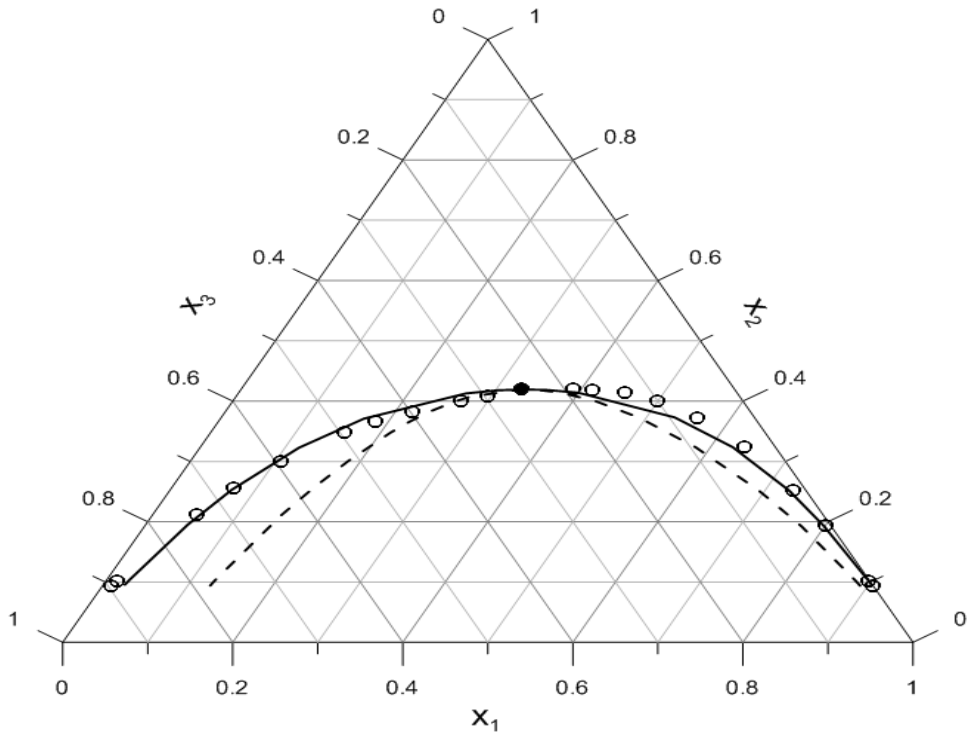

Figure 2.3-1 Binodal & Spinodal curves for 2-Propanol (1) + Water (2) + Hexane (3) Experimental points (o), Binodal curve from NRTL (—), Spinodal curve (- -), and critical point (•) @ 298.15 K.

The graphical results of the binodal curve, spinodal curve, and critical temperature are illustrated in figures 2.3-1 to 2.3-4 for each ternary system. All of the ternary systems treated in this group conform to the anticipated theoretical behaviour, where both the spinodal and binodal curves converge at exactly the critical point.

Spinodal curves for each of the ternary system studied here were in close proximity to the binodal curve, resulting in a very narrow metastable region. In fact, the spinodal curve grows closer to the binodal curve as it progresses from C6 to C9. Additionally, all spinodal curves are slightly skewed to the right, which in effect leads to a relatively wider metastable region in the alkane rich phase (x_1<0.6).

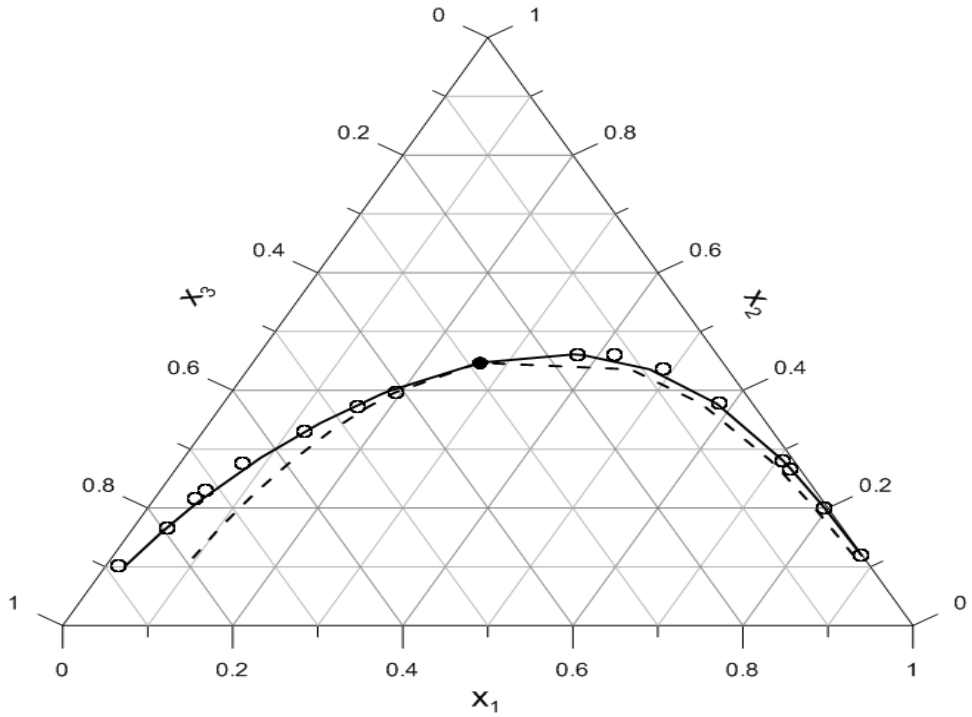

Figure 2.3-2: Binodal & Spinodal curves for 2-Propanol (1) + Water (2) + Heptane (3) Experimental points (o), Binodal curve from NRTL (—), Spinodal curve (- -), and critical point (•), @ 298.15 K.

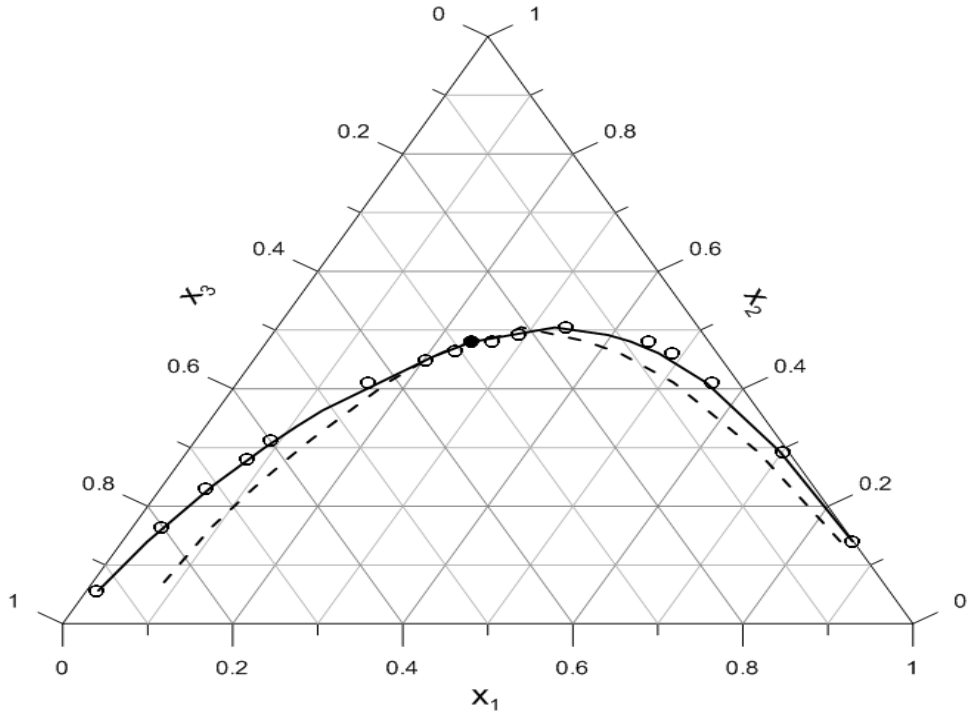

Figure 2.3-3: Binodal & Spinodal curves for 2-Propanol (1) + Water (2) + Octane (3) Experimental points (o), Binodal curve from NRTL (—), Spinodal curve (- -), and critical point (•), 298.15 K.

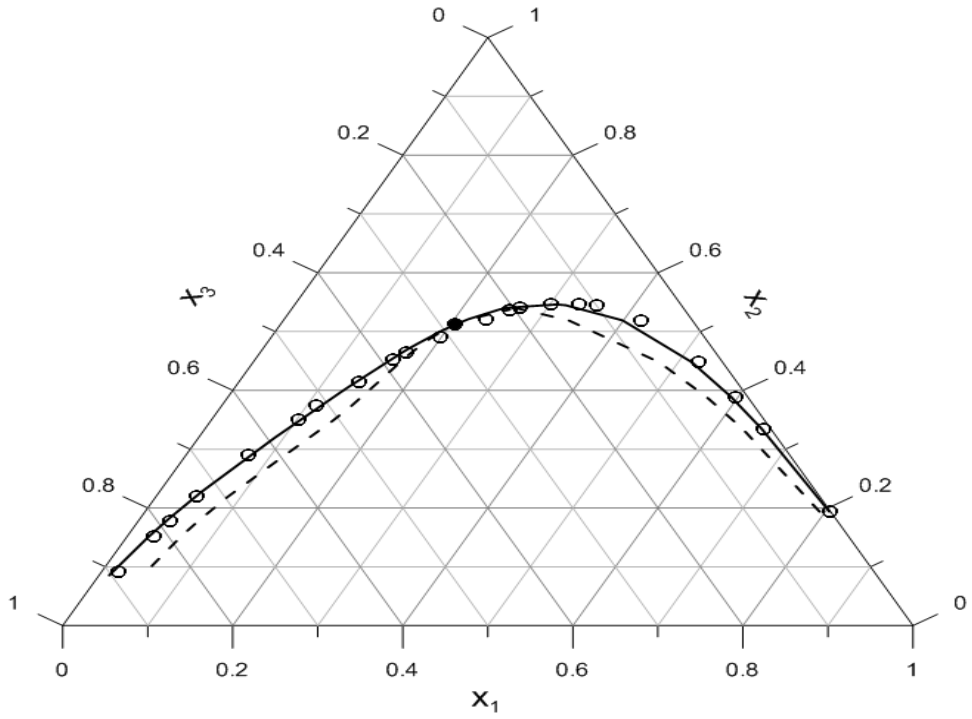

Figure 2.3-4: Binodal & Spinodal curves for 2-Propanol (1) + Water (2) + Nonane (3) Experimental points (o), Binodal curve from NRTL (—), Spinodal curve (- -), and critical point (•), 298.15 K.

The critical point for all 2-Propanol (1) + Water (2) 9+ Alkanes ternary systems are reported in table 2.3-1. Unfortunately, there are no reported literature data for the critical points of these systems to compare results. However, in the absence of the literature data, the results can be evaluated based on two criteria: first, how well the binodal curve predicted by NRTL model using the regressed binary interaction parameters; and second, more importantly, on the behaviour of the spinodal curve and if it intersects with the binodal curve at precisely the critical point. The results obtained here show good agreement based on the above criteria.

Graphically, the critical point seems to be less affected by molecular size. At first sight, there is no pronounced change or trend for the critical point from C6-C8. Yet upon further observation, the critical point is seen to actually shift to the left towards the alkane rich phase. This conclusion can be also be deduced by studying table 2.3-1.

Table 2.3-1 Critical composition calculated for 2-Propanol (1) + Water (2) + Alkanes (3) ternary systems @ 298.15 K.

	Critical composition		
System	x_1	x_2	x_3
2- Propanol (1)+ Water (2) + Hexane (3)	0.331	0.419	0.249
2- Propanol (1)+ Water (2) + Heptane (3)	0.267	0.447	0.286
2- Propanol (1)+ Water (2) + Octane (3)	0.240	0.479	0.28
2- Propanol (1)+ Water (2) + Nonane (3)	0.206	0.512	0.283

2.3.2 2-Propanone + Water + Alcohols

The ternary systems for 2-Propanone (1) + Water (2) + Butanol (3), 2-Propanone (1) + Water (2) + Hexanol (3), 2-Propanone (1) + Water (2) + Heptanol (3), and 2-Propanone (1) + Water (2) + Octanol (3) were analysed in terms of the stability limits. The experimental LLE data points were taken at 303.15 K. The binary interaction parameters needed for optimum fit of NRTL model were reported in DECHEMAVol. 3 [99].

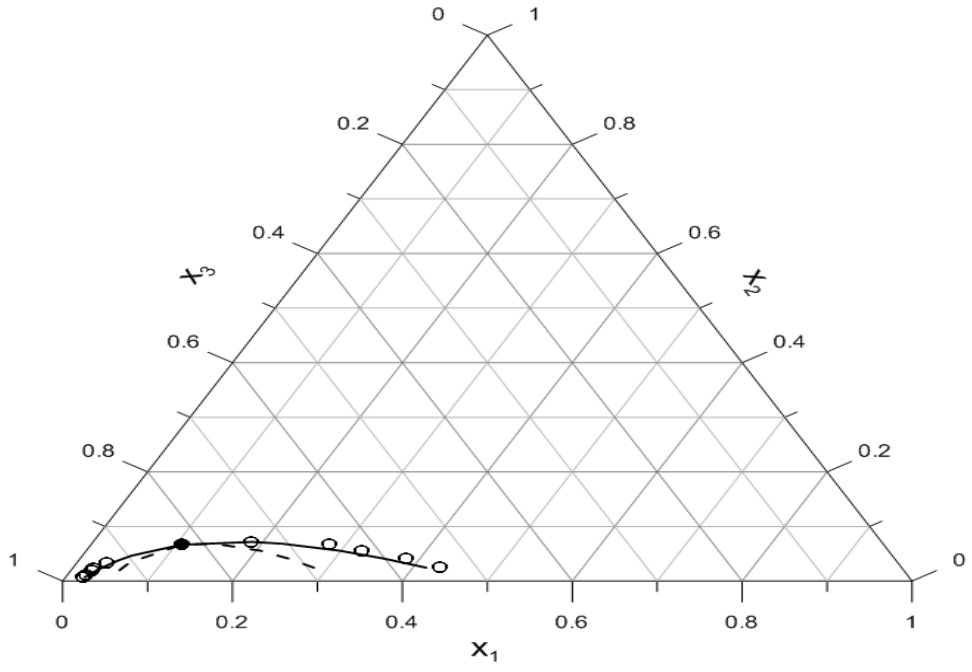

Figure 2.3-5: Binodal & Spinodal curves for 2-Propanone (1) + Water (2) + Butanol (3) Experimental points (o), Binodal curve from NRTL (—), Spinodal curve (- -), and critical point (•) at 303.15 K.

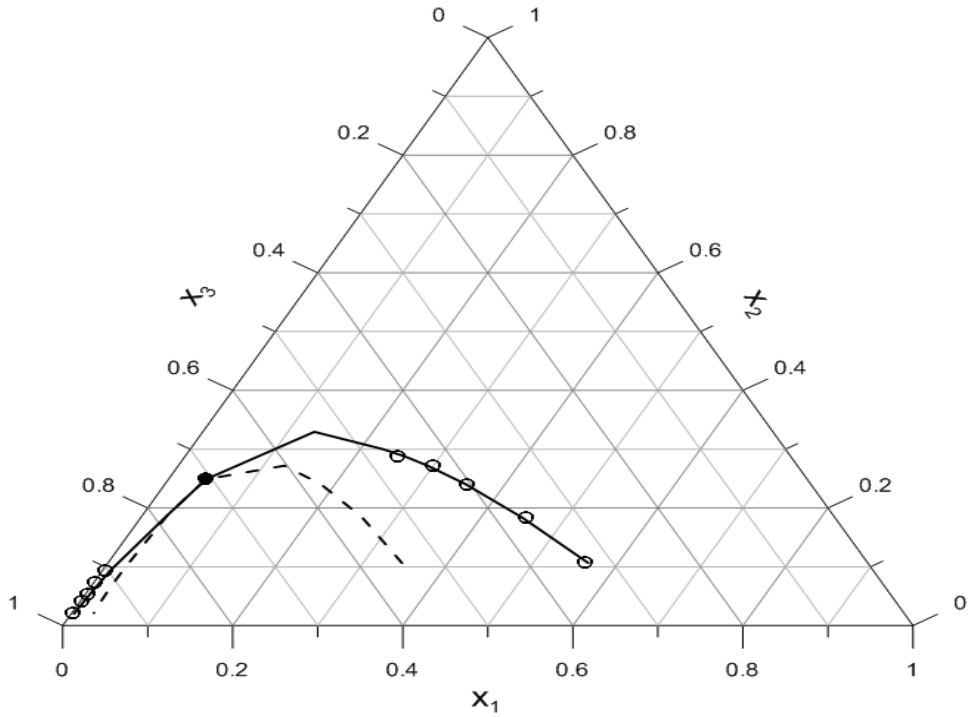

Figure 2.3-6: Binodal & Spinodal curves for 2-Propanone (1) + Water (2) + Hexanol (3) Experimental points (o), Binodal curve from NRTL (—), Spinodal curve (- -), and critical point (•) at 303.15 K.

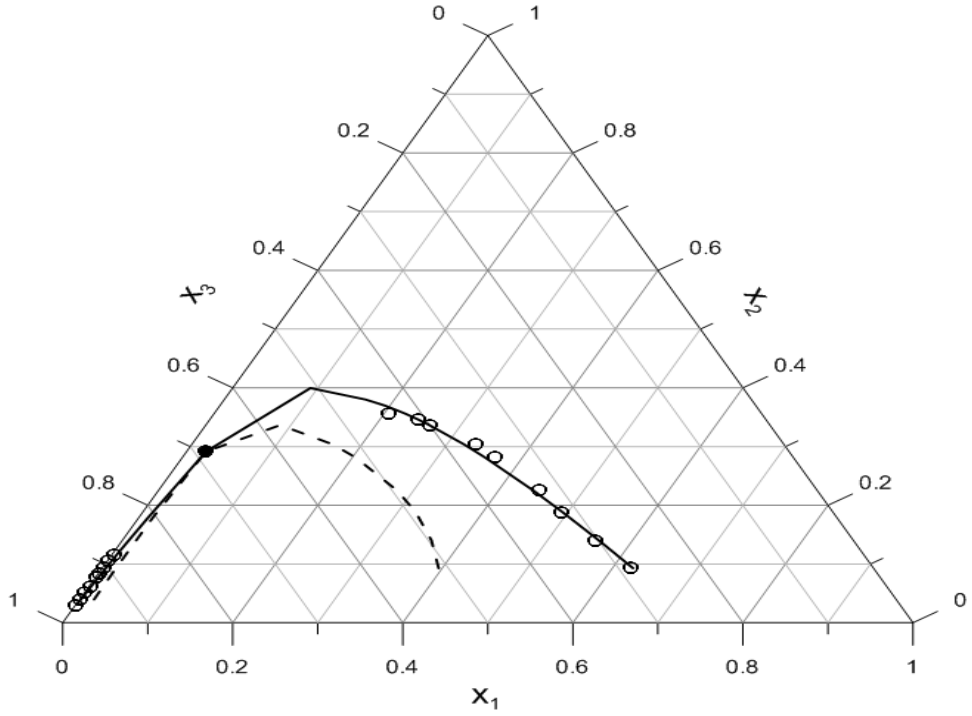

Figure 2.3-7: Binodal & Spinodal curves for 2-Propanone (1) + Water (2) + Heptanol (3) Experimental points (o), Binodal curve from NRTL (—), Spinodal curve (- -), and critical point (•) at 303.15 K.

The results of the binodal curve, spinodal curve, and critical temperature are illustrated in figures 2.3-5 to 2.3-8. All ternary systems studied follow the expected theoretical behaviour, as both binodal and spinodal curves converge at precisely the critical point. The binodal curves were reproduced reasonably well by the regressed binary interaction parameters, as shown in figures 2.3-5 to 2.3-8.

All spinodal curves are highly skewed to the left, with a more pronounced trend for higher molecular size alcohols. The spinodal curve on the left side (alcohol rich phase) is almost graphically inseparable from the binodal curve, in contrast to the right side (2-Propanone rich phase) where the metastable region is reasonably very wide. Subsequently, the metastable region can be easily achieved from the right side as compared to the left side.

The critical point for all 2-Propanone (1) + Water (2) 9+ Alcohols ternary systems are reported in table 2.3-2. There are no reported literature data for the critical points of these systems to compare with the results obtained. Yet, the results conform to the analytical behaviour, as both the binodal and spinodal curves intersected at the critical point, and the binodal curves were accurately predicted by the experimental points—giving confidence in the calculated results.

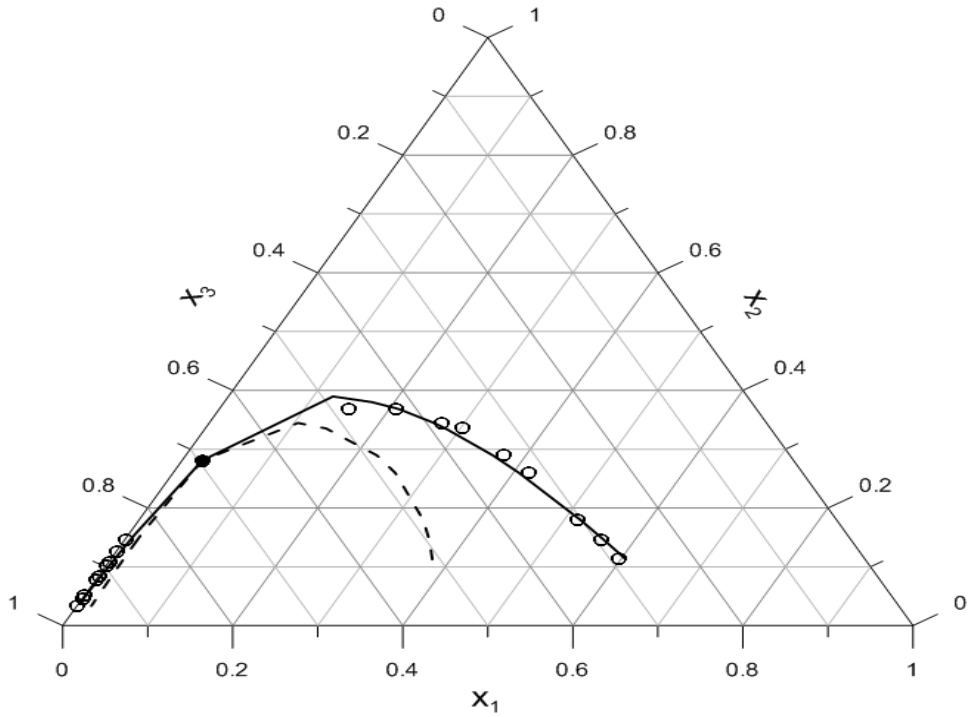

Figure 2.3-8: Binodal & Spinodal curves for 2-Propanone (1) + Water (2) + Octanol (3) Experimental points (o), Binodal curve from NRTL (—), Spinodal curve (- -), and critical point (•) at 303.15 K.

There is no confirmed trend for the critical point. The location of the critical point seems to be slightly affected by the molecular size, even though the mutual solubility increases with the component size, as shown in figures 2.3-5 to 2.3-8. Yet, there is big jump of critical point moving from Butanol to Hexanol ternary systems in figures 2.3-5 & 2.3-6. This behaviour has not been observed for Hexanol and Octanol. Essentially, the critical point becomes less affected by molecular size, as seen by the change from the C4 to C6 alcohols.

Table 2.3-2 Critical composition calculated for 2-Propanone (1)+ Water (2) + Alcohols (3) ternary systems @ 303.15 K.

	Critical composition		
System	x_1	x_2	x_3
2-Propanone (1) + Water (3) + Butanol (3)	0.107	0.067	0.827
2-Propanone (1) + Water (3) + Hexanol (3)	0.044	0.249	0.707
2-Propanone (1) + Water (3) + Heptanol (3)	0.023	0.292	0.686
2-Propanone (1) + Water (3) + Octanol (3)	0.024	0.281	0.695

2.3.3 Ethyl Acetate + Water + Carboxylic acids

Table 2.3-3 illustrates the different ternary systems studied for Ethyl Acetate (1) + Water (2) + Carboxylic Acids, together with the references citing the temperature at which the LLE data were collected. The binary interaction parameters of NRTL that provide the best fit of experimental data were reported in DECHEMA Vol. 3 [99].

Table 2.3-3 Temperature of experimental data for Ethyl Acetate (1) + Water (2) +Carboxylic Acids (3) ternary systems.

System	Temperature (K)
Ethyl Acetate (1) + Water (2) + Formic Acid (3)	308.15
Ethyl Acetate (1) + Water (2) + Acetic Acid (3)	303.15
Ethyl Acetate (1) + Water (2) + Propanoic Acid (3)	303.15

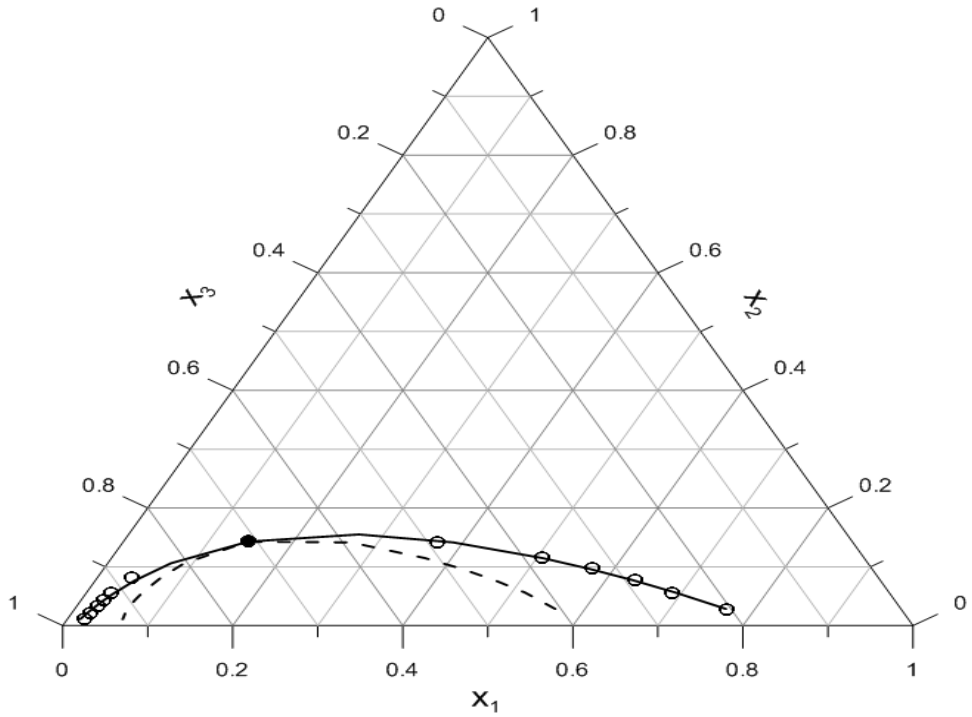

Figure 2.3-9: Binodal & Spinodal curves for Ethyl Acetate (1) + Water (2) + Formic Acid (3) Experimental points (o), Binodal curve from NRTL (—), Spinodal curve (- -), and critical point (•).

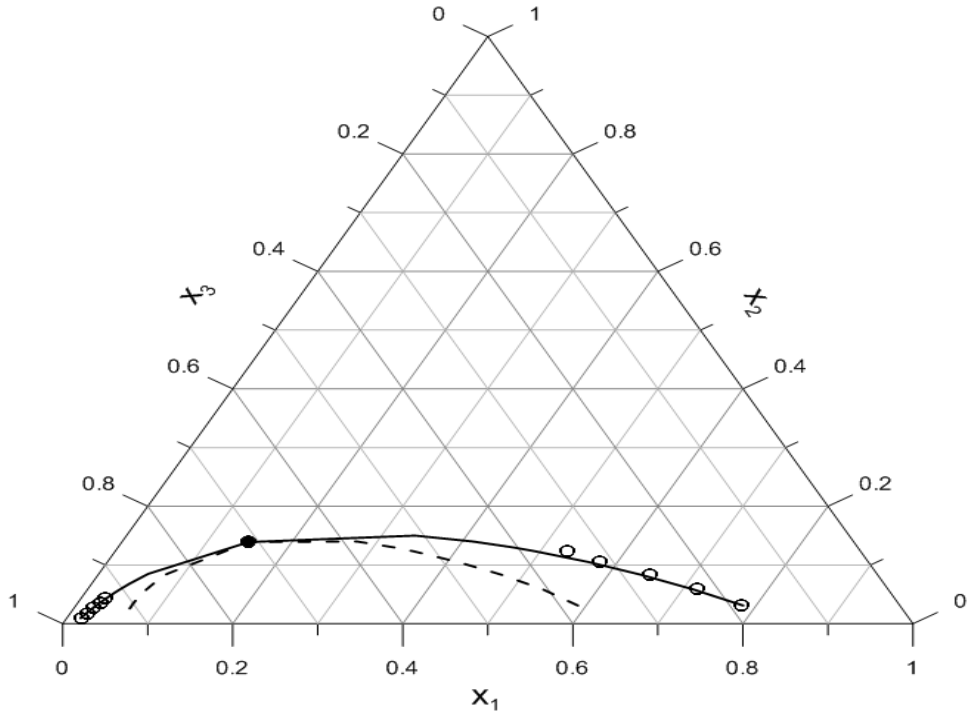

Figure 2.3-10: Binodal & Spinodal curves for Ethyl Acetate (1) + Water (2) + Acetic Acid (3) Experimental points (o), Binodal curve from NRTL (—), Spinodal curve (- -), and critical point (•).

Figures 2.3-9 to 2.3-11, represent the graphical results of binodal curve, spinodal curve, and critical point of each ternary system studied for this series. The results represented show that the ternary systems perform well within the expected theoretical behaviour with the binodal and spinodal curves converging at exactly the critical points. The binodal curve calculated from NRTL exceedingly agrees with the experimental data, except for Ethyl Acetate (1) + Water (2) + Propanoic Acid (3), where poor prediction of experimental binodal points in the Ethyl Acetate rich phase is depicted.

The spinodal curves of Ethyl Acetate (1) + Water (2) ternary systems are slightly skewed to the left and the metastable region on the right side (Ethyl Acetate rich phase) is wider as compared to the left side (Carboxylic Acid rich phase). This trend is consistent for all three ternary systems studied here.

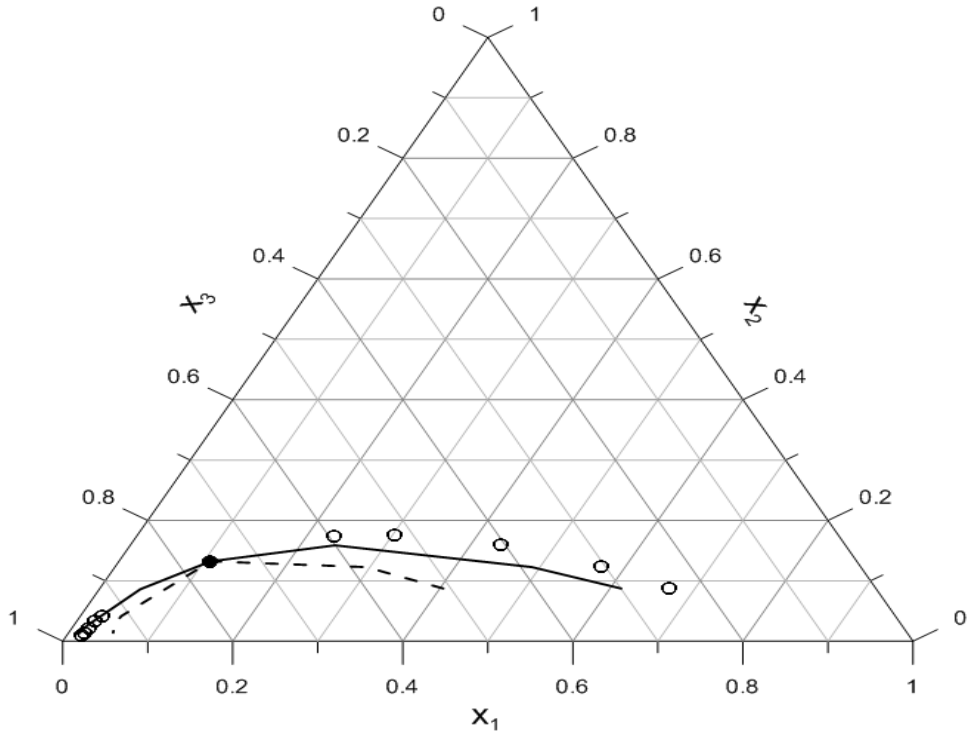

Figure 2.3-11: Binodal & Spinodal curves for Ethyl Acetate (1) + Water (2) + Propanoic Acid (3) Experimental points (o), Binodal curve from NRTL (—), Spinodal curve (- -), and critical point (•).

The results of the critical points for Ethyl Acetate (1) + Water (2) + Carboxylic Acids (3) are given in table 2.3-4. Upon examination of the table and figures, it can be established

that the critical point has not much been affected by the size of carboxylic acids and there was no noticeable change in the mutual solubility.

Table 2.3-4 Critical composition calculated for Ethyl Acetate (1) + Water (2) + Carboxylic Acids (3) ternary systems.

	Critical composition		
System	x_1	x_2	x_3
Ethyl Acetate (1) + Water (2) + Formic Acid (3)	0.147	0.143	0.711
Ethyl Acetate (1) + Water (2) + Acetic Acid (3)	0.149	0.139	0.712
Ethyl Acetate (1) + Water (2) + Propanoic Acid (3)	0.108	0.132	0.76

2.3.4 Dibutyl Ether + Alcohols + Water

The stability limits were determined for Dibutyl Ether (1) + Methanol (2) + Water (3), Dibutyl Ether (1) + Ethanol (2) + Water (3), Dibutyl Ether (1) + 1-Propanol (2) + Water (3), Dibutyl Ether (1) + 2-Propanol (2) + Water (3), and Dibutyl Ether (1) + Butanol (2) + Water (3). The LLE data points and the optimized binary interaction parameters required by the NRTL model for each ternary system were reported in the literature [104]. The experimental data points were collected at 298.15 K.

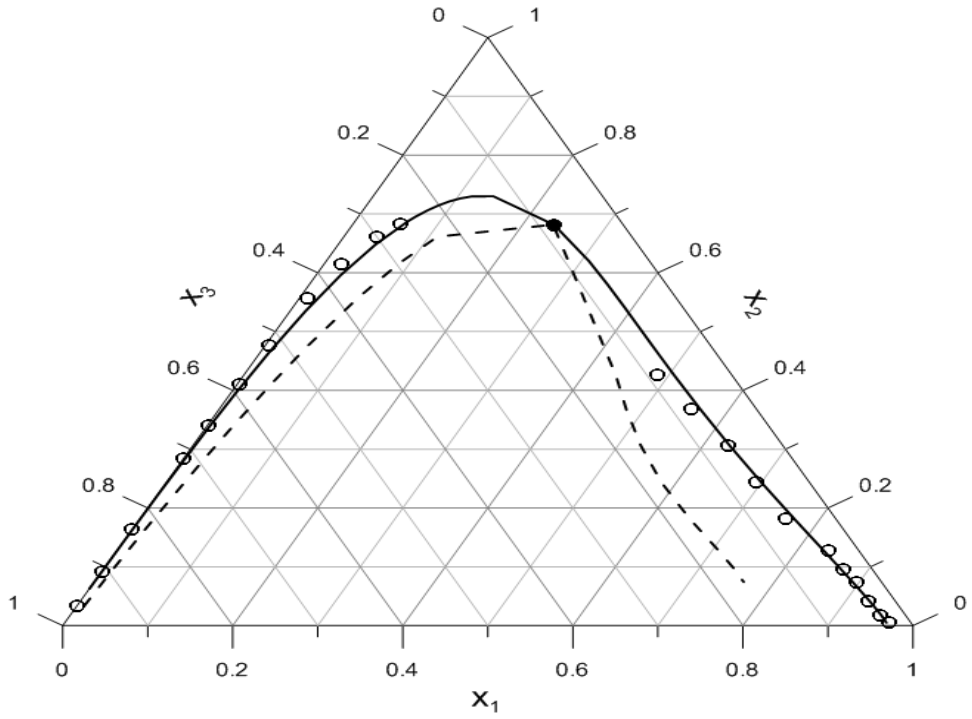

Figure 2.3-12: Binodal & Spinodal curves for Dibutyl Ether (1) + Methanol (2) + Water (3) Experimental points (o), Binodal curve from NRTL (—), Spinodal curve (- -), and critical point (•).

The results of the binodal curve, spinodal curve, and critical temperature are illustrated in figures 2.3-12 to 2.3-16 for each of the ternary system treated. Ternary systems are found to confirm the anticipated theoretical behaviour, with both spinodal and binodal curves converging at exactly the critical point, for those that have a critical point.

The binodal curve produced by NRTL agrees very well with the experimental binodal curve, except for Dibutyl Ether (1) + Butanol (2) + Water (3). This is attributed to the abundance of experimental points which ensures that regression of the NRTL parameters is precise.

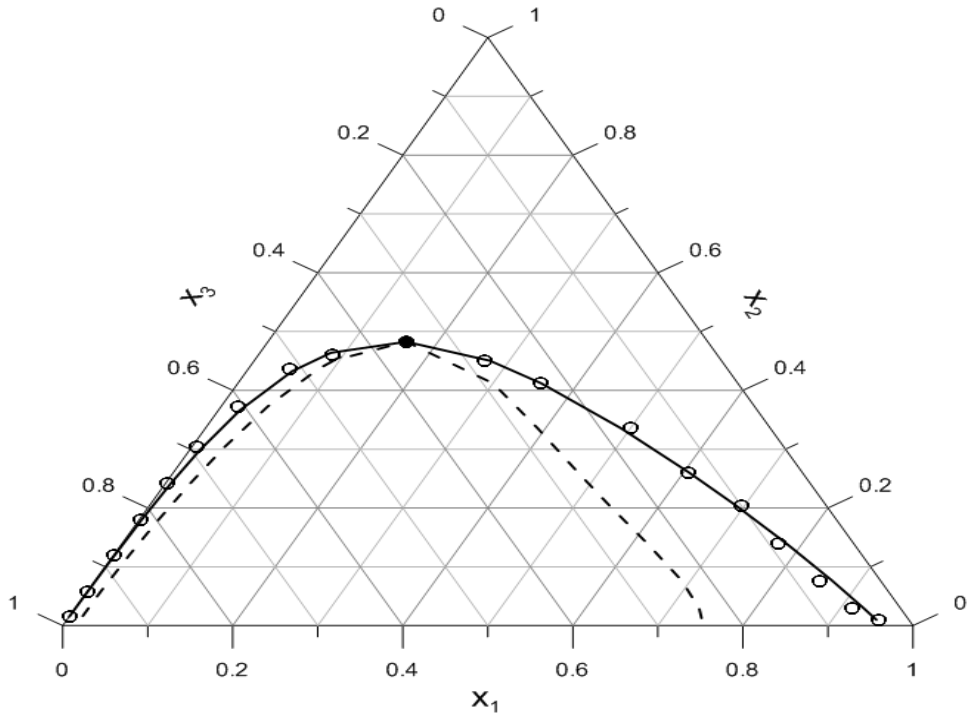

Figure 2.3-13: Binodal & Spinodal curves for Dibutyl Ether (1) + Ethanol (2) + Water (3) Experimental points (o), Binodal curve from NRTL (—), Spinodal curve (- -), and critical point (•).

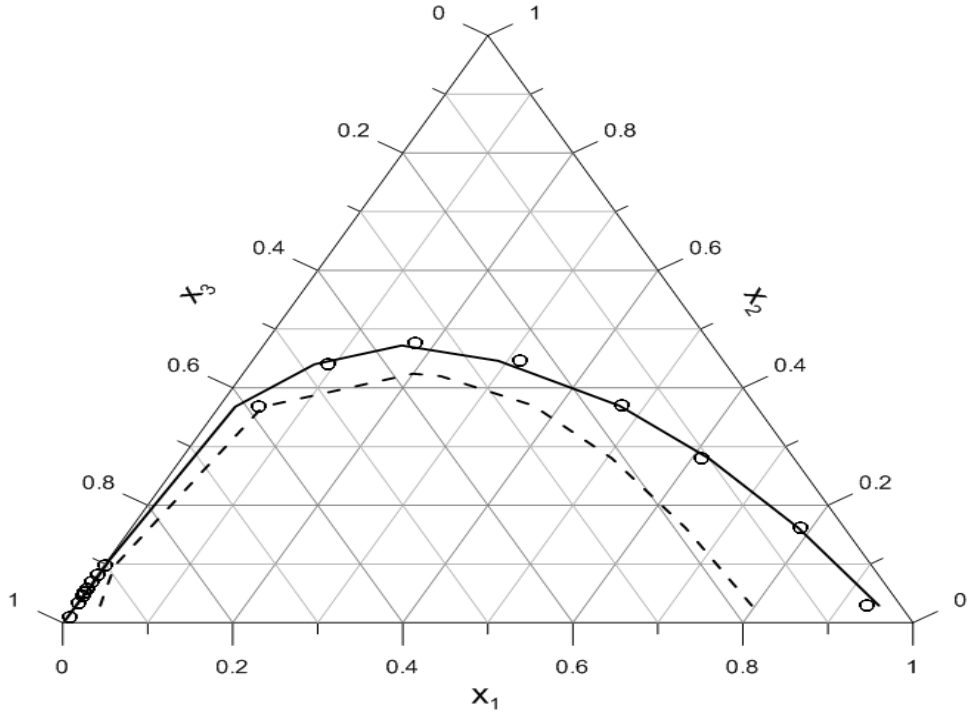

Figure 2.3-14: Binodal & Spinodal curves for Dibutyl Ether (1) + 1-Propanol (2) + Water (3) Experimental points (o), Binodal curve from NRTL (—), Spinodal curve (- -), and critical point (•).

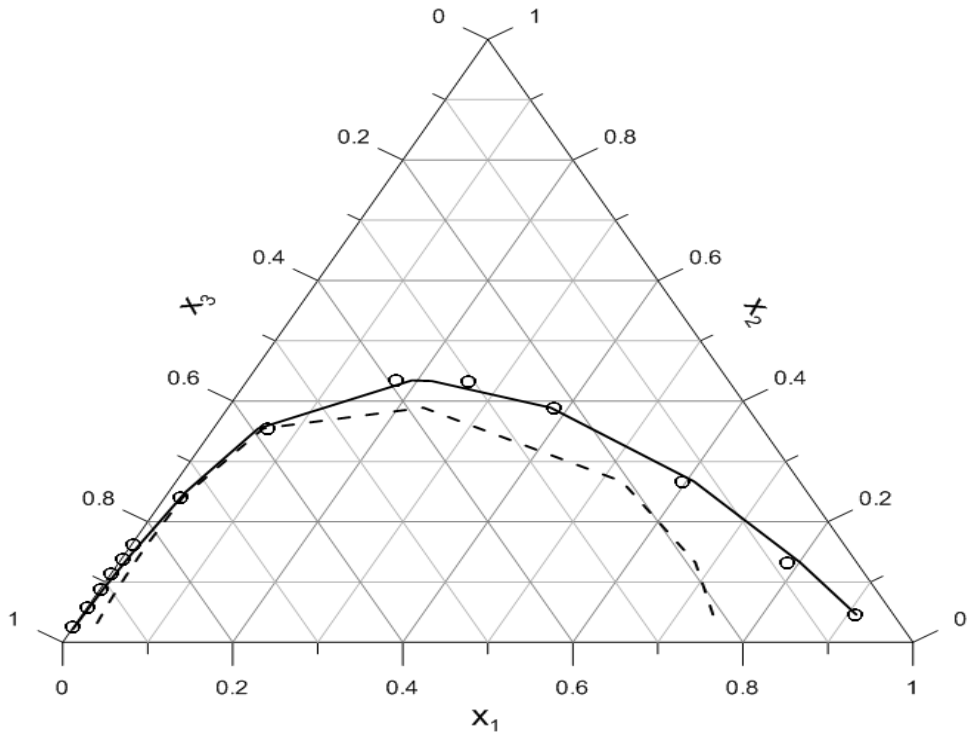

Figure 2.3-15: Binodal & Spinodal curves for Dibutyl Ether (1) + 2-Propanol (2) + Water (3) Experimental points (o), Binodal curve from NRTL (—), Spinodal curve (- -), and critical point (•).

All spinodal curves of Dibutyl Ether + Alcohols+ Water are skewed to the right which subsequently produces a wider metastable region on the right side (Dibutyl Ether rich phase) as compared to the left side (Alcohols rich region). For 1-Propanol, 2-Propanol, and Butanol ternary systems, the spinodal curves do not intersect the binodal curve as the critical point for these systems are non-existent, even though graphically they look like they are intersecting but they are actually just very close to the binodal curve.

The results for the critical point are only reported for Dibutyl Ether (1) + Methanol (2) + Water (3), and Dibutyl Ether (1) + Ethanol (2) + Water (3) are reported in table 2.3-5, as all other ternary systems show no critical point. The critical point location seems to be highly affected by the molecular size by comparing the Methanol and Ethanol ternary systems. Additionally, the mutual solubility decreases with the increase of alcohol molecular size. In any case, this trend cannot be confirmed as there are only two ternary systems that have critical point.

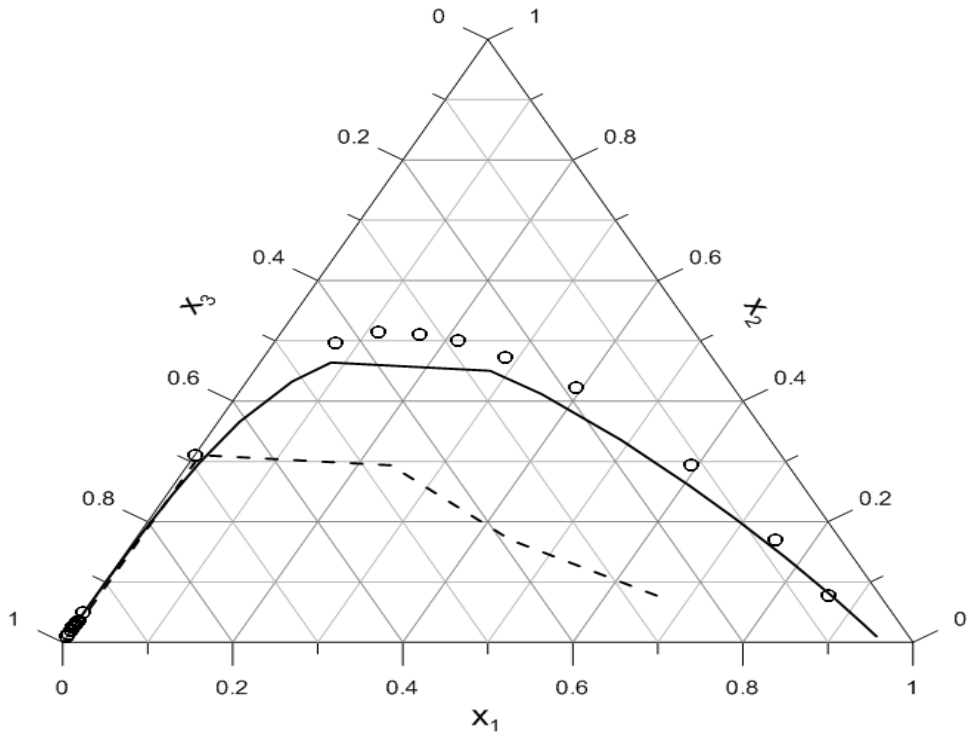

Figure 2.3-16: Binodal & Spinodal curves for Dibutyl Ether (1) + Butanol (2) + Water (3) Experimental points (o), Binodal curve from NRTL (—), Spinodal curve (- -), and critical point (•).

Table 2.3-5 Critical composition calculated for Dibutyl Ether (1)+ Water (2) + Alcohols (3) ternary systems.

System	Critical composition		
	x_1	x_2	x_3
Dibutyl Ether (1) + Methanol (2) + Water (3)	0.236	0.682	0.082
Dibutyl Ether (1) + Ethanol (2) + Water (3)	0.163	0.483	0.355
Dibutyl Ether (1) + 1-Propanol (2) + Water (3)	-	-	-
Dibutyl Ether (1) + 2-Propanol (2) + Water (3)	-	-	-
Dibutyl Ether (1) + Butanol (2) + Water (3)	-	-	-

2.3.5 Water + Ethanol + Toluenes

Water (1) + Ethanol (2) + Toluenes (3) ternary systems were analysed and the stability limits were determined. Similar to other ternary systems, the experimental data points and the optimized binary interaction parameters of NRTL were taken from DECHEMA Vol3 [99] All experimental work for the ternary systems was carried out at 298.15 K.

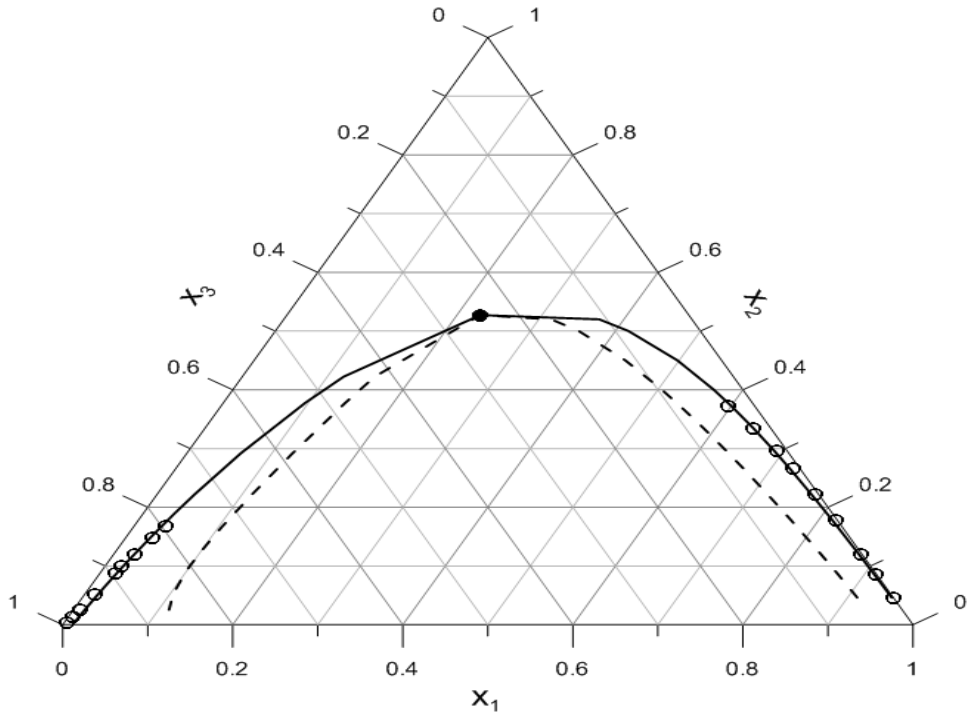

Figure 2.3-17: Binodal & Spinodal curves for Water (1) + Ethanol (2) + Toluene (3) Experimental points (o), Binodal curve from NRTL (—), Spinodal curve (- -), and critical point (•).

The graphical results of the binodal curve, spinodal curve, and critical temperature are illustrated in figures 2.3-17 to 2.3-20 for each ternary system. All the ternary systems treated in this group conform to the anticipated theoretical behaviour, where both spinodal and binodal curves converge at exactly the critical point.

The binodal curve constructed using NRTL model agrees well with the experimental data points. This is attributed to the abundance and the quality of experimental data that has enabled effective regression for binary interaction parameters of NRTL and has

subsequently produced a good fit of the binodal curve when compared to the experimental binodal curve.

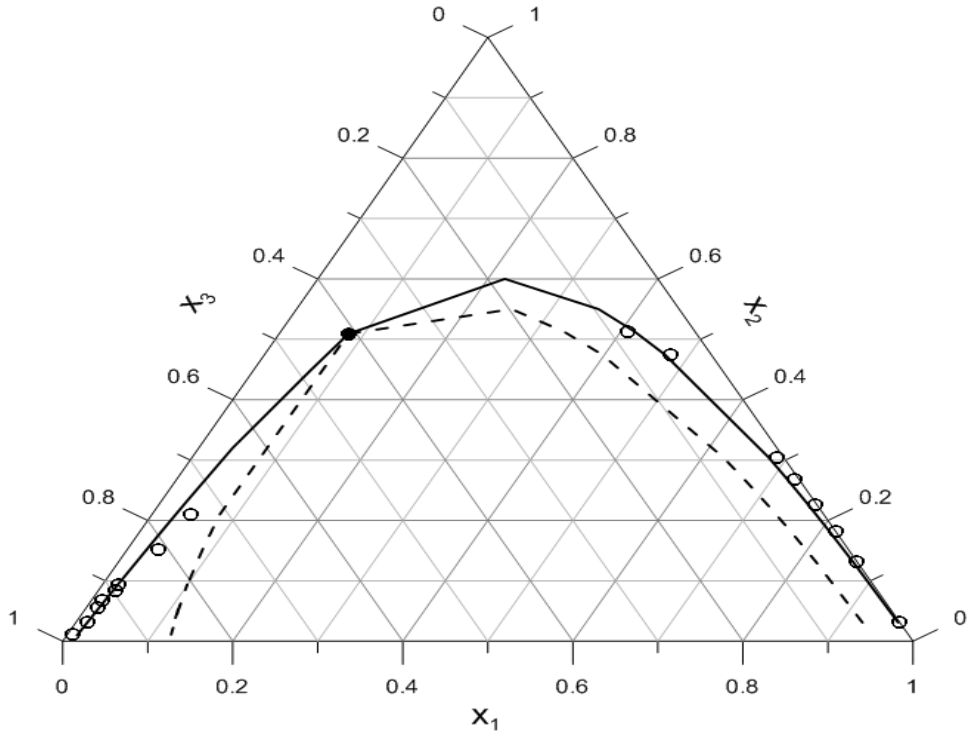

Figure 2.3-18: Binodal & Spinodal curves for Water (1) + Ethanol (2) + 2-ChloroToluene (3) Experimental points (o), Binodal curve from NRTL (—), Spinodal curve (- -), and critical point (•).

All spinodal curves are slightly skewed to the left. It is usually observed that for ternary systems that are skewed to the left, there is a wider region of metastability on the right. However, this ternary series deviates from this observation for other ternary systems. There is a wider metastability region at low Water and Ethanol composition range. Nevertheless, the metastability region is broader on the right side in the proximity of the critical region. It is also observed that the skew becomes more pronounced in Cholor toluene ternary systems as compared to the toluene system.

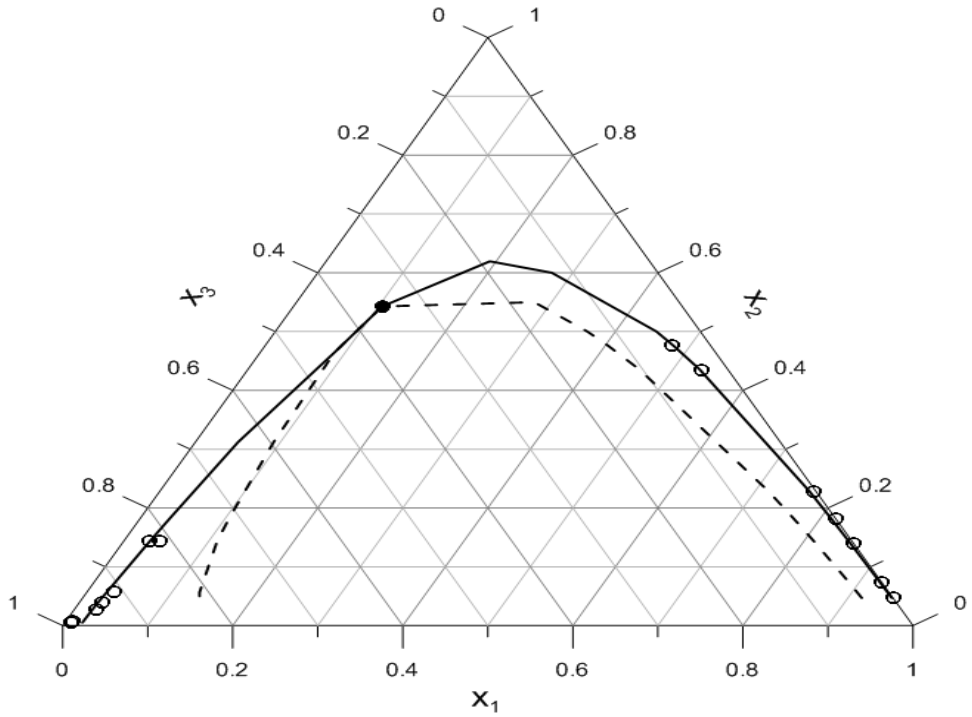

Figure 2.3-19: Binodal & Spinodal curves for Water (1) + Ethanol (2) + 3-ChloroToluene (3) Experimental points (o), Binodal curve from NRTL (—), Spinodal curve (- -), and critical point (•).

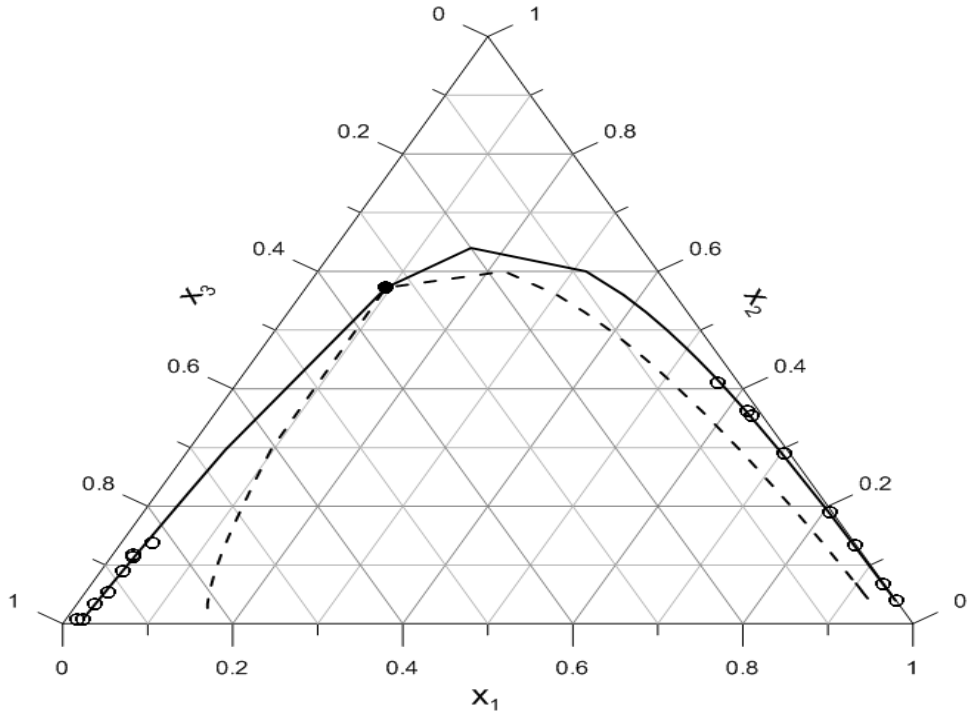

Figure 2.3-20: Binodal & Spinodal curves for Water (1) + Ethanol (2) + 4-ChloroToluene (3) Experimental points (o), Binodal curve from NRTL (—), Spinodal curve (- -), and critical point (•).

The critical point for all Water (1) + Ethanol (2) + Toluenes ternary systems are reported in table 2.3-6. The critical point for ternary systems are scarcely reported in literature, thus, no reported literature values of critical point are found for these ternary systems to compare the results. Nevertheless, the results obtained showed good quality of the binodal curve calculated by NRTL and all ternary systems, studied here, correspond to the expected analytical behaviour, with the binodal and spinodal curve converging at exactly the critical point. These factors assure confidence in the results obtained here.

The location of the critical points for Chloro Toluenes ternary systems are quite similar and no established trend can be observed. In addition, the size of the mutual solubility is more or less the same. Nevertheless, the size of the mutual solubility increases from Toluene to Chloro Toluenes ternary systems and the location of the critical point shifts more to the left.

Table 2.3-6 Critical composition for Water (1)+ Ethanol (2) + Toluene (3) ternary systems.

System	Critical composition		
	x_1	x_2	x_3
Water (1) + Ethanol (2) + Toluene (3)	0.227	0.527	0.245
Water (1) + Ethanol (2) + 2-Chloro Toluene (3)	0.082	0.509	0.409
Water (1) + Ethanol (2) + 3-Chloro Toluene (3)	0.104	0.543	0.353
Water (1) + Ethanol (2) + 4-Chloro Toluene (3)	0.094	0.572	0.334

2.3.6 Water + Ethanol + Benzenes

The stability limits were determine for Water (1) + Ethanol (2) + Benzene (3), Water (1) + Ethanol (2) + Toluene (3), Water (1) + Ethanol (2) + 1,2 Dimethyl Benzene (3) , and Water (1) + Ethanol (2) + 1,3 Dimethyl Benzene (3). The LLE data for each ternary systems, together with the optimized binary interaction parameters were taken from DECHEMA Vol 3 [99]. The experimental data points were collected at 298.15 K.

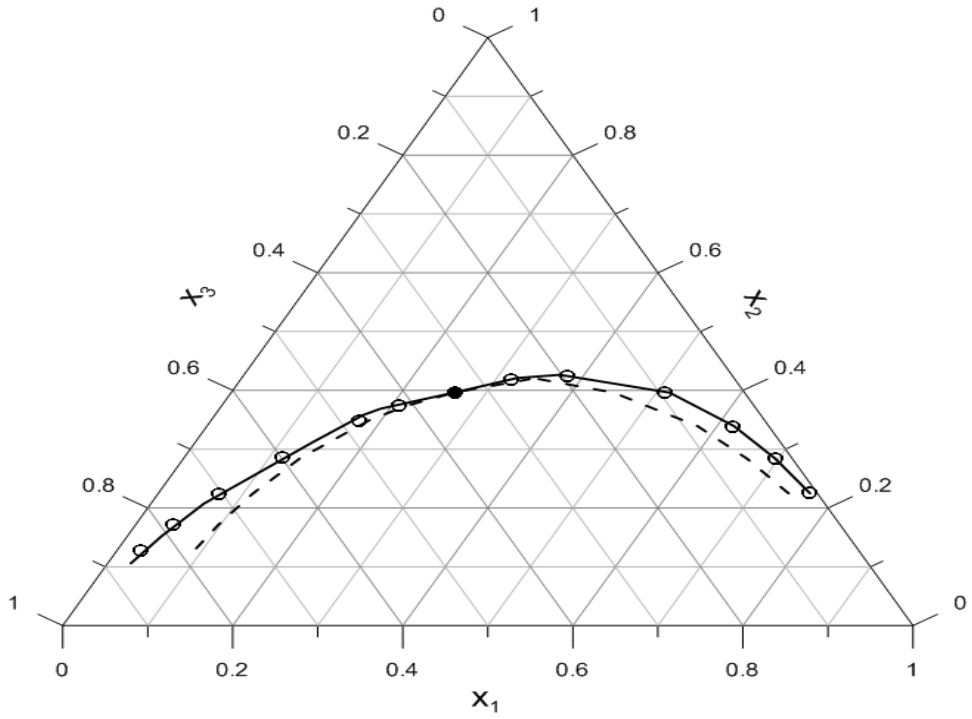

Figure 2.3-21: Binodal & Spinodal curves for Water (1) + Ethanol (2) + Benzene (3) Experimental points (o), Binodal curve from NRTL (—), Spinodal curve (- -), and critical point (•).

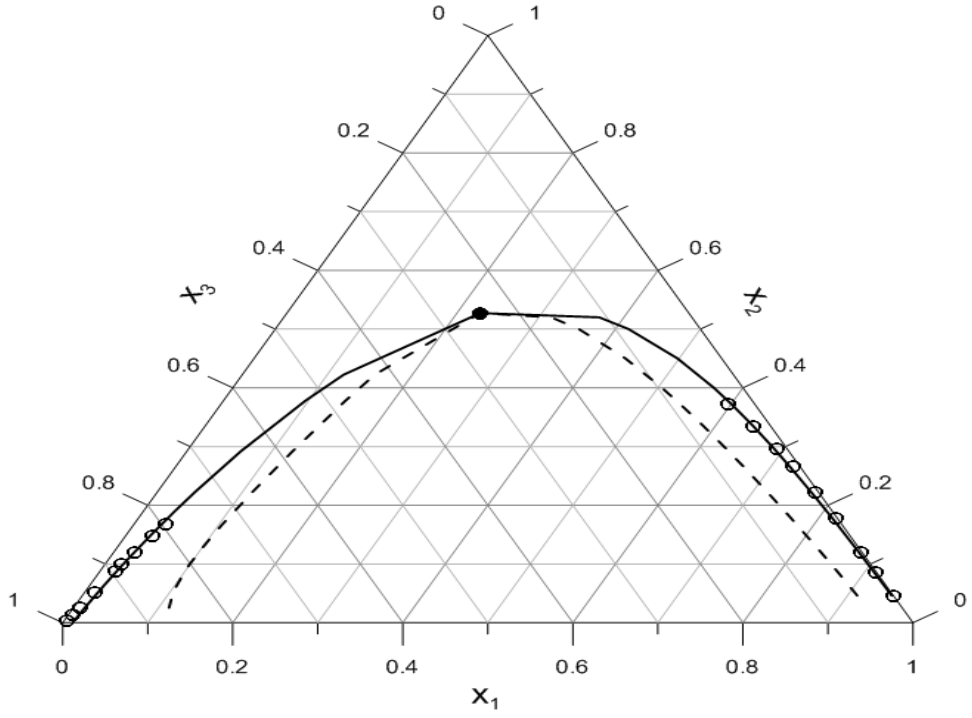

Figure 2.3-22: Binodal & Spinodal curves for Water (1) + Ethanol (2) + Toluene (3) Experimental points (o), Binodal curve from NRTL (—), Spinodal curve (- -), and critical point (•).

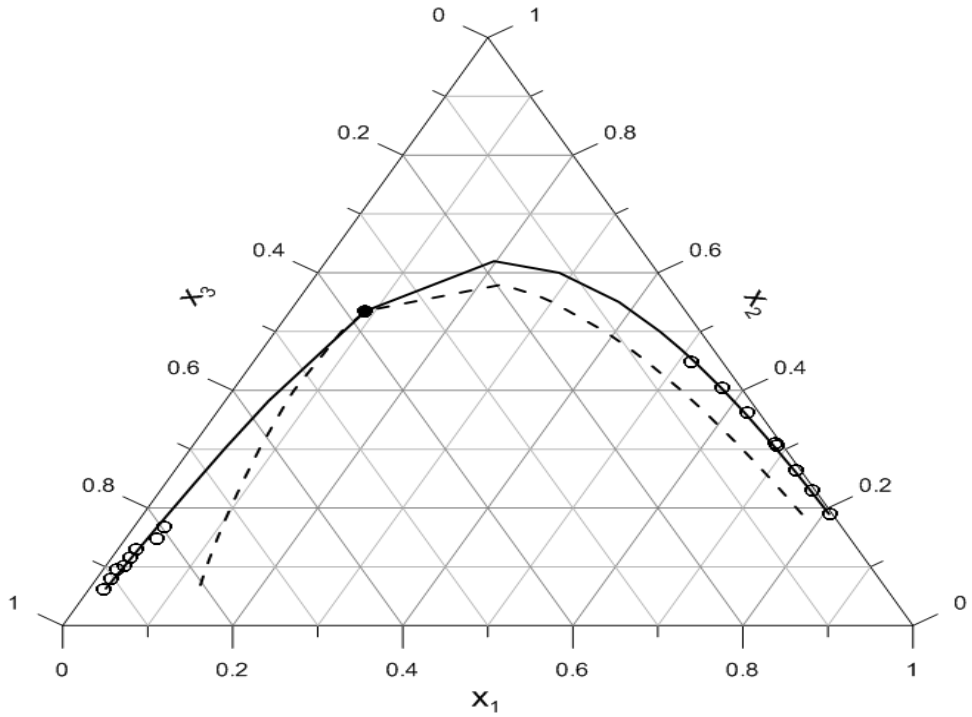

Figure 2.3-23: Binodal & Spinodal curves for Water (1) + Ethanol (2) + 1,2 Dimethyl Benzene (3) Experimental points (o), Binodal curve from NRTL (—), Spinodal curve (- -), and critical point (•).

The results of the binodal curve, spinodal curve, and critical temperature are illustrated in figures 2.3-21 to 2.3-24. All ternary systems studied follow the expected theoretical behaviour, having the binodal and spinodal curve converge at precisely the critical point. The binodal curves were reproduced reasonably well by the regressed binary interaction parameters. This is attributed to the abundance of experimental data points, which makes it possible to find the optimum fit of binary interaction parameters that can satisfactory reproduce the experimental data points.

There is established trend of having the spinodal curve skew more to the left with the molecular size. Even though, all spinodal curves are skewed to the left, the metastability region on the left side is wider than the right. This contradicts the general observation of having a wider metastability region on the right side when the curves are skewed to the left.

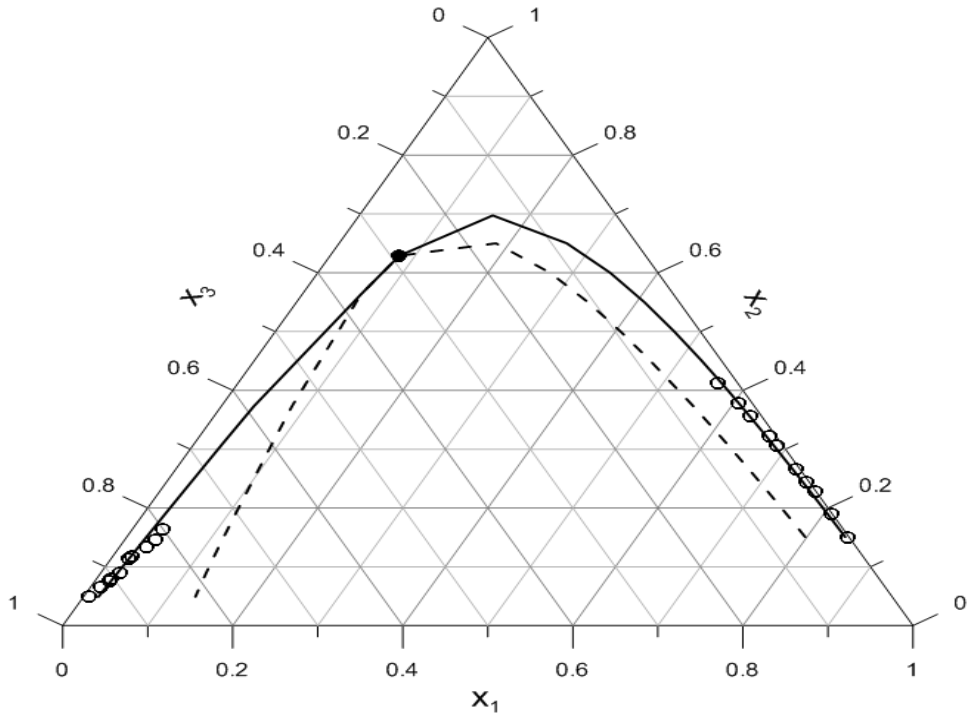

Figure 2.3-24: Binodal & Spinodal curves for Water (1) + Ethanol (2) + 1,3 Dimethyl Benzene (3) Experimental points (o), Binodal curve from NRTL (—), Spinodal curve (- -), and critical point (•).

The results of the critical points for Water (1) + Ethanol (2) + Benzenes (3) are given in table 2.3-7. Looking at table 2.3-13 and figures 2.3-21 to 24, it can be established that the mutual solubility and the critical point has increased with the molecular size. It is interesting to note that even though Water (1) + Ethanol (2) + 1,2 Dimethyl Benzene (3) and Water (1) + Ethanol (2) + 1,3 Dimethyl Benzene (3) are of the same size, their critical point and solubility change is more than the observed change for Benzene and Toluene ternary systems.

Table 2.3-7 Critical composition calculated for Water (1)+ Ethanol (2) + Benzenes (3) ternary systems.

System	Critical composition		
	x_1	x_2	x_3
Water (1) + Ethanol (2) + Benzene (3)	0.264	0.397	0.339
Water (1) + Ethanol (2) + Toluene (3)	0.227	0.527	0.245
Water (1) + Ethanol (2) + 1,2 Dimethyl Benzene (3)	0.088	0.535	0.376
Water (1) + Ethanol (2) + 1,3 Dimethyl Benzene (3)	0.082	0.629	0.289

2.3.7 Limonene+ Linalool+ 2-Aminoethanol

In this section, a single ternary system is studied rather than series of ternary systems. The stability limits for Limonene (1) + Linalool (2) + 2-Aminoethanol (3) were determined at temperatures of 298.15 K, 308.15 K, and 318.15 K. The optimised binary interactions parameters for NRTL model are reported in the same reference [108].

The results of the binodal curve, spinodal curve, and critical temperature are illustrated in figures 2.3-25 to 27 for each of the ternary system treated. Ternary systems are found to validate the anticipated theoretical behaviour, with both spinodal and binodal curves converging at exactly the critical point, for the ones who actually have critical point. The binodal curve produced by NRTL agrees very well with the experimental binodal curve demonstrating that the binary interaction parameters were successfully regressed. This is attributed to the abundance of experimental points that makes regression of the NRTL parameters precise.

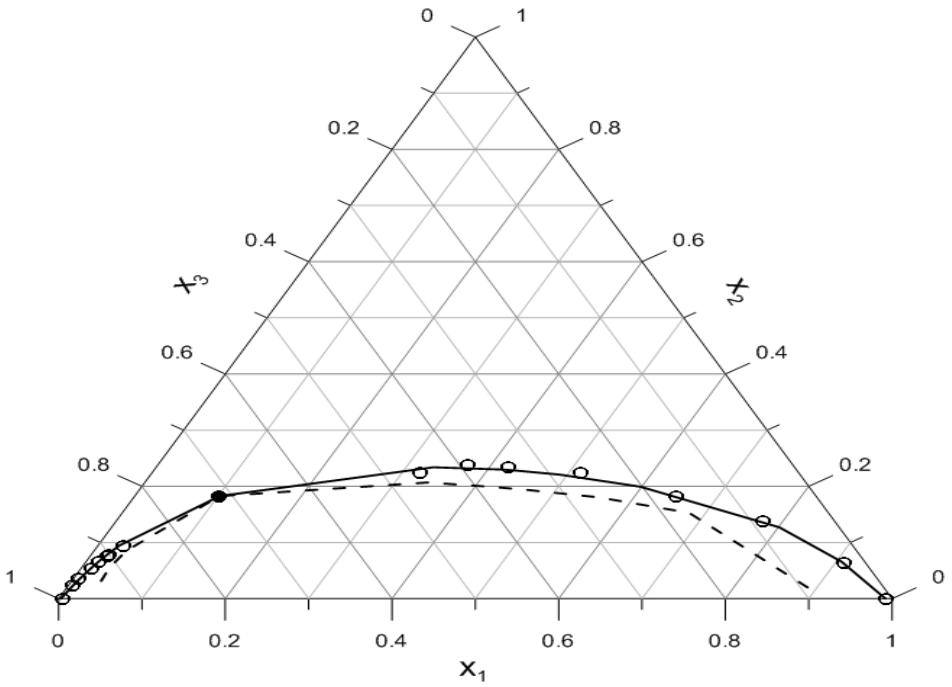

Figure 2.3-25: Binodal & Spinodal curves for Limonene (1) + Linalool (2) + 2-Aminoethanol (3) Experimental points (o), Binodal curve from NRTL (—), Spinodal curve (- -), and critical point (•) @ 298.15 K.

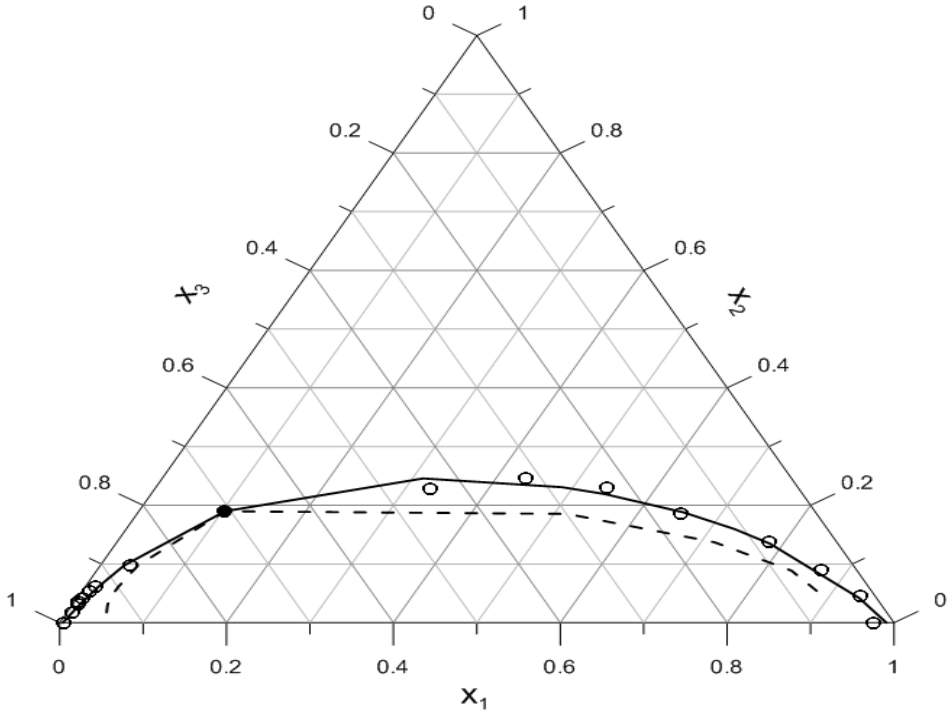

Figure 2.3-26: Binodal & Spinodal curves for Limonene (1) + Linalool (2) + 2-Aminoethanol (3) Experimental points (o), Binodal curve from NRTL (—), Spinodal curve (- -), and critical point (•) @ 308.15 K.

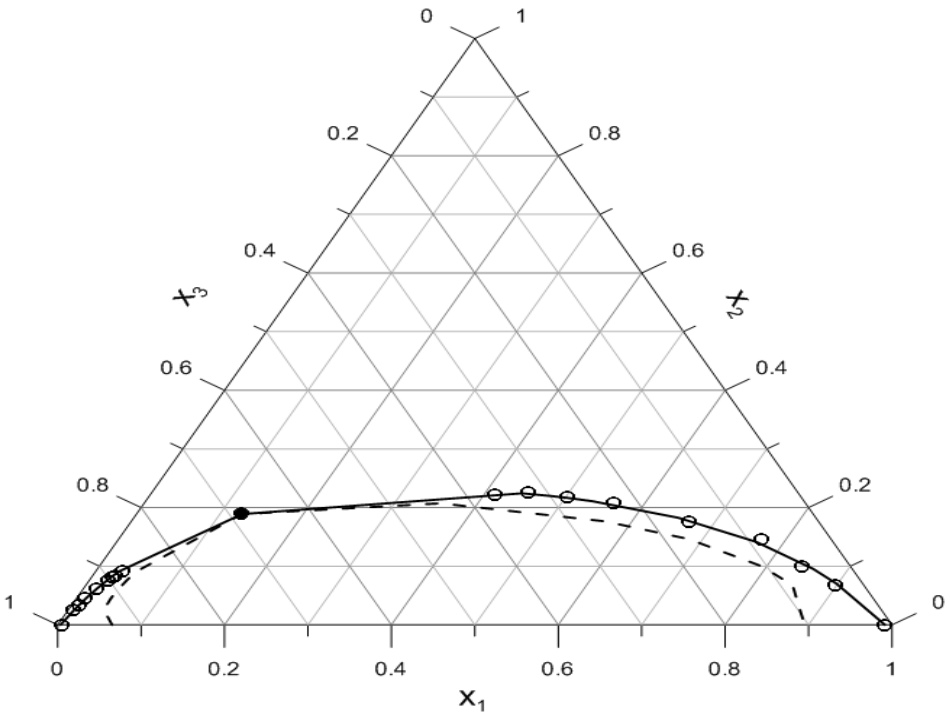

Figure 2.3-27: Binodal & Spinodal curves for Limonene (1) + Linalool (2) + 2-Aminoethanol (3) Experimental points (o), Binodal curve from NRTL (—), Spinodal curve (- -), and critical point (•) @ 318.15 K.

The spinodal curve of Limonene (1) + Linalool (2) + 2-Aminethanol (3) are skewed to the left. This is sustained with increasing temperature, which is expected since the temperature has little influence on LLE behaviour.

The calculated critical points are given in table 2.3-8. Fortunately, a literature value was found for the critical point at 298.15 K. The calculated critical point shows good agreement with the literature's reported value. The critical point has not changed with the increasing temperature—confirming the fact that temperature has little influence on the behaviour of LLE, as expected.

Table 2.3-8 Critical composition calculated for Water (1)+ Ethanol (2) + Benzene (3) ternary systems.

System	Critical composition		
	x_1	x_2	x_3
298.15	0.102	0.183	0.716
298.15 (literature value)	0.095	0.19	0.715
308.15	0.103	0.189	0.707
318.15	0.127	0.189	0.685

Chapter 3
Conclusions & Recommendations

In this thesis, The NRTL liquid phase model was used to predict the stability limits of selected binary and ternary liquid systems. The working model equations were derived based on the rigorous thermodynamic criteria for spinodal limits and criticality conditions in terms of the liquid phase Gibbs free energy.

The applicability of the NRTL model to predict stability limits and critical conditions was tested for fifty three binary systems belonging to six distinct groups of chemical species and twenty six ternary systems that also span six groups of chemically different groups. The groups encompassing binary systems include; acetonitrile + hydrocarbons, N-formylmorpholine (NFM)+ alkanes, perfluoroalkanes + n-alkanes, sulfolane + hydrocarbons, 1,3- propanediol + ionic liquids, and N-methyl-α -pyrrolidone + n-alkanes. Those of the ternary systems include; 2-propanol + water + alkanes, 2-propanone + water + alcohols, ethyl acetate + water + carboxylic acids, dibutyl ether + alcohols + water, water + ethanol + toluenes, and water + ethanol + benzene. Whenever available, the generated critical temperatures and compositions were compared with the corresponding experimental values reported in the technical literature. Good agreement was found between NRTL-predicted values and those reported in the literature.
The generated critical conditions for binary and ternary mixtures were verified for conformation with the universal critical phenomenon for the behavior of properties in the proximity of the critical region. The predicted critical exponents from the liquid-liquid systems studied in this work were found in agreement with those describing magnetic and vapor-liquid systems near their critical region.

The computational procedure followed in this thesis for the prediction of stability limits and criticality conditions is a very tedious one. It involves a very hefty derivation as clear from the reported working equations in the appendix. It is recommended, therefore, to

attempt simplifying the computational algorithm by trying other approaches based on fugacity coefficients and cubic equation of state in lieu of liquid phase models based on activity coefficient approach.

It is also recommended to apply these rigorous computational methods to predict stability limits and critical conditions for some newly-emerging systems of special practical importance such as those involving emulsion stability and polymeric criticality and stability conditions.

References

[1] J. W. Tester and M. Modell, *Thermodynamics and its applications*, 3rd ed. Upper Saddle River, N.J.: Prentice Hall PTR, 1997.

[2] P. G. Debenedetti, *Metastable Liquids: Concepts and Principles*. New Jersey: Princeton University Press, 1996.

[3] R. E. Apfel, "Water superheated to 279.5.deg. at atmospheric pressure," *Nature (London), Phys. Sci.*, vol. 238, pp. 63-4, 1972.

[4] B. M. Cwilong, "Sublimation in a Wilson chamber," *Proc. R. Soc. London, Ser. A*, vol. 190, pp. 137-43, 1947.

[5] P. C. Wankat, *Separation Process Engineering*: Pearson Education, 2006.

[6] R. C. Reid, *et al.*, *The properties of gases and liquids*. New York: McGraw-Hill, 1987.

[7] F. Garcia-Sanchez, *et al.*, "Modeling of multiphase liquid equilibria for multicomponent mixtures," *Fluid Phase Equilib.*, vol. 121, pp. 207-225, 1996.

[8] V. J. Klenin and Editor, *Thermodynamics of Systems Containing Flexible-Chain Polymers*: Elsevier, 1999.

[9] E. Salzano and R. Bubbico, "Acoustic analysis of explosive LNG rapid phase transition on water,", pp. ACSAICHE-99138. 2008.

[10] N. A. Darwish and S. A. Al-Muhtaseb, "A comparison between four cubic equations of state in predicting the inversion curve and spinodal curve loci of methane," *Thermochim. Acta*, vol. 287, pp. 43-52, 1996.

[11] R. P. Koopman and D. L. Ermak, "Lessons learned from LNG safety research," *J. Hazard. Mater.*, vol. 140, pp. 412-428, 2007.

[12] R. C. Reid, "Superheated liquids. A laboratory curiosity and, possibly, an industrial curse. Part 3: Discussion and conclusions," *Chem. Eng. Educ.*, vol. 12, pp. 194-6, 203-6, 1978.

[13] R. C. Reid, "Superheated liquids: a laboratory curiosity and, possibly, an industrial curse. Part 2: Industrial vapor explosions," *Chem. Eng. Educ.*, vol. 12, pp. 108-11, 127-9, 1978.

[14] R. C. Reid, "Superheated liquids: a laboratory curiosity and, possibly, an industrial curse. Part 1: Laboratory studies and theory," *Chem. Eng. Educ.*, vol. 12, pp. 60-3, 83-7, 1978.

[15] R. C. Reid, "Rapid phase transitions from liquid to vapor," *Adv. Chem. Eng.*, vol. 12, pp. 105-208, 1983.

[16] H. K. Fauske, "Mechanism of uranium dioxide-sodium explosive interactions," *Nucl. Sci. Eng.*, vol. 51, pp. 95-101, 1973.

[17] P. D. Hess and K. J. Brondyke, "Causes of molten aluminum-water explosions and their prevention," *Metal Progr.*, vol. 95, pp. 93-4, 96, 98, 100, 1969.

[18] American Institute of Chemical Engineers, *Guidelines for Consequence Analysis of Chemical Releases, Center for Chemical Process Safety*. New York, 1999.

[19] T. Abbasi and S. A. Abbasi, "The boiling liquid expanding vapour explosion (BLEVE): Mechanism, consequence assessment, management," *Journal of Hazardous Materials,* vol. 141, pp. 489-519, 2007.

[20] R. C. Reid, "Possible mechanism for pressurized-liquid tank explosions or BLEVE's," *Science (Washington, D. C.),* vol. 203, pp. 1263-5, 1979.

[21] M. E. Kim-E and R. C. Reid, "The rapid depressurization of hot, high pressure liquids or supercritical fluids,", pp. 81-100, 1983.

[22] J. Wu, *et al.*, "Molecular-thermodynamic framework for asphaltene-oil equilibria," *AIChE J.*, vol. 44, p. 2568, 1998.

[23] A. Firoozabadi, Thermodynamics of Hydrocarbon Reservoirs: McGraw-Hill, 1999.

[24] G. P. S. Association, "GPSA Engineering Data Book 13th Ed," in *Dehydration* ed, 2012.

[25] J. M. Campbell, *Gas conditioning and processing*: Campbell Petroleum Series, 1976.

[26] P. Licence, "Clathrate Hydrates of Natural Gases by E. Dendy Sloan, A. Koh Carolyn," *Fuel,* vol. 87, p. 3158, 2008.

[27] J. Long and E. D. Sloan, Jr., "Quantized water clusters around apolar molecules," *Mol. Simul.*, vol. 11, pp. 145-61, 1993.

[28] L. Del Villano and M. A. Kelland, "Tetrahydrofuran hydrate crystal growth inhibition by hyperbranched poly(ester amide)s," *Chemical Engineering Science*, vol. 64, pp. 3197-3200, 2009.

[29] A. L. DeVries, "Freezing resistance in fishes," in Fish Physiology Conference, New York, pp. 157-90, 1971.

[30] F. Franks, *Biochemistry and Biophysics at Low Temperatures*. Cambridge: Cambridge University Press, 1985.

[31] D. W. Wu, *et al.*, "Enhancement of insect antifreeze protein activity by antibodies," *Biochim Biophys Acta*, vol. 1076, pp. 416-20, 1991.

[32] A. L. DeVries, *et al.*, "Primary structure of freezing point-depressing glycoproteins," *J. Biol. Chem.*, vol. 246, pp. 305-8, 1971.

[33] K. E. Zachariassen and J. A. Husby, "Antifreeze effect of thermal hysteresis agents protects highly supercooled insects," *Nature*, vol. 298, pp. 865-867, 1982.

[34] K. Sassen, *et al.*, "Highly supercooled cirrus cloud water: confirmation and climatic implications," *Science*, vol. 227, pp. 411-3, 1985.

[35] K. Sassen, "Evidence for liquid-phase cirrus cloud formation from volcanic aerosols: climatic implications," *Science*, vol. 257, pp. 516-9, 1992.

[36] B. Vonnegut, "Nucleation of ice formation by silver iodide," *J. Appl. Phys.*, vol. 18, pp. 593-5, 1947.

[37] P. A. Wells, *et al.*, "Experimental determination of the spinodal P-T-x surface for the system 2-butoxyethanol/water using the 'PPICS' apparatus," *Fluid Phase Equilib.*, vol. 106, pp. 185-202, 1995.

[38] J. P. Novak, *et al.*, "Critical curves of liquid-liquid equilibria in ternary systems Description by a regular-solution model," *Fluid Phase Equilib.*, vol. 208, pp. 199-221, 2003.

[39] J. M. Smith, *et al.*, *Introduction to Chemical Engineering Thermodynamics*: McGraw-Hill Companies, Incorporated, 2004.

[40] J. M. Sørensen and W. Arlt, *Liquid-liquid Equilibrium Data Collection: Binary systems*: DECHEMA, Deutsche Gesellschaft für Chemisches Apparatewesen, 1979.

[41] J. M. Prausnitz, *et al.*, *Molecular Thermodynamics of Fluid-Phase Equilibria*: Pearson Education, 1998.

[42] D. C. Jones and H. F. Betts, "Some miscibility relations of acetic anhydride," *J. Chem. Soc.*, pp. 1177-92, 1928.

[43] R. Eustaquio-Rincon, *et al.*, "Experimental liquid-liquid phase equilibria for binary systems: ethanenitrile with several hydrocarbon isomers," *Fluid Phase Equilib.*, vol. 149, pp. 177-189, 1998.

[44] U. Domanska, *et al.*, "Liquid-Liquid Phase Equilibria of Binary Systems Containing Hyperbranched Polymer B-U3000: Experimental Study and Modeling in Terms of Lattice Cluster Theory," *J. Chem. Eng. Data*, vol. 55, pp. 3842-3846, 2010.

[45] A. F. Frolov, *et al.*, "Solubility and liquid-liquid equilibrium in amethyl vinyl ketone-acetone-water-[organic]solvent system," *Zh. Prikl. Khim. (Leningrad)*, vol. 42, pp. 2095-104, 1969.

[46] W. Zhang, "Phase behavior and phase separation kinetics in polymer solutions under high pressure", Ph.D. dissertation, Dept. Chem. Eng. Virginia Polytechnic Institute and State University, Blacksburg, VA, 2005.

[47] R. R. Parvatiker and B. C. McEwen, "Studies in mutual solubility. III. The mutual solubility of glycerol and amino-and hydroxy-compounds," *J. Chem. Soc., Trans.*, vol. 125, pp. 1484-92, 1924.

[48] J. Matous, *et al.*, "Phase equilibriums in the system tetrahydrofuran(1)-water(2)," *Collect. Czech. Chem. Commun.*, vol. 37, pp. 2653-63, 1972.

[49] B. H. Chang and Y. C. Bae, "Liquid-liquid equilibria of binary polymer solutions with specific interactions," *Polymer*, vol. 39, pp. 6449-6454, 1998.

[50] P. A. Schacht and J. T. Koberstein, "The effects of end groups on thermodynamics of polymer blends. III LCST phase diagrams," *Polymer*, vol. 43, pp. 6527-6534, 2002.

[51] C. Browarzik and D. Browarzik, "Liquid-liquid equilibrium calculation in binary water+nonionic surfactant CiEj systems with a new mass-action law model based on continuous thermodynamics," *Fluid Phase Equilib.,* vol. 235, pp. 127-138, 2005.

[52] J. Yang, *et al.,* "Liquid-liquid equilibria of polymer solutions with oriented interactions," *Fluid Phase Equilib.,* vol. 249, pp. 192-197, 2006.

[53] F. A. H. Schreinemakers, "On the equilibrium in systems with three components, in which two or three liquid phases can be present. [machine translation]," *Archives neerland. sc. exact, et nat.,* vol. 3, pp. 1-78, 1899.

[54] J. L. Zurita, *et al.,* "Equilibrium diagrams of water + succinic acid + (n-butanol or + benzyl alcohol or + tributyl phosphate) ternary systems at 303.15 K," *Afinidad,* vol. 52, pp. 419-24, 1995.

[55] G. Hradetzky, *et al.,* "Liquid-liquid equilibrium. Methanol-hexane system," *Int. DATA Ser., Sel. Data Mixtures, Ser. A,* p. 294, 1991.

[56] M. A. C. Gomez, *et al.,* "Influence of temperature on the liquid-liquid equilibria containing two pairs of partially miscible liquids Water + furfural + 1-butanol ternary system," *Fluid Phase Equilib.,* vol. 153, pp. 279-292, 1998.

[57] V. P. Sazonov, *et al.,* "Influence of Temperature on the Liquid-Liquid Equilibria of the Ternary System Nitromethane + 1-Hexanol + Octanoic Acid," *J. Chem. Eng. Data,* vol. 47, pp. 599-602, 2002.

[58] F. A. H. Schreinemakers, "Equilibria in the system: water, phenol, and acetone," *Zeit. physikal. Chem.,* vol. 33, pp. 78-98, 1900.

[59] F. Becker and P. Richter, "Nonaqueous ternary mixtures with 'island' miscibility gaps," *Fluid Phase Equilib.,* vol. 49, pp. 157-6, 1989.

[60] E. Raub and A. Engel, "The ternary system gold-copper-nickel. II. The transformations of gold-copper alloys in the ternary system gold-copper-nickel," *Metallforschung,* vol. 2, pp. 147-58, 1947.

[61] P. A. Meerburg, "Equilibria in systems of three components, the formation of two liquid phases being possible," *Zeit. physikal. Chem.,* vol. 40, pp. 641-88, 1902.

[62] K. Rehak, *et al.,* "Phase equilibria of phenol + tetrahydrofuran + water system and its thermodynamic description," *Fluid Phase Equilib.,* vol. 109, pp. 113-29, 1995.

[63] W. Li, *et al.*, "Measurement and calculation of liquid–liquid equilibria of binary aqueous polymer solutions," *Chemical Engineering Journal,* vol. 78, pp. 179-185, 2000.

[64] A. E. Hill, "Mutual solubility of liquids. I. Mutual solubility of ethyl ether and water. II. Solubility of water in benzene," *J. Am. Chem. Soc.,* vol. 45, pp. 1143-55, 1923.

[65] K. Řehák, *et al.*, "Revision of the volumetric method for measurements of liquid–liquid equilibria in binary systems," *Fluid Phase Equilibria,* vol. 230, pp. 109-120, 2005.

[66] M. Mohsen-Nia, *et al.*, "Binodal curve measurements for (water + propionic acid + dichloromethane) ternary system by cloud point method," *J. Chem. Thermodyn.,* vol. 41, pp. 859-863, 2009.

[67] B. Chu and F. J. Schoenes, "Diffusion coefficient of the isobutyric acid-water system in the critical region," *Phys. Rev. Lett.,* vol. 21, pp. 6-9, 1968.

[68] C. M. Sorensen, "Dynamic light-scattering of tetrahydrofuran and water solutions," *J. Phys. Chem.,* vol. 92, pp. 2367-70, 1988.

[69] P. Debye, "Angular dissymmetry of the critical opalescence in liquid mixtures," *J. Chem. Phys.,* vol. 31, pp. 680-7, 1959.

[70] H. Galina, *et al.*, "Pulse-induced critical scattering (PICS), its methods and its role in characterization,", pp. 267-98, 1986.

[71] P. A. Wells, *et al.*, "Experimental determination of the spinodal P-T-x surface for the system 2-butoxyethanol/water using the 'PPICS' apparatus," *Fluid Phase Equilib.,* vol. 106, pp. 185-202, 1995.

[72] J. Maugey, *et al.*, "Small angle light scattering investigation of polymerization induced phase separation mechanisms," *Polymer,* vol. 42, pp. 4353-4366, 2001.

[73] S. Chaikunchuensakun, "A combined optimization algorithm for stability, phase, and chemical equilibria," Ph.d, Chemical Engineering, Polytechnic University, 2000.

[74] L. E. Baker, *et al.*, "Gibbs energy analysis of phase equilibriums [for oil reservoirs]," *SPEJ, Soc. Pet. Eng. J.,* vol. 22, pp. 731-42, 1982.

[75] M. L. Michelsen, "The isothermal flash problem. Part I. Stability," *Fluid Phase Equilib.*, vol. 9, pp. 1-19, 1982.

[76] S. K. Wasylkiewicz, *et al.*, "Global Stability Analysis and Calculation of Liquid-Liquid Equilibrium in Multicomponent Mixtures," *Ind. Eng. Chem. Res.*, vol. 35, pp. 1395-408, 1996.

[77] A. C. Sun and W. D. Seider, "Homotopy-continuation method for stability analysis in the global minimization of the Gibbs free energy," *Fluid Phase Equilib.*, vol. 103, pp. 213-49, 1995.

[78] C. A. Floudas, Deterministic Global Optimization: Theory, Methods and Applications. New Jersey: Springer, pp. 45-84, 1999.

[79] J. Z. Huaa, *et al.*, "Reliable computation of phase stability using interval analysis: cubic equation of state models," *Comput. Chem. Eng.*, vol. 22, pp. 1207-1214, 1998.

[80] R. L. Rowley, Statistical mechanics for thermophysical property calculations: Prentice Hall, 1994.

[81] A. Kumar, et al., "Equilibrium critical phenomena in binary liquid mixtures," Physics Reports, vol. 98, pp. 57-143, 1983.

[82] J. V. Sengers and J. M. H. L. Sengers, "Thermodynamic behavior of fluids near the critical point," Annu. Rev. Phys. Chem., vol. 37, pp. 189-222, 1986.

[83] R. F. Chang, et al., "Correlation function near the critical mixing point of a binary liquid," Phys. Rev. A, vol. 19, pp. 866-82, 1979.

[84] T. A. Edison, et al., "Critical scaling laws and an excess Gibbs energy model," Fluid Phase Equilib., vol. 150, 151, pp. 429-438, 1998.

[85] A. van ’t Hof, et al., "Description of liquid–liquid equilibria including the critical region with the crossover-NRTL model," Fluid Phase Equilibria, vol. 192, pp. 27-48, 2001.

[86] J. J. De Pablo and J. M. Prausnitz, "Liquid-liquid equilibria for binary and ternary systems including the critical region. Transformation to non-classical coordinates," Fluid Phase Equilibria, vol. 50, pp. 101-131, 1989.

[87] M. Ko, *et al.*, "Liquid-Liquid Equilibria for the Binary Systems of Sulfolane with Alkanes," *J. Chem. Eng. Data*, vol. 52, pp. 1464-1467, 2007.

[88] K. Kurihara, *et al.*, "Determination and correlation of liquid-liquid equilibria for nine binary acetonitrile + n-alkane systems," *Fluid Phase Equilib.*, vol. 302, pp. 109-114, 2011.

[89] R. Eustaquio-Rincon, *et al.*, "Experimental liquid-liquid phase equilibria for binary systems: ethanenitrile with several hydrocarbon isomers," *Fluid Phase Equilib.*, vol. 149, pp. 177-189, 1998.

[90] K. Zieborak and K. Olszewski, "Heteropolyazeotropic systems. II. Acetonitrile-n-paraffinic hydrocarbons," *Bull. Acad. Pol. Sci., Cl. 3,* vol. 4, pp. 823-7, 1956.

[91] H. Matsuda, *et al.*, "Liquid–liquid equilibrium data for binary perfluoroalkane (C6 and C8);n-alkane systems," *Fluid Phase Equilibria,* vol. 297, pp. 187-191, 2010.

[92] M. Ko, *et al.*, "Liquid-Liquid Equilibria for the Binary Systems of N-Formylmorpholine with Branched Cycloalkanes," *J. Chem. Eng. Data,* vol. 48, pp. 699-702, 2003.

[93] M. Ko, *et al.*, "Liquid-Liquid Equilibria for Binary Systems Containing N-Formylmorpholine," *J. Chem. Eng. Data,* vol. 47, pp. 923-926, 2002.

[94] J. Im, *et al.*, "Liquid-liquid equilibria for the binary systems of sulfolane with branched cycloalkanes," *Fluid Phase Equilib.,* vol. 246, pp. 34-38, 2006.

[95] M. B. Shiflett and A. Yokozeki, "Liquid-Liquid Equilibria in Binary Mixtures of 1,3-Propanediol + Ionic Liquids [bmim][PF6], [bmim][BF4], and [emim][BF4]," *J. Chem. Eng. Data,* vol. 52, pp. 1302-1306, 2007.

[96] H. J. Bittrich, *et al.*, "Liquid-liquid equilibria in binary mixtures of N-methyl-α-pyrrolidone and saturated hydrocarbons. Part II," *Fluid Phase Equilib.,* vol. 126, pp. 115-125, 1996.

[97] R. Alcalde, *et al.*, "Liquid-liquid equilibria of lactam containing binary systems," *Fluid Phase Equilib.,* vol. 266, pp. 90-100, 2008.

[98] L. Han, *et al.*, "The liquid-liquid critical behaviour of binary solutions for (N-methyl-2-pyrrolidone + cycloalkanes)," *Phys. Chem. Chem. Phys.*, vol. 1, pp. 2733-2736, 1999.

[99] J. M. Sørensen and W. Arlt, Liquid-liquid Equilibrium Data Collection: Ternary systems: DECHEMA, Deutsche Gesellschaft für Chemisches Apparatewesen, 1980.

[100] A. Venkataratnam, et al., "Ternary liquid equilibriums. Systems: acetone-water-esters," Chem. Eng. Sci., vol. 7, pp. 102-10, 1957.

[101] R. E. Treybal and O. J. Vondrak, "Distribution of ketones in water-hydrocarbon system," J. Ind. Eng. Chem. (Washington, D. C.), vol. 41, pp. 1761-3, 1949.

[102] V. V. Udovenko and L. P. Aleksandrova, "Solubility in the formic acid-1,2-dichloroethane-water system," Zh. Fiz. Khim., vol. 32, pp. 1889-92, 1958.

[103] A. S. Dubovskaya and M. K. Karapet'yants, "Mutual solubility in water-1,2-dichloroethane-alkanoic acid systems," Zh. Fiz. Khim., vol. 44, pp. 2299-305, 1970.

[104] S.-J. Park, et al., "Binary Liquid-Liquid Equilibrium (LLE) for Dibutyl Ether (DBE) + Water from (288.15 to 318.15) K and Ternary LLE for Systems of DBE + C1 - C4 Alcohols + Water at 298.15 K," J. Chem. Eng. Data, vol. 53, pp. 2089-2094, 2008.

[105] E. R. Washburn, et al., "The ternary system: ethyl alcohol, toluene and water at 25°," J. Am. Chem. Soc., vol. 61, pp. 1694-5, 1939.

[106] S. Nam, et al., "Mutual solubility and equilibrium data for ternary systems," J. Chem. Eng. Jap., vol. 5, pp. 327-34, 1972.

[107] S. F. Taylor, "Mass law studies. I. [Solubility of benzene in aqueous alcohol.]," J. Physical Chem., vol. 1, pp. 301-3, 1897.

[108] A. Arce, et al., "Phase stability of the system limonene + linalool + 2-aminoethanol," Fluid Phase Equilib., vol. 226, pp. 121-127, 2004.

Appendix I: Legendre Transform [1]

Legendre transform is useful tool that enables the transformation of a function in terms of other variables without losing the information content of the original function. It plays an important role in calculus thermodynamics to transform functions in terms of other variables that easily measured or dealt with. It is used to transform fundamental property relation, which is expressed in the extensive form as

$$d\bar{U} = T\, d\bar{S} - P\, d\bar{V} \qquad \text{(AI.1)}$$

Now, this equation is expressed in terms of entropy and volume. This might not be helpful because entropy cannot readily be measured and it would be more useful if it can be expressed in terms of other variables that are easier to measure or to deal with such as temperature and pressure. Moreover, it is not possible to transform it by simply differentiating as this will reduce the information content of the equation. Legendre transformation can be used to express this equation in terms of other variables, without losing the original information content given by fundamental property relation equation, given that it must be restricted to its conical variables, which are: Temperature & Entropy, and Pressure & Volume. Legendre transformation can be done using the following equations:

$$y^{(0)} = f(x_1,...,x_m) \qquad \text{(AI.2)}$$

x_1 can be transformed to its conical variable which is in this case is ξ_1 by differentiating

$$\zeta_i = \left(\frac{\partial y^{(0)}}{\partial x_i} \right) \qquad \text{(AI.3)}$$

The integrated form of the original function can be found by

$$y^{(k)} = y^{(0)} - \sum_{i=1}^{k} x_i \zeta_i \qquad \text{(AI.4)}$$

The differential can also be obtained by

$$dy^{(k)} = -\sum_{i=1}^{k} x_i d\zeta_i + \sum_{i=k+1}^{m} \zeta_i dx_i \qquad \text{(AI.5)}$$

$y^{(k)}$ refers to Legendre transform of kth degree. Now, applying Legendre transformation and using fundamental property relation as the basis function as follows

$$\bar{U} = f(\bar{S}, \bar{V}, N_1 \ldots., N_n) \qquad \text{(AI.6)}$$

Now, to get rid of entropy as variable, it can be done but it must be restricted to transforming it to temperature, which it's conical variables as follows

$$\xi_1 = \left(\frac{\partial \bar{U}}{\partial \bar{S}}\right)_{\bar{V},N} = T \quad \text{(AI.7)}$$

Now, equations A1.4 & A1.5 used to find the final form of the new function

$$y^{(1)} = \bar{U} - \bar{S}T \equiv \bar{A} \quad \text{(AI.8)}$$

And

$$dy^{(1)} \equiv d\bar{A} = -\bar{S}dT + Pd\bar{V} + \sum_{i=1}^{n} \mu_i \, dN_i \quad \text{(AI.9)}$$

Internal energy is now transformed to Helmholtz free energy, which is the 1st Legendre transform, without losing any information.

Next, to obtain second Legendre transform using U as our basis function again,

$$\xi_1 = \left(\frac{\partial \bar{U}}{\partial \bar{S}}\right)_{\bar{V},N} = T \quad \text{(AI.10)}$$

$$\xi_2 = \left(\frac{\partial \bar{U}}{\partial \bar{V}}\right)_{\bar{S},N} = -P \quad \text{(AI.11)}$$

The 2nd Legendre transform becomes,

$$y^{(2)} = \bar{U} - \bar{S}T - (-P\bar{V}) \equiv \bar{G} \quad \text{(AI.12)}$$

And the differential form is

$$dy^{(2)} \equiv d\bar{G} = -\bar{S}dT + \bar{V}dP + \sum_{i=1}^{n} \mu_i \, dN_i \quad \text{(AI.13)}$$

Finally, Total Legendre transform is

$$y^{(n+2)} = \bar{U} - \bar{S}T - (-P\bar{V}) \equiv \bar{G} \quad \text{(AI.14)}$$

$$dy^{(n+2)} = -\bar{S}dT + \bar{V}dP - \sum_{i=1}^{n} N_i \, d\mu_i \quad \text{(AI.15)}$$

Appendix II: Derivatives From NRTL Model

$$\left(\frac{\partial^2 \bar{G}^M}{\partial {x_1}^2}\right)_{T,P,x_2}$$
$$= 2\left[\frac{(x_1 + x_2G_{21} + x_3G_{31})(-G_{31}\tau_{31}) - (x_2G_{21}\tau_{21} + x_3G_{31}\tau_{31})(1 - G_{31})}{(x_1 + x_2G_{21} + x_3G_{31})^2}\right]$$
$$- 2\,x_1\left[\frac{(x_1 + x_2G_{21} + x_3G_{31})(-G_{31}\tau_{31}) - (x_2G_{21}\tau_{21} + x_3G_{31}\tau_{31})(1 - G_{31})}{(x_1 + x_2G_{21} + x_3G_{31})^3}\right](1 - G_{31})$$
$$- 2\,x_2\left[\frac{(x_1G_{12} + x_2 + x_3G_{32})(G_{12}\tau_{12} - G_{32}\tau_{32}) - (x_1G_{12}\tau_{12} + x_3G_{32}\tau_{32})(G_{12} - G_{32})}{(x_1G_{12} + x_2 + x_3G_{32})^3}\right](G_{12} - G_{32})$$
$$- 2\left[\frac{(x_1G_{13} + x_2G_{23} + x_3)(G_{13}\tau_{13}) - (x_1G_{13}\tau_{13} + x_2G_{23}\tau_{23})(G_{13} - 1)}{(x_1G_{13} + x_2G_{23} + x_3)^2}\right] + \frac{1}{x_1} + \frac{1}{x_3}$$
$$- 2\,x_3\left[\frac{(x_1G_{13} + x_2G_{23} + x_3)(G_{13}\tau_{13}) - (x_1G_{13}\tau_{13} + x_2G_{23}\tau_{23})(G_{13} - 1)}{(x_1G_{13} + x_2G_{23} + x_3)^3}\right](G_{13} - 1)$$

(AII.1)

$$\left(\frac{\partial^2 \bar{G}^M}{\partial {x_2}^2}\right)_{T,P,x_1}$$
$$= -2x_1\left[\frac{(x_1 + x_2G_{21} + x_3G_{31})(G_{21}\tau_{21} + G_{31}\tau_{31}) - (x_2G_{21}\tau_{21} + x_3G_{31}\tau_{31})(G_{21} - G_{31})}{(x_1 + x_2G_{21} + x_3G_{31})^3}\right](G_{21} - G_{31})$$
$$+ 2\left[\frac{(x_1G_{12} + x_2 + x_3G_{32})(-G_{32}\tau_{32}) - (x_1G_{12}\tau_{12} + x_3G_{32}\tau_{32})(1 - G_{32})}{(x_1G_{12} + x_2 + x_3G_{32})^2}\right]$$
$$- 2\,x_2\left[\frac{(x_1G_{12} + x_2 + x_3G_{32})(-G_{32}\tau_{32}) - (x_1G_{12}\tau_{12} + x_3G_{32}\tau_{32})(1 - G_{32})}{(x_1G_{12} + x_2 + x_3G_{32})^3}\right](1 - G_{32})$$
$$- 2\left[\frac{(x_1G_{13} + x_2G_{23} + x_3)(G_{23}\tau_{23}) - (x_1G_{13}\tau_{13} + x_2G_{23}\tau_{23})(G_{23} - 1)}{(x_1G_{13} + x_2G_{23} + x_3)^2}\right] + \frac{1}{x_2} + \frac{1}{x_3}$$
$$- 2\,x_3\left[\frac{(x_1G_{13} + x_2G_{23} + x_3)(G_{23}\tau_{23}) - (x_1G_{13}\tau_{13} + x_2G_{23}\tau_{23})(G_{23} - 1)}{(x_1G_{13} + x_2G_{23} + x_3)^3}\right](G_{23} - 1)$$

(AII.2)

$$\left(\frac{\partial^2 \bar{G}^M}{\partial x_1 \partial x_2}\right)_{T,P,x_1}$$

$$= -2x_1\left[\frac{(x_1 + x_2G_{21} + x_3G_{31})(G_{21}\tau_{21} + G_{31}\tau_{31}) - (x_2G_{21}\tau_{21} + x_3G_{31}\tau_{31})(G_{21} - G_{31})}{(x_1 + x_2G_{21} + x_3G_{31})^2}\right]$$

$$+ x_1\left[\begin{array}{c}\dfrac{(x_1 + x_2G_{21} + x_3G_{31})[(G_{21} - G_{31})(-G_{31}\tau_{31}) - (G_{21}\tau_{21} - G_{31}\tau_{31})(1 - G_{31})]}{(x_1 + x_2G_{21} + x_3G_{31})^3} \\ -2(G_{21} - G_{31})\ \dfrac{[(x_1 + x_2G_{21} + x_3G_{31})(-G_{31}\tau_{31}) - (x_2G_{21}\tau_{21} + x_3G_{31}\tau_{31})(1 - G_{31})]}{(x_1 + x_2G_{21} + x_3G_{31})^3}\end{array}\right]$$

$$+\left[\frac{(x_1G_{12} + x_2 + x_3G_{32})(G_{12}\tau_{12} - G_{32}\tau_{32}) - (x_1G_{12}\tau_{12} + x_3G_{32}\tau_{32})(G_{12} - G_{32})}{(x_1G_{12} + x_2 + x_3G_{32})^2}\right]$$

$$+\ x_2\left[\begin{array}{c}\dfrac{(x_1G_{12} + x_2 + x_3G_{32})[(G_{32}\tau_{32})(G_{12} - G_{32}) + (G_{12}\tau_{12} - G_{32}\tau_{32})(1 - G_{32})]}{(x_1G_{12} + x_2 + x_3G_{32})^3} \\ -2(1 - G_{32})\dfrac{[(x_1G_{12} + x_2 + x_3G_{32})(G_{12}\tau_{12} - G_{32}\tau_{32}) - (x_1G_{12}\tau_{12} + x_3G_{32}\tau_{32})(G_{12} - G_{32})]}{(x_1G_{12} + x_2 + x_3G_{32})^3}\end{array}\right]$$

$$-\left[\frac{(x_1G_{13} + x_2G_{23} + x_3)(G_{23}\tau_{23}) - (x_1G_{13}\tau_{13} + x_2G_{23}\tau_{23})(G_{23} - 1)}{(x_1G_{13} + x_2G_{23} + x_3)^2}\right]$$

$$-\left[\frac{(x_1G_{13} + x_2G_{23} + x_3)(G_{13}\tau_{13}) - (x_1G_{13}\tau_{13} + x_2G_{23}\tau_{23})(G_{13} - 1)}{(x_1G_{13} + x_2G_{23} + x_3)^2}\right] + \frac{1}{x_3}$$

$$+ x_3\left[\begin{array}{c}\dfrac{(x_1G_{13} + x_2G_{23} + x_3)[(G_{23} - 1)(G_{13}\tau_{13}) - (G_{23}\tau_{23})(G_{13} - 1)]}{(x_1G_{13} + x_2G_{23} + x_3)^3} \\ -2(G_{23} - 1)\ \dfrac{[(x_1G_{13} + x_2G_{23} + x_3)(G_{13}\tau_{13}) - (x_1G_{13}\tau_{13} + x_2G_{23}\tau_{23})(G_{13} - 1)]}{(x_1G_{13} + x_2G_{23} + x_3)^3}\end{array}\right]$$

(AII.3)

$$\left(\frac{\partial^3 \bar{G}^M}{\partial {x_1}^3}\right)_{T,P,x_2}$$

$$= -6(1 - G_{31})\left[\frac{(x_1 + x_2G_{21} + x_3G_{31})(-G_{31}\tau_{31}) - (x_2G_{21}\tau_{21} + x_3G_{31}\tau_{31})(1 - G_{31})}{(x_1 + x_2G_{21} + x_3G_{31})^3}\right]$$

$$+ 6\ x_1\left[\frac{(x_1 + x_2G_{21} + x_3G_{31})(-G_{31}\tau_{31}) - (x_2G_{21}\tau_{21} + x_3G_{31}\tau_{31})(1 - G_{31})}{(x_1 + x_2G_{21} + x_3G_{31})^4}\right](1 - G_{31})^2$$

$$+ 6\ x_2\left[\frac{(x_1G_{12} + x_2 + x_3G_{32})(G_{12}\tau_{12} - G_{32}\tau_{32}) - (x_1G_{12}\tau_{12} + x_3G_{32}\tau_{32})(G_{12} - G_{32})}{(x_1G_{12} + x_2 + x_3G_{32})^3}\right](G_{12} - G_{32})^2$$

$$+ 6\left[\frac{(x_1G_{13} + x_2G_{23} + x_3)(G_{13}\tau_{13}) - (x_1G_{13}\tau_{13} + x_2G_{23}\tau_{23})(G_{13} - 1)}{(x_1G_{13} + x_2G_{23} + x_3)^2}\right](G_{13} - 1) + \frac{1}{{x_1}^2} + \frac{1}{{x_3}^2}$$

$$+ 6\ x_3\left[\frac{(x_1G_{13} + x_2G_{23} + x_3)(G_{13}\tau_{13}) - (x_1G_{13}\tau_{13} + x_2G_{23}\tau_{23})(G_{13} - 1)}{(x_1G_{13} + x_2G_{23} + x_3)^3}\right](G_{13} - 1)^2$$

(AII.4)

$$\left(\frac{\partial^3 \bar{G}^M}{\partial {x_2}^3}\right)_{T,P,x_1}$$

$$= 6x_1\left[\frac{(x_1+x_2G_{21}+x_3G_{31})(G_{21}\tau_{21}+G_{31}\tau_{31})-(x_2G_{21}\tau_{21}+x_3G_{31}\tau_{31})(G_{21}-G_{31})}{(x_1+x_2G_{21}+x_3G_{31})^4}\right](G_{21}-G_{31})^2$$
$$-6\left[\frac{(x_1G_{12}+x_2+x_3G_{32})(-G_{32}\tau_{32})-(x_1G_{12}\tau_{12}+x_3G_{32}\tau_{32})(1-G_{32})}{(x_1G_{12}+x_2+x_3G_{32})^3}\right](1-G_{32})$$
$$+6\,x_2\left[\frac{(x_1G_{12}+x_2+x_3G_{32})(-G_{32}\tau_{32})-(x_1G_{12}\tau_{12}+x_3G_{32}\tau_{32})(1-G_{32})}{(x_1G_{12}+x_2+x_3G_{32})^4}\right](1-G_{32})^2$$
$$+6\left[\frac{(x_1G_{13}+x_2G_{23}+x_3)(G_{23}\tau_{23})-(x_1G_{13}\tau_{13}+x_2G_{23}\tau_{23})(G_{23}-1)}{(x_1G_{13}+x_2G_{23}+x_3)^3}\right](G_{23}-1)$$
$$+6\,x_3\left[\frac{(x_1G_{13}+x_2G_{23}+x_3)(G_{23}\tau_{23})-(x_1G_{13}\tau_{13}+x_2G_{23}\tau_{23})(G_{23}-1)}{(x_1G_{13}+x_2G_{23}+x_3)^3}\right](G_{23}-1)^2$$
$$-\frac{1}{{x_2}^2}+\frac{1}{{x_3}^2}$$

(AII.5)

$$\left(\frac{\partial^3 \bar{G}^M}{\partial {x_1}^2\,\partial x_2}\right)_{T,P,x_1}$$

$$= 2\left[\begin{array}{c}\dfrac{(x_1+x_2G_{21}+x_3G_{31})[(G_{21}-G_{31})(-G_{31}\tau_{31})-(G_{21}\tau_{21}+G_{31}\tau_{31})(1-G_{31})]}{(x_1+x_2G_{21}+x_3G_{31})^3}\\ -2(G_{21}-G_{31})\dfrac{[(x_1+x_2G_{21}+x_3G_{31})(-G_{31}\tau_{31})-(x_2G_{21}\tau_{21}+x_3G_{31}\tau_{31})(1-G_{31})]}{(x_1+x_2G_{21}+x_3G_{31})^3}\end{array}\right]$$
$$-\,x_1\left[\begin{array}{c}\dfrac{(x_1+x_2G_{21}+x_3G_{31})[(-G_{31}\tau_{31})(1-G_{31})(G_{21}-G_{31})-(G_{21}\tau_{21}+G_{31}\tau_{31})(1-G_{31})^2]}{(x_1+x_2G_{21}+x_3G_{31})^4}\\ -6(1-G_{31})(G_{21}-G_{31})\dfrac{[(x_1+x_2G_{21}+x_3G_{31})(-G_{31}\tau_{31})-(x_2G_{21}\tau_{21}+x_3G_{31}\tau_{31})(1-G_{31})]}{(x_1+x_2G_{21}+x_3G_{31})^4}\end{array}\right]$$
$$-2\left[\frac{(x_1G_{12}+x_2+x_3G_{32})(G_{12}\tau_{12}-G_{32}\tau_{32})-(x_1G_{12}\tau_{12}+x_3G_{32}\tau_{32})(G_{12}-G_{32})}{(x_1G_{12}+x_2+x_3G_{32})^3}\right](G_{12}-G_{32})$$
$$+\,x_2\left[\begin{array}{c}2\dfrac{(x_1G_{13}+x_2G_{23}+x_3)[(G_{12}\tau_{12}-G_{32}\tau_{32})(1-G_{32})(G_{12}-G_{32})+(G_{32}\tau_{32})(G_{12}-G_{32})^2]}{(x_1G_{12}+x_2+x_3G_{32})^4}\\ -6(G_{12}-G_{32})(1-G_{32})\dfrac{[(x_1G_{12}+x_2+x_3G_{32})(G_{12}\tau_{12}-G_{32}\tau_{32})-(x_1G_{12}\tau_{12}+x_3G_{32}\tau_{32})(G_{12}-G_{32})]}{(x_1G_{12}+x_2+x_3G_{32})^4}\end{array}\right]$$
$$+2\left[\frac{(x_1G_{13}+x_2G_{23}+x_3)(G_{13}\tau_{13})-(x_1G_{13}\tau_{13}+x_2G_{23}\tau_{23})(G_{13}-1)}{(x_1G_{13}+x_2G_{23}+x_3)^3}\right](G_{13}-1)+\frac{1}{{x_3}^2}$$
$$-\,2\,x_3\left[\begin{array}{c}\dfrac{(x_1G_{13}+x_2G_{23}+x_3)[(G_{13}\tau_{13})(G_{13}-1)(G_{23}-1)-(G_{23}\tau_{23})(G_{13}-1)^2]}{(x_1G_{13}+x_2G_{23}+x_3)^4}\\ 6(G_{13}-1)(G_{23}-1)\dfrac{[(x_1G_{13}+x_2G_{23}+x_3)(G_{13}\tau_{13})-(x_1G_{13}\tau_{13}+x_2G_{23}\tau_{23})(G_{13}-1)]}{(x_1G_{13}+x_2G_{23}+x_3)^4}\end{array}\right]$$

(AII.6)

$$\left(\frac{\partial^3 \bar{G}^M}{\partial {x_2}^2 \partial x_1}\right)_{T,P,x_2}$$

$$= -2\left[\frac{(x_1 + x_2G_{21} + x_3G_{31})(G_{21}\tau_{21} + G_{31}\tau_{31}) - (x_2G_{21}\tau_{21} + x_3G_{31}\tau_{31})(G_{21} - G_{31})}{(x_1 + x_2G_{21} + x_3G_{31})^3}\right](G_{21} - G_{31})$$

$$- 2\,x_1\left[\begin{array}{c}\dfrac{(x_1 + x_2G_{21} + x_3G_{31})[(G_{21}\tau_{21} - G_{31}\tau_{31})(G_{21} - G_{31})(1 - G_{31}) + (G_{31}\tau_{31})(1 - G_{31})(G_{21} - G_{31})]}{(x_1 + x_2G_{21} + x_3G_{31})^4} \\ 6(G_{21} - G_{31})(1 - G_{31})\dfrac{[(x_1 + x_2G_{21} + x_3G_{31})(G_{21}\tau_{21} + G_{31}\tau_{31}) - (x_2G_{21}\tau_{21} + x_3G_{31}\tau_{31})(G_{21} - G_{31})]}{(x_1 + x_2G_{21} + x_3G_{31})^4}\end{array}\right]$$

$$+ 2\left[\begin{array}{c}\dfrac{(x_1G_{12} + x_2 + x_3G_{32})[(-G_{32}\tau_{32})(G_{12} - G_{32}) - (G_{12}\tau_{12} - G_{32}\tau_{32})(1 - G_{32})]}{(x_1G_{12} + x_2 + x_3G_{32})^3} \\ 2(G_{12} - G_{32})\dfrac{[(x_1G_{12} + x_2 + x_3G_{32})(-G_{32}\tau_{32}) - (x_1G_{12}\tau_{12} + x_3G_{32}\tau_{32})(1 - G_{32})]}{(x_1G_{12} + x_2 + x_3G_{32})^3}\end{array}\right]$$

$$- 2\,x_2\left[\begin{array}{c}\dfrac{(x_1G_{12} + x_2 + x_3G_{32})[(-G_{32}\tau_{32})(1 - G_{32})(G_{12} - G_{32}) - (G_{12}\tau_{12} - G_{32}\tau_{32})(1 - G_{32})^2]}{(x_1G_{12} + x_2 + x_3G_{32})^3} \\ 6\,(1 - G_{32})(G_{12} - G_{32})\dfrac{[(x_1G_{12} + x_2 + x_3G_{32})(-G_{32}\tau_{32}) - (x_1G_{12}\tau_{12} + x_3G_{32}\tau_{32})(1 - G_{32})]}{(x_1G_{12} + x_2 + x_3G_{32})^4}\end{array}\right]$$

$$- 2\left[\begin{array}{c}\dfrac{(x_1G_{13} + x_2G_{23} + x_3)[(G_{23}\tau_{23})(G_{13} - 1) - (G_{13}\tau_{13})(G_{23} - 1)]}{(x_1G_{13} + x_2G_{23} + x_3)^3} \\ \dfrac{2(G_{13} - 1)[(x_1G_{13} + x_2G_{23} + x_3)(G_{23}\tau_{23}) - (x_1G_{13}\tau_{13} + x_2G_{23}\tau_{23})(G_{23} - 1)]}{(x_1G_{13} + x_2G_{23} + x_3)^3}\end{array}\right] + \frac{1}{{x_3}^2}$$

$$+ \left[\frac{(x_1G_{13} + x_2G_{23} + x_3)(G_{23}\tau_{23}) - (x_1G_{13}\tau_{13} + x_2G_{23}\tau_{23})(G_{23} - 1)}{(x_1G_{13} + x_2G_{23} + x_3)^3}\right]$$

$$- 2\,x_3\left[\begin{array}{c}\dfrac{(x_1G_{13} + x_2G_{23} + x_3)[(G_{23} - 1)(G_{13} - 1)(G_{23}\tau_{23}) - (G_{23}\tau_{23})(G_{23} - 1)^2]}{(x_1G_{13} + x_2G_{23} + x_3)^4} \\ \dfrac{6\,(G_{23} - 1)(G_{13} - 1)[(x_1G_{13} + x_2G_{23} + x_3)(G_{23}\tau_{23}) - (x_1G_{13}\tau_{13} + x_2G_{23}\tau_{23})(G_{23} - 1)]}{(x_1G_{13} + x_2G_{23} + x_3)^4}\end{array}\right]$$

(AII.7)

Appendix III: Matlab© Coding for spinodal and critical locii of binary and ternary systems

Limits of stability for binary system

```
function [f]=spin7(x1)
global T
% Spinodal limits for NFM (1) + Hpetane (2)
x2=1-x1;
% Non-randomness parameters
a12=0.2;
a21=0.2;
% Binary interaction parameters
t12=-5.0594691+2512.54372/T;
t21=1.67759807+166.132276/T;
g12=exp(-a12*t12);
g21=exp(-a21*t21);
%Equation for spinodal limits
f=-2*x2*(t21*(g21/(x1+x2*g21))^2+g12*t12/((x2+x1*g12)^2))+x2^2*(-
2*t21*g21^2*(1-g21)/((x1+x2*g21)^3)-2*g12*t12*(g12-
1)/((x2+x1*g12)^3))+1/x1;
```

```
global T
% Setting T & finding the correspondent composition for spinodal curve
T=301.12
xi=0.09; % Initial guess for spinodal curve composition
[x,fval,jacobian]=fsolve(@spin7,xi)
```

Critical Point Determination for Binary Systems

```
function [f]=critical7(x)
global x1
% Critical temperature & composition for NFM (1) + Hpetane (2)
T=x(1);
x1=x(2);
x2=1-x(2);
% Non-randomness parameters
a12=0.2;
a21=0.2;
% Binary interaction parameters
t12=-5.0594691+2512.54372/T;
t21=1.67759807+166.132276/T;
g12=exp(-a12*t12);
g21=exp(-a21*t21);
% The equations below are solved simultaneously to find the critical
% temperature and composition
f(1)=-2*x2*(t21*(g21/(x1+x2*g21))^2+g12*t12/((x2+x1*g12)^2))-
2*x2^2*(t21*g21^2*(1-g21)/((x1+x2*g21)^3)+g12*t12*(g12-
1)/((x2+x1*g12)^3))+1/x1;
f(2)=2*(t21*(g21/(x1+x2*g21))^2+g12*t12/((x2+x1*g12)^2))+8*x2*(t21*g21^
2*(1-g21)/((x1+x2*g21)^3)+g12*t12*(g12-
1)/((x2+x1*g12)^3))+6*x2^2*(t21*g21^2*(1-
g21)^2/((x1+x2*g21)^4)+g12*t12*(g12-1)^2/((x2+x1*g12)^4))-1/(x1^2);


g=[525; 0.46 ]; % Initial guess
options = optimset('Display','iter','TolFun',1e-20);
[x,fval,jacobian]=fsolve(@critical7,g,options)%fsolve routine
```

Limits of stability for ternary system

```
function [f]=spinodal31(x1)
global x2
% Spinodal curve for DBE (1) + Water (2) + Methanol (3)
T=298.15;
% Binary interaction parameters for all binary combinations
s12=-196.39;
s21=875.83;
s23=-695.99;
s32=406.53;
s13=709.68;
s31=2958.6;
t12=s12/(T);
t21=s21/(T);
t13=s13/(T);
t31=s31/(T);
t23=s23/(T);
t32=s32/(T);
G12=exp(-0.2*t12);
G21=exp(-0.2*t21);
G13=exp(-0.2*t13);
G31=exp(-0.2*t31);
G23=exp(-0.2*t23);
G32=exp(-0.2*t32);

% (dlngam1/dx1)
B11=(G31*t31*(x1+x2-1)-G21*t21*x2)/(x1+G21*x2-G31*(x1+x2-1))^2-
(G31*t31)/(x1+G21*x2-G31*(x1+x2-1))-((G31*t31*(x1+x2-1)-
G21*t21*x2)*(G31-1))/(x1+G21*x2-G31*(x1+x2-1))^2-(G13*(t13-
(G13*t13*x1+G23*t23*x2)/(G13*x1-x2-x1+G23*x2+1)))/(G13*x1-x2-
x1+G23*x2+1)+(2*x1*(G31*t31*(x1+x2-1)-G21*t21*x2)*(G31-1))/(x1+G21*x2-
G31*(x1+x2-1))^3-(G12*x2*((G12*t12-G32*t32)/(x2+G12*x1-G32*(x1+x2-
1))+((G12-G32)*(G32*t32*(x1+x2-1)-G12*t12*x1))/(x2+G12*x1-G32*(x1+x2-
1))^2))/(x2+G12*x1-G32*(x1+x2-1))+(G31*t31*x1)/(x1+G21*x2-G31*(x1+x2-
1))^2-(G13*(((G13*t13*x1+G23*t23*x2)*(G13-1))/(G13*x1-x2-
x1+G23*x2+1)^2-(G13*t13)/(G13*x1-x2-x1+G23*x2+1))*(x1+x2-1))/(G13*x1-
x2-x1+G23*x2+1)-(G12*x2*(G12-G32)*(t12+(G32*t32*(x1+x2-1)-
G12*t12*x1)/(x2+G12*x1-G32*(x1+x2-1))))/(x2+G12*x1-G32*(x1+x2-
1))^2+(G13*(t13-(G13*t13*x1+G23*t23*x2)/(G13*x1-x2-x1+G23*x2+1))*(G13-
1)*(x1+x2-1))/(G13*x1-x2-x1+G23*x2+1)^2;
% (dlngam3/dx1)
B31=(G13*t13*x1+G23*t23*x2)/(G13*x1-x2-x1+G23*x2+1)^2-
((G13*t13*x1+G23*t23*x2)*(G13-1))/(G13*x1-x2-
x1+G23*x2+1)^2+(G13*t13)/(G13*x1-x2-
x1+G23*x2+1)+(G31*(t31+(G31*t31*(x1+x2-1)-G21*t21*x2)/(x1+G21*x2-
G31*(x1+x2-1))))/(x1+G21*x2-G31*(x1+x2-1))+(G13*t13*(x1+x2-1))/(G13*x1-
x2-x1+G23*x2+1)^2-(G32*x2*((G12*t12-G32*t32)/(x2+G12*x1-G32*(x1+x2-
1))+((G12-G32)*(G32*t32*(x1+x2-1)-G12*t12*x1))/(x2+G12*x1-G32*(x1+x2-
1))^2))/(x2+G12*x1-G32*(x1+x2-1))-(2*(G13*t13*x1+G23*t23*x2)*(G13-
1)*(x1+x2-1))/(G13*x1-x2-x1+G23*x2+1)^3+(G31*x1*((G31*t31)/(x1+G21*x2-
G31*(x1+x2-1))+((G31*t31*(x1+x2-1)-G21*t21*x2)*(G31-1))/(x1+G21*x2-
G31*(x1+x2-1))^2))/(x1+G21*x2-G31*(x1+x2-1))-(G32*x2*(G12-
G32)*(t32+(G32*t32*(x1+x2-1)-G12*t12*x1)/(x2+G12*x1-G32*(x1+x2-
```

```
1))))/(x2+G12*x1-G32*(x1+x2-1))^2+(G31*x1*(G31-1)*(t31+(G31*t31*(x1+x2-
1)-G21*t21*x2)/(x1+G21*x2-G31*(x1+x2-1))))/(x1+G21*x2-G31*(x1+x2-1))^2;
% (dlngam2/dx2)
B22=(G32*t32*(x1+x2-1)-G12*t12*x1)/(x2+G12*x1-G32*(x1+x2-1))^2-
(G32*t32)/(x2+G12*x1-G32*(x1+x2-1))-((G32*t32*(x1+x2-1)-
G12*t12*x1)*(G32-1))/(x2+G12*x1-G32*(x1+x2-1))^2-(G23*(t23-
(G13*t13*x1+G23*t23*x2)/(G13*x1-x2-x1+G23*x2+1)))/(G13*x1-x2-
x1+G23*x2+1)+(2*x2*(G32*t32*(x1+x2-1)-G12*t12*x1)*(G32-1))/(x2+G12*x1-
G32*(x1+x2-1))^3-(G21*x1*((G21*t21-G31*t31)/(x1+G21*x2-G31*(x1+x2-
1))+((G21-G31)*(G31*t31*(x1+x2-1)-G21*t21*x2))/(x1+G21*x2-G31*(x1+x2-
1))^2))/(x1+G21*x2-G31*(x1+x2-1))+(G32*t32*x2)/(x2+G12*x1-G32*(x1+x2-
1))^2-(G23*(((G13*t13*x1+G23*t23*x2)*(G23-1))/(G13*x1-x2-
x1+G23*x2+1)^2-(G23*t23)/(G13*x1-x2-x1+G23*x2+1))*(x1+x2-1))/(G13*x1-
x2-x1+G23*x2+1)-(G21*x1*(G21-G31)*(t21+(G31*t31*(x1+x2-1)-
G21*t21*x2)/(x1+G21*x2-G31*(x1+x2-1))))/(x1+G21*x2-G31*(x1+x2-
1))^2+(G23*(t23-(G13*t13*x1+G23*t23*x2)/(G13*x1-x2-x1+G23*x2+1))*(G23-
1)*(x1+x2-1))/(G13*x1-x2-x1+G23*x2+1)^2;
% (dlngam3/dx2)
B32=(G13*t13*x1+G23*t23*x2)/(G13*x1-x2-x1+G23*x2+1)^2-
((G13*t13*x1+G23*t23*x2)*(G23-1))/(G13*x1-x2-
x1+G23*x2+1)^2+(G23*t23)/(G13*x1-x2-
x1+G23*x2+1)+(G32*(t32+(G32*t32*(x1+x2-1)-G12*t12*x1)/(x2+G12*x1-
G32*(x1+x2-1))))/(x2+G12*x1-G32*(x1+x2-1))+(G23*t23*(x1+x2-1))/(G13*x1-
x2-x1+G23*x2+1)^2-(G31*x1*((G21*t21-G31*t31)/(x1+G21*x2-G31*(x1+x2-
1))+((G21-G31)*(G31*t31*(x1+x2-1)-G21*t21*x2))/(x1+G21*x2-G31*(x1+x2-
1))^2))/(x1+G21*x2-G31*(x1+x2-1))-(2*(G13*t13*x1+G23*t23*x2)*(G23-
1)*(x1+x2-1))/(G13*x1-x2-x1+G23*x2+1)^3+(G32*x2*((G32*t32)/(x2+G12*x1-
G32*(x1+x2-1))+((G32*t32*(x1+x2-1)-G12*t12*x1)*(G32-1))/(x2+G12*x1-
G32*(x1+x2-1))^2))/(x2+G12*x1-G32*(x1+x2-1))-(G31*x1*(G21-
G31)*(t31+(G31*t31*(x1+x2-1)-G21*t21*x2)/(x1+G21*x2-G31*(x1+x2-
1))))/(x1+G21*x2-G31*(x1+x2-1))^2+(G32*x2*(G32-1)*(t32+(G32*t32*(x1+x2-
1)-G12*t12*x1)/(x2+G12*x1-G32*(x1+x2-1))))/(x2+G12*x1-G32*(x1+x2-1))^2;
% (dlngam1/dx2)
B12=(G21*t21-G31*t31)/(x1+G21*x2-G31*(x1+x2-1))+((G21-
G31)*(G31*t31*(x1+x2-1)-G21*t21*x2))/(x1+G21*x2-G31*(x1+x2-1))^2-
(G13*(t13-(G13*t13*x1+G23*t23*x2)/(G13*x1-x2-x1+G23*x2+1)))/(G13*x1-x2-
x1+G23*x2+1)-(x1*(G21*t21-G31*t31))/(x1+G21*x2-G31*(x1+x2-
1))^2+(G12*(t12+(G32*t32*(x1+x2-1)-G12*t12*x1)/(x2+G12*x1-G32*(x1+x2-
1))))/(x2+G12*x1-G32*(x1+x2-1))-(2*x1*(G21-G31)*(G31*t31*(x1+x2-1)-
G21*t21*x2))/(x1+G21*x2-G31*(x1+x2-1))^3+(G12*x2*((G32*t32)/(x2+G12*x1-
G32*(x1+x2-1))+((G32*t32*(x1+x2-1)-G12*t12*x1)*(G32-1))/(x2+G12*x1-
G32*(x1+x2-1))^2))/(x2+G12*x1-G32*(x1+x2-1))-
(G13*(((G13*t13*x1+G23*t23*x2)*(G23-1))/(G13*x1-x2-x1+G23*x2+1)^2-
(G23*t23)/(G13*x1-x2-x1+G23*x2+1))*(x1+x2-1))/(G13*x1-x2-
x1+G23*x2+1)+(G13*(t13-(G13*t13*x1+G23*t23*x2)/(G13*x1-x2-
x1+G23*x2+1))*(G23-1)*(x1+x2-1))/(G13*x1-x2-
x1+G23*x2+1)^2+(G12*x2*(G32-1)*(t12+(G32*t32*(x1+x2-1)-
G12*t12*x1)/(x2+G12*x1-G32*(x1+x2-1))))/(x2+G12*x1-G32*(x1+x2-1))^2;
% (dlngam2/dx1)
B21=(G12*t12-G32*t32)/(x2+G12*x1-G32*(x1+x2-1))+((G12-
G32)*(G32*t32*(x1+x2-1)-G12*t12*x1))/(x2+G12*x1-G32*(x1+x2-1))^2-
(G23*(t23-(G13*t13*x1+G23*t23*x2)/(G13*x1-x2-x1+G23*x2+1)))/(G13*x1-x2-
x1+G23*x2+1)-(x2*(G12*t12-G32*t32))/(x2+G12*x1-G32*(x1+x2-
1))^2+(G21*(t21+(G31*t31*(x1+x2-1)-G21*t21*x2)/(x1+G21*x2-G31*(x1+x2-
1))))/(x1+G21*x2-G31*(x1+x2-1))-(2*x2*(G12-G32)*(G32*t32*(x1+x2-1)-
G12*t12*x1))/(x2+G12*x1-G32*(x1+x2-1))^3+(G21*x1*((G31*t31)/(x1+G21*x2-
G31*(x1+x2-1))+((G31*t31*(x1+x2-1)-G21*t21*x2)*(G31-1))/(x1+G21*x2-
```

```
G31*(x1+x2-1))^2))/(x1+G21*x2-G31*(x1+x2-1))-
(G23*(((G13*t13*x1+G23*t23*x2)*(G13-1))/(G13*x1-x2-x1+G23*x2+1)^2-
(G13*t13)/(G13*x1-x2-x1+G23*x2+1))*(x1+x2-1))/(G13*x1-x2-
x1+G23*x2+1)+(G23*(t23-(G13*t13*x1+G23*t23*x2)/(G13*x1-x2-
x1+G23*x2+1))*(G13-1)*(x1+x2-1))/(G13*x1-x2-
x1+G23*x2+1)^2+(G21*x1*(G31-1)*(t21+(G31*t31*(x1+x2-1)-
G21*t21*x2)/(x1+G21*x2-G31*(x1+x2-1))))/(x1+G21*x2-G31*(x1+x2-1))^2;
% (d2lngam1/d(x1)^2)
B111=(2*G31*t31)/(x1+G21*x2-G31*(x1+x2-1))^2-(2*(G31*t31*(x1+x2-1)-
G21*t21*x2)*(G31-1)^2)/(x1+G21*x2-G31*(x1+x2-1))^3+(4*(G31*t31*(x1+x2-
1)-G21*t21*x2)*(G31-1))/(x1+G21*x2-G31*(x1+x2-1))^3-
(2*G13*(((G13*t13*x1+G23*t23*x2)*(G13-1))/(G13*x1-x2-x1+G23*x2+1)^2-
(G13*t13)/(G13*x1-x2-x1+G23*x2+1)))/(G13*x1-x2-
x1+G23*x2+1)+(G13*((2*(G13*t13*x1+G23*t23*x2)*(G13-1)^2)/(G13*x1-x2-
x1+G23*x2+1)^3-(2*G13*t13*(G13-1))/(G13*x1-x2-x1+G23*x2+1)^2)*(x1+x2-
1))/(G13*x1-x2-x1+G23*x2+1)-(2*G31*t31*(G31-1))/(x1+G21*x2-G31*(x1+x2-
1))^2+(G12*x2*((2*(G12-G32)*(G12*t12-G32*t32))/(x2+G12*x1-G32*(x1+x2-
1))^2+(2*(G12-G32)^2*(G32*t32*(x1+x2-1)-G12*t12*x1))/(x2+G12*x1-
G32*(x1+x2-1))^3))/(x2+G12*x1-G32*(x1+x2-1))+(2*G13*(t13-
(G13*t13*x1+G23*t23*x2)/(G13*x1-x2-x1+G23*x2+1))*(G13-1))/(G13*x1-x2-
x1+G23*x2+1)^2+(6*x1*(G31*t31*(x1+x2-1)-G21*t21*x2)*(G31-
1)^2)/(x1+G21*x2-G31*(x1+x2-1))^4-(2*G13*(t13-
(G13*t13*x1+G23*t23*x2)/(G13*x1-x2-x1+G23*x2+1))*(G13-1)^2*(x1+x2-
1))/(G13*x1-x2-x1+G23*x2+1)^3+(4*G31*t31*x1*(G31-1))/(x1+G21*x2-
G31*(x1+x2-1))^3+(2*G13*(((G13*t13*x1+G23*t23*x2)*(G13-1))/(G13*x1-x2-
x1+G23*x2+1)^2-(G13*t13)/(G13*x1-x2-x1+G23*x2+1))*(G13-1)*(x1+x2-
1))/(G13*x1-x2-x1+G23*x2+1)^2+(2*G12*x2*(G12-G32)*((G12*t12-
G32*t32)/(x2+G12*x1-G32*(x1+x2-1))+((G12-G32)*(G32*t32*(x1+x2-1)-
G12*t12*x1))/(x2+G12*x1-G32*(x1+x2-1))^2))/(x2+G12*x1-G32*(x1+x2-
1))^2+(2*G12*x2*(G12-G32)^2*(t12+(G32*t32*(x1+x2-1)-
G12*t12*x1)/(x2+G12*x1-G32*(x1+x2-1))))/(x2+G12*x1-G32*(x1+x2-1))^3;
% (d2lngam2/d(x1)^2)
B211=(2*G21*((G31*t31)/(x1+G21*x2-G31*(x1+x2-1))+((G31*t31*(x1+x2-1)-
G21*t21*x2)*(G31-1))/(x1+G21*x2-G31*(x1+x2-1))^2))/(x1+G21*x2-
G31*(x1+x2-1))-(2*(G12-G32)*(G12*t12-G32*t32))/(x2+G12*x1-G32*(x1+x2-
1))^2-(2*G23*(((G13*t13*x1+G23*t23*x2)*(G13-1))/(G13*x1-x2-
x1+G23*x2+1)^2-(G13*t13)/(G13*x1-x2-x1+G23*x2+1)))/(G13*x1-x2-
x1+G23*x2+1)-(2*(G12-G32)^2*(G32*t32*(x1+x2-1)-G12*t12*x1))/(x2+G12*x1-
G32*(x1+x2-1))^3+(G23*((2*(G13*t13*x1+G23*t23*x2)*(G13-1)^2)/(G13*x1-
x2-x1+G23*x2+1)^3-(2*G13*t13*(G13-1))/(G13*x1-x2-
x1+G23*x2+1)^2)*(x1+x2-1))/(G13*x1-x2-x1+G23*x2+1)+(4*x2*(G12-
G32)*(G12*t12-G32*t32))/(x2+G12*x1-G32*(x1+x2-1))^3+(6*x2*(G12-
G32)^2*(G32*t32*(x1+x2-1)-G12*t12*x1))/(x2+G12*x1-G32*(x1+x2-
1))^4+(2*G23*(t23-(G13*t13*x1+G23*t23*x2)/(G13*x1-x2-
x1+G23*x2+1))*(G13-1))/(G13*x1-x2-x1+G23*x2+1)^2+(2*G21*(G31-
1)*(t21+(G31*t31*(x1+x2-1)-G21*t21*x2)/(x1+G21*x2-G31*(x1+x2-
1))))/(x1+G21*x2-G31*(x1+x2-1))^2+(G21*x1*((2*(G31*t31*(x1+x2-1)-
G21*t21*x2)*(G31-1)^2)/(x1+G21*x2-G31*(x1+x2-1))^3+(2*G31*t31*(G31-
1))/(x1+G21*x2-G31*(x1+x2-1))^2))/(x1+G21*x2-G31*(x1+x2-1))-
(2*G23*(t23-(G13*t13*x1+G23*t23*x2)/(G13*x1-x2-x1+G23*x2+1))*(G13-
1)^2*(x1+x2-1))/(G13*x1-x2-x1+G23*x2+1)^3+(2*G21*x1*(G31-
1)^2*(t21+(G31*t31*(x1+x2-1)-G21*t21*x2)/(x1+G21*x2-G31*(x1+x2-
1))))/(x1+G21*x2-G31*(x1+x2-1))^3+(2*G21*x1*((G31*t31)/(x1+G21*x2-
G31*(x1+x2-1))+((G31*t31*(x1+x2-1)-G21*t21*x2)*(G31-1))/(x1+G21*x2-
G31*(x1+x2-1))^2)*(G31-1))/(x1+G21*x2-G31*(x1+x2-
1))^2+(2*G23*(((G13*t13*x1+G23*t23*x2)*(G13-1))/(G13*x1-x2-
```

```
x1+G23*x2+1)^2-(G13*t13)/(G13*x1-x2-x1+G23*x2+1))*(G13-1)*(x1+x2-
1))/(G13*x1-x2-x1+G23*x2+1)^2;
% (d2lngam3/d(x1)^2)
B311=(2*G31*((G31*t31)/(x1+G21*x2-G31*(x1+x2-1))+((G31*t31*(x1+x2-1)-
G21*t21*x2)*(G31-1))/(x1+G21*x2-G31*(x1+x2-1))^2))/(x1+G21*x2-
G31*(x1+x2-1))-(4*(G13*t13*x1+G23*t23*x2)*(G13-1))/(G13*x1-x2-
x1+G23*x2+1)^3+(2*(G13*t13*x1+G23*t23*x2)*(G13-1)^2)/(G13*x1-x2-
x1+G23*x2+1)^3+(2*G13*t13)/(G13*x1-x2-x1+G23*x2+1)^2+(G32*x2*((2*(G12-
G32)*(G12*t12-G32*t32))/(x2+G12*x1-G32*(x1+x2-1))^2+(2*(G12-
G32)^2*(G32*t32*(x1+x2-1)-G12*t12*x1))/(x2+G12*x1-G32*(x1+x2-
1))^3))/(x2+G12*x1-G32*(x1+x2-1))-(2*G13*t13*(G13-1))/(G13*x1-x2-
x1+G23*x2+1)^2+(2*G31*(G31-1)*(t31+(G31*t31*(x1+x2-1)-
G21*t21*x2)/(x1+G21*x2-G31*(x1+x2-1))))/(x1+G21*x2-G31*(x1+x2-
1))^2+(6*(G13*t13*x1+G23*t23*x2)*(G13-1)^2*(x1+x2-1))/(G13*x1-x2-
x1+G23*x2+1)^4+(G31*x1*((2*(G31*t31*(x1+x2-1)-G21*t21*x2)*(G31-
1)^2)/(x1+G21*x2-G31*(x1+x2-1))^3+(2*G31*t31*(G31-1))/(x1+G21*x2-
G31*(x1+x2-1))^2))/(x1+G21*x2-G31*(x1+x2-1))+(2*G31*x1*(G31-
1)^2*(t31+(G31*t31*(x1+x2-1)-G21*t21*x2)/(x1+G21*x2-G31*(x1+x2-
1))))/(x1+G21*x2-G31*(x1+x2-1))^3+(2*G31*x1*((G31*t31)/(x1+G21*x2-
G31*(x1+x2-1))+((G31*t31*(x1+x2-1)-G21*t21*x2)*(G31-1))/(x1+G21*x2-
G31*(x1+x2-1))^2)*(G31-1))/(x1+G21*x2-G31*(x1+x2-1))^2+(2*G32*x2*(G12-
G32)*((G12*t12-G32*t32)/(x2+G12*x1-G32*(x1+x2-1))+((G12-
G32)*(G32*t32*(x1+x2-1)-G12*t12*x1))/(x2+G12*x1-G32*(x1+x2-
1))^2))/(x2+G12*x1-G32*(x1+x2-1))^2-(4*G13*t13*(G13-1)*(x1+x2-
1))/(G13*x1-x2-x1+G23*x2+1)^3+(2*G32*x2*(G12-
G32)^2*(t32+(G32*t32*(x1+x2-1)-G12*t12*x1)/(x2+G12*x1-G32*(x1+x2-
1))))/(x2+G12*x1-G32*(x1+x2-1))^3;
% (d2lngam1/d(x2)^2)
B122=(2*G12*((G32*t32)/(x2+G12*x1-G32*(x1+x2-1))+((G32*t32*(x1+x2-1)-
G12*t12*x1)*(G32-1))/(x2+G12*x1-G32*(x1+x2-1))^2))/(x2+G12*x1-
G32*(x1+x2-1))-(2*(G21-G31)*(G21*t21-G31*t31))/(x1+G21*x2-G31*(x1+x2-
1))^2-(2*G13*(((G13*t13*x1+G23*t23*x2)*(G23-1))/(G13*x1-x2-
x1+G23*x2+1)^2-(G23*t23)/(G13*x1-x2-x1+G23*x2+1)))/(G13*x1-x2-
x1+G23*x2+1)-(2*(G21-G31)^2*(G31*t31*(x1+x2-1)-G21*t21*x2))/(x1+G21*x2-
G31*(x1+x2-1))^3+(G13*((2*(G13*t13*x1+G23*t23*x2)*(G23-1)^2)/(G13*x1-
x2-x1+G23*x2+1)^3-(2*G23*t23*(G23-1))/(G13*x1-x2-
x1+G23*x2+1)^2)*(x1+x2-1))/(G13*x1-x2-x1+G23*x2+1)+(4*x1*(G21-
G31)*(G21*t21-G31*t31))/(x1+G21*x2-G31*(x1+x2-1))^3+(6*x1*(G21-
G31)^2*(G31*t31*(x1+x2-1)-G21*t21*x2))/(x1+G21*x2-G31*(x1+x2-
1))^4+(2*G13*(t13-(G13*t13*x1+G23*t23*x2)/(G13*x1-x2-
x1+G23*x2+1))*(G23-1))/(G13*x1-x2-x1+G23*x2+1)^2+(2*G12*(G32-
1)*(t12+(G32*t32*(x1+x2-1)-G12*t12*x1)/(x2+G12*x1-G32*(x1+x2-
1))))/(x2+G12*x1-G32*(x1+x2-1))^2+(G12*x2*((2*(G32*t32*(x1+x2-1)-
G12*t12*x1)*(G32-1)^2)/(x2+G12*x1-G32*(x1+x2-1))^3+(2*G32*t32*(G32-
1))/(x2+G12*x1-G32*(x1+x2-1))^2))/(x2+G12*x1-G32*(x1+x2-1))-
(2*G13*(t13-(G13*t13*x1+G23*t23*x2)/(G13*x1-x2-x1+G23*x2+1))*(G23-
1)^2*(x1+x2-1))/(G13*x1-x2-x1+G23*x2+1)^3+(2*G12*x2*(G32-
1)^2*(t12+(G32*t32*(x1+x2-1)-G12*t12*x1)/(x2+G12*x1-G32*(x1+x2-
1))))/(x2+G12*x1-G32*(x1+x2-1))^3+(2*G12*x2*((G32*t32)/(x2+G12*x1-
G32*(x1+x2-1))+((G32*t32*(x1+x2-1)-G12*t12*x1)*(G32-1))/(x2+G12*x1-
G32*(x1+x2-1))^2)*(G32-1))/(x2+G12*x1-G32*(x1+x2-
1))^2+(2*G13*(((G13*t13*x1+G23*t23*x2)*(G23-1))/(G13*x1-x2-
x1+G23*x2+1)^2-(G23*t23)/(G13*x1-x2-x1+G23*x2+1))*(G23-1)*(x1+x2-
1))/(G13*x1-x2-x1+G23*x2+1)^2;
% (d2lngam2/d(x2)^2)
B222=(2*G32*t32)/(x2+G12*x1-G32*(x1+x2-1))^2-(2*(G32*t32*(x1+x2-1)-
G12*t12*x1)*(G32-1)^2)/(x2+G12*x1-G32*(x1+x2-1))^3+(4*(G32*t32*(x1+x2-
```

```
1)-G12*t12*x1)*(G32-1))/(x2+G12*x1-G32*(x1+x2-1))^3-
(2*G23*(((G13*t13*x1+G23*t23*x2)*(G23-1))/(G13*x1-x2-x1+G23*x2+1)^2-
(G23*t23)/(G13*x1-x2-x1+G23*x2+1)))/(G13*x1-x2-
x1+G23*x2+1)+(G23*((2*(G13*t13*x1+G23*t23*x2)*(G23-1)^2)/(G13*x1-x2-
x1+G23*x2+1)^3-(2*G23*t23*(G23-1))/(G13*x1-x2-x1+G23*x2+1)^2)*(x1+x2-
1))/(G13*x1-x2-x1+G23*x2+1)-(2*G32*t32*(G32-1))/(x2+G12*x1-G32*(x1+x2-
1))^2+(G21*x1*((2*(G21-G31)*(G21*t21-G31*t31))/(x1+G21*x2-G31*(x1+x2-
1))^2+(2*(G21-G31)^2*(G31*t31*(x1+x2-1)-G21*t21*x2))/(x1+G21*x2-
G31*(x1+x2-1))^3))/(x1+G21*x2-G31*(x1+x2-1))+(2*G23*(t23-
(G13*t13*x1+G23*t23*x2)/(G13*x1-x2-x1+G23*x2+1))*(G23-1))/(G13*x1-x2-
x1+G23*x2+1)^2+(6*x2*(G32*t32*(x1+x2-1)-G12*t12*x1)*(G32-
1)^2)/(x2+G12*x1-G32*(x1+x2-1))^4-(2*G23*(t23-
(G13*t13*x1+G23*t23*x2)/(G13*x1-x2-x1+G23*x2+1))*(G23-1)^2*(x1+x2-
1))/(G13*x1-x2-x1+G23*x2+1)^3+(4*G32*t32*x2*(G32-1))/(x2+G12*x1-
G32*(x1+x2-1))^3+(2*G23*(((G13*t13*x1+G23*t23*x2)*(G23-1))/(G13*x1-x2-
x1+G23*x2+1)^2-(G23*t23)/(G13*x1-x2-x1+G23*x2+1))*(G23-1)*(x1+x2-
1))/(G13*x1-x2-x1+G23*x2+1)^2+(2*G21*x1*(G21-G31)*((G21*t21-
G31*t31)/(x1+G21*x2-G31*(x1+x2-1))+((G21-G31)*(G31*t31*(x1+x2-1)-
G21*t21*x2))/(x1+G21*x2-G31*(x1+x2-1))^2))/(x1+G21*x2-G31*(x1+x2-
1))^2+(2*G21*x1*(G21-G31)^2*(t21+(G31*t31*(x1+x2-1)-
G21*t21*x2)/(x1+G21*x2-G31*(x1+x2-1))))/(x1+G21*x2-G31*(x1+x2-1))^3;
% (d2lngam3/d(x2)^2)
B322=(2*G32*((G32*t32)/(x2+G12*x1-G32*(x1+x2-1))+((G32*t32*(x1+x2-1)-
G12*t12*x1)*(G32-1))/(x2+G12*x1-G32*(x1+x2-1))^2))/(x2+G12*x1-
G32*(x1+x2-1))-(4*(G13*t13*x1+G23*t23*x2)*(G23-1))/(G13*x1-x2-
x1+G23*x2+1)^3+(2*(G13*t13*x1+G23*t23*x2)*(G23-1)^2)/(G13*x1-x2-
x1+G23*x2+1)^3+(2*G23*t23)/(G13*x1-x2-x1+G23*x2+1)^2+(G31*x1*((2*(G21-
G31)*(G21*t21-G31*t31))/(x1+G21*x2-G31*(x1+x2-1))^2+(2*(G21-
G31)^2*(G31*t31*(x1+x2-1)-G21*t21*x2))/(x1+G21*x2-G31*(x1+x2-
1))^3))/(x1+G21*x2-G31*(x1+x2-1))-(2*G23*t23*(G23-1))/(G13*x1-x2-
x1+G23*x2+1)^2+(2*G32*(G32-1)*(t32+(G32*t32*(x1+x2-1)-
G12*t12*x1)/(x2+G12*x1-G32*(x1+x2-1))))/(x2+G12*x1-G32*(x1+x2-
1))^2+(6*(G13*t13*x1+G23*t23*x2)*(G23-1)^2*(x1+x2-1))/(G13*x1-x2-
x1+G23*x2+1)^4+(G32*x2*((2*(G32*t32*(x1+x2-1)-G12*t12*x1)*(G32-
1)^2)/(x2+G12*x1-G32*(x1+x2-1))^3+(2*G32*t32*(G32-1))/(x2+G12*x1-
G32*(x1+x2-1))^2))/(x2+G12*x1-G32*(x1+x2-1))+(2*G32*x2*(G32-
1)^2*(t32+(G32*t32*(x1+x2-1)-G12*t12*x1)/(x2+G12*x1-G32*(x1+x2-
1))))/(x2+G12*x1-G32*(x1+x2-1))^3+(2*G32*x2*((G32*t32)/(x2+G12*x1-
G32*(x1+x2-1))+((G32*t32*(x1+x2-1)-G12*t12*x1)*(G32-1))/(x2+G12*x1-
G32*(x1+x2-1))^2)*(G32-1))/(x2+G12*x1-G32*(x1+x2-1))^2+(2*G31*x1*(G21-
G31)*((G21*t21-G31*t31)/(x1+G21*x2-G31*(x1+x2-1))+((G21-
G31)*(G31*t31*(x1+x2-1)-G21*t21*x2))/(x1+G21*x2-G31*(x1+x2-
1))^2))/(x1+G21*x2-G31*(x1+x2-1))^2-(4*G23*t23*(G23-1)*(x1+x2-
1))/(G13*x1-x2-x1+G23*x2+1)^3+(2*G31*x1*(G21-
G31)^2*(t31+(G31*t31*(x1+x2-1)-G21*t21*x2)/(x1+G21*x2-G31*(x1+x2-
1))))/(x1+G21*x2-G31*(x1+x2-1))^3;
% (d2lngam1/dx1 dx2)
B112=((G21*t21-G31*t31)*(G31-1))/(x1+G21*x2-G31*(x1+x2-1))^2-(2*(G21-
G31)*(G31*t31*(x1+x2-1)-G21*t21*x2))/(x1+G21*x2-G31*(x1+x2-1))^3-
(G13*(((G13*t13*x1+G23*t23*x2)*(G13-1))/(G13*x1-x2-x1+G23*x2+1)^2-
(G13*t13)/(G13*x1-x2-x1+G23*x2+1)))/(G13*x1-x2-x1+G23*x2+1)-
(G13*(((G13*t13*x1+G23*t23*x2)*(G23-1))/(G13*x1-x2-x1+G23*x2+1)^2-
(G23*t23)/(G13*x1-x2-x1+G23*x2+1)))/(G13*x1-x2-x1+G23*x2+1)-(G21*t21-
G31*t31)/(x1+G21*x2-G31*(x1+x2-1))^2-(G12*((G12*t12-
G32*t32)/(x2+G12*x1-G32*(x1+x2-1))+((G12-G32)*(G32*t32*(x1+x2-1)-
G12*t12*x1))/(x2+G12*x1-G32*(x1+x2-1))^2))/(x2+G12*x1-G32*(x1+x2-1))-
(G12*(G12-G32)*(t12+(G32*t32*(x1+x2-1)-G12*t12*x1)/(x2+G12*x1-
```

```
G32*(x1+x2-1))))/(x2+G12*x1-G32*(x1+x2-1))^2+(G13*(t13-
(G13*t13*x1+G23*t23*x2)/(G13*x1-x2-x1+G23*x2+1))*(G13-1))/(G13*x1-x2-
x1+G23*x2+1)^2+(G13*(t13-(G13*t13*x1+G23*t23*x2)/(G13*x1-x2-
x1+G23*x2+1))*(G23-1))/(G13*x1-x2-x1+G23*x2+1)^2-(2*x1*(G21*t21-
G31*t31)*(G31-1))/(x1+G21*x2-G31*(x1+x2-1))^3-(G12*x2*(((G12*t12-
G32*t32)*(G32-1))/(x2+G12*x1-G32*(x1+x2-1))^2+(G32*t32*(G12-
G32))/(x2+G12*x1-G32*(x1+x2-1))^2+(2*(G12-G32)*(G32*t32*(x1+x2-1)-
G12*t12*x1)*(G32-1))/(x2+G12*x1-G32*(x1+x2-1))^3))/(x2+G12*x1-
G32*(x1+x2-1))+(G31*t31*(G21-G31))/(x1+G21*x2-G31*(x1+x2-1))^2-
(G13*((G13*t13*(G23-1))/(G13*x1-x2-x1+G23*x2+1)^2+(G23*t23*(G13-
1))/(G13*x1-x2-x1+G23*x2+1)^2-(2*(G13*t13*x1+G23*t23*x2)*(G13-1)*(G23-
1))/(G13*x1-x2-x1+G23*x2+1)^3)*(x1+x2-1))/(G13*x1-x2-
x1+G23*x2+1)+(2*(G21-G31)*(G31*t31*(x1+x2-1)-G21*t21*x2)*(G31-
1))/(x1+G21*x2-G31*(x1+x2-1))^3-(G12*x2*(G32-1)*((G12*t12-
G32*t32)/(x2+G12*x1-G32*(x1+x2-1))+((G12-G32)*(G32*t32*(x1+x2-1)-
G12*t12*x1))/(x2+G12*x1-G32*(x1+x2-1))^2))/(x2+G12*x1-G32*(x1+x2-1))^2-
(2*G31*t31*x1*(G21-G31))/(x1+G21*x2-G31*(x1+x2-1))^3-(G12*x2*(G12-
G32)*((G32*t32)/(x2+G12*x1-G32*(x1+x2-1))+((G32*t32*(x1+x2-1)-
G12*t12*x1)*(G32-1))/(x2+G12*x1-G32*(x1+x2-1))^2))/(x2+G12*x1-
G32*(x1+x2-1))^2-(6*x1*(G21-G31)*(G31*t31*(x1+x2-1)-G21*t21*x2)*(G31-
1))/(x1+G21*x2-G31*(x1+x2-1))^4+(G13*(((G13*t13*x1+G23*t23*x2)*(G13-
1))/(G13*x1-x2-x1+G23*x2+1)^2-(G13*t13)/(G13*x1-x2-x1+G23*x2+1))*(G23-
1)*(x1+x2-1))/(G13*x1-x2-
x1+G23*x2+1)^2+(G13*(((G13*t13*x1+G23*t23*x2)*(G23-1))/(G13*x1-x2-
x1+G23*x2+1)^2-(G23*t23)/(G13*x1-x2-x1+G23*x2+1))*(G13-1)*(x1+x2-
1))/(G13*x1-x2-x1+G23*x2+1)^2-(2*G12*x2*(G12-G32)*(G32-
1)*(t12+(G32*t32*(x1+x2-1)-G12*t12*x1)/(x2+G12*x1-G32*(x1+x2-
1))))/(x2+G12*x1-G32*(x1+x2-1))^3-(2*G13*(t13-
(G13*t13*x1+G23*t23*x2)/(G13*x1-x2-x1+G23*x2+1))*(G13-1)*(G23-
1)*(x1+x2-1))/(G13*x1-x2-x1+G23*x2+1)^3;
% (d2lngam2/dx1 dx2)
B212=((G12*t12-G32*t32)*(G32-1))/(x2+G12*x1-G32*(x1+x2-1))^2-(2*(G12-
G32)*(G32*t32*(x1+x2-1)-G12*t12*x1))/(x2+G12*x1-G32*(x1+x2-1))^3-
(G23*(((G13*t13*x1+G23*t23*x2)*(G13-1))/(G13*x1-x2-x1+G23*x2+1)^2-
(G13*t13)/(G13*x1-x2-x1+G23*x2+1)))/(G13*x1-x2-x1+G23*x2+1)-
(G23*(((G13*t13*x1+G23*t23*x2)*(G23-1))/(G13*x1-x2-x1+G23*x2+1)^2-
(G23*t23)/(G13*x1-x2-x1+G23*x2+1)))/(G13*x1-x2-x1+G23*x2+1)-(G12*t12-
G32*t32)/(x2+G12*x1-G32*(x1+x2-1))^2-(G21*((G21*t21-
G31*t31)/(x1+G21*x2-G31*(x1+x2-1))+((G21-G31)*(G31*t31*(x1+x2-1)-
G21*t21*x2))/(x1+G21*x2-G31*(x1+x2-1))^2))/(x1+G21*x2-G31*(x1+x2-1))-
(G21*(G21-G31)*(t21+(G31*t31*(x1+x2-1)-G21*t21*x2)/(x1+G21*x2-
G31*(x1+x2-1))))/(x1+G21*x2-G31*(x1+x2-1))^2+(G23*(t23-
(G13*t13*x1+G23*t23*x2)/(G13*x1-x2-x1+G23*x2+1))*(G13-1))/(G13*x1-x2-
x1+G23*x2+1)^2+(G23*(t23-(G13*t13*x1+G23*t23*x2)/(G13*x1-x2-
x1+G23*x2+1))*(G23-1))/(G13*x1-x2-x1+G23*x2+1)^2-(2*x2*(G12*t12-
G32*t32)*(G32-1))/(x2+G12*x1-G32*(x1+x2-1))^3-(G21*x1*(((G21*t21-
G31*t31)*(G31-1))/(x1+G21*x2-G31*(x1+x2-1))^2+(G31*t31*(G21-
G31))/(x1+G21*x2-G31*(x1+x2-1))^2+(2*(G21-G31)*(G31*t31*(x1+x2-1)-
G21*t21*x2)*(G31-1))/(x1+G21*x2-G31*(x1+x2-1))^3))/(x1+G21*x2-
G31*(x1+x2-1))+(G32*t32*(G12-G32))/(x2+G12*x1-G32*(x1+x2-1))^2-
(G23*((G13*t13*(G23-1))/(G13*x1-x2-x1+G23*x2+1)^2+(G23*t23*(G13-
1))/(G13*x1-x2-x1+G23*x2+1)^2-(2*(G13*t13*x1+G23*t23*x2)*(G13-1)*(G23-
1))/(G13*x1-x2-x1+G23*x2+1)^3)*(x1+x2-1))/(G13*x1-x2-
x1+G23*x2+1)+(2*(G12-G32)*(G32*t32*(x1+x2-1)-G12*t12*x1)*(G32-
1))/(x2+G12*x1-G32*(x1+x2-1))^3-(G21*x1*(G31-1)*((G21*t21-
G31*t31)/(x1+G21*x2-G31*(x1+x2-1))+((G21-G31)*(G31*t31*(x1+x2-1)-
G21*t21*x2))/(x1+G21*x2-G31*(x1+x2-1))^2))/(x1+G21*x2-G31*(x1+x2-1))^2-
```

```
(2*G32*t32*x2*(G12-G32))/(x2+G12*x1-G32*(x1+x2-1))^3-(G21*x1*(G21-
G31)*((G31*t31)/(x1+G21*x2-G31*(x1+x2-1))+((G31*t31*(x1+x2-1)-
G21*t21*x2)*(G31-1))/(x1+G21*x2-G31*(x1+x2-1))^2))/(x1+G21*x2-
G31*(x1+x2-1))^2-(6*x2*(G12-G32)*(G32*t32*(x1+x2-1)-G12*t12*x1)*(G32-
1))/(x2+G12*x1-G32*(x1+x2-1))^4+(G23*(((G13*t13*x1+G23*t23*x2)*(G13-
1))/(G13*x1-x2-x1+G23*x2+1)^2-(G13*t13)/(G13*x1-x2-x1+G23*x2+1))*(G23-
1)*(x1+x2-1))/(G13*x1-x2-
x1+G23*x2+1)^2+(G23*(((G13*t13*x1+G23*t23*x2)*(G23-1))/(G13*x1-x2-
x1+G23*x2+1)^2-(G23*t23)/(G13*x1-x2-x1+G23*x2+1))*(G13-1)*(x1+x2-
1))/(G13*x1-x2-x1+G23*x2+1)^2-(2*G21*x1*(G21-G31)*(G31-
1)*(t21+(G31*t31*(x1+x2-1)-G21*t21*x2)/(x1+G21*x2-G31*(x1+x2-
1))))/(x1+G21*x2-G31*(x1+x2-1))^3-(2*G23*(t23-
(G13*t13*x1+G23*t23*x2)/(G13*x1-x2-x1+G23*x2+1))*(G13-1)*(G23-
1)*(x1+x2-1))/(G13*x1-x2-x1+G23*x2+1)^3;
% (d2lngam3/dx1 dx2)
B312=(G13*t13)/(G13*x1-x2-x1+G23*x2+1)^2-
(2*(G13*t13*x1+G23*t23*x2)*(G23-1))/(G13*x1-x2-x1+G23*x2+1)^3-
(2*(G13*t13*x1+G23*t23*x2)*(G13-1))/(G13*x1-x2-
x1+G23*x2+1)^3+(G23*t23)/(G13*x1-x2-x1+G23*x2+1)^2-(G32*((G12*t12-
G32*t32)/(x2+G12*x1-G32*(x1+x2-1))+((G12-G32)*(G32*t32*(x1+x2-1)-
G12*t12*x1))/(x2+G12*x1-G32*(x1+x2-1))^2))/(x2+G12*x1-G32*(x1+x2-1))-
(G31*((G21*t21-G31*t31)/(x1+G21*x2-G31*(x1+x2-1))+((G21-
G31)*(G31*t31*(x1+x2-1)-G21*t21*x2))/(x1+G21*x2-G31*(x1+x2-
1))^2))/(x1+G21*x2-G31*(x1+x2-1))-(G32*(G12-G32)*(t32+(G32*t32*(x1+x2-
1)-G12*t12*x1)/(x2+G12*x1-G32*(x1+x2-1))))/(x2+G12*x1-G32*(x1+x2-1))^2-
(G31*(G21-G31)*(t31+(G31*t31*(x1+x2-1)-G21*t21*x2)/(x1+G21*x2-
G31*(x1+x2-1))))/(x1+G21*x2-G31*(x1+x2-1))^2-(G32*x2*((G12*t12-
G32*t32)*(G32-1))/(x2+G12*x1-G32*(x1+x2-1))^2+(G32*t32*(G12-
G32))/(x2+G12*x1-G32*(x1+x2-1))^2+(2*(G12-G32)*(G32*t32*(x1+x2-1)-
G12*t12*x1)*(G32-1))/(x2+G12*x1-G32*(x1+x2-1))^3))/(x2+G12*x1-
G32*(x1+x2-1))-(G31*x1*(((G21*t21-G31*t31)*(G31-1))/(x1+G21*x2-
G31*(x1+x2-1))^2+(G31*t31*(G21-G31))/(x1+G21*x2-G31*(x1+x2-
1))^2+(2*(G21-G31)*(G31*t31*(x1+x2-1)-G21*t21*x2)*(G31-1))/(x1+G21*x2-
G31*(x1+x2-1))^3))/(x1+G21*x2-G31*(x1+x2-1))-(G13*t13*(G23-1))/(G13*x1-
x2-x1+G23*x2+1)^2-(G23*t23*(G13-1))/(G13*x1-x2-
x1+G23*x2+1)^2+(2*(G13*t13*x1+G23*t23*x2)*(G13-1)*(G23-1))/(G13*x1-x2-
x1+G23*x2+1)^3-(G32*x2*(G32-1)*((G12*t12-G32*t32)/(x2+G12*x1-
G32*(x1+x2-1))+((G12-G32)*(G32*t32*(x1+x2-1)-G12*t12*x1))/(x2+G12*x1-
G32*(x1+x2-1))^2))/(x2+G12*x1-G32*(x1+x2-1))^2-(G31*x1*(G31-
1)*((G21*t21-G31*t31)/(x1+G21*x2-G31*(x1+x2-1))+((G21-
G31)*(G31*t31*(x1+x2-1)-G21*t21*x2))/(x1+G21*x2-G31*(x1+x2-
1))^2))/(x1+G21*x2-G31*(x1+x2-1))^2+(6*(G13*t13*x1+G23*t23*x2)*(G13-
1)*(G23-1)*(x1+x2-1))/(G13*x1-x2-x1+G23*x2+1)^4-(G32*x2*(G12-
G32)*((G32*t32)/(x2+G12*x1-G32*(x1+x2-1))+((G32*t32*(x1+x2-1)-
G12*t12*x1)*(G32-1))/(x2+G12*x1-G32*(x1+x2-1))^2))/(x2+G12*x1-
G32*(x1+x2-1))^2-(G31*x1*(G21-G31)*((G31*t31)/(x1+G21*x2-G31*(x1+x2-
1))+((G31*t31*(x1+x2-1)-G21*t21*x2)*(G31-1))/(x1+G21*x2-G31*(x1+x2-
1))^2))/(x1+G21*x2-G31*(x1+x2-1))^2-(2*G13*t13*(G23-1)*(x1+x2-
1))/(G13*x1-x2-x1+G23*x2+1)^3-(2*G23*t23*(G13-1)*(x1+x2-1))/(G13*x1-x2-
x1+G23*x2+1)^3-(2*G32*x2*(G12-G32)*(G32-1)*(t32+(G32*t32*(x1+x2-1)-
G12*t12*x1)/(x2+G12*x1-G32*(x1+x2-1))))/(x2+G12*x1-G32*(x1+x2-1))^3-
(2*G31*x1*(G21-G31)*(G31-1)*(t31+(G31*t31*(x1+x2-1)-
G21*t21*x2)/(x1+G21*x2-G31*(x1+x2-1))))/(x1+G21*x2-G31*(x1+x2-1))^3;

% (d2Gm/d(x2)^2)
G22=x1*B122+2*B22+2/x2+x2*(B222-1/(x2^2))-2*B32+2/(1-x2-x1)+(1-x2-
x1)*(B322-(1/((1-x2-x1)^2)));
```

```
% (d2Gm/dx1 dx2)
Gm12=B12+x1*B112+x2*B212-B32+2/(1-x2-x1)-B31+(1-x2-x1)*(B312-(1/((1-x2-
x1)^2)))+B21;
% (d2Gm/d(x2)^2)
G11=2*B11+2/x1+x1*(B111-1/(x1^2))+x2*B211-2*B31+2/(1-x2-x1)+(1-x2-
x1)*(B311-(1/((1-x2-x1)^2)));

%Solving equation below for spinodal limits
f=G11*G22-(Gm12)^2;


%Solving equation below for spinodal limits
xi=0.001; % Initial guess
x1=0.0217; % x1
% solving routine
options=optimset('Display','iter','FunValCheck','on');
[x,fval,jacobian]=fsolve(@spinodal3,xi,options)
fplot(@spinodal3,[0 0.3])
grid on
```

Critical Point Determination for Ternary Systems

```
function [f]=critical1(x)
% Critical point solving for DBE (1) + Water (2) + Methanol (3)
T=298.15;
x1=x(1);
x2=x(2);
% Binary interaction parameters for all binary combinations
s12=-196.39;
s21=875.83;
s23=-695.99;
s32=406.53;
s13=709.68;
s31=2958.6;
t12=s12/(T);
t21=s21/(T);
t13=s13/(T);
t31=s31/(T);
t23=s23/(T);
t32=s32/(T);
G12=exp(-0.2*t12);
G21=exp(-0.2*t21);
G13=exp(-0.2*t13);
G31=exp(-0.2*t31);
G23=exp(-0.2*t23);
G32=exp(-0.2*t32);

% (dlngam1/dx1)
B11=(G31*t31*(x1+x2-1)-G21*t21*x2)/(x1+G21*x2-G31*(x1+x2-1))^2-
(G31*t31)/(x1+G21*x2-G31*(x1+x2-1))-((G31*t31*(x1+x2-1)-
G21*t21*x2)*(G31-1))/(x1+G21*x2-G31*(x1+x2-1))^2-(G13*(t13-
(G13*t13*x1+G23*t23*x2)/(G13*x1-x2-x1+G23*x2+1)))/(G13*x1-x2-
x1+G23*x2+1)+(2*x1*(G31*t31*(x1+x2-1)-G21*t21*x2)*(G31-1))/(x1+G21*x2-
G31*(x1+x2-1))^3-(G12*x2*((G12*t12-G32*t32)/(x2+G12*x1-G32*(x1+x2-
1))+((G12-G32)*(G32*t32*(x1+x2-1)-G12*t12*x1))/(x2+G12*x1-G32*(x1+x2-
```

```
1))^2))/(x2+G12*x1-G32*(x1+x2-1))+(G31*t31*x1)/(x1+G21*x2-G31*(x1+x2-
1))^2-(G13*(((G13*t13*x1+G23*t23*x2)*(G13-1))/(G13*x1-x2-
x1+G23*x2+1)^2-(G13*t13)/(G13*x1-x2-x1+G23*x2+1))*(x1+x2-1))/(G13*x1-
x2-x1+G23*x2+1)-(G12*x2*(G12-G32)*(t12+(G32*t32*(x1+x2-1)-
G12*t12*x1)/(x2+G12*x1-G32*(x1+x2-1))))/(x2+G12*x1-G32*(x1+x2-
1))^2+(G13*(t13-(G13*t13*x1+G23*t23*x2)/(G13*x1-x2-x1+G23*x2+1))*(G13-
1)*(x1+x2-1))/(G13*x1-x2-x1+G23*x2+1)^2;
% (dlngam3/dx1)
B31=(G13*t13*x1+G23*t23*x2)/(G13*x1-x2-x1+G23*x2+1)^2-
((G13*t13*x1+G23*t23*x2)*(G13-1))/(G13*x1-x2-
x1+G23*x2+1)^2+(G13*t13)/(G13*x1-x2-
x1+G23*x2+1)+(G31*(t31+(G31*t31*(x1+x2-1)-G21*t21*x2)/(x1+G21*x2-
G31*(x1+x2-1))))/(x1+G21*x2-G31*(x1+x2-1))+(G13*t13*(x1+x2-1))/(G13*x1-
x2-x1+G23*x2+1)^2-(G32*x2*((G12*t12-G32*t32)/(x2+G12*x1-G32*(x1+x2-
1))+((G12-G32)*(G32*t32*(x1+x2-1)-G12*t12*x1))/(x2+G12*x1-G32*(x1+x2-
1))^2))/(x2+G12*x1-G32*(x1+x2-1))-(2*(G13*t13*x1+G23*t23*x2)*(G13-
1)*(x1+x2-1))/(G13*x1-x2-x1+G23*x2+1)^3+(G31*x1*((G31*t31)/(x1+G21*x2-
G31*(x1+x2-1))+((G31*t31*(x1+x2-1)-G21*t21*x2)*(G31-1))/(x1+G21*x2-
G31*(x1+x2-1))^2))/(x1+G21*x2-G31*(x1+x2-1))-(G32*x2*(G12-
G32)*(t32+(G32*t32*(x1+x2-1)-G12*t12*x1)/(x2+G12*x1-G32*(x1+x2-
1))))/(x2+G12*x1-G32*(x1+x2-1))^2+(G31*x1*(G31-1)*(t31+(G31*t31*(x1+x2-
1)-G21*t21*x2)/(x1+G21*x2-G31*(x1+x2-1))))/(x1+G21*x2-G31*(x1+x2-1))^2;
% (dlngam2/dx2)
B22=(G32*t32*(x1+x2-1)-G12*t12*x1)/(x2+G12*x1-G32*(x1+x2-1))^2-
(G32*t32)/(x2+G12*x1-G32*(x1+x2-1))-((G32*t32*(x1+x2-1)-
G12*t12*x1)*(G32-1))/(x2+G12*x1-G32*(x1+x2-1))^2-(G23*(t23-
(G13*t13*x1+G23*t23*x2)/(G13*x1-x2-x1+G23*x2+1)))/(G13*x1-x2-
x1+G23*x2+1)+(2*x2*(G32*t32*(x1+x2-1)-G12*t12*x1)*(G32-1))/(x2+G12*x1-
G32*(x1+x2-1))^3-(G21*x1*((G21*t21-G31*t31)/(x1+G21*x2-G31*(x1+x2-
1))+((G21-G31)*(G31*t31*(x1+x2-1)-G21*t21*x2))/(x1+G21*x2-G31*(x1+x2-
1))^2))/(x1+G21*x2-G31*(x1+x2-1))+(G32*t32*x2)/(x2+G12*x1-G32*(x1+x2-
1))^2-(G23*(((G13*t13*x1+G23*t23*x2)*(G23-1))/(G13*x1-x2-
x1+G23*x2+1)^2-(G23*t23)/(G13*x1-x2-x1+G23*x2+1))*(x1+x2-1))/(G13*x1-
x2-x1+G23*x2+1)-(G21*x1*(G21-G31)*(t21+(G31*t31*(x1+x2-1)-
G21*t21*x2)/(x1+G21*x2-G31*(x1+x2-1))))/(x1+G21*x2-G31*(x1+x2-
1))^2+(G23*(t23-(G13*t13*x1+G23*t23*x2)/(G13*x1-x2-x1+G23*x2+1))*(G23-
1)*(x1+x2-1))/(G13*x1-x2-x1+G23*x2+1)^2;
% (dlngam3/dx2)
B32=(G13*t13*x1+G23*t23*x2)/(G13*x1-x2-x1+G23*x2+1)^2-
((G13*t13*x1+G23*t23*x2)*(G23-1))/(G13*x1-x2-
x1+G23*x2+1)^2+(G23*t23)/(G13*x1-x2-
x1+G23*x2+1)+(G32*(t32+(G32*t32*(x1+x2-1)-G12*t12*x1)/(x2+G12*x1-
G32*(x1+x2-1))))/(x2+G12*x1-G32*(x1+x2-1))+(G23*t23*(x1+x2-1))/(G13*x1-
x2-x1+G23*x2+1)^2-(G31*x1*((G21*t21-G31*t31)/(x1+G21*x2-G31*(x1+x2-
1))+((G21-G31)*(G31*t31*(x1+x2-1)-G21*t21*x2))/(x1+G21*x2-G31*(x1+x2-
1))^2))/(x1+G21*x2-G31*(x1+x2-1))-(2*(G13*t13*x1+G23*t23*x2)*(G23-
1)*(x1+x2-1))/(G13*x1-x2-x1+G23*x2+1)^3+(G32*x2*((G32*t32)/(x2+G12*x1-
G32*(x1+x2-1))+((G32*t32*(x1+x2-1)-G12*t12*x1)*(G32-1))/(x2+G12*x1-
G32*(x1+x2-1))^2))/(x2+G12*x1-G32*(x1+x2-1))-(G31*x1*(G21-
G31)*(t31+(G31*t31*(x1+x2-1)-G21*t21*x2)/(x1+G21*x2-G31*(x1+x2-
1))))/(x1+G21*x2-G31*(x1+x2-1))^2+(G32*x2*(G32-1)*(t32+(G32*t32*(x1+x2-
1)-G12*t12*x1)/(x2+G12*x1-G32*(x1+x2-1))))/(x2+G12*x1-G32*(x1+x2-1))^2;
% (dlngam1/dx2)
B12=(G21*t21-G31*t31)/(x1+G21*x2-G31*(x1+x2-1))+((G21-
G31)*(G31*t31*(x1+x2-1)-G21*t21*x2))/(x1+G21*x2-G31*(x1+x2-1))^2-
(G13*(t13-(G13*t13*x1+G23*t23*x2)/(G13*x1-x2-x1+G23*x2+1)))/(G13*x1-x2-
x1+G23*x2+1)-(x1*(G21*t21-G31*t31))/(x1+G21*x2-G31*(x1+x2-
```

```
1))^2+(G12*(t12+(G32*t32*(x1+x2-1)-G12*t12*x1)/(x2+G12*x1-G32*(x1+x2-
1))))/(x2+G12*x1-G32*(x1+x2-1))-(2*x1*(G21-G31)*(G31*t31*(x1+x2-1)-
G21*t21*x2))/(x1+G21*x2-G31*(x1+x2-1))^3+(G12*x2*((G32*t32)/(x2+G12*x1-
G32*(x1+x2-1))+((G32*t32*(x1+x2-1)-G12*t12*x1)*(G32-1))/(x2+G12*x1-
G32*(x1+x2-1))^2))/(x2+G12*x1-G32*(x1+x2-1))-
(G13*(((G13*t13*x1+G23*t23*x2)*(G23-1))/(G13*x1-x2-x1+G23*x2+1)^2-
(G23*t23)/(G13*x1-x2-x1+G23*x2+1))*(x1+x2-1))/(G13*x1-x2-
x1+G23*x2+1)+(G13*(t13-(G13*t13*x1+G23*t23*x2)/(G13*x1-x2-
x1+G23*x2+1))*(G23-1)*(x1+x2-1))/(G13*x1-x2-
x1+G23*x2+1)^2+(G12*x2*(G32-1)*(t12+(G32*t32*(x1+x2-1)-
G12*t12*x1)/(x2+G12*x1-G32*(x1+x2-1))))/(x2+G12*x1-G32*(x1+x2-1))^2;
% (dlngam2/dx1)
B21=(G12*t12-G32*t32)/(x2+G12*x1-G32*(x1+x2-1))+((G12-
G32)*(G32*t32*(x1+x2-1)-G12*t12*x1))/(x2+G12*x1-G32*(x1+x2-1))^2-
(G23*(t23-(G13*t13*x1+G23*t23*x2)/(G13*x1-x2-x1+G23*x2+1)))/(G13*x1-x2-
x1+G23*x2+1)-(x2*(G12*t12-G32*t32))/(x2+G12*x1-G32*(x1+x2-
1))^2+(G21*(t21+(G31*t31*(x1+x2-1)-G21*t21*x2)/(x1+G21*x2-G31*(x1+x2-
1))))/(x1+G21*x2-G31*(x1+x2-1))-(2*x2*(G12-G32)*(G32*t32*(x1+x2-1)-
G12*t12*x1))/(x2+G12*x1-G32*(x1+x2-1))^3+(G21*x1*((G31*t31)/(x1+G21*x2-
G31*(x1+x2-1))+((G31*t31*(x1+x2-1)-G21*t21*x2)*(G31-1))/(x1+G21*x2-
G31*(x1+x2-1))^2))/(x1+G21*x2-G31*(x1+x2-1))-
(G23*(((G13*t13*x1+G23*t23*x2)*(G13-1))/(G13*x1-x2-x1+G23*x2+1)^2-
(G13*t13)/(G13*x1-x2-x1+G23*x2+1))*(x1+x2-1))/(G13*x1-x2-
x1+G23*x2+1)+(G23*(t23-(G13*t13*x1+G23*t23*x2)/(G13*x1-x2-
x1+G23*x2+1))*(G13-1)*(x1+x2-1))/(G13*x1-x2-
x1+G23*x2+1)^2+(G21*x1*(G31-1)*(t21+(G31*t31*(x1+x2-1)-
G21*t21*x2)/(x1+G21*x2-G31*(x1+x2-1))))/(x1+G21*x2-G31*(x1+x2-1))^2;
% (d2lngam1/d(x1)^2)
B111=(2*G31*t31)/(x1+G21*x2-G31*(x1+x2-1))^2-(2*(G31*t31*(x1+x2-1)-
G21*t21*x2)*(G31-1)^2)/(x1+G21*x2-G31*(x1+x2-1))^3+(4*(G31*t31*(x1+x2-
1)-G21*t21*x2)*(G31-1))/(x1+G21*x2-G31*(x1+x2-1))^3-
(2*G13*(((G13*t13*x1+G23*t23*x2)*(G13-1))/(G13*x1-x2-x1+G23*x2+1)^2-
(G13*t13)/(G13*x1-x2-x1+G23*x2+1)))/(G13*x1-x2-
x1+G23*x2+1)+(G13*((2*(G13*t13*x1+G23*t23*x2)*(G13-1)^2)/(G13*x1-x2-
x1+G23*x2+1)^3-(2*G13*t13*(G13-1))/(G13*x1-x2-x1+G23*x2+1)^2)*(x1+x2-
1))/(G13*x1-x2-x1+G23*x2+1)-(2*G31*t31*(G31-1))/(x1+G21*x2-G31*(x1+x2-
1))^2+(G12*x2*((2*(G12-G32)*(G12*t12-G32*t32))/(x2+G12*x1-G32*(x1+x2-
1))^2+(2*(G12-G32)^2*(G32*t32*(x1+x2-1)-G12*t12*x1))/(x2+G12*x1-
G32*(x1+x2-1))^3))/(x2+G12*x1-G32*(x1+x2-1))+(2*G13*(t13-
(G13*t13*x1+G23*t23*x2)/(G13*x1-x2-x1+G23*x2+1))*(G13-1))/(G13*x1-x2-
x1+G23*x2+1)^2+(6*x1*(G31*t31*(x1+x2-1)-G21*t21*x2)*(G31-
1)^2)/(x1+G21*x2-G31*(x1+x2-1))^4-(2*G13*(t13-
(G13*t13*x1+G23*t23*x2)/(G13*x1-x2-x1+G23*x2+1))*(G13-1)^2*(x1+x2-
1))/(G13*x1-x2-x1+G23*x2+1)^3+(4*G31*t31*x1*(G31-1))/(x1+G21*x2-
G31*(x1+x2-1))^3+(2*G13*(((G13*t13*x1+G23*t23*x2)*(G13-1))/(G13*x1-x2-
x1+G23*x2+1)^2-(G13*t13)/(G13*x1-x2-x1+G23*x2+1))*(G13-1)*(x1+x2-
1))/(G13*x1-x2-x1+G23*x2+1)^2+(2*G12*x2*(G12-G32)*((G12*t12-
G32*t32)/(x2+G12*x1-G32*(x1+x2-1))+((G12-G32)*(G32*t32*(x1+x2-1)-
G12*t12*x1))/(x2+G12*x1-G32*(x1+x2-1))^2))/(x2+G12*x1-G32*(x1+x2-
1))^2+(2*G12*x2*(G12-G32)^2*(t12+(G32*t32*(x1+x2-1)-
G12*t12*x1)/(x2+G12*x1-G32*(x1+x2-1))))/(x2+G12*x1-G32*(x1+x2-1))^3;
% (d2lngam2/d(x1)^2)
B211=(2*G21*((G31*t31)/(x1+G21*x2-G31*(x1+x2-1))+((G31*t31*(x1+x2-1)-
G21*t21*x2)*(G31-1))/(x1+G21*x2-G31*(x1+x2-1))^2))/(x1+G21*x2-
G31*(x1+x2-1))-(2*(G12-G32)*(G12*t12-G32*t32))/(x2+G12*x1-G32*(x1+x2-
1))^2-(2*G23*(((G13*t13*x1+G23*t23*x2)*(G13-1))/(G13*x1-x2-
x1+G23*x2+1)^2-(G13*t13)/(G13*x1-x2-x1+G23*x2+1)))/(G13*x1-x2-
```

```
x1+G23*x2+1)-(2*(G12-G32)^2*(G32*t32*(x1+x2-1)-G12*t12*x1))/(x2+G12*x1-
G32*(x1+x2-1))^3+(G23*((2*(G13*t13*x1+G23*t23*x2)*(G13-1)^2)/(G13*x1-
x2-x1+G23*x2+1)^3-(2*G13*t13*(G13-1))/(G13*x1-x2-
x1+G23*x2+1)^2)*(x1+x2-1))/(G13*x1-x2-x1+G23*x2+1)+(4*x2*(G12-
G32)*(G12*t12-G32*t32))/(x2+G12*x1-G32*(x1+x2-1))^3+(6*x2*(G12-
G32)^2*(G32*t32*(x1+x2-1)-G12*t12*x1))/(x2+G12*x1-G32*(x1+x2-
1))^4+(2*G23*(t23-(G13*t13*x1+G23*t23*x2)/(G13*x1-x2-
x1+G23*x2+1))*(G13-1))/(G13*x1-x2-x1+G23*x2+1)^2+(2*G21*(G31-
1)*(t21+(G31*t31*(x1+x2-1)-G21*t21*x2)/(x1+G21*x2-G31*(x1+x2-
1))))/(x1+G21*x2-G31*(x1+x2-1))^2+(G21*x1*((2*(G31*t31*(x1+x2-1)-
G21*t21*x2)*(G31-1)^2)/(x1+G21*x2-G31*(x1+x2-1))^3+(2*G31*t31*(G31-
1))/(x1+G21*x2-G31*(x1+x2-1))^2))/(x1+G21*x2-G31*(x1+x2-1))-
(2*G23*(t23-(G13*t13*x1+G23*t23*x2)/(G13*x1-x2-x1+G23*x2+1))*(G13-
1)^2*(x1+x2-1))/(G13*x1-x2-x1+G23*x2+1)^3+(2*G21*x1*(G31-
1)^2*(t21+(G31*t31*(x1+x2-1)-G21*t21*x2)/(x1+G21*x2-G31*(x1+x2-
1))))/(x1+G21*x2-G31*(x1+x2-1))^3+(2*G21*x1*((G31*t31)/(x1+G21*x2-
G31*(x1+x2-1))+((G31*t31*(x1+x2-1)-G21*t21*x2)*(G31-1))/(x1+G21*x2-
G31*(x1+x2-1))^2)*(G31-1))/(x1+G21*x2-G31*(x1+x2-
1))^2+(2*G23*(((G13*t13*x1+G23*t23*x2)*(G13-1))/(G13*x1-x2-
x1+G23*x2+1)^2-(G13*t13)/(G13*x1-x2-x1+G23*x2+1))*(G13-1)*(x1+x2-
1))/(G13*x1-x2-x1+G23*x2+1)^2;
% (d2lngam3/d(x1)^2)
B311=(2*G31*((G31*t31)/(x1+G21*x2-G31*(x1+x2-1))+((G31*t31*(x1+x2-1)-
G21*t21*x2)*(G31-1))/(x1+G21*x2-G31*(x1+x2-1))^2))/(x1+G21*x2-
G31*(x1+x2-1))-(4*(G13*t13*x1+G23*t23*x2)*(G13-1))/(G13*x1-x2-
x1+G23*x2+1)^3+(2*(G13*t13*x1+G23*t23*x2)*(G13-1)^2)/(G13*x1-x2-
x1+G23*x2+1)^3+(2*G13*t13)/(G13*x1-x2-x1+G23*x2+1)^2+(G32*x2*((2*(G12-
G32)*(G12*t12-G32*t32))/(x2+G12*x1-G32*(x1+x2-1))^2+(2*(G12-
G32)^2*(G32*t32*(x1+x2-1)-G12*t12*x1))/(x2+G12*x1-G32*(x1+x2-
1))^3))/(x2+G12*x1-G32*(x1+x2-1))-(2*G13*t13*(G13-1))/(G13*x1-x2-
x1+G23*x2+1)^2+(2*G31*(G31-1)*(t31+(G31*t31*(x1+x2-1)-
G21*t21*x2)/(x1+G21*x2-G31*(x1+x2-1))))/(x1+G21*x2-G31*(x1+x2-
1))^2+(6*(G13*t13*x1+G23*t23*x2)*(G13-1)^2*(x1+x2-1))/(G13*x1-x2-
x1+G23*x2+1)^4+(G31*x1*((2*(G31*t31*(x1+x2-1)-G21*t21*x2)*(G31-
1)^2)/(x1+G21*x2-G31*(x1+x2-1))^3+(2*G31*t31*(G31-1))/(x1+G21*x2-
G31*(x1+x2-1))^2))/(x1+G21*x2-G31*(x1+x2-1))+(2*G31*x1*(G31-
1)^2*(t31+(G31*t31*(x1+x2-1)-G21*t21*x2)/(x1+G21*x2-G31*(x1+x2-
1))))/(x1+G21*x2-G31*(x1+x2-1))^3+(2*G31*x1*((G31*t31)/(x1+G21*x2-
G31*(x1+x2-1))+((G31*t31*(x1+x2-1)-G21*t21*x2)*(G31-1))/(x1+G21*x2-
G31*(x1+x2-1))^2)*(G31-1))/(x1+G21*x2-G31*(x1+x2-1))^2+(2*G32*x2*(G12-
G32)*((G12*t12-G32*t32)/(x2+G12*x1-G32*(x1+x2-1))+((G12-
G32)*(G32*t32*(x1+x2-1)-G12*t12*x1))/(x2+G12*x1-G32*(x1+x2-
1))^2))/(x2+G12*x1-G32*(x1+x2-1))^2-(4*G13*t13*(G13-1)*(x1+x2-
1))/(G13*x1-x2-x1+G23*x2+1)^3+(2*G32*x2*(G12-
G32)^2*(t32+(G32*t32*(x1+x2-1)-G12*t12*x1)/(x2+G12*x1-G32*(x1+x2-
1))))/(x2+G12*x1-G32*(x1+x2-1))^3;
% (d2lngam1/d(x2)^2)
B122=(2*G12*((G32*t32)/(x2+G12*x1-G32*(x1+x2-1))+((G32*t32*(x1+x2-1)-
G12*t12*x1)*(G32-1))/(x2+G12*x1-G32*(x1+x2-1))^2))/(x2+G12*x1-
G32*(x1+x2-1))-(2*(G21-G31)*(G21*t21-G31*t31))/(x1+G21*x2-G31*(x1+x2-
1))^2-(2*G13*(((G13*t13*x1+G23*t23*x2)*(G23-1))/(G13*x1-x2-
x1+G23*x2+1)^2-(G23*t23)/(G13*x1-x2-x1+G23*x2+1)))/(G13*x1-x2-
x1+G23*x2+1)-(2*(G21-G31)^2*(G31*t31*(x1+x2-1)-G21*t21*x2))/(x1+G21*x2-
G31*(x1+x2-1))^3+(G13*((2*(G13*t13*x1+G23*t23*x2)*(G23-1)^2)/(G13*x1-
x2-x1+G23*x2+1)^3-(2*G23*t23*(G23-1))/(G13*x1-x2-
x1+G23*x2+1)^2)*(x1+x2-1))/(G13*x1-x2-x1+G23*x2+1)+(4*x1*(G21-
G31)*(G21*t21-G31*t31))/(x1+G21*x2-G31*(x1+x2-1))^3+(6*x1*(G21-
```

```
G31)^2*(G31*t31*(x1+x2-1)-G21*t21*x2))/(x1+G21*x2-G31*(x1+x2-
1))^4+(2*G13*(t13-(G13*t13*x1+G23*t23*x2)/(G13*x1-x2-
x1+G23*x2+1))*(G23-1))/(G13*x1-x2-x1+G23*x2+1)^2+(2*G12*(G32-
1)*(t12+(G32*t32*(x1+x2-1)-G12*t12*x1)/(x2+G12*x1-G32*(x1+x2-
1))))/(x2+G12*x1-G32*(x1+x2-1))^2+(G12*x2*((2*(G32*t32*(x1+x2-1)-
G12*t12*x1)*(G32-1)^2)/(x2+G12*x1-G32*(x1+x2-1))^3+(2*G32*t32*(G32-
1))/(x2+G12*x1-G32*(x1+x2-1))^2))/(x2+G12*x1-G32*(x1+x2-1))-
(2*G13*(t13-(G13*t13*x1+G23*t23*x2)/(G13*x1-x2-x1+G23*x2+1))*(G23-
1)^2*(x1+x2-1))/(G13*x1-x2-x1+G23*x2+1)^3+(2*G12*x2*(G32-
1)^2*(t12+(G32*t32*(x1+x2-1)-G12*t12*x1)/(x2+G12*x1-G32*(x1+x2-
1))))/(x2+G12*x1-G32*(x1+x2-1))^3+(2*G12*x2*((G32*t32)/(x2+G12*x1-
G32*(x1+x2-1))+((G32*t32*(x1+x2-1)-G12*t12*x1)*(G32-1))/(x2+G12*x1-
G32*(x1+x2-1))^2)*(G32-1))/(x2+G12*x1-G32*(x1+x2-
1))^2+(2*G13*(((G13*t13*x1+G23*t23*x2)*(G23-1))/(G13*x1-x2-
x1+G23*x2+1)^2-(G23*t23)/(G13*x1-x2-x1+G23*x2+1))*(G23-1)*(x1+x2-
1))/(G13*x1-x2-x1+G23*x2+1)^2;
% (d2lngam2/d(x2)^2)
B222=(2*G32*t32)/(x2+G12*x1-G32*(x1+x2-1))^2-(2*(G32*t32*(x1+x2-1)-
G12*t12*x1)*(G32-1)^2)/(x2+G12*x1-G32*(x1+x2-1))^3+(4*(G32*t32*(x1+x2-
1)-G12*t12*x1)*(G32-1))/(x2+G12*x1-G32*(x1+x2-1))^3-
(2*G23*(((G13*t13*x1+G23*t23*x2)*(G23-1))/(G13*x1-x2-x1+G23*x2+1)^2-
(G23*t23)/(G13*x1-x2-x1+G23*x2+1)))/(G13*x1-x2-
x1+G23*x2+1)+(G23*((2*(G13*t13*x1+G23*t23*x2)*(G23-1)^2)/(G13*x1-x2-
x1+G23*x2+1)^3-(2*G23*t23*(G23-1))/(G13*x1-x2-x1+G23*x2+1)^2)*(x1+x2-
1))/(G13*x1-x2-x1+G23*x2+1)-(2*G32*t32*(G32-1))/(x2+G12*x1-G32*(x1+x2-
1))^2+(G21*x1*((2*(G21-G31)*(G21*t21-G31*t31))/(x1+G21*x2-G31*(x1+x2-
1))^2+(2*(G21-G31)^2*(G31*t31*(x1+x2-1)-G21*t21*x2))/(x1+G21*x2-
G31*(x1+x2-1))^3))/(x1+G21*x2-G31*(x1+x2-1))+(2*G23*(t23-
(G13*t13*x1+G23*t23*x2)/(G13*x1-x2-x1+G23*x2+1))*(G23-1))/(G13*x1-x2-
x1+G23*x2+1)^2+(6*x2*(G32*t32*(x1+x2-1)-G12*t12*x1)*(G32-
1)^2)/(x2+G12*x1-G32*(x1+x2-1))^4-(2*G23*(t23-
(G13*t13*x1+G23*t23*x2)/(G13*x1-x2-x1+G23*x2+1))*(G23-1)^2*(x1+x2-
1))/(G13*x1-x2-x1+G23*x2+1)^3+(4*G32*t32*x2*(G32-1))/(x2+G12*x1-
G32*(x1+x2-1))^3+(2*G23*(((G13*t13*x1+G23*t23*x2)*(G23-1))/(G13*x1-x2-
x1+G23*x2+1)^2-(G23*t23)/(G13*x1-x2-x1+G23*x2+1))*(G23-1)*(x1+x2-
1))/(G13*x1-x2-x1+G23*x2+1)^2+(2*G21*x1*(G21-G31)*((G21*t21-
G31*t31)/(x1+G21*x2-G31*(x1+x2-1))+((G21-G31)*(G31*t31*(x1+x2-1)-
G21*t21*x2))/(x1+G21*x2-G31*(x1+x2-1))^2))/(x1+G21*x2-G31*(x1+x2-
1))^2+(2*G21*x1*(G21-G31)^2*(t21+(G31*t31*(x1+x2-1)-
G21*t21*x2)/(x1+G21*x2-G31*(x1+x2-1))))/(x1+G21*x2-G31*(x1+x2-1))^3;
% (d2lngam3/d(x2)^2)
B322=(2*G32*((G32*t32)/(x2+G12*x1-G32*(x1+x2-1))+((G32*t32*(x1+x2-1)-
G12*t12*x1)*(G32-1))/(x2+G12*x1-G32*(x1+x2-1))^2))/(x2+G12*x1-
G32*(x1+x2-1))-(4*(G13*t13*x1+G23*t23*x2)*(G23-1))/(G13*x1-x2-
x1+G23*x2+1)^3+(2*(G13*t13*x1+G23*t23*x2)*(G23-1)^2)/(G13*x1-x2-
x1+G23*x2+1)^3+(2*G23*t23)/(G13*x1-x2-x1+G23*x2+1)^2+(G31*x1*((2*(G21-
G31)*(G21*t21-G31*t31))/(x1+G21*x2-G31*(x1+x2-1))^2+(2*(G21-
G31)^2*(G31*t31*(x1+x2-1)-G21*t21*x2))/(x1+G21*x2-G31*(x1+x2-
1))^3))/(x1+G21*x2-G31*(x1+x2-1))-(2*G23*t23*(G23-1))/(G13*x1-x2-
x1+G23*x2+1)^2+(2*G32*(G32-1)*(t32+(G32*t32*(x1+x2-1)-
G12*t12*x1)/(x2+G12*x1-G32*(x1+x2-1))))/(x2+G12*x1-G32*(x1+x2-
1))^2+(6*(G13*t13*x1+G23*t23*x2)*(G23-1)^2*(x1+x2-1))/(G13*x1-x2-
x1+G23*x2+1)^4+(G32*x2*((2*(G32*t32*(x1+x2-1)-G12*t12*x1)*(G32-
1)^2)/(x2+G12*x1-G32*(x1+x2-1))^3+(2*G32*t32*(G32-1))/(x2+G12*x1-
G32*(x1+x2-1))^2))/(x2+G12*x1-G32*(x1+x2-1))+(2*G32*x2*(G32-
1)^2*(t32+(G32*t32*(x1+x2-1)-G12*t12*x1)/(x2+G12*x1-G32*(x1+x2-
1))))/(x2+G12*x1-G32*(x1+x2-1))^3+(2*G32*x2*((G32*t32)/(x2+G12*x1-
```

```
G32*(x1+x2-1))+((G32*t32*(x1+x2-1)-G12*t12*x1)*(G32-1))/(x2+G12*x1-
G32*(x1+x2-1))^2)*(G32-1))/(x2+G12*x1-G32*(x1+x2-1))^2+(2*G31*x1*(G21-
G31)*((G21*t21-G31*t31)/(x1+G21*x2-G31*(x1+x2-1))+((G21-
G31)*(G31*t31*(x1+x2-1)-G21*t21*x2))/(x1+G21*x2-G31*(x1+x2-
1))^2))/(x1+G21*x2-G31*(x1+x2-1))^2-(4*G23*t23*(G23-1)*(x1+x2-
1))/(G13*x1-x2-x1+G23*x2+1)^3+(2*G31*x1*(G21-
G31)^2*(t31+(G31*t31*(x1+x2-1)-G21*t21*x2)/(x1+G21*x2-G31*(x1+x2-
1))))/(x1+G21*x2-G31*(x1+x2-1))^3;
% (d2lngam1/dx1 dx2)
B112=((G21*t21-G31*t31)*(G31-1))/(x1+G21*x2-G31*(x1+x2-1))^2-(2*(G21-
G31)*(G31*t31*(x1+x2-1)-G21*t21*x2))/(x1+G21*x2-G31*(x1+x2-1))^3-
(G13*(((G13*t13*x1+G23*t23*x2)*(G13-1))/(G13*x1-x2-x1+G23*x2+1)^2-
(G13*t13)/(G13*x1-x2-x1+G23*x2+1)))/(G13*x1-x2-x1+G23*x2+1)-
(G13*(((G13*t13*x1+G23*t23*x2)*(G23-1))/(G13*x1-x2-x1+G23*x2+1)^2-
(G23*t23)/(G13*x1-x2-x1+G23*x2+1)))/(G13*x1-x2-x1+G23*x2+1)-(G21*t21-
G31*t31)/(x1+G21*x2-G31*(x1+x2-1))^2-(G12*((G12*t12-
G32*t32)/(x2+G12*x1-G32*(x1+x2-1))+((G12-G32)*(G32*t32*(x1+x2-1)-
G12*t12*x1))/(x2+G12*x1-G32*(x1+x2-1))^2))/(x2+G12*x1-G32*(x1+x2-1))-
(G12*(G12-G32)*(t12+(G32*t32*(x1+x2-1)-G12*t12*x1)/(x2+G12*x1-
G32*(x1+x2-1))))/(x2+G12*x1-G32*(x1+x2-1))^2+(G13*(t13-
(G13*t13*x1+G23*t23*x2)/(G13*x1-x2-x1+G23*x2+1))*(G13-1))/(G13*x1-x2-
x1+G23*x2+1)^2+(G13*(t13-(G13*t13*x1+G23*t23*x2)/(G13*x1-x2-
x1+G23*x2+1))*(G23-1))/(G13*x1-x2-x1+G23*x2+1)^2-(2*x1*(G21*t21-
G31*t31)*(G31-1))/(x1+G21*x2-G31*(x1+x2-1))^3-(G12*x2*(((G12*t12-
G32*t32)*(G32-1))/(x2+G12*x1-G32*(x1+x2-1))^2+(G32*t32*(G12-
G32))/(x2+G12*x1-G32*(x1+x2-1))^2+(2*(G12-G32)*(G32*t32*(x1+x2-1)-
G12*t12*x1)*(G32-1))/(x2+G12*x1-G32*(x1+x2-1))^3))/(x2+G12*x1-
G32*(x1+x2-1))+(G31*t31*(G21-G31))/(x1+G21*x2-G31*(x1+x2-1))^2-
(G13*((G13*t13*(G23-1))/(G13*x1-x2-x1+G23*x2+1)^2+(G23*t23*(G13-
1))/(G13*x1-x2-x1+G23*x2+1)^2-(2*(G13*t13*x1+G23*t23*x2)*(G13-1)*(G23-
1))/(G13*x1-x2-x1+G23*x2+1)^3)*(x1+x2-1))/(G13*x1-x2-
x1+G23*x2+1)+(2*(G21-G31)*(G31*t31*(x1+x2-1)-G21*t21*x2)*(G31-
1))/(x1+G21*x2-G31*(x1+x2-1))^3-(G12*x2*(G32-1)*((G12*t12-
G32*t32)/(x2+G12*x1-G32*(x1+x2-1))+((G12-G32)*(G32*t32*(x1+x2-1)-
G12*t12*x1))/(x2+G12*x1-G32*(x1+x2-1))^2))/(x2+G12*x1-G32*(x1+x2-1))^2-
(2*G31*t31*x1*(G21-G31))/(x1+G21*x2-G31*(x1+x2-1))^3-(G12*x2*(G12-
G32)*((G32*t32)/(x2+G12*x1-G32*(x1+x2-1))+((G32*t32*(x1+x2-1)-
G12*t12*x1)*(G32-1))/(x2+G12*x1-G32*(x1+x2-1))^2))/(x2+G12*x1-
G32*(x1+x2-1))^2-(6*x1*(G21-G31)*(G31*t31*(x1+x2-1)-G21*t21*x2)*(G31-
1))/(x1+G21*x2-G31*(x1+x2-1))^4+(G13*(((G13*t13*x1+G23*t23*x2)*(G13-
1))/(G13*x1-x2-x1+G23*x2+1)^2-(G13*t13)/(G13*x1-x2-x1+G23*x2+1))*(G23-
1)*(x1+x2-1))/(G13*x1-x2-
x1+G23*x2+1)^2+(G13*(((G13*t13*x1+G23*t23*x2)*(G23-1))/(G13*x1-x2-
x1+G23*x2+1)^2-(G23*t23)/(G13*x1-x2-x1+G23*x2+1))*(G13-1)*(x1+x2-
1))/(G13*x1-x2-x1+G23*x2+1)^2-(2*G12*x2*(G12-G32)*(G32-
1)*(t12+(G32*t32*(x1+x2-1)-G12*t12*x1)/(x2+G12*x1-G32*(x1+x2-
1))))/(x2+G12*x1-G32*(x1+x2-1))^3-(2*G13*(t13-
(G13*t13*x1+G23*t23*x2)/(G13*x1-x2-x1+G23*x2+1))*(G13-1)*(G23-
1)*(x1+x2-1))/(G13*x1-x2-x1+G23*x2+1)^3;
% (d2lngam2/dx1 dx2)
B212=((G12*t12-G32*t32)*(G32-1))/(x2+G12*x1-G32*(x1+x2-1))^2-(2*(G12-
G32)*(G32*t32*(x1+x2-1)-G12*t12*x1))/(x2+G12*x1-G32*(x1+x2-1))^3-
(G23*(((G13*t13*x1+G23*t23*x2)*(G13-1))/(G13*x1-x2-x1+G23*x2+1)^2-
(G13*t13)/(G13*x1-x2-x1+G23*x2+1)))/(G13*x1-x2-x1+G23*x2+1)-
(G23*(((G13*t13*x1+G23*t23*x2)*(G23-1))/(G13*x1-x2-x1+G23*x2+1)^2-
(G23*t23)/(G13*x1-x2-x1+G23*x2+1)))/(G13*x1-x2-x1+G23*x2+1)-(G12*t12-
G32*t32)/(x2+G12*x1-G32*(x1+x2-1))^2-(G21*((G21*t21-
```

```
G31*t31)/(x1+G21*x2-G31*(x1+x2-1))+((G21-G31)*(G31*t31*(x1+x2-1)-
G21*t21*x2))/(x1+G21*x2-G31*(x1+x2-1))^2))/(x1+G21*x2-G31*(x1+x2-1))-
(G21*(G21-G31)*(t21+(G31*t31*(x1+x2-1)-G21*t21*x2)/(x1+G21*x2-
G31*(x1+x2-1))))/(x1+G21*x2-G31*(x1+x2-1))^2+(G23*(t23-
(G13*t13*x1+G23*t23*x2)/(G13*x1-x2-x1+G23*x2+1))*(G13-1))/(G13*x1-x2-
x1+G23*x2+1)^2+(G23*(t23-(G13*t13*x1+G23*t23*x2)/(G13*x1-x2-
x1+G23*x2+1))*(G23-1))/(G13*x1-x2-x1+G23*x2+1)^2-(2*x2*(G12*t12-
G32*t32)*(G32-1))/(x2+G12*x1-G32*(x1+x2-1))^3-(G21*x1*(((G21*t21-
G31*t31)*(G31-1))/(x1+G21*x2-G31*(x1+x2-1))^2+(G31*t31*(G21-
G31))/(x1+G21*x2-G31*(x1+x2-1))^2+(2*(G21-G31)*(G31*t31*(x1+x2-1)-
G21*t21*x2)*(G31-1))/(x1+G21*x2-G31*(x1+x2-1))^3))/(x1+G21*x2-
G31*(x1+x2-1))+(G32*t32*(G12-G32))/(x2+G12*x1-G32*(x1+x2-1))^2-
(G23*((G13*t13*(G23-1))/(G13*x1-x2-x1+G23*x2+1)^2+(G23*t23*(G13-
1))/(G13*x1-x2-x1+G23*x2+1)^2-(2*(G13*t13*x1+G23*t23*x2)*(G13-1)*(G23-
1))/(G13*x1-x2-x1+G23*x2+1)^3)*(x1+x2-1))/(G13*x1-x2-
x1+G23*x2+1)+(2*(G12-G32)*(G32*t32*(x1+x2-1)-G12*t12*x1)*(G32-
1))/(x2+G12*x1-G32*(x1+x2-1))^3-(G21*x1*(G31-1)*((G21*t21-
G31*t31)/(x1+G21*x2-G31*(x1+x2-1))+((G21-G31)*(G31*t31*(x1+x2-1)-
G21*t21*x2))/(x1+G21*x2-G31*(x1+x2-1))^2))/(x1+G21*x2-G31*(x1+x2-1))^2-
(2*G32*t32*x2*(G12-G32))/(x2+G12*x1-G32*(x1+x2-1))^3-(G21*x1*(G21-
G31)*((G31*t31)/(x1+G21*x2-G31*(x1+x2-1))+((G31*t31*(x1+x2-1)-
G21*t21*x2)*(G31-1))/(x1+G21*x2-G31*(x1+x2-1))^2))/(x1+G21*x2-
G31*(x1+x2-1))^2-(6*x2*(G12-G32)*(G32*t32*(x1+x2-1)-G12*t12*x1)*(G32-
1))/(x2+G12*x1-G32*(x1+x2-1))^4+(G23*(((G13*t13*x1+G23*t23*x2)*(G13-
1))/(G13*x1-x2-x1+G23*x2+1)^2-(G13*t13)/(G13*x1-x2-x1+G23*x2+1))*(G23-
1)*(x1+x2-1))/(G13*x1-x2-
x1+G23*x2+1)^2+(G23*(((G13*t13*x1+G23*t23*x2)*(G23-1))/(G13*x1-x2-
x1+G23*x2+1)^2-(G23*t23)/(G13*x1-x2-x1+G23*x2+1))*(G13-1)*(x1+x2-
1))/(G13*x1-x2-x1+G23*x2+1)^2-(2*G21*x1*(G21-G31)*(G31-
1)*(t21+(G31*t31*(x1+x2-1)-G21*t21*x2)/(x1+G21*x2-G31*(x1+x2-
1))))/(x1+G21*x2-G31*(x1+x2-1))^3-(2*G23*(t23-
(G13*t13*x1+G23*t23*x2)/(G13*x1-x2-x1+G23*x2+1))*(G13-1)*(G23-
1)*(x1+x2-1))/(G13*x1-x2-x1+G23*x2+1)^3;
% (d2lngam3/dx1 dx2)
B312=(G13*t13)/(G13*x1-x2-x1+G23*x2+1)^2-
(2*(G13*t13*x1+G23*t23*x2)*(G23-1))/(G13*x1-x2-x1+G23*x2+1)^3-
(2*(G13*t13*x1+G23*t23*x2)*(G13-1))/(G13*x1-x2-
x1+G23*x2+1)^3+(G23*t23)/(G13*x1-x2-x1+G23*x2+1)^2-(G32*((G12*t12-
G32*t32)/(x2+G12*x1-G32*(x1+x2-1))+((G12-G32)*(G32*t32*(x1+x2-1)-
G12*t12*x1))/(x2+G12*x1-G32*(x1+x2-1))^2))/(x2+G12*x1-G32*(x1+x2-1))-
(G31*((G21*t21-G31*t31)/(x1+G21*x2-G31*(x1+x2-1))+((G21-
G31)*(G31*t31*(x1+x2-1)-G21*t21*x2))/(x1+G21*x2-G31*(x1+x2-
1))^2))/(x1+G21*x2-G31*(x1+x2-1))-(G32*(G12-G32)*(t32+(G32*t32*(x1+x2-
1)-G12*t12*x1)/(x2+G12*x1-G32*(x1+x2-1))))/(x2+G12*x1-G32*(x1+x2-1))^2-
(G31*(G21-G31)*(t31+(G31*t31*(x1+x2-1)-G21*t21*x2)/(x1+G21*x2-
G31*(x1+x2-1))))/(x1+G21*x2-G31*(x1+x2-1))^2-(G32*x2*(((G12*t12-
G32*t32)*(G32-1))/(x2+G12*x1-G32*(x1+x2-1))^2+(G32*t32*(G12-
G32))/(x2+G12*x1-G32*(x1+x2-1))^2+(2*(G12-G32)*(G32*t32*(x1+x2-1)-
G12*t12*x1)*(G32-1))/(x2+G12*x1-G32*(x1+x2-1))^3))/(x2+G12*x1-
G32*(x1+x2-1))-(G31*x1*(((G21*t21-G31*t31)*(G31-1))/(x1+G21*x2-
G31*(x1+x2-1))^2+(G31*t31*(G21-G31))/(x1+G21*x2-G31*(x1+x2-
1))^2+(2*(G21-G31)*(G31*t31*(x1+x2-1)-G21*t21*x2)*(G31-1))/(x1+G21*x2-
G31*(x1+x2-1))^3))/(x1+G21*x2-G31*(x1+x2-1))-(G13*t13*(G23-1))/(G13*x1-
x2-x1+G23*x2+1)^2-(G23*t23*(G13-1))/(G13*x1-x2-
x1+G23*x2+1)^2+(2*(G13*t13*x1+G23*t23*x2)*(G13-1)*(G23-1))/(G13*x1-x2-
x1+G23*x2+1)^3-(G32*x2*(G32-1)*((G12*t12-G32*t32)/(x2+G12*x1-
G32*(x1+x2-1))+((G12-G32)*(G32*t32*(x1+x2-1)-G12*t12*x1))/(x2+G12*x1-
```

```
G32*(x1+x2-1))^2))/(x2+G12*x1-G32*(x1+x2-1))^2-(G31*x1*(G31-
1)*((G21*t21-G31*t31)/(x1+G21*x2-G31*(x1+x2-1))+((G21-
G31)*(G31*t31*(x1+x2-1)-G21*t21*x2))/(x1+G21*x2-G31*(x1+x2-
1))^2))/(x1+G21*x2-G31*(x1+x2-1))^2+(6*(G13*t13*x1+G23*t23*x2)*(G13-
1)*(G23-1)*(x1+x2-1))/(G13*x1-x2-x1+G23*x2+1)^4-(G32*x2*(G12-
G32)*((G32*t32)/(x2+G12*x1-G32*(x1+x2-1))+((G32*t32*(x1+x2-1)-
G12*t12*x1)*(G32-1))/(x2+G12*x1-G32*(x1+x2-1))^2))/(x2+G12*x1-
G32*(x1+x2-1))^2-(G31*x1*(G21-G31)*((G31*t31)/(x1+G21*x2-G31*(x1+x2-
1))+((G31*t31*(x1+x2-1)-G21*t21*x2)*(G31-1))/(x1+G21*x2-G31*(x1+x2-
1))^2))/(x1+G21*x2-G31*(x1+x2-1))^2-(2*G13*t13*(G23-1)*(x1+x2-
1))/(G13*x1-x2-x1+G23*x2+1)^3-(2*G23*t23*(G13-1)*(x1+x2-1))/(G13*x1-x2-
x1+G23*x2+1)^3-(2*G32*x2*(G12-G32)*(G32-1)*(t32+(G32*t32*(x1+x2-1)-
G12*t12*x1)/(x2+G12*x1-G32*(x1+x2-1))))/(x2+G12*x1-G32*(x1+x2-1))^3-
(2*G31*x1*(G21-G31)*(G31-1)*(t31+(G31*t31*(x1+x2-1)-
G21*t21*x2)/(x1+G21*x2-G31*(x1+x2-1))))/(x1+G21*x2-G31*(x1+x2-1))^3;
% (d3lngam1/d (x1)^3)
B1111=(18*(G31*t31*(x1+x2-1)-G21*t21*x2)*(G31-1)^2)/(x1+G21*x2-
G31*(x1+x2-1))^4-(6*(G31*t31*(x1+x2-1)-G21*t21*x2)*(G31-
1)^3)/(x1+G21*x2-G31*(x1+x2-
1))^4+(3*G13*((2*(G13*t13*x1+G23*t23*x2)*(G13-1)^2)/(G13*x1-x2-
x1+G23*x2+1)^3-(2*G13*t13*(G13-1))/(G13*x1-x2-x1+G23*x2+1)^2))/(G13*x1-
x2-x1+G23*x2+1)+(12*G31*t31*(G31-1))/(x1+G21*x2-G31*(x1+x2-
1))^3+(6*G13*(((G13*t13*x1+G23*t23*x2)*(G13-1))/(G13*x1-x2-
x1+G23*x2+1)^2-(G13*t13)/(G13*x1-x2-x1+G23*x2+1))*(G13-1))/(G13*x1-x2-
x1+G23*x2+1)^2-(G13*((6*(G13*t13*x1+G23*t23*x2)*(G13-1)^3)/(G13*x1-x2-
x1+G23*x2+1)^4-(6*G13*t13*(G13-1)^2)/(G13*x1-x2-x1+G23*x2+1)^3)*(x1+x2-
1))/(G13*x1-x2-x1+G23*x2+1)-(6*G31*t31*(G31-1)^2)/(x1+G21*x2-
G31*(x1+x2-1))^3-(G12*x2*((6*(G12-G32)^3*(G32*t32*(x1+x2-1)-
G12*t12*x1))/(x2+G12*x1-G32*(x1+x2-1))^4+(6*(G12-G32)^2*(G12*t12-
G32*t32))/(x2+G12*x1-G32*(x1+x2-1))^3))/(x2+G12*x1-G32*(x1+x2-
1))+(24*x1*(G31*t31*(x1+x2-1)-G21*t21*x2)*(G31-1)^3)/(x1+G21*x2-
G31*(x1+x2-1))^5-(6*G13*(t13-(G13*t13*x1+G23*t23*x2)/(G13*x1-x2-
x1+G23*x2+1))*(G13-1)^2)/(G13*x1-x2-x1+G23*x2+1)^3-
(6*G13*(((G13*t13*x1+G23*t23*x2)*(G13-1))/(G13*x1-x2-x1+G23*x2+1)^2-
(G13*t13)/(G13*x1-x2-x1+G23*x2+1))*(G13-1)^2*(x1+x2-1))/(G13*x1-x2-
x1+G23*x2+1)^3+(6*G13*(t13-(G13*t13*x1+G23*t23*x2)/(G13*x1-x2-
x1+G23*x2+1))*(G13-1)^3*(x1+x2-1))/(G13*x1-x2-x1+G23*x2+1)^4-
(6*G12*x2*(G12-G32)^2*((G12*t12-G32*t32)/(x2+G12*x1-G32*(x1+x2-
1))+((G12-G32)*(G32*t32*(x1+x2-1)-G12*t12*x1))/(x2+G12*x1-G32*(x1+x2-
1))^2))/(x2+G12*x1-G32*(x1+x2-1))^3-(3*G12*x2*(G12-G32)*((2*(G12-
G32)*(G12*t12-G32*t32))/(x2+G12*x1-G32*(x1+x2-1))^2+(2*(G12-
G32)^2*(G32*t32*(x1+x2-1)-G12*t12*x1))/(x2+G12*x1-G32*(x1+x2-
1))^3))/(x2+G12*x1-G32*(x1+x2-1))^2-
(3*G13*((2*(G13*t13*x1+G23*t23*x2)*(G13-1)^2)/(G13*x1-x2-
x1+G23*x2+1)^3-(2*G13*t13*(G13-1))/(G13*x1-x2-x1+G23*x2+1)^2)*(G13-
1)*(x1+x2-1))/(G13*x1-x2-x1+G23*x2+1)^2+(18*G31*t31*x1*(G31-
1)^2)/(x1+G21*x2-G31*(x1+x2-1))^4-(6*G12*x2*(G12-
G32)^3*(t12+(G32*t32*(x1+x2-1)-G12*t12*x1)/(x2+G12*x1-G32*(x1+x2-
1))))/(x2+G12*x1-G32*(x1+x2-1))^4;
% (d3lngam2/d (x1)^3)
B2111=(3*G21*((2*(G31*t31*(x1+x2-1)-G21*t21*x2)*(G31-1)^2)/(x1+G21*x2-
G31*(x1+x2-1))^3+(2*G31*t31*(G31-1))/(x1+G21*x2-G31*(x1+x2-
1))^2))/(x1+G21*x2-G31*(x1+x2-1))+(6*(G12-G32)^3*(G32*t32*(x1+x2-1)-
G12*t12*x1))/(x2+G12*x1-G32*(x1+x2-
1))^4+(3*G23*((2*(G13*t13*x1+G23*t23*x2)*(G13-1)^2)/(G13*x1-x2-
x1+G23*x2+1)^3-(2*G13*t13*(G13-1))/(G13*x1-x2-x1+G23*x2+1)^2))/(G13*x1-
x2-x1+G23*x2+1)+(6*(G12-G32)^2*(G12*t12-G32*t32))/(x2+G12*x1-
```

```
G32*(x1+x2-1))^3+(6*G21*((G31*t31)/(x1+G21*x2-G31*(x1+x2-
1))+((G31*t31*(x1+x2-1)-G21*t21*x2)*(G31-1))/(x1+G21*x2-G31*(x1+x2-
1))^2)*(G31-1))/(x1+G21*x2-G31*(x1+x2-1))^2-(24*x2*(G12-
G32)^3*(G32*t32*(x1+x2-1)-G12*t12*x1))/(x2+G12*x1-G32*(x1+x2-
1))^5+(G21*x1*((6*(G31*t31*(x1+x2-1)-G21*t21*x2)*(G31-1)^3)/(x1+G21*x2-
G31*(x1+x2-1))^4+(6*G31*t31*(G31-1)^2)/(x1+G21*x2-G31*(x1+x2-
1))^3))/(x1+G21*x2-G31*(x1+x2-
1))+(6*G23*(((G13*t13*x1+G23*t23*x2)*(G13-1))/(G13*x1-x2-
x1+G23*x2+1)^2-(G13*t13)/(G13*x1-x2-x1+G23*x2+1))*(G13-1))/(G13*x1-x2-
x1+G23*x2+1)^2-(G23*((6*(G13*t13*x1+G23*t23*x2)*(G13-1)^3)/(G13*x1-x2-
x1+G23*x2+1)^4-(6*G13*t13*(G13-1)^2)/(G13*x1-x2-x1+G23*x2+1)^3)*(x1+x2-
1))/(G13*x1-x2-x1+G23*x2+1)-(18*x2*(G12-G32)^2*(G12*t12-
G32*t32))/(x2+G12*x1-G32*(x1+x2-1))^4-(6*G23*(t23-
(G13*t13*x1+G23*t23*x2)/(G13*x1-x2-x1+G23*x2+1))*(G13-1)^2)/(G13*x1-x2-
x1+G23*x2+1)^3+(6*G21*(G31-1)^2*(t21+(G31*t31*(x1+x2-1)-
G21*t21*x2)/(x1+G21*x2-G31*(x1+x2-1))))/(x1+G21*x2-G31*(x1+x2-1))^3-
(6*G23*(((G13*t13*x1+G23*t23*x2)*(G13-1))/(G13*x1-x2-x1+G23*x2+1)^2-
(G13*t13)/(G13*x1-x2-x1+G23*x2+1))*(G13-1)^2*(x1+x2-1))/(G13*x1-x2-
x1+G23*x2+1)^3+(6*G23*(t23-(G13*t13*x1+G23*t23*x2)/(G13*x1-x2-
x1+G23*x2+1))*(G13-1)^3*(x1+x2-1))/(G13*x1-x2-
x1+G23*x2+1)^4+(6*G21*x1*(G31-1)^3*(t21+(G31*t31*(x1+x2-1)-
G21*t21*x2)/(x1+G21*x2-G31*(x1+x2-1))))/(x1+G21*x2-G31*(x1+x2-
1))^4+(3*G21*x1*((2*(G31*t31*(x1+x2-1)-G21*t21*x2)*(G31-
1)^2)/(x1+G21*x2-G31*(x1+x2-1))^3+(2*G31*t31*(G31-1))/(x1+G21*x2-
G31*(x1+x2-1))^2)*(G31-1))/(x1+G21*x2-G31*(x1+x2-1))^2-
(3*G23*((2*(G13*t13*x1+G23*t23*x2)*(G13-1)^2)/(G13*x1-x2-
x1+G23*x2+1)^3-(2*G13*t13*(G13-1))/(G13*x1-x2-x1+G23*x2+1)^2)*(G13-
1)*(x1+x2-1))/(G13*x1-x2-
x1+G23*x2+1)^2+(6*G21*x1*((G31*t31)/(x1+G21*x2-G31*(x1+x2-
1))+((G31*t31*(x1+x2-1)-G21*t21*x2)*(G31-1))/(x1+G21*x2-G31*(x1+x2-
1))^2)*(G31-1)^2)/(x1+G21*x2-G31*(x1+x2-1))^3;
% (d3lngam3/d (x1)^3)
B3111=(3*G31*((2*(G31*t31*(x1+x2-1)-G21*t21*x2)*(G31-1)^2)/(x1+G21*x2-
G31*(x1+x2-1))^3+(2*G31*t31*(G31-1))/(x1+G21*x2-G31*(x1+x2-
1))^2))/(x1+G21*x2-G31*(x1+x2-1))+(18*(G13*t13*x1+G23*t23*x2)*(G13-
1)^2)/(G13*x1-x2-x1+G23*x2+1)^4-(6*(G13*t13*x1+G23*t23*x2)*(G13-
1)^3)/(G13*x1-x2-x1+G23*x2+1)^4+(6*G31*((G31*t31)/(x1+G21*x2-
G31*(x1+x2-1))+((G31*t31*(x1+x2-1)-G21*t21*x2)*(G31-1))/(x1+G21*x2-
G31*(x1+x2-1))^2)*(G31-1))/(x1+G21*x2-G31*(x1+x2-
1))^2+(G31*x1*((6*(G31*t31*(x1+x2-1)-G21*t21*x2)*(G31-1)^3)/(x1+G21*x2-
G31*(x1+x2-1))^4+(6*G31*t31*(G31-1)^2)/(x1+G21*x2-G31*(x1+x2-
1))^3))/(x1+G21*x2-G31*(x1+x2-1))-(12*G13*t13*(G13-1))/(G13*x1-x2-
x1+G23*x2+1)^3-(G32*x2*((6*(G12-G32)^3*(G32*t32*(x1+x2-1)-
G12*t12*x1))/(x2+G12*x1-G32*(x1+x2-1))^4+(6*(G12-G32)^2*(G12*t12-
G32*t32))/(x2+G12*x1-G32*(x1+x2-1))^3))/(x2+G12*x1-G32*(x1+x2-
1))+(6*G13*t13*(G13-1)^2)/(G13*x1-x2-x1+G23*x2+1)^3+(6*G31*(G31-
1)^2*(t31+(G31*t31*(x1+x2-1)-G21*t21*x2)/(x1+G21*x2-G31*(x1+x2-
1))))/(x1+G21*x2-G31*(x1+x2-1))^3-(24*(G13*t13*x1+G23*t23*x2)*(G13-
1)^3*(x1+x2-1))/(G13*x1-x2-x1+G23*x2+1)^5-(6*G32*x2*(G12-
G32)^2*((G12*t12-G32*t32)/(x2+G12*x1-G32*(x1+x2-1))+((G12-
G32)*(G32*t32*(x1+x2-1)-G12*t12*x1))/(x2+G12*x1-G32*(x1+x2-
1))^2))/(x2+G12*x1-G32*(x1+x2-1))^3+(18*G13*t13*(G13-1)^2*(x1+x2-
1))/(G13*x1-x2-x1+G23*x2+1)^4+(6*G31*x1*(G31-1)^3*(t31+(G31*t31*(x1+x2-
1)-G21*t21*x2)/(x1+G21*x2-G31*(x1+x2-1))))/(x1+G21*x2-G31*(x1+x2-1))^4-
(3*G32*x2*(G12-G32)*((2*(G12-G32)*(G12*t12-G32*t32))/(x2+G12*x1-
G32*(x1+x2-1))^2+(2*(G12-G32)^2*(G32*t32*(x1+x2-1)-
G12*t12*x1))/(x2+G12*x1-G32*(x1+x2-1))^3))/(x2+G12*x1-G32*(x1+x2-
```

```
1))^2+(3*G31*x1*((2*(G31*t31*(x1+x2-1)-G21*t21*x2)*(G31-
1)^2)/(x1+G21*x2-G31*(x1+x2-1))^3+(2*G31*t31*(G31-1))/(x1+G21*x2-
G31*(x1+x2-1))^2)*(G31-1))/(x1+G21*x2-G31*(x1+x2-
1))^2+(6*G31*x1*((G31*t31)/(x1+G21*x2-G31*(x1+x2-1))+((G31*t31*(x1+x2-
1)-G21*t21*x2)*(G31-1))/(x1+G21*x2-G31*(x1+x2-1))^2)*(G31-
1)^2)/(x1+G21*x2-G31*(x1+x2-1))^3-(6*G32*x2*(G12-
G32)^3*(t32+(G32*t32*(x1+x2-1)-G12*t12*x1)/(x2+G12*x1-G32*(x1+x2-
1))))/(x2+G12*x1-G32*(x1+x2-1))^4;
% (d3lngam1/d (x2)^3)
B1222=(3*G12*((2*(G32*t32*(x1+x2-1)-G12*t12*x1)*(G32-1)^2)/(x2+G12*x1-
G32*(x1+x2-1))^3+(2*G32*t32*(G32-1))/(x2+G12*x1-G32*(x1+x2-
1))^2))/(x2+G12*x1-G32*(x1+x2-1))+(6*(G21-G31)^3*(G31*t31*(x1+x2-1)-
G21*t21*x2))/(x1+G21*x2-G31*(x1+x2-
1))^4+(3*G13*((2*(G13*t13*x1+G23*t23*x2)*(G23-1)^2)/(G13*x1-x2-
x1+G23*x2+1)^3-(2*G23*t23*(G23-1))/(G13*x1-x2-x1+G23*x2+1)^2))/(G13*x1-
x2-x1+G23*x2+1)+(6*(G21-G31)^2*(G21*t21-G31*t31))/(x1+G21*x2-
G31*(x1+x2-1))^3+(6*G12*((G32*t32)/(x2+G12*x1-G32*(x1+x2-
1))+((G32*t32*(x1+x2-1)-G12*t12*x1)*(G32-1))/(x2+G12*x1-G32*(x1+x2-
1))^2)*(G32-1))/(x2+G12*x1-G32*(x1+x2-1))^2-(24*x1*(G21-
G31)^3*(G31*t31*(x1+x2-1)-G21*t21*x2))/(x1+G21*x2-G31*(x1+x2-
1))^5+(G12*x2*((6*(G32*t32*(x1+x2-1)-G12*t12*x1)*(G32-1)^3)/(x2+G12*x1-
G32*(x1+x2-1))^4+(6*G32*t32*(G32-1)^2)/(x2+G12*x1-G32*(x1+x2-
1))^3))/(x2+G12*x1-G32*(x1+x2-
1))+(6*G13*(((G13*t13*x1+G23*t23*x2)*(G23-1))/(G13*x1-x2-
x1+G23*x2+1)^2-(G23*t23)/(G13*x1-x2-x1+G23*x2+1))*(G23-1))/(G13*x1-x2-
x1+G23*x2+1)^2-(G13*((6*(G13*t13*x1+G23*t23*x2)*(G23-1)^3)/(G13*x1-x2-
x1+G23*x2+1)^4-(6*G23*t23*(G23-1)^2)/(G13*x1-x2-x1+G23*x2+1)^3)*(x1+x2-
1))/(G13*x1-x2-x1+G23*x2+1)-(18*x1*(G21-G31)^2*(G21*t21-
G31*t31))/(x1+G21*x2-G31*(x1+x2-1))^4-(6*G13*(t13-
(G13*t13*x1+G23*t23*x2)/(G13*x1-x2-x1+G23*x2+1))*(G23-1)^2)/(G13*x1-x2-
x1+G23*x2+1)^3+(6*G12*(G32-1)^2*(t12+(G32*t32*(x1+x2-1)-
G12*t12*x1)/(x2+G12*x1-G32*(x1+x2-1))))/(x2+G12*x1-G32*(x1+x2-1))^3-
(6*G13*(((G13*t13*x1+G23*t23*x2)*(G23-1))/(G13*x1-x2-x1+G23*x2+1)^2-
(G23*t23)/(G13*x1-x2-x1+G23*x2+1))*(G23-1)^2*(x1+x2-1))/(G13*x1-x2-
x1+G23*x2+1)^3+(6*G13*(t13-(G13*t13*x1+G23*t23*x2)/(G13*x1-x2-
x1+G23*x2+1))*(G23-1)^3*(x1+x2-1))/(G13*x1-x2-
x1+G23*x2+1)^4+(6*G12*x2*(G32-1)^3*(t12+(G32*t32*(x1+x2-1)-
G12*t12*x1)/(x2+G12*x1-G32*(x1+x2-1))))/(x2+G12*x1-G32*(x1+x2-
1))^4+(3*G12*x2*((2*(G32*t32*(x1+x2-1)-G12*t12*x1)*(G32-
1)^2)/(x2+G12*x1-G32*(x1+x2-1))^3+(2*G32*t32*(G32-1))/(x2+G12*x1-
G32*(x1+x2-1))^2)*(G32-1))/(x2+G12*x1-G32*(x1+x2-1))^2-
(3*G13*((2*(G13*t13*x1+G23*t23*x2)*(G23-1)^2)/(G13*x1-x2-
x1+G23*x2+1)^3-(2*G23*t23*(G23-1))/(G13*x1-x2-x1+G23*x2+1)^2)*(G23-
1)*(x1+x2-1))/(G13*x1-x2-
x1+G23*x2+1)^2+(6*G12*x2*((G32*t32)/(x2+G12*x1-G32*(x1+x2-
1))+((G32*t32*(x1+x2-1)-G12*t12*x1)*(G32-1))/(x2+G12*x1-G32*(x1+x2-
1))^2)*(G32-1)^2)/(x2+G12*x1-G32*(x1+x2-1))^3;
% (d3lngam2/d (x2)^3)
B2222=(18*(G32*t32*(x1+x2-1)-G12*t12*x1)*(G32-1)^2)/(x2+G12*x1-
G32*(x1+x2-1))^4-(6*(G32*t32*(x1+x2-1)-G12*t12*x1)*(G32-
1)^3)/(x2+G12*x1-G32*(x1+x2-
1))^4+(3*G23*((2*(G13*t13*x1+G23*t23*x2)*(G23-1)^2)/(G13*x1-x2-
x1+G23*x2+1)^3-(2*G23*t23*(G23-1))/(G13*x1-x2-x1+G23*x2+1)^2))/(G13*x1-
x2-x1+G23*x2+1)+(12*G32*t32*(G32-1))/(x2+G12*x1-G32*(x1+x2-
1))^3+(6*G23*(((G13*t13*x1+G23*t23*x2)*(G23-1))/(G13*x1-x2-
x1+G23*x2+1)^2-(G23*t23)/(G13*x1-x2-x1+G23*x2+1))*(G23-1))/(G13*x1-x2-
x1+G23*x2+1)^2-(G23*((6*(G13*t13*x1+G23*t23*x2)*(G23-1)^3)/(G13*x1-x2-
```

```
x1+G23*x2+1)^4-(6*G23*t23*(G23-1)^2)/(G13*x1-x2-x1+G23*x2+1)^3)*(x1+x2-
1))/(G13*x1-x2-x1+G23*x2+1)-(6*G32*t32*(G32-1)^2)/(x2+G12*x1-
G32*(x1+x2-1))^3-(G21*x1*((6*(G21-G31)^3*(G31*t31*(x1+x2-1)-
G21*t21*x2))/(x1+G21*x2-G31*(x1+x2-1))^4+(6*(G21-G31)^2*(G21*t21-
G31*t31))/(x1+G21*x2-G31*(x1+x2-1))^3))/(x1+G21*x2-G31*(x1+x2-
1))+(24*x2*(G32*t32*(x1+x2-1)-G12*t12*x1)*(G32-1)^3)/(x2+G12*x1-
G32*(x1+x2-1))^5-(6*G23*(t23-(G13*t13*x1+G23*t23*x2)/(G13*x1-x2-
x1+G23*x2+1))*(G23-1)^2)/(G13*x1-x2-x1+G23*x2+1)^3-
(6*G23*(((G13*t13*x1+G23*t23*x2)*(G23-1))/(G13*x1-x2-x1+G23*x2+1)^2-
(G23*t23)/(G13*x1-x2-x1+G23*x2+1))*(G23-1)^2*(x1+x2-1))/(G13*x1-x2-
x1+G23*x2+1)^3+(6*G23*(t23-(G13*t13*x1+G23*t23*x2)/(G13*x1-x2-
x1+G23*x2+1))*(G23-1)^3*(x1+x2-1))/(G13*x1-x2-x1+G23*x2+1)^4-
(6*G21*x1*(G21-G31)^2*((G21*t21-G31*t31)/(x1+G21*x2-G31*(x1+x2-
1))+((G21-G31)*(G31*t31*(x1+x2-1)-G21*t21*x2))/(x1+G21*x2-G31*(x1+x2-
1))^2))/(x1+G21*x2-G31*(x1+x2-1))^3-(3*G21*x1*(G21-G31)*((2*(G21-
G31)*(G21*t21-G31*t31))/(x1+G21*x2-G31*(x1+x2-1))^2+(2*(G21-
G31)^2*(G31*t31*(x1+x2-1)-G21*t21*x2))/(x1+G21*x2-G31*(x1+x2-
1))^3))/(x1+G21*x2-G31*(x1+x2-1))^2-
(3*G23*((2*(G13*t13*x1+G23*t23*x2)*(G23-1)^2)/(G13*x1-x2-
x1+G23*x2+1)^3-(2*G23*t23*(G23-1))/(G13*x1-x2-x1+G23*x2+1)^2)*(G23-
1)*(x1+x2-1))/(G13*x1-x2-x1+G23*x2+1)^2+(18*G32*t32*x2*(G32-
1)^2)/(x2+G12*x1-G32*(x1+x2-1))^4-(6*G21*x1*(G21-
G31)^3*(t21+(G31*t31*(x1+x2-1)-G21*t21*x2)/(x1+G21*x2-G31*(x1+x2-
1))))/(x1+G21*x2-G31*(x1+x2-1))^4;
% (d3lngam3/d (x2)^3)
B3222=(3*G32*((2*(G32*t32*(x1+x2-1)-G12*t12*x1)*(G32-1)^2)/(x2+G12*x1-
G32*(x1+x2-1))^3+(2*G32*t32*(G32-1))/(x2+G12*x1-G32*(x1+x2-
1))^2))/(x2+G12*x1-G32*(x1+x2-1))+(18*(G13*t13*x1+G23*t23*x2)*(G23-
1)^2)/(G13*x1-x2-x1+G23*x2+1)^4-(6*(G13*t13*x1+G23*t23*x2)*(G23-
1)^3)/(G13*x1-x2-x1+G23*x2+1)^4+(6*G32*((G32*t32)/(x2+G12*x1-
G32*(x1+x2-1))+((G32*t32*(x1+x2-1)-G12*t12*x1)*(G32-1))/(x2+G12*x1-
G32*(x1+x2-1))^2)*(G32-1))/(x2+G12*x1-G32*(x1+x2-
1))^2+(G32*x2*((6*(G32*t32*(x1+x2-1)-G12*t12*x1)*(G32-1)^3)/(x2+G12*x1-
G32*(x1+x2-1))^4+(6*G32*t32*(G32-1)^2)/(x2+G12*x1-G32*(x1+x2-
1))^3))/(x2+G12*x1-G32*(x1+x2-1))-(12*G23*t23*(G23-1))/(G13*x1-x2-
x1+G23*x2+1)^3-(G31*x1*((6*(G21-G31)^3*(G31*t31*(x1+x2-1)-
G21*t21*x2))/(x1+G21*x2-G31*(x1+x2-1))^4+(6*(G21-G31)^2*(G21*t21-
G31*t31))/(x1+G21*x2-G31*(x1+x2-1))^3))/(x1+G21*x2-G31*(x1+x2-
1))+(6*G23*t23*(G23-1)^2)/(G13*x1-x2-x1+G23*x2+1)^3+(6*G32*(G32-
1)^2*(t32+(G32*t32*(x1+x2-1)-G12*t12*x1)/(x2+G12*x1-G32*(x1+x2-
1))))/(x2+G12*x1-G32*(x1+x2-1))^3-(24*(G13*t13*x1+G23*t23*x2)*(G23-
1)^3*(x1+x2-1))/(G13*x1-x2-x1+G23*x2+1)^5-(6*G31*x1*(G21-
G31)^2*((G21*t21-G31*t31)/(x1+G21*x2-G31*(x1+x2-1))+((G21-
G31)*(G31*t31*(x1+x2-1)-G21*t21*x2))/(x1+G21*x2-G31*(x1+x2-
1))^2))/(x1+G21*x2-G31*(x1+x2-1))^3+(18*G23*t23*(G23-1)^2*(x1+x2-
1))/(G13*x1-x2-x1+G23*x2+1)^4+(6*G32*x2*(G32-1)^3*(t32+(G32*t32*(x1+x2-
1)-G12*t12*x1)/(x2+G12*x1-G32*(x1+x2-1))))/(x2+G12*x1-G32*(x1+x2-1))^4-
(3*G31*x1*(G21-G31)*((2*(G21-G31)*(G21*t21-G31*t31))/(x1+G21*x2-
G31*(x1+x2-1))^2+(2*(G21-G31)^2*(G31*t31*(x1+x2-1)-
G21*t21*x2))/(x1+G21*x2-G31*(x1+x2-1))^3))/(x1+G21*x2-G31*(x1+x2-
1))^2+(3*G32*x2*((2*(G32*t32*(x1+x2-1)-G12*t12*x1)*(G32-
1)^2)/(x2+G12*x1-G32*(x1+x2-1))^3+(2*G32*t32*(G32-1))/(x2+G12*x1-
G32*(x1+x2-1))^2)*(G32-1))/(x2+G12*x1-G32*(x1+x2-
1))^2+(6*G32*x2*((G32*t32)/(x2+G12*x1-G32*(x1+x2-1))+((G32*t32*(x1+x2-
1)-G12*t12*x1)*(G32-1))/(x2+G12*x1-G32*(x1+x2-1))^2)*(G32-
1)^2)/(x2+G12*x1-G32*(x1+x2-1))^3-(6*G31*x1*(G21-
```

```
G31)^3*(t31+(G31*t31*(x1+x2-1)-G21*t21*x2)/(x1+G21*x2-G31*(x1+x2-
1))))/(x1+G21*x2-G31*(x1+x2-1))^4;
% (d3lngam1/d (x1)^2 dx2)
B1112=(2*(G21*t21-G31*t31)*(G31-1)^2)/(x1+G21*x2-G31*(x1+x2-1))^3-
(2*G13*((G13*t13*(G23-1))/(G13*x1-x2-x1+G23*x2+1)^2+(G23*t23*(G13-
1))/(G13*x1-x2-x1+G23*x2+1)^2-(2*(G13*t13*x1+G23*t23*x2)*(G13-1)*(G23-
1))/(G13*x1-x2-x1+G23*x2+1)^3))/(G13*x1-x2-x1+G23*x2+1)+(G12*((2*(G12-
G32)*(G12*t12-G32*t32))/(x2+G12*x1-G32*(x1+x2-1))^2+(2*(G12-
G32)^2*(G32*t32*(x1+x2-1)-G12*t12*x1))/(x2+G12*x1-G32*(x1+x2-
1))^3))/(x2+G12*x1-G32*(x1+x2-
1))+(G13*((2*(G13*t13*x1+G23*t23*x2)*(G13-1)^2)/(G13*x1-x2-
x1+G23*x2+1)^3-(2*G13*t13*(G13-1))/(G13*x1-x2-x1+G23*x2+1)^2))/(G13*x1-
x2-x1+G23*x2+1)-(4*(G21*t21-G31*t31)*(G31-1))/(x1+G21*x2-G31*(x1+x2-
1))^3+(G13*(x1+x2-1)*((2*G23*t23*(G13-1)^2)/(G13*x1-x2-x1+G23*x2+1)^3-
(6*(G13*t13*x1+G23*t23*x2)*(G13-1)^2*(G23-1))/(G13*x1-x2-
x1+G23*x2+1)^4+(4*G13*t13*(G13-1)*(G23-1))/(G13*x1-x2-
x1+G23*x2+1)^3))/(G13*x1-x2-x1+G23*x2+1)+(2*G12*(G12-G32)*((G12*t12-
G32*t32)/(x2+G12*x1-G32*(x1+x2-1))+((G12-G32)*(G32*t32*(x1+x2-1)-
G12*t12*x1))/(x2+G12*x1-G32*(x1+x2-1))^2))/(x2+G12*x1-G32*(x1+x2-
1))^2+(2*G13*(((G13*t13*x1+G23*t23*x2)*(G13-1))/(G13*x1-x2-
x1+G23*x2+1)^2-(G13*t13)/(G13*x1-x2-x1+G23*x2+1))*(G13-1))/(G13*x1-x2-
x1+G23*x2+1)^2+(2*G13*(((G13*t13*x1+G23*t23*x2)*(G13-1))/(G13*x1-x2-
x1+G23*x2+1)^2-(G13*t13)/(G13*x1-x2-x1+G23*x2+1))*(G23-1))/(G13*x1-x2-
x1+G23*x2+1)^2+(2*G13*(((G13*t13*x1+G23*t23*x2)*(G23-1))/(G13*x1-x2-
x1+G23*x2+1)^2-(G23*t23)/(G13*x1-x2-x1+G23*x2+1))*(G13-1))/(G13*x1-x2-
x1+G23*x2+1)^2+(6*(G21-G31)*(G31*t31*(x1+x2-1)-G21*t21*x2)*(G31-
1)^2)/(x1+G21*x2-G31*(x1+x2-1))^4+(G12*x2*((2*G32*t32*(G12-
G32)^2)/(x2+G12*x1-G32*(x1+x2-1))^3+(4*(G12-G32)*(G12*t12-
G32*t32)*(G32-1))/(x2+G12*x1-G32*(x1+x2-1))^3+(6*(G12-
G32)^2*(G32*t32*(x1+x2-1)-G12*t12*x1)*(G32-1))/(x2+G12*x1-G32*(x1+x2-
1))^4))/(x2+G12*x1-G32*(x1+x2-1))+(2*G12*(G12-
G32)^2*(t12+(G32*t32*(x1+x2-1)-G12*t12*x1)/(x2+G12*x1-G32*(x1+x2-
1))))/(x2+G12*x1-G32*(x1+x2-1))^3-(4*G31*t31*(G21-G31))/(x1+G21*x2-
G31*(x1+x2-1))^3-(2*G13*(t13-(G13*t13*x1+G23*t23*x2)/(G13*x1-x2-
x1+G23*x2+1))*(G13-1)^2)/(G13*x1-x2-x1+G23*x2+1)^3-(6*x1*(G21*t21-
G31*t31)*(G31-1)^2)/(x1+G21*x2-G31*(x1+x2-1))^4-(12*(G21-
G31)*(G31*t31*(x1+x2-1)-G21*t21*x2)*(G31-1))/(x1+G21*x2-G31*(x1+x2-
1))^4-(4*G13*(t13-(G13*t13*x1+G23*t23*x2)/(G13*x1-x2-
x1+G23*x2+1))*(G13-1)*(G23-1))/(G13*x1-x2-x1+G23*x2+1)^3-
(2*G13*(((G13*t13*x1+G23*t23*x2)*(G23-1))/(G13*x1-x2-x1+G23*x2+1)^2-
(G23*t23)/(G13*x1-x2-x1+G23*x2+1))*(G13-1)^2*(x1+x2-1))/(G13*x1-x2-
x1+G23*x2+1)^3+(4*G31*t31*(G21-G31)*(G31-1))/(x1+G21*x2-G31*(x1+x2-
1))^3+(2*G13*(G13-1)*((G13*t13*(G23-1))/(G13*x1-x2-
x1+G23*x2+1)^2+(G23*t23*(G13-1))/(G13*x1-x2-x1+G23*x2+1)^2-
(2*(G13*t13*x1+G23*t23*x2)*(G13-1)*(G23-1))/(G13*x1-x2-
x1+G23*x2+1)^3)*(x1+x2-1))/(G13*x1-x2-x1+G23*x2+1)^2+(2*G12*x2*(G12-
G32)^2*((G32*t32)/(x2+G12*x1-G32*(x1+x2-1))+((G32*t32*(x1+x2-1)-
G12*t12*x1)*(G32-1))/(x2+G12*x1-G32*(x1+x2-1))^2))/(x2+G12*x1-
G32*(x1+x2-1))^3-(G13*((2*(G13*t13*x1+G23*t23*x2)*(G13-1)^2)/(G13*x1-
x2-x1+G23*x2+1)^3-(2*G13*t13*(G13-1))/(G13*x1-x2-x1+G23*x2+1)^2)*(G23-
1)*(x1+x2-1))/(G13*x1-x2-x1+G23*x2+1)^2+(2*G12*x2*(G12-G32)*(((G12*t12-
G32*t32)*(G32-1))/(x2+G12*x1-G32*(x1+x2-1))^2+(G32*t32*(G12-
G32))/(x2+G12*x1-G32*(x1+x2-1))^2+(2*(G12-G32)*(G32*t32*(x1+x2-1)-
G12*t12*x1)*(G32-1))/(x2+G12*x1-G32*(x1+x2-1))^3))/(x2+G12*x1-
G32*(x1+x2-1))^2+(G12*x2*((2*(G12-G32)*(G12*t12-G32*t32))/(x2+G12*x1-
G32*(x1+x2-1))^2+(2*(G12-G32)^2*(G32*t32*(x1+x2-1)-
G12*t12*x1))/(x2+G12*x1-G32*(x1+x2-1))^3)*(G32-1))/(x2+G12*x1-
```

```
G32*(x1+x2-1))^2-(24*x1*(G21-G31)*(G31*t31*(x1+x2-1)-G21*t21*x2)*(G31-
1)^2)/(x1+G21*x2-G31*(x1+x2-1))^5-
(4*G13*(((G13*t13*x1+G23*t23*x2)*(G13-1))/(G13*x1-x2-x1+G23*x2+1)^2-
(G13*t13)/(G13*x1-x2-x1+G23*x2+1))*(G13-1)*(G23-1)*(x1+x2-1))/(G13*x1-
x2-x1+G23*x2+1)^3+(4*G12*x2*(G12-G32)*(G32-1)*((G12*t12-
G32*t32)/(x2+G12*x1-G32*(x1+x2-1))+((G12-G32)*(G32*t32*(x1+x2-1)-
G12*t12*x1))/(x2+G12*x1-G32*(x1+x2-1))^2))/(x2+G12*x1-G32*(x1+x2-
1))^3+(6*G12*x2*(G12-G32)^2*(G32-1)*(t12+(G32*t32*(x1+x2-1)-
G12*t12*x1)/(x2+G12*x1-G32*(x1+x2-1))))/(x2+G12*x1-G32*(x1+x2-
1))^4+(6*G13*(t13-(G13*t13*x1+G23*t23*x2)/(G13*x1-x2-
x1+G23*x2+1))*(G13-1)^2*(G23-1)*(x1+x2-1))/(G13*x1-x2-x1+G23*x2+1)^4-
(12*G31*t31*x1*(G21-G31)*(G31-1))/(x1+G21*x2-G31*(x1+x2-1))^4;
% (d3lngam3/d (x1)^2 dx2)
B3112=(G32*((2*(G12-G32)*(G12*t12-G32*t32))/(x2+G12*x1-G32*(x1+x2-
1))^2+(2*(G12-G32)^2*(G32*t32*(x1+x2-1)-G12*t12*x1))/(x2+G12*x1-
G32*(x1+x2-1))^3))/(x2+G12*x1-G32*(x1+x2-
1))+(6*(G13*t13*x1+G23*t23*x2)*(G13-1)^2)/(G13*x1-x2-x1+G23*x2+1)^4-
(2*G31*(((G21*t21-G31*t31)*(G31-1))/(x1+G21*x2-G31*(x1+x2-
1))^2+(G31*t31*(G21-G31))/(x1+G21*x2-G31*(x1+x2-1))^2+(2*(G21-
G31)*(G31*t31*(x1+x2-1)-G21*t21*x2)*(G31-1))/(x1+G21*x2-G31*(x1+x2-
1))^3))/(x1+G21*x2-G31*(x1+x2-1))+(2*G32*(G12-G32)*((G12*t12-
G32*t32)/(x2+G12*x1-G32*(x1+x2-1))+((G12-G32)*(G32*t32*(x1+x2-1)-
G12*t12*x1))/(x2+G12*x1-G32*(x1+x2-1))^2))/(x2+G12*x1-G32*(x1+x2-1))^2-
(6*(G13*t13*x1+G23*t23*x2)*(G13-1)^2*(G23-1))/(G13*x1-x2-
x1+G23*x2+1)^4-(4*G13*t13*(G13-1))/(G13*x1-x2-x1+G23*x2+1)^3-
(4*G13*t13*(G23-1))/(G13*x1-x2-x1+G23*x2+1)^3-(4*G23*t23*(G13-
1))/(G13*x1-x2-x1+G23*x2+1)^3+(G32*x2*((2*G32*t32*(G12-
G32)^2)/(x2+G12*x1-G32*(x1+x2-1))^3+(4*(G12-G32)*(G12*t12-
G32*t32)*(G32-1))/(x2+G12*x1-G32*(x1+x2-1))^3+(6*(G12-
G32)^2*(G32*t32*(x1+x2-1)-G12*t12*x1)*(G32-1))/(x2+G12*x1-G32*(x1+x2-
1))^4))/(x2+G12*x1-G32*(x1+x2-1))+(2*G32*(G12-
G32)^2*(t32+(G32*t32*(x1+x2-1)-G12*t12*x1)/(x2+G12*x1-G32*(x1+x2-
1))))/(x2+G12*x1-G32*(x1+x2-1))^3-(2*G31*(G31-1)*((G21*t21-
G31*t31)/(x1+G21*x2-G31*(x1+x2-1))+((G21-G31)*(G31*t31*(x1+x2-1)-
G21*t21*x2))/(x1+G21*x2-G31*(x1+x2-1))^2))/(x1+G21*x2-G31*(x1+x2-1))^2-
(2*G31*(G21-G31)*((G31*t31)/(x1+G21*x2-G31*(x1+x2-1))+((G31*t31*(x1+x2-
1)-G21*t21*x2)*(G31-1))/(x1+G21*x2-G31*(x1+x2-1))^2))/(x1+G21*x2-
G31*(x1+x2-1))^2-(G31*x1*((2*(G21*t21-G31*t31)*(G31-1)^2)/(x1+G21*x2-
G31*(x1+x2-1))^3+(6*(G21-G31)*(G31*t31*(x1+x2-1)-G21*t21*x2)*(G31-
1)^2)/(x1+G21*x2-G31*(x1+x2-1))^4+(4*G31*t31*(G21-G31)*(G31-
1))/(x1+G21*x2-G31*(x1+x2-1))^3))/(x1+G21*x2-G31*(x1+x2-
1))+(2*G23*t23*(G13-1)^2)/(G13*x1-x2-
x1+G23*x2+1)^3+(12*(G13*t13*x1+G23*t23*x2)*(G13-1)*(G23-1))/(G13*x1-x2-
x1+G23*x2+1)^4-(2*G31*x1*(G31-1)*(((G21*t21-G31*t31)*(G31-
1))/(x1+G21*x2-G31*(x1+x2-1))^2+(G31*t31*(G21-G31))/(x1+G21*x2-
G31*(x1+x2-1))^2+(2*(G21-G31)*(G31*t31*(x1+x2-1)-G21*t21*x2)*(G31-
1))/(x1+G21*x2-G31*(x1+x2-1))^3))/(x1+G21*x2-G31*(x1+x2-
1))^2+(4*G13*t13*(G13-1)*(G23-1))/(G13*x1-x2-
x1+G23*x2+1)^3+(6*G23*t23*(G13-1)^2*(x1+x2-1))/(G13*x1-x2-
x1+G23*x2+1)^4-(G31*x1*(G21-G31)*((2*(G31*t31*(x1+x2-1)-
G21*t21*x2)*(G31-1)^2)/(x1+G21*x2-G31*(x1+x2-1))^3+(2*G31*t31*(G31-
1))/(x1+G21*x2-G31*(x1+x2-1))^2))/(x1+G21*x2-G31*(x1+x2-1))^2-
(2*G31*x1*(G31-1)^2*((G21*t21-G31*t31)/(x1+G21*x2-G31*(x1+x2-1))+((G21-
G31)*(G31*t31*(x1+x2-1)-G21*t21*x2))/(x1+G21*x2-G31*(x1+x2-
1))^2))/(x1+G21*x2-G31*(x1+x2-1))^3-(24*(G13*t13*x1+G23*t23*x2)*(G13-
1)^2*(G23-1)*(x1+x2-1))/(G13*x1-x2-x1+G23*x2+1)^5+(2*G32*x2*(G12-
G32)^2*((G32*t32)/(x2+G12*x1-G32*(x1+x2-1))+((G32*t32*(x1+x2-1)-
```

```
G12*t12*x1)*(G32-1))/(x2+G12*x1-G32*(x1+x2-1))^2))/(x2+G12*x1-
G32*(x1+x2-1))^3+(2*G32*x2*(G12-G32)*(((G12*t12-G32*t32)*(G32-
1))/(x2+G12*x1-G32*(x1+x2-1))^2+(G32*t32*(G12-G32))/(x2+G12*x1-
G32*(x1+x2-1))^2+(2*(G12-G32)*(G32*t32*(x1+x2-1)-G12*t12*x1)*(G32-
1))/(x2+G12*x1-G32*(x1+x2-1))^3))/(x2+G12*x1-G32*(x1+x2-
1))^2+(G32*x2*((2*(G12-G32)*(G12*t12-G32*t32))/(x2+G12*x1-G32*(x1+x2-
1))^2+(2*(G12-G32)^2*(G32*t32*(x1+x2-1)-G12*t12*x1))/(x2+G12*x1-
G32*(x1+x2-1))^3)*(G32-1))/(x2+G12*x1-G32*(x1+x2-1))^2-(4*G31*(G21-
G31)*(G31-1)*(t31+(G31*t31*(x1+x2-1)-G21*t21*x2)/(x1+G21*x2-G31*(x1+x2-
1))))/(x1+G21*x2-G31*(x1+x2-1))^3+(4*G32*x2*(G12-G32)*(G32-
1)*((G12*t12-G32*t32)/(x2+G12*x1-G32*(x1+x2-1))+((G12-
G32)*(G32*t32*(x1+x2-1)-G12*t12*x1))/(x2+G12*x1-G32*(x1+x2-
1))^2))/(x2+G12*x1-G32*(x1+x2-1))^3+(12*G13*t13*(G13-1)*(G23-1)*(x1+x2-
1))/(G13*x1-x2-x1+G23*x2+1)^4+(6*G32*x2*(G12-G32)^2*(G32-
1)*(t32+(G32*t32*(x1+x2-1)-G12*t12*x1)/(x2+G12*x1-G32*(x1+x2-
1))))/(x2+G12*x1-G32*(x1+x2-1))^4-(6*G31*x1*(G21-G31)*(G31-
1)^2*(t31+(G31*t31*(x1+x2-1)-G21*t21*x2)/(x1+G21*x2-G31*(x1+x2-
1))))/(x1+G21*x2-G31*(x1+x2-1))^4-(4*G31*x1*(G21-
G31)*((G31*t31)/(x1+G21*x2-G31*(x1+x2-1))+((G31*t31*(x1+x2-1)-
G21*t21*x2)*(G31-1))/(x1+G21*x2-G31*(x1+x2-1))^2)*(G31-1))/(x1+G21*x2-
G31*(x1+x2-1))^3;
% (d3lngam1/d (x2)^2 dx1)
B1122=(4*(G21-G31)*(G21*t21-G31*t31))/(x1+G21*x2-G31*(x1+x2-1))^3-
(2*G13*((G13*t13*(G23-1))/(G13*x1-x2-x1+G23*x2+1)^2+(G23*t23*(G13-
1))/(G13*x1-x2-x1+G23*x2+1)^2-(2*(G13*t13*x1+G23*t23*x2)*(G13-1)*(G23-
1))/(G13*x1-x2-x1+G23*x2+1)^3))/(G13*x1-x2-x1+G23*x2+1)+(6*(G21-
G31)^2*(G31*t31*(x1+x2-1)-G21*t21*x2))/(x1+G21*x2-G31*(x1+x2-
1))^4+(G13*((2*(G13*t13*x1+G23*t23*x2)*(G23-1)^2)/(G13*x1-x2-
x1+G23*x2+1)^3-(2*G23*t23*(G23-1))/(G13*x1-x2-x1+G23*x2+1)^2))/(G13*x1-
x2-x1+G23*x2+1)-(2*G12*(((G12*t12-G32*t32)*(G32-1))/(x2+G12*x1-
G32*(x1+x2-1))^2+(G32*t32*(G12-G32))/(x2+G12*x1-G32*(x1+x2-
1))^2+(2*(G12-G32)*(G32*t32*(x1+x2-1)-G12*t12*x1)*(G32-1))/(x2+G12*x1-
G32*(x1+x2-1))^3))/(x2+G12*x1-G32*(x1+x2-1))-(2*G31*t31*(G21-
G31)^2)/(x1+G21*x2-G31*(x1+x2-1))^3+(G13*(x1+x2-1)*((2*G13*t13*(G23-
1)^2)/(G13*x1-x2-x1+G23*x2+1)^3-(6*(G13*t13*x1+G23*t23*x2)*(G13-
1)*(G23-1)^2)/(G13*x1-x2-x1+G23*x2+1)^4+(4*G23*t23*(G13-1)*(G23-
1))/(G13*x1-x2-x1+G23*x2+1)^3))/(G13*x1-x2-x1+G23*x2+1)-(4*(G21-
G31)*(G21*t21-G31*t31)*(G31-1))/(x1+G21*x2-G31*(x1+x2-
1))^3+(2*G13*(((G13*t13*x1+G23*t23*x2)*(G13-1))/(G13*x1-x2-
x1+G23*x2+1)^2-(G13*t13)/(G13*x1-x2-x1+G23*x2+1))*(G23-1))/(G13*x1-x2-
x1+G23*x2+1)^2+(2*G13*(((G13*t13*x1+G23*t23*x2)*(G23-1))/(G13*x1-x2-
x1+G23*x2+1)^2-(G23*t23)/(G13*x1-x2-x1+G23*x2+1))*(G13-1))/(G13*x1-x2-
x1+G23*x2+1)^2+(2*G13*(((G13*t13*x1+G23*t23*x2)*(G23-1))/(G13*x1-x2-
x1+G23*x2+1)^2-(G23*t23)/(G13*x1-x2-x1+G23*x2+1))*(G23-1))/(G13*x1-x2-
x1+G23*x2+1)^2-(6*(G21-G31)^2*(G31*t31*(x1+x2-1)-G21*t21*x2)*(G31-
1))/(x1+G21*x2-G31*(x1+x2-1))^4-(2*G12*(G32-1)*((G12*t12-
G32*t32)/(x2+G12*x1-G32*(x1+x2-1))+((G12-G32)*(G32*t32*(x1+x2-1)-
G12*t12*x1))/(x2+G12*x1-G32*(x1+x2-1))^2))/(x2+G12*x1-G32*(x1+x2-1))^2-
(2*G12*(G12-G32)*((G32*t32)/(x2+G12*x1-G32*(x1+x2-1))+((G32*t32*(x1+x2-
1)-G12*t12*x1)*(G32-1))/(x2+G12*x1-G32*(x1+x2-1))^2))/(x2+G12*x1-
G32*(x1+x2-1))^2-(2*G13*(t13-(G13*t13*x1+G23*t23*x2)/(G13*x1-x2-
x1+G23*x2+1))*(G23-1)^2)/(G13*x1-x2-x1+G23*x2+1)^3-
(G12*x2*((2*(G12*t12-G32*t32)*(G32-1)^2)/(x2+G12*x1-G32*(x1+x2-
1))^3+(6*(G12-G32)*(G32*t32*(x1+x2-1)-G12*t12*x1)*(G32-
1)^2)/(x2+G12*x1-G32*(x1+x2-1))^4+(4*G32*t32*(G12-G32)*(G32-
1))/(x2+G12*x1-G32*(x1+x2-1))^3))/(x2+G12*x1-G32*(x1+x2-1))-
(4*G13*(t13-(G13*t13*x1+G23*t23*x2)/(G13*x1-x2-x1+G23*x2+1))*(G13-
```

```
1)*(G23-1))/(G13*x1-x2-x1+G23*x2+1)^3-
(2*G13*(((G13*t13*x1+G23*t23*x2)*(G13-1))/(G13*x1-x2-x1+G23*x2+1)^2-
(G13*t13)/(G13*x1-x2-x1+G23*x2+1))*(G23-1)^2*(x1+x2-1))/(G13*x1-x2-
x1+G23*x2+1)^3-(2*G12*x2*(G32-1)*(((G12*t12-G32*t32)*(G32-
1))/(x2+G12*x1-G32*(x1+x2-1))^2+(G32*t32*(G12-G32))/(x2+G12*x1-
G32*(x1+x2-1))^2+(2*(G12-G32)*(G32*t32*(x1+x2-1)-G12*t12*x1)*(G32-
1))/(x2+G12*x1-G32*(x1+x2-1))^3))/(x2+G12*x1-G32*(x1+x2-1))^2-
(G12*x2*(G12-G32)*((2*(G32*t32*(x1+x2-1)-G12*t12*x1)*(G32-
1)^2)/(x2+G12*x1-G32*(x1+x2-1))^3+(2*G32*t32*(G32-1))/(x2+G12*x1-
G32*(x1+x2-1))^2))/(x2+G12*x1-G32*(x1+x2-1))^2+(2*G13*(G23-
1)*((G13*t13*(G23-1))/(G13*x1-x2-x1+G23*x2+1)^2+(G23*t23*(G13-
1))/(G13*x1-x2-x1+G23*x2+1)^2-(2*(G13*t13*x1+G23*t23*x2)*(G13-1)*(G23-
1))/(G13*x1-x2-x1+G23*x2+1)^3)*(x1+x2-1))/(G13*x1-x2-x1+G23*x2+1)^2-
(2*G12*x2*(G32-1)^2*((G12*t12-G32*t32)/(x2+G12*x1-G32*(x1+x2-1))+((G12-
G32)*(G32*t32*(x1+x2-1)-G12*t12*x1))/(x2+G12*x1-G32*(x1+x2-
1))^2))/(x2+G12*x1-G32*(x1+x2-1))^3+(6*G31*t31*x1*(G21-
G31)^2)/(x1+G21*x2-G31*(x1+x2-1))^4-
(G13*((2*(G13*t13*x1+G23*t23*x2)*(G23-1)^2)/(G13*x1-x2-x1+G23*x2+1)^3-
(2*G23*t23*(G23-1))/(G13*x1-x2-x1+G23*x2+1)^2)*(G13-1)*(x1+x2-
1))/(G13*x1-x2-x1+G23*x2+1)^2+(12*x1*(G21-G31)*(G21*t21-G31*t31)*(G31-
1))/(x1+G21*x2-G31*(x1+x2-1))^4-(4*G12*(G12-G32)*(G32-
1)*(t12+(G32*t32*(x1+x2-1)-G12*t12*x1)/(x2+G12*x1-G32*(x1+x2-
1))))/(x2+G12*x1-G32*(x1+x2-1))^3+(24*x1*(G21-G31)^2*(G31*t31*(x1+x2-
1)-G21*t21*x2)*(G31-1))/(x1+G21*x2-G31*(x1+x2-1))^5-
(4*G13*(((G13*t13*x1+G23*t23*x2)*(G23-1))/(G13*x1-x2-x1+G23*x2+1)^2-
(G23*t23)/(G13*x1-x2-x1+G23*x2+1))*(G13-1)*(G23-1)*(x1+x2-1))/(G13*x1-
x2-x1+G23*x2+1)^3-(6*G12*x2*(G12-G32)*(G32-1)^2*(t12+(G32*t32*(x1+x2-
1)-G12*t12*x1)/(x2+G12*x1-G32*(x1+x2-1))))/(x2+G12*x1-G32*(x1+x2-
1))^4+(6*G13*(t13-(G13*t13*x1+G23*t23*x2)/(G13*x1-x2-
x1+G23*x2+1))*(G13-1)*(G23-1)^2*(x1+x2-1))/(G13*x1-x2-x1+G23*x2+1)^4-
(4*G12*x2*(G12-G32)*((G32*t32)/(x2+G12*x1-G32*(x1+x2-
1))+((G32*t32*(x1+x2-1)-G12*t12*x1)*(G32-1))/(x2+G12*x1-G32*(x1+x2-
1))^2)*(G32-1))/(x2+G12*x1-G32*(x1+x2-1))^3;
% (d3lngam2/d (x2)^2 dx1)
B2122=(2*(G12*t12-G32*t32)*(G32-1)^2)/(x2+G12*x1-G32*(x1+x2-1))^3-
(2*G23*((G13*t13*(G23-1))/(G13*x1-x2-x1+G23*x2+1)^2+(G23*t23*(G13-
1))/(G13*x1-x2-x1+G23*x2+1)^2-(2*(G13*t13*x1+G23*t23*x2)*(G13-1)*(G23-
1))/(G13*x1-x2-x1+G23*x2+1)^3))/(G13*x1-x2-x1+G23*x2+1)+(G21*((2*(G21-
G31)*(G21*t21-G31*t31))/(x1+G21*x2-G31*(x1+x2-1))^2+(2*(G21-
G31)^2*(G31*t31*(x1+x2-1)-G21*t21*x2))/(x1+G21*x2-G31*(x1+x2-
1))^3))/(x1+G21*x2-G31*(x1+x2-
1))+(G23*((2*(G13*t13*x1+G23*t23*x2)*(G23-1)^2)/(G13*x1-x2-
x1+G23*x2+1)^3-(2*G23*t23*(G23-1))/(G13*x1-x2-x1+G23*x2+1)^2))/(G13*x1-
x2-x1+G23*x2+1)-(4*(G12*t12-G32*t32)*(G32-1))/(x2+G12*x1-G32*(x1+x2-
1))^3+(G23*(x1+x2-1)*((2*G13*t13*(G23-1)^2)/(G13*x1-x2-x1+G23*x2+1)^3-
(6*(G13*t13*x1+G23*t23*x2)*(G13-1)*(G23-1)^2)/(G13*x1-x2-
x1+G23*x2+1)^4+(4*G23*t23*(G13-1)*(G23-1))/(G13*x1-x2-
x1+G23*x2+1)^3))/(G13*x1-x2-x1+G23*x2+1)+(2*G21*(G21-G31)*((G21*t21-
G31*t31)/(x1+G21*x2-G31*(x1+x2-1))+((G21-G31)*(G31*t31*(x1+x2-1)-
G21*t21*x2))/(x1+G21*x2-G31*(x1+x2-1))^2))/(x1+G21*x2-G31*(x1+x2-
1))^2+(2*G23*(((G13*t13*x1+G23*t23*x2)*(G13-1))/(G13*x1-x2-
x1+G23*x2+1)^2-(G13*t13)/(G13*x1-x2-x1+G23*x2+1))*(G23-1))/(G13*x1-x2-
x1+G23*x2+1)^2+(2*G23*(((G13*t13*x1+G23*t23*x2)*(G23-1))/(G13*x1-x2-
x1+G23*x2+1)^2-(G23*t23)/(G13*x1-x2-x1+G23*x2+1))*(G13-1))/(G13*x1-x2-
x1+G23*x2+1)^2+(2*G23*(((G13*t13*x1+G23*t23*x2)*(G23-1))/(G13*x1-x2-
x1+G23*x2+1)^2-(G23*t23)/(G13*x1-x2-x1+G23*x2+1))*(G23-1))/(G13*x1-x2-
x1+G23*x2+1)^2+(6*(G12-G32)*(G32*t32*(x1+x2-1)-G12*t12*x1)*(G32-
```

```
1)^2)/(x2+G12*x1-G32*(x1+x2-1))^4+(G21*x1*((2*G31*t31*(G21-
G31)^2)/(x1+G21*x2-G31*(x1+x2-1))^3+(4*(G21-G31)*(G21*t21-
G31*t31)*(G31-1))/(x1+G21*x2-G31*(x1+x2-1))^3+(6*(G21-
G31)^2*(G31*t31*(x1+x2-1)-G21*t21*x2)*(G31-1))/(x1+G21*x2-G31*(x1+x2-
1))^4))/(x1+G21*x2-G31*(x1+x2-1))+(2*G21*(G21-
G31)^2*(t21+(G31*t31*(x1+x2-1)-G21*t21*x2)/(x1+G21*x2-G31*(x1+x2-
1))))/(x1+G21*x2-G31*(x1+x2-1))^3-(4*G32*t32*(G12-G32))/(x2+G12*x1-
G32*(x1+x2-1))^3-(2*G23*(t23-(G13*t13*x1+G23*t23*x2)/(G13*x1-x2-
x1+G23*x2+1))*(G23-1)^2)/(G13*x1-x2-x1+G23*x2+1)^3-(6*x2*(G12*t12-
G32*t32)*(G32-1)^2)/(x2+G12*x1-G32*(x1+x2-1))^4-(12*(G12-
G32)*(G32*t32*(x1+x2-1)-G12*t12*x1)*(G32-1))/(x2+G12*x1-G32*(x1+x2-
1))^4-(4*G23*(t23-(G13*t13*x1+G23*t23*x2)/(G13*x1-x2-
x1+G23*x2+1))*(G13-1)*(G23-1))/(G13*x1-x2-x1+G23*x2+1)^3-
(2*G23*(((G13*t13*x1+G23*t23*x2)*(G13-1))/(G13*x1-x2-x1+G23*x2+1)^2-
(G13*t13)/(G13*x1-x2-x1+G23*x2+1))*(G23-1)^2*(x1+x2-1))/(G13*x1-x2-
x1+G23*x2+1)^3+(4*G32*t32*(G12-G32)*(G32-1))/(x2+G12*x1-G32*(x1+x2-
1))^3+(2*G23*(G23-1)*((G13*t13*(G23-1))/(G13*x1-x2-
x1+G23*x2+1)^2+(G23*t23*(G13-1))/(G13*x1-x2-x1+G23*x2+1)^2-
(2*(G13*t13*x1+G23*t23*x2)*(G13-1)*(G23-1))/(G13*x1-x2-
x1+G23*x2+1)^3)*(x1+x2-1))/(G13*x1-x2-x1+G23*x2+1)^2+(2*G21*x1*(G21-
G31)^2*((G31*t31)/(x1+G21*x2-G31*(x1+x2-1))+((G31*t31*(x1+x2-1)-
G21*t21*x2)*(G31-1))/(x1+G21*x2-G31*(x1+x2-1))^2))/(x1+G21*x2-
G31*(x1+x2-1))^3-(G23*((2*(G13*t13*x1+G23*t23*x2)*(G23-1)^2)/(G13*x1-
x2-x1+G23*x2+1)^3-(2*G23*t23*(G23-1))/(G13*x1-x2-x1+G23*x2+1)^2)*(G13-
1)*(x1+x2-1))/(G13*x1-x2-x1+G23*x2+1)^2+(2*G21*x1*(G21-G31)*(((G21*t21-
G31*t31)*(G31-1))/(x1+G21*x2-G31*(x1+x2-1))^2+(G31*t31*(G21-
G31))/(x1+G21*x2-G31*(x1+x2-1))^2+(2*(G21-G31)*(G31*t31*(x1+x2-1)-
G21*t21*x2)*(G31-1))/(x1+G21*x2-G31*(x1+x2-1))^3))/(x1+G21*x2-
G31*(x1+x2-1))^2+(G21*x1*((2*(G21-G31)*(G21*t21-G31*t31))/(x1+G21*x2-
G31*(x1+x2-1))^2+(2*(G21-G31)^2*(G31*t31*(x1+x2-1)-
G21*t21*x2))/(x1+G21*x2-G31*(x1+x2-1))^3)*(G31-1))/(x1+G21*x2-
G31*(x1+x2-1))^2-(24*x2*(G12-G32)*(G32*t32*(x1+x2-1)-G12*t12*x1)*(G32-
1)^2)/(x2+G12*x1-G32*(x1+x2-1))^5-
(4*G23*(((G13*t13*x1+G23*t23*x2)*(G23-1))/(G13*x1-x2-x1+G23*x2+1)^2-
(G23*t23)/(G13*x1-x2-x1+G23*x2+1))*(G13-1)*(G23-1)*(x1+x2-1))/(G13*x1-
x2-x1+G23*x2+1)^3+(4*G21*x1*(G21-G31)*(G31-1)*((G21*t21-
G31*t31)/(x1+G21*x2-G31*(x1+x2-1))+((G21-G31)*(G31*t31*(x1+x2-1)-
G21*t21*x2))/(x1+G21*x2-G31*(x1+x2-1))^2))/(x1+G21*x2-G31*(x1+x2-
1))^3+(6*G21*x1*(G21-G31)^2*(G31-1)*(t21+(G31*t31*(x1+x2-1)-
G21*t21*x2)/(x1+G21*x2-G31*(x1+x2-1))))/(x1+G21*x2-G31*(x1+x2-
1))^4+(6*G23*(t23-(G13*t13*x1+G23*t23*x2)/(G13*x1-x2-
x1+G23*x2+1))*(G13-1)*(G23-1)^2*(x1+x2-1))/(G13*x1-x2-x1+G23*x2+1)^4-
(12*G32*t32*x2*(G12-G32)*(G32-1))/(x2+G12*x1-G32*(x1+x2-1))^4;
% (d3lngam3/d (x2)^2 dx1)
B3122=(G31*((2*(G21-G31)*(G21*t21-G31*t31))/(x1+G21*x2-G31*(x1+x2-
1))^2+(2*(G21-G31)^2*(G31*t31*(x1+x2-1)-G21*t21*x2))/(x1+G21*x2-
G31*(x1+x2-1))^3))/(x1+G21*x2-G31*(x1+x2-
1))+(6*(G13*t13*x1+G23*t23*x2)*(G23-1)^2)/(G13*x1-x2-x1+G23*x2+1)^4-
(2*G32*(((G12*t12-G32*t32)*(G32-1))/(x2+G12*x1-G32*(x1+x2-
1))^2+(G32*t32*(G12-G32))/(x2+G12*x1-G32*(x1+x2-1))^2+(2*(G12-
G32)*(G32*t32*(x1+x2-1)-G12*t12*x1)*(G32-1))/(x2+G12*x1-G32*(x1+x2-
1))^3))/(x2+G12*x1-G32*(x1+x2-1))+(2*G31*(G21-G31)*((G21*t21-
G31*t31)/(x1+G21*x2-G31*(x1+x2-1))+((G21-G31)*(G31*t31*(x1+x2-1)-
G21*t21*x2))/(x1+G21*x2-G31*(x1+x2-1))^2))/(x1+G21*x2-G31*(x1+x2-1))^2-
(6*(G13*t13*x1+G23*t23*x2)*(G13-1)*(G23-1)^2)/(G13*x1-x2-
x1+G23*x2+1)^4-(4*G13*t13*(G23-1))/(G13*x1-x2-x1+G23*x2+1)^3-
(4*G23*t23*(G13-1))/(G13*x1-x2-x1+G23*x2+1)^3-(4*G23*t23*(G23-
```

```
1))/(G13*x1-x2-x1+G23*x2+1)^3+(G31*x1*((2*G31*t31*(G21-
G31)^2)/(x1+G21*x2-G31*(x1+x2-1))^3+(4*(G21-G31)*(G21*t21-
G31*t31)*(G31-1))/(x1+G21*x2-G31*(x1+x2-1))^3+(6*(G21-
G31)^2*(G31*t31*(x1+x2-1)-G21*t21*x2)*(G31-1))/(x1+G21*x2-G31*(x1+x2-
1))^4))/(x1+G21*x2-G31*(x1+x2-1))+(2*G31*(G21-
G31)^2*(t31+(G31*t31*(x1+x2-1)-G21*t21*x2)/(x1+G21*x2-G31*(x1+x2-
1))))/(x1+G21*x2-G31*(x1+x2-1))^3-(2*G32*(G32-1)*((G12*t12-
G32*t32)/(x2+G12*x1-G32*(x1+x2-1))+((G12-G32)*(G32*t32*(x1+x2-1)-
G12*t12*x1))/(x2+G12*x1-G32*(x1+x2-1))^2))/(x2+G12*x1-G32*(x1+x2-1))^2-
(2*G32*(G12-G32)*((G32*t32)/(x2+G12*x1-G32*(x1+x2-1))+((G32*t32*(x1+x2-
1)-G12*t12*x1)*(G32-1))/(x2+G12*x1-G32*(x1+x2-1))^2))/(x2+G12*x1-
G32*(x1+x2-1))^2-(G32*x2*((2*(G12*t12-G32*t32)*(G32-1)^2)/(x2+G12*x1-
G32*(x1+x2-1))^3+(6*(G12-G32)*(G32*t32*(x1+x2-1)-G12*t12*x1)*(G32-
1)^2)/(x2+G12*x1-G32*(x1+x2-1))^4+(4*G32*t32*(G12-G32)*(G32-
1))/(x2+G12*x1-G32*(x1+x2-1))^3))/(x2+G12*x1-G32*(x1+x2-
1))+(2*G13*t13*(G23-1)^2)/(G13*x1-x2-
x1+G23*x2+1)^3+(12*(G13*t13*x1+G23*t23*x2)*(G13-1)*(G23-1))/(G13*x1-x2-
x1+G23*x2+1)^4-(2*G32*x2*(G32-1)*(((G12*t12-G32*t32)*(G32-
1))/(x2+G12*x1-G32*(x1+x2-1))^2+(G32*t32*(G12-G32))/(x2+G12*x1-
G32*(x1+x2-1))^2+(2*(G12-G32)*(G32*t32*(x1+x2-1)-G12*t12*x1)*(G32-
1))/(x2+G12*x1-G32*(x1+x2-1))^3))/(x2+G12*x1-G32*(x1+x2-
1))^2+(4*G23*t23*(G13-1)*(G23-1))/(G13*x1-x2-
x1+G23*x2+1)^3+(6*G13*t13*(G23-1)^2*(x1+x2-1))/(G13*x1-x2-
x1+G23*x2+1)^4-(G32*x2*(G12-G32)*((2*(G32*t32*(x1+x2-1)-
G12*t12*x1)*(G32-1)^2)/(x2+G12*x1-G32*(x1+x2-1))^3+(2*G32*t32*(G32-
1))/(x2+G12*x1-G32*(x1+x2-1))^2))/(x2+G12*x1-G32*(x1+x2-1))^2-
(2*G32*x2*(G32-1)^2*((G12*t12-G32*t32)/(x2+G12*x1-G32*(x1+x2-1))+((G12-
G32)*(G32*t32*(x1+x2-1)-G12*t12*x1))/(x2+G12*x1-G32*(x1+x2-
1))^2))/(x2+G12*x1-G32*(x1+x2-1))^3-(24*(G13*t13*x1+G23*t23*x2)*(G13-
1)*(G23-1)^2*(x1+x2-1))/(G13*x1-x2-x1+G23*x2+1)^5+(2*G31*x1*(G21-
G31)^2*((G31*t31)/(x1+G21*x2-G31*(x1+x2-1))+((G31*t31*(x1+x2-1)-
G21*t21*x2)*(G31-1))/(x1+G21*x2-G31*(x1+x2-1))^2))/(x1+G21*x2-
G31*(x1+x2-1))^3+(2*G31*x1*(G21-G31)*(((G21*t21-G31*t31)*(G31-
1))/(x1+G21*x2-G31*(x1+x2-1))^2+(G31*t31*(G21-G31))/(x1+G21*x2-
G31*(x1+x2-1))^2+(2*(G21-G31)*(G31*t31*(x1+x2-1)-G21*t21*x2)*(G31-
1))/(x1+G21*x2-G31*(x1+x2-1))^3))/(x1+G21*x2-G31*(x1+x2-
1))^2+(G31*x1*((2*(G21-G31)*(G21*t21-G31*t31))/(x1+G21*x2-G31*(x1+x2-
1))^2+(2*(G21-G31)^2*(G31*t31*(x1+x2-1)-G21*t21*x2))/(x1+G21*x2-
G31*(x1+x2-1))^3)*(G31-1))/(x1+G21*x2-G31*(x1+x2-1))^2-(4*G32*(G12-
G32)*(G32-1)*(t32+(G32*t32*(x1+x2-1)-G12*t12*x1)/(x2+G12*x1-G32*(x1+x2-
1))))/(x2+G12*x1-G32*(x1+x2-1))^3+(4*G31*x1*(G21-G31)*(G31-
1)*((G21*t21-G31*t31)/(x1+G21*x2-G31*(x1+x2-1))+((G21-
G31)*(G31*t31*(x1+x2-1)-G21*t21*x2))/(x1+G21*x2-G31*(x1+x2-
1))^2))/(x1+G21*x2-G31*(x1+x2-1))^3+(12*G23*t23*(G13-1)*(G23-1)*(x1+x2-
1))/(G13*x1-x2-x1+G23*x2+1)^4-(6*G32*x2*(G12-G32)*(G32-
1)^2*(t32+(G32*t32*(x1+x2-1)-G12*t12*x1)/(x2+G12*x1-G32*(x1+x2-
1))))/(x2+G12*x1-G32*(x1+x2-1))^4+(6*G31*x1*(G21-G31)^2*(G31-
1)*(t31+(G31*t31*(x1+x2-1)-G21*t21*x2)/(x1+G21*x2-G31*(x1+x2-
1))))/(x1+G21*x2-G31*(x1+x2-1))^4-(4*G32*x2*(G12-
G32)*((G32*t32)/(x2+G12*x1-G32*(x1+x2-1))+((G32*t32*(x1+x2-1)-
G12*t12*x1)*(G32-1))/(x2+G12*x1-G32*(x1+x2-1))^2)*(G32-1))/(x2+G12*x1-
G32*(x1+x2-1))^3;
% (d3lngam2/d (x1)^2 dx2)
B2112=(4*(G12-G32)*(G12*t12-G32*t32))/(x2+G12*x1-G32*(x1+x2-1))^3-
(2*G23*((G13*t13*(G23-1))/(G13*x1-x2-x1+G23*x2+1)^2+(G23*t23*(G13-
1))/(G13*x1-x2-x1+G23*x2+1)^2-(2*(G13*t13*x1+G23*t23*x2)*(G13-1)*(G23-
1))/(G13*x1-x2-x1+G23*x2+1)^3))/(G13*x1-x2-x1+G23*x2+1)+(6*(G12-
```

```
G32)^2*(G32*t32*(x1+x2-1)-G12*t12*x1))/(x2+G12*x1-G32*(x1+x2-
1))^4+(G23*((2*(G13*t13*x1+G23*t23*x2)*(G13-1)^2)/(G13*x1-x2-
x1+G23*x2+1)^3-(2*G13*t13*(G13-1))/(G13*x1-x2-x1+G23*x2+1)^2))/(G13*x1-
x2-x1+G23*x2+1)-(2*G21*(((G21*t21-G31*t31)*(G31-1))/(x1+G21*x2-
G31*(x1+x2-1))^2+(G31*t31*(G21-G31))/(x1+G21*x2-G31*(x1+x2-
1))^2+(2*(G21-G31)*(G31*t31*(x1+x2-1)-G21*t21*x2)*(G31-1))/(x1+G21*x2-
G31*(x1+x2-1))^3))/(x1+G21*x2-G31*(x1+x2-1))-(2*G32*t32*(G12-
G32)^2)/(x2+G12*x1-G32*(x1+x2-1))^3+(G23*(x1+x2-1)*((2*G23*t23*(G13-
1)^2)/(G13*x1-x2-x1+G23*x2+1)^3-(6*(G13*t13*x1+G23*t23*x2)*(G13-
1)^2*(G23-1))/(G13*x1-x2-x1+G23*x2+1)^4+(4*G13*t13*(G13-1)*(G23-
1))/(G13*x1-x2-x1+G23*x2+1)^3))/(G13*x1-x2-x1+G23*x2+1)-(4*(G12-
G32)*(G12*t12-G32*t32)*(G32-1))/(x2+G12*x1-G32*(x1+x2-
1))^3+(2*G23*(((G13*t13*x1+G23*t23*x2)*(G13-1))/(G13*x1-x2-
x1+G23*x2+1)^2-(G13*t13)/(G13*x1-x2-x1+G23*x2+1))*(G13-1))/(G13*x1-x2-
x1+G23*x2+1)^2+(2*G23*(((G13*t13*x1+G23*t23*x2)*(G13-1))/(G13*x1-x2-
x1+G23*x2+1)^2-(G13*t13)/(G13*x1-x2-x1+G23*x2+1))*(G23-1))/(G13*x1-x2-
x1+G23*x2+1)^2+(2*G23*(((G13*t13*x1+G23*t23*x2)*(G23-1))/(G13*x1-x2-
x1+G23*x2+1)^2-(G23*t23)/(G13*x1-x2-x1+G23*x2+1))*(G13-1))/(G13*x1-x2-
x1+G23*x2+1)^2-(6*(G12-G32)^2*(G32*t32*(x1+x2-1)-G12*t12*x1)*(G32-
1))/(x2+G12*x1-G32*(x1+x2-1))^4-(2*G21*(G31-1)*((G21*t21-
G31*t31)/(x1+G21*x2-G31*(x1+x2-1))+((G21-G31)*(G31*t31*(x1+x2-1)-
G21*t21*x2))/(x1+G21*x2-G31*(x1+x2-1))^2))/(x1+G21*x2-G31*(x1+x2-1))^2-
(2*G21*(G21-G31)*((G31*t31)/(x1+G21*x2-G31*(x1+x2-1))+((G31*t31*(x1+x2-
1)-G21*t21*x2)*(G31-1))/(x1+G21*x2-G31*(x1+x2-1))^2))/(x1+G21*x2-
G31*(x1+x2-1))^2-(2*G23*(t23-(G13*t13*x1+G23*t23*x2)/(G13*x1-x2-
x1+G23*x2+1))*(G13-1)^2)/(G13*x1-x2-x1+G23*x2+1)^3-
(G21*x1*((2*(G21*t21-G31*t31)*(G31-1)^2)/(x1+G21*x2-G31*(x1+x2-
1))^3+(6*(G21-G31)*(G31*t31*(x1+x2-1)-G21*t21*x2)*(G31-
1)^2)/(x1+G21*x2-G31*(x1+x2-1))^4+(4*G31*t31*(G21-G31)*(G31-
1))/(x1+G21*x2-G31*(x1+x2-1))^3))/(x1+G21*x2-G31*(x1+x2-1))-
(4*G23*(t23-(G13*t13*x1+G23*t23*x2)/(G13*x1-x2-x1+G23*x2+1))*(G13-
1)*(G23-1))/(G13*x1-x2-x1+G23*x2+1)^3-
(2*G23*(((G13*t13*x1+G23*t23*x2)*(G23-1))/(G13*x1-x2-x1+G23*x2+1)^2-
(G23*t23)/(G13*x1-x2-x1+G23*x2+1))*(G13-1)^2*(x1+x2-1))/(G13*x1-x2-
x1+G23*x2+1)^3-(2*G21*x1*(G31-1)*(((G21*t21-G31*t31)*(G31-
1))/(x1+G21*x2-G31*(x1+x2-1))^2+(G31*t31*(G21-G31))/(x1+G21*x2-
G31*(x1+x2-1))^2+(2*(G21-G31)*(G31*t31*(x1+x2-1)-G21*t21*x2)*(G31-
1))/(x1+G21*x2-G31*(x1+x2-1))^3))/(x1+G21*x2-G31*(x1+x2-1))^2-
(G21*x1*(G21-G31)*((2*(G31*t31*(x1+x2-1)-G21*t21*x2)*(G31-
1)^2)/(x1+G21*x2-G31*(x1+x2-1))^3+(2*G31*t31*(G31-1))/(x1+G21*x2-
G31*(x1+x2-1))^2))/(x1+G21*x2-G31*(x1+x2-1))^2+(2*G23*(G13-
1)*((G13*t13*(G23-1))/(G13*x1-x2-x1+G23*x2+1)^2+(G23*t23*(G13-
1))/(G13*x1-x2-x1+G23*x2+1)^2-(2*(G13*t13*x1+G23*t23*x2)*(G13-1)*(G23-
1))/(G13*x1-x2-x1+G23*x2+1)^3)*(x1+x2-1))/(G13*x1-x2-x1+G23*x2+1)^2-
(2*G21*x1*(G31-1)^2*((G21*t21-G31*t31)/(x1+G21*x2-G31*(x1+x2-1))+((G21-
G31)*(G31*t31*(x1+x2-1)-G21*t21*x2))/(x1+G21*x2-G31*(x1+x2-
1))^2))/(x1+G21*x2-G31*(x1+x2-1))^3+(6*G32*t32*x2*(G12-
G32)^2)/(x2+G12*x1-G32*(x1+x2-1))^4-
(G23*((2*(G13*t13*x1+G23*t23*x2)*(G13-1)^2)/(G13*x1-x2-x1+G23*x2+1)^3-
(2*G13*t13*(G13-1))/(G13*x1-x2-x1+G23*x2+1)^2)*(G23-1)*(x1+x2-
1))/(G13*x1-x2-x1+G23*x2+1)^2+(12*x2*(G12-G32)*(G12*t12-G32*t32)*(G32-
1))/(x2+G12*x1-G32*(x1+x2-1))^4-(4*G21*(G21-G31)*(G31-
1)*(t21+(G31*t31*(x1+x2-1)-G21*t21*x2)/(x1+G21*x2-G31*(x1+x2-
1))))/(x1+G21*x2-G31*(x1+x2-1))^3+(24*x2*(G12-G32)^2*(G32*t32*(x1+x2-
1)-G12*t12*x1)*(G32-1))/(x2+G12*x1-G32*(x1+x2-1))^5-
(4*G23*(((G13*t13*x1+G23*t23*x2)*(G13-1))/(G13*x1-x2-x1+G23*x2+1)^2-
(G13*t13)/(G13*x1-x2-x1+G23*x2+1))*(G13-1)*(G23-1)*(x1+x2-1))/(G13*x1-
```

```
x2-x1+G23*x2+1)^3-(6*G21*x1*(G21-G31)*(G31-1)^2*(t21+(G31*t31*(x1+x2-
1)-G21*t21*x2)/(x1+G21*x2-G31*(x1+x2-1))))/(x1+G21*x2-G31*(x1+x2-
1))^4+(6*G23*(t23-(G13*t13*x1+G23*t23*x2)/(G13*x1-x2-
x1+G23*x2+1))*(G13-1)^2*(G23-1)*(x1+x2-1))/(G13*x1-x2-x1+G23*x2+1)^4-
(4*G21*x1*(G21-G31)*((G31*t31)/(x1+G21*x2-G31*(x1+x2-
1))+((G31*t31*(x1+x2-1)-G21*t21*x2)*(G31-1))/(x1+G21*x2-G31*(x1+x2-
1))^2)*(G31-1))/(x1+G21*x2-G31*(x1+x2-1))^3;



% (d2Gm/d(x2)^2)
G22=x1*B122+2*B22+2/x2+x2*(B222-1/(x2^2))-2*B32+2/(1-x2-x1)+(1-x2-
x1)*(B322-(1/((1-x2-x1)^2)));
% (d2Gm/dx1 dx2)
Gm12=B12+x1*B112+x2*B212-B32+2/(1-x2-x1)-B31+(1-x2-x1)*(B312-(1/((1-x2-
x1)^2)))+B21;
% (d2Gm/d(x2)^2)
G11=2*B11+2/x1+x1*(B111-1/(x1^2))+x2*B211-2*B31+2/(1-x2-x1)+(1-x2-
x1)*(B311-(1/((1-x2-x1)^2)));
% (d3Gm/d(x1)^3)
G111=3*B111-3/(x1^2)+x1*(B1111+2/(x1^3))+x2*B2111-3*B311+3/((1-x2-
x1)^2)+(1-x2-x1)*(B3111-2/((1-x2-x1)^3));
% (d3Gm/d(x2)^3)
G222=x1*B1222+3*B222-3/(x2^2)+x2*(B2222+2/(x2^3))-3*B322+3/((1-x2-
x1)^2)+(1-x2-x1)*(B3222-2/((1-x2-x1)^3));
% (d3Gm/d(x1)^2 dx2)
G112=2*B112+x1*B1112+B211+x2*B2112-2*B312+3/((1-x2-x1)^2)-B311+(1-x2-
x1)*(B3112-2/((1-x2-x1)^3));
% (d3Gm/dx1 d(x2)^2)
G122=B122+x1*B1122+2*B212+x2*B2122-B322-2*B312+3/((1-x2-x1)^2)+(1-x2-
x1)*(B3122-2/((1-x2-x1)^3));

% Both equations below are solved simultaneously to find critical point
of
% ternary system
f(1)=G11*G22-(Gm12)^2;
f(2)=G111*G22^2+G11*G122*G22-3*Gm12*G112*G22-
G11*G222*Gm12+2*Gm12^2*G122;
```

Vita

Fahad Al-Sadoon was born on April 18, 1986, in Basrah, Iraq. He was educated in public and private schools in Iraq, Jordan, and UAE. He graduated from Sharjah Public School in 2005 and enrolled in American University of Sharjah to graduate with bachelor degree of chemical engineering and graduated in fall 2008. He joined the MSc program of chemical engineering at American University of Sharjah in Fall 2009.

Mr. Al-Sadoon is currently working as process engineer in Petrofac Int Ltd, Sharjah.